Università degli Studi di Torino
Scuola di Dottorato

Defects in Conformal Field Theory with O(N) Symmetry

Elia de Sabbata

Università degli Studi di Torino
Scuola di Dottorato

Dottorato in Fisica

Defects in Conformal Field Theory with O(N) Symmetry

Elia de Sabbata

PhD Advisor: Lorenzo Bianchi

Doch im Erstarren such' ich nicht mein Heil,
Das Schaudern ist der Menschheit bestes Theil;
Wie auch die Welt ihm das Gefühl vertheure,
Ergriffen, fühlt er tief das Ungeheure.
[And yet in torpor there's no gain for me;
The thrill of awe is man's best quality.
Although the world may stifle every sense,
Enthralled, man deeply senses the Immense.]

Faust to Mephistopheles

Abstract

Conformal field theories (CFTs) are essential tools in quantum field theory and statistical physics, providing a framework for understanding critical phenomena and renormalisation group flows, with further applications to other formal areas of theoretical physics. In recent years, extended excitations within these theories–such as conformal defects–have gained prominence as powerful probes of quantum field theories, offering insights into dualities and symmetries. Moreover, conformal defects are widely employed in statistical physics, where they model the critical behaviour of systems with impurities, finite-size effects, or interfaces.

This thesis explores various aspects of the role that conformal defects play in CFTs. It begins by reviewing the fundamental concepts of CFTs, conformal defects, defect renormalisation group flows, and bootstrap methods. The focus then shifts to the study of specific conformal defects in CFTs with $O(N)$ internal symmetry, though the techniques employed are readily applicable to more general contexts. The localised magnetic field and the magnetic impurity in the critical $O(N)$ model are introduced and analysed extensively using the analytic bootstrap. Next, the concept of transdimensional defects is explored through concrete examples in free $O(N)$ field theory and the critical $O(N)$ model. Finally, several constructions of conformal defects in generalised free field theories and long-range $O(N)$ models are examined.

Contents

1 Introduction **1**
- 1.1 General introduction . . . 1
- 1.2 Main results and structure of the thesis . . . 4

2 Conformal field theory and defects **9**
- 2.1 Conformal field theory . . . 9
  - 2.1.1 The conformal group . . . 10
  - 2.1.2 The conformal algebra . . . 11
  - 2.1.3 Representation theory . . . 12
  - 2.1.4 Correlators and Ward identities . . . 14
  - 2.1.5 Radial quantisation . . . 16
  - 2.1.6 The operator product expansion . . . 18
  - 2.1.7 The conformal bootstrap . . . 20
- 2.2 Conformal defects . . . 23
  - 2.2.1 Defect conformal symmetry . . . 24
  - 2.2.2 Correlators in the defect theory . . . 25
  - 2.2.3 Displacement and Tilt operators . . . 29
  - 2.2.4 The defect OPE . . . 30
  - 2.2.5 The defect conformal bootstrap . . . 31
- 2.3 RG flows and conformal fixed points . . . 33
  - 2.3.1 Defect RG flows . . . 35

3 The critical O(N) model and its defects **39**
- 3.1 The critical O(N) model . . . 39
  - 3.1.1 The field theory description . . . 41
- 3.2 The localised magnetic field . . . 44
  - 3.2.1 The bulk two-point function . . . 47
- 3.3 The magnetic impurity . . . 50
  - 3.3.1 Defect β-function for free and interacting bulks 51
  - 3.3.2 Correlators and discrete symmetries . . . 53
  - 3.3.3 The defect spectrum . . . 56
- 3.4 Other defects in the critical O(N) model . . . 72
  - 3.4.1 Weakly-coupled defects . . . 72
  - 3.4.2 Strongly-coupled defects . . . 76

4 Analytic bootstrap for line defects in the O(N) model 81
4.1 Lorentzian inversion formulae and dispersion relation . 81
4.2 Analytic bootstrap for the localised magnetic field . . . 84
4.2.1 Tree level 84
4.2.2 One loop 87
4.2.3 The full result 89
4.3 Analytic bootstrap for the magnetic impurity 98
4.3.1 Free bulk 99
4.3.2 Interacting bulk 105
4.3.3 Diagrammatic computation 109

5 Transdimensional defects 117
5.1 Transdimensional defects in the $O(N)$ model 117
5.1.1 Free $O(N)$ field theory 118
5.1.2 The interacting $O(N)$ model to all orders in the defect coupling 121
5.2 Large-N analysis for $4 < d < 6$ 125

6 The long-range O(N) model and its defects 129
6.1 The long range O(N) model 129
6.2 Defects in the long-range O(N) model 133
6.2.1 Non-local defects 137
6.2.2 Defects close to $d = 4$ 145
6.2.3 Semiclassical construction of defects 153

7 Outlook 159

Appendices 163

A Bulk and defect blocks 165

B Explicit computations 167
B.1 Computation of the one-loop bulk two-point function for the localised magnetic field 167
B.1.1 The correlator from the dispersion relation . . . 167
B.1.2 Generating function of the bulk inversion 169
B.1.3 Feynman diagrams 169
B.2 Computation of the β-function for the magnetic impurity 172
B.2.1 Summary of the strategy 173
B.2.2 Expectation value of defect at three loops . . . 174
B.2.3 Expectation value of vertex at three loops . . . 175
B.2.4 Integrals 177
B.2.5 Computation of the β-function 179
B.2.6 β-function in the interacting bulk case 179
B.2.7 Two-point function of defect spin operators . . . 182

B.3 Diagrams and recursion for transdimensional defects . . 183
B.4 Diagrams for defects in the long-range O(N) model . . 192
B.4.1 Diagrams for the defect coupling renormalisation 193
B.4.2 Diagrams for the g-function close to four dimensions 194
B.4.3 Useful integrals 195

Chapter 1

Introduction

1.1 General introduction

Quantum field theories (QFTs) constitute the main paradigm through which modern physics has provided accurate descriptions of a wide range of physical phenomena. They were initially introduced to describe the interactions of particles at a fundamental quantum level, in accordance with the symmetries imposed by special relativity. The search for a consistent quantum theory of interactions between photons and electrons led to the development of the first QFT: quantum electrodynamics (QED). Following a series of outstanding breakthroughs, other particles and interactions were incorporated into this framework over the years, culminating in the development of the Standard Model of fundamental interactions. In parallel, shortly after the development of QED, it was realised that QFTs are also well-suited to describe the interactions of low-energy excitations in condensed matter systems in the continuum limit.

A crucial role in understanding the structure of QFTs is played by the *renormalisation group* (RG). Initially, renormalisation was introduced as a formal procedure to "cure" the infinities that arise in loop calculations in QFTs. This led to the celebrated theoretical prediction of the anomalous magnetic moment of the electron, one of the most accurate predictions ever made in theoretical physics. Later, a deeper understanding of the physical meaning of renormalisation came from its application in statistical field theory, once again demonstrating how rich and fruitful the exchange of ideas between high-energy theory and statistical physics can be. In the modern perspective, renormalisation is essentially a connection between descriptions of the same physical system at different length (or energy) scales. This connection provides a flow, known as the *renormalisation group flow*, which can be used to probe the space of QFTs. Within this framework, it is natural to

consider the limits of very large or very small energy scales. In some cases, these limits may be trivial, while in others, they may lead to a non-trivial, scale-invariant theory. In the context of statistical physics, it was recognised that these theories can be used to model second-order phase transitions in the continuum limit, where the correlation length of typical fluctuations diverges and scale invariance emerges. This applies both to statistical systems at finite temperature and to quantum many-body systems at zero temperature. A particularly interesting property of these scale-invariant theories is *universality*: second-order phase transitions in entirely different systems may be described by the same theory. Moreover, in most physically relevant cases, these scale-invariant theories turn out to be invariant under a larger spacetime symmetry group: the *conformal group*. Theories that are invariant under this group are known as *conformal field theories* (CFTs). Investigating the properties of CFTs provides deep insights into various aspects of statistical physics and condensed matter theory. Moreover, from a purely field-theoretical perspective, it has become clear that understanding CFTs is also essential to understanding QFTs, as most interesting QFTs are either conformal or correspond to points in the RG flow between CFTs. CFTs also have independent relevance in other formal aspects of theoretical physics, including the worldsheet description of string theory, the AdS/CFT correspondence, the study of dualities in QFTs, and more. For these reasons, the classification and characterisation of CFTs has become a long-term endeavour and remains one of the most active areas of research in modern theoretical physics.

One of the most notable approaches to the classification of CFTs is the *conformal bootstrap programme*. In brief, the aim of this programme is to study CFTs using very general principles, rather than focusing on specific models. The requirement that a CFT obeys conformal symmetry, together with other general assumptions–such as unitarity and locality–has proven to be so constraining that it allows for the derivation of a significant amount of information. The conformal bootstrap was initially applied to solve a particular family of CFTs in two dimensions: the *minimal models*, exploiting the fact that in two dimensions, the conformal group is infinite-dimensional [1]. More recently, thanks to the clever numerical implementations and the growth of computational power, and to the development of powerful new analytic techniques, the conformal bootstrap has also achieved remarkable results for CFTs in $d \geqslant 3$ dimensions [2–6]. The most celebrated of these results is the accurate numerical prediction of the critical exponents of the Ising and $O(N)$ models [7–9], which describe the critical behaviour of physically relevant statistical systems.

This thesis focuses on specific aspects of the broader endeavour to classify CFTs, using a variety of methods and techniques within the paradigm of the conformal bootstrap. More specifically, it investigates the behaviour of certain CFTs in the presence of extended excitations, known as *defects*. In fact, in recent years it has been recognised that QFTs should not be studied solely through the behaviour of their localised excitations, as it was initially believed, but that extended excitations must also be considered. The study of defects provides novel insights that contribute to the classification of QFTs. Defects are indeed powerful tools for exploring dualities and (generalised) symmetries, they give rise to novel observables, such as entropy-like quantities and order parameters for confining phases, and they also have direct phenomenological applications, as they describe impurities and boundaries in statistical systems [10–13]. Even more recently, the study of defects has merged with the conformal bootstrap philosophy, and investigating *conformal defects* (defects that are left invariant by a certain amount of conformal symmetry) within CFTs through symmetry constraints has become an independent, fertile, and rapidly developing line of research. For a partial list of reference see [14–27].

An important class of conformal defects, on which this thesis focuses, consists of those that can be realised in CFTs with internal $O(N)$ symmetry. The main example of the latter is the critical $O(N)$ model, although other examples, such as the free $O(N)$ field theory and the long-range $O(N)$ model, are also considered. The reason for this is twofold.
First, such theories are of great interest in statistical physics, as for different values of N, they describe the critical behaviour of a variety of physically relevant statistical systems. Examples include the liquid-vapour transition of water near the critical point and the phase transition of uniaxial magnets for $N = 1$, the helium superfluid transition for $N = 2$, and the ferromagnetic phase transition in isotropic magnets for $N = 3$. For this reason, much information about these CFTs is already available, providing a solid foundation for the analysis of conformal defects that these theories admit and their associated properties. Moreover, some defects in these models have already been considered in condensed matter theory [28–30].
Some of these defects may also have direct interpretations in terms of experimentally realisable systems. For example, the *magnetic impurity* discussed in Section 3.3 serves as a simple model for a two-dimensional doped quantum anti-ferromagnet. These systems are experimentally significant as they represent certain classes of high-temperature superconductors and spin-gap insulators [29]. The *localised magnetic field* defect introduced in Section 3.2 could also be realised experimentally

for $N = 1$ by immersing an elongated cylindrical colloidal particle in a critical classical binary mixture of liquids [31]. Other defects considered in this thesis, such as *transdimensional* defects and those in the long-range $O(N)$ model, although lacking direct experimental realisation at present, remain of considerable interest. On the one hand, they may find experimental interpretations in the future, and on the other hand, they provide new models in which general techniques for studying defects can be developed.

Second, the $O(N)$ model and its defects admit a simple Lagrangian description in terms of N scalar fields, which allows for the computation of observables using techniques such as the ε-expansion and the large-N expansion [32, 33]. These expansions play a crucial role in the application of analytic bootstrap techniques, which become particularly powerful when combined with them. Moreover, the ability to compute observables using Lagrangian techniques also provides a series of useful consistency checks for the results of the bootstrap analysis. Nevertheless, despite the simple Lagrangian formulation, defects in $O(N)$ and similar models exhibit a wide variety of consistent defects with particularly rich dynamics. This allows for the investigation of important questions such as the consequences of symmetry breaking of internal symmetries, the non-perturbative existence of non-trivial defects in certain regimes, the relationship between bulk and defect operators, and many others.

1.2 Main results and structure of the thesis

The primary goal of this thesis is to introduce and discuss selected topics on conformal defects in CFTs with $O(N)$ internal symmetry. Assuming only basic knowledge of QFTs, the main concepts of CFTs, the conformal bootstrap, and conformal defects are introduced. Moreover, some of the techniques widely used in current research are developed and applied, with an overview of the relevant literature provided along the way. The ideas and tools introduced will then be employed to discuss the content of the following original research works:

- [34] L. Bianchi, D. Bonomi and E. de Sabbata, "Analytic bootstrap for the localized magnetic field," JHEP **04** (2023), 069
- [35] L. Bianchi, D. Bonomi, E. de Sabbata and A. Gimenez-Grau, "Analytic bootstrap for magnetic impurities," JHEP **05** (2024), 080
- [36] E. de Sabbata, N. Drukker and A. Stergiou, "Transdimensional Defects," arXiv:2411.17809 [hep-th]

- [37] L. Bianchi, L. S. Cardinale and E. de Sabbata, "Defects in the long-range O(N) model," arXiv:2412.08697 [hep-th]

Summary of the results

It is worth emphasising the original results achieved in each of the works mentioned above. Articles [34] and [35] aims at advancing the current understanding of known conformal defects in CFTs through the efficient computation of new observables, using a powerful technique called *analytic bootstrap*. The practical application to specific models also serves as a demonstration of the validity and generality of these methods.

Article [34] focuses on a specific defect: the *the localised magnetic field* in the $O(N)$ model. The bulk two-point function of two fundamental fields in the ε-expansion is considered as the main observable. First, this two-point function is computed at one-loop using bootstrap techniques, with the only input being the anomalous dimension of a single bulk operator. The result is then employed to extract anomalous dimensions of defect operators and bulk-to-defect OPE coefficients, as presented in (4.34) and (4.49). The same observable is also used to compute the one-point function coefficients of bulk operators, as presented in (4.54). Some technical issues related to low-spin ambiguities are discussed, and several perturbative computations are performed to check the bootstrap results.

Article [35] follows a similar strategy for another defect in the $O(3)$ model: the *magnetic impurity*. The case in which the bulk is the free theory of N scalars is also considered. In this latter case, the beta-function is computed to three loops in the ε-expansion using perturbation theory, with the result presented in (3.45). Next, the lowest twist spectrum of the defect theory is carefully analysed in both the free and interacting bulk cases. A list of these operators, along with their quantum numbers and scaling dimensions, is provided in Tables 3.1 and 3.2. Subsequently, a bootstrap analysis of the bulk two-point function of two fundamental fields is performed. In the free bulk case, the correlator is determined at all orders in ε from this analysis. The result is given in (4.67) and (4.68), and is used to argue that in three dimensions (or at $\varepsilon = 1$), there is no fixed-point defect CFT. Finally, a bootstrap analysis of the interacting bulk case is also carried out, yielding the results at order ε^2 for the correlator and the related defect data, as presented in (4.102) and (4.103)–(4.108), respectively. Once again, several perturbative computations are performed to check the validity of the bootstrap results.

On the other hand, Articles [36] and [37] aim to construct new and interesting examples of conformal defects by generalising known constructions and introducing novel ones. These works focus on defects for specific bulk theories, such as the standard $O(N)$ model and its long-range version. However, the constructions can be generalised to other bulk theories and primarily serve as a proof of principle.

Article [36] introduces the concept of *transdimensional* defects. These are conformal defects with continuously adjustable dimensions. The idea is illustrated using the prototypical example of a symmetry preserving defect with dimension $p = 2+\delta$ in the $O(N)$ model in $d = 4-\varepsilon$ dimensions. By working to all orders in δ, it is possible to extrapolate to the cases $p = 3-\varepsilon$ and $p = 3$. The former represents a new symmetry preserving interface with low-lying spectrum presented in (5.28). In the latter case, by focusing solely on defect operators, a non-local three-dimensional CFT is obtained, with the conformal dimensions of the lightest operators given in (5.29) and (5.30). At $\varepsilon = 0$, the non-local three-dimensional CFT is described by generalised free fields with dimension $\hat{\Delta}_{\hat{\phi}} = 2$, and for $\varepsilon \neq 0$, a new interacting deformation of generalised free fields arises.
As another example, the $O(N)$ model in the range $4 \leqslant d \leqslant 6$ is considered in the large-N limit. It is known that there exists an $O(N)$-breaking line defect near $d = 4$ and an $O(N)$-breaking surface defect near $d = 6$. In Section 5.2 it is demonstrated that transdimensional defects can be used to interpolate between these two cases, and that the dimensions and bulk one-point function coefficients obtained analytically at large N in d match the expected results when expanded around $d = 4$ and $d = 6$.

Article [37] investigates the defects that can be realised in the long-range $O(N)$ model. Three different constructions are considered.
The first, presented in Section 6.2.1, involves the introduction of non-local defect degrees of freedom coupled to the bulk. One important consequence of this approach is that it enables the construction of non-trivial defects in generalised free field theory.
The second, discussed in Section 6.2.2, treats the non-locality of the model as a perturbation of the four-dimensional local theory. Several observables are computed using perturbation theory.
The third, presented in Section 6.2.3, is based on a semiclassical analysis that identifies new saddle-point solutions describing line defects. The implementation of perturbation theory around these saddles is also discussed.

Structure of the thesis

The thesis is structured as follows.

In Chapter 2, fundamental aspects of conformal field theories, conformal defects, and renormalisation group flows are reviewed. The review covers the main concepts and provides the essential references necessary for understanding the core results of the thesis. All the results in Chapter 2 are well-known in the literature.
In particular, Section 2.1 discusses the basics of conformal invariance and the conformal group, the consequences of these symmetries on correlators, the powerful product operator expansions, and the fundamental idea behind the conformal bootstrap.
Section 2.2 introduces conformal defects, and, in analogy with the previous section, discusses symmetries, their consequences on correlators, operator product expansions, and the defect version of the bootstrap.
In Section 2.3, basics aspects of renormalisation group flows, defect renormalisation group flows, and their fixed points are covered.

In Chapter 3, the critical $O(N)$ model and its conformal defects are examined. In Section 3.1, after a brief general introduction, the field theory construction of the $O(N)$ model is reviewed, with particular emphasis on the ε-expansion.
In Section 3.2, the localised magnetic field is considered, the computation of some basic observables is reviewed, and the first consequences of conformal invariance are analysed, laying the groundwork for a more refined bootstrap analysis.
Similarly, in Section 3.3, the magnetic impurity is discussed. Once again, the basic knowledge required for the bootstrap analysis is established. Moreover, a detailed analysis of the low-lying defect spectrum is carried out, following the presentation in [35].
For completeness, Section 3.4 describes other defects in the critical $O(N)$ model that are not analysed later using bootstrap methods. Some new perturbative results concerning a surface defect are presented, following the discussion in [36].

Chapter 4 is devoted to the introduction and application of analytic bootstrap techniques in the context of conformal defects.
In Section 4.1, the main tools, such as the Lorentzian inversion formulae and the dispersion relation, are briefly reviewed.
In Section 4.2, the analytic bootstrap is applied to the localised magnetic field, as presented in [34].
In Section 3.3, similar methods are employed for the magnetic impurity, following [35].

In Chapter 5, the construction of transdimensional defects is explored through two prototypical examples in the $O(N)$ model, following [36]. In particular, Section 5.1 examines the construction of a symmetry-preserving defect in the ε-expansion, while Section 5.2 focuses on a symmetry-breaking transdimensional defect in the large-N limit.

In Chapter 6, conformal defects in the long-range $O(N)$ model are investigated.
Section 6.1 provides a brief review of the long-range $O(N)$ model.
Section 6.2 discusses possible constructions of conformal defects in this long-range CFT, considering several possibilities, as presented in [37].

Finally, Chapter 7 briefly outlines potential directions for future research, stemming from both natural generalisations and direct applications of the techniques and concepts discussed in this thesis.

Chapter 2

Conformal field theory and defects

2.1 Conformal field theory

The study of Conformal Field Theories (CFTs) is a major line of research in modern theoretical physics. A deep understanding of CFTs is an essential tool to investigate quantum field theories beyond the perturbative regime and to understand properties of renormalisation group (RG) flows. Moreover, CFTs also have a wide-range of applications to other areas of high energy physics, most notably they provide a framework to study aspects of quantum gravity trough holography. Finally, they also provides deep insights into statistical physics and condensed matter theory, as universality classes of critical phenomena such as second-order phase transitions are typically described by CFTs.

A CFT is usually defined in physical terms as a QFT whose spacetime symmetries are described by the *conformal group*, an extension of the Poincaré group that includes transformations preserving angles (though not necessarily distances), which will be defined more precisely shortly. However, what is the exact definition of QFT itself is still a problem that has not yet received a conclusive answer. Several attempts have been made to provide axiomatic definitions, although none of them is unanimously thought to perfectly characterise the meaning of the word "QFT" as it is used in practice by physicists. In fact, as it will be better explained later, it seems more likely that a precise axiomatic definition of a CFT could be achieved by other means, for example through the bootstrap equations, without having to invoke a wide and still mathematically vague concept such as QFTs.

Nevertheless, as it is often the case in physics, starting with a raw list of abstract axioms is not the most insightful way to introduce an

idea. Consequently, in this review section, CFTs are presented as it is commonly done in the literature: by assuming that the reader already knows what a QFT is in a heuristic way. No attempt is made at mathematical rigour, nor at giving an original or exhaustive presentation of the concepts. The main purpose of this section is to fix notation and conventions, and to make the topics of this thesis more self-contained as possible. Several reviews and references to topics that are not covered are given throughout the section.

2.1.1 The conformal group

Given a (pseudo-)Riemannian manifold $\mathcal{M}$ with metric g,[1] the *conformal group* over $\mathcal{M}$ is defined as the set of *conformal transformations* from $\mathcal{M}$ to itself, where the group product is obviously given by composition. A *conformal transformation* is a diffeomorphism under which the metric transforms by collecting a space-dependent scale factor. Using coordinates such that $g(x) \equiv g_{\mu\nu}(x)dx^\mu dx^\nu$, for a conformal transformation $x \mapsto x'$ one has

$$g'_{\mu\nu}(x') = \frac{\partial x'^\mu}{\partial x^\rho}\frac{\partial x'^\nu}{\partial x^\sigma} g_{\rho\sigma}(x) = \Omega^2(x) g_{\mu\nu}(x)\,. \tag{2.1}$$

In practice, the effect of $\Omega^2(x)$ is to "stretch" distances at any point with different rates, but the transformation does not change angles between intersecting lines. It is often useful to introduce the infinitesimal version of conformal transformations: $x \mapsto x' = x + \varepsilon(x)$. Neglecting non-linear corrections, (2.1) becomes the conformal Killing equation

$$\nabla_\mu \varepsilon_\nu + \nabla_\nu \varepsilon_\mu = \frac{2}{d}\nabla_\rho \varepsilon^\rho g_{\mu\nu}\,, \tag{2.2}$$

where ∇ is the covariant derivative associated to the Levi-Civita connection.

For the purposes of studying CFTs, one can focus on the specific case $\mathcal{M} = \mathbb{R}^d$ (or $\mathbb{M}^d$) with the Euclidean (or Minkowskian) metric.[2] Moreover, the theories considered in this thesis are "higher dimensional" CFTs, that is to say, $d > 2$. Several reviews are available in the literature [38–44] . Of course two-dimensional CFTs are also of profound interest in theoretical physics, on the one hand because of their application to string theory, on the other hand because the conformal group becomes infinite-dimensional, allowing for extremely powerful methods that cannot be generalised to the higher-dimensional case. For modern

[1] More precisely, one should talk about an equivalence class $[g]$ of metrics, where two metrics are equivalent if and only if one is the product of the other with a positive smooth function (usually called conformal factor).

[2] Or any pair $(\mathcal{M}, g)$ that is conformally equivalent to these.

reviews of this topic see [45, 46] and references therein.

Setting $\mathcal{M} = \mathbb{R}^d$ with $d > 2$, equipped with the flat metric $g = \delta_{\mu\nu}dx^\mu dx^\nu$, it is possible to show that the most general solution to the conformal Killing equation (2.2) is

$$\varepsilon^\mu(x) = a^\mu + \omega^{\mu\nu}x_\nu + \lambda x^\mu + b^\mu x^2 - 2x^\mu(b\cdot x)\,. \tag{2.3}$$

The real constants a^μ, $\omega^{\mu\nu} = -\omega^{\nu\mu}$, λ, and b^μ correspond to translations, rotations, dilatations, and special conformal transformations, respectively. It is also possible to show that the most general infinitesimal conformal transformation (2.3) can be extended to a finite transformation that is globally defined.[3] For example, the finite version of special conformal transformation is

$$x'^\mu = \frac{x^\mu - b^\mu x^2}{1 - 2b\cdot x + b^2x^2}\,. \tag{2.4}$$

In (2.3), there are $\frac{1}{2}(d+2)(d+2)$ free real parameters. Indeed, it turns out that this group is isomorphic to $SO(d+1,1)$ (or $SO(d,2)$ in the Minkowskian case). This will become evident in the next section, by looking at the algebra generated by infinitesimal transformations. There is yet another interesting global conformal transformation that does not belong to the component connected to the identity of the conformal group: the inversion. This discrete transformation is

$$x'^\mu = \frac{x^\mu}{x^2}\,, \tag{2.5}$$

and it squares to the identity. Together with inversion, the conformal group becomes $O(d+1,1)$ (or $O(d,2)$ in the Minkowskian case). Not all CFTs are necessarily invariant under inversion.[4] On the other hand, any scale-invariant theory that is also invariant under inversion must be fully conformally invariant, since it can be shown that special conformal transformations are translations conjugated by inversion.

2.1.2 The conformal algebra

The conformal Killing vector fields (2.3) with the Lie brackets form a Lie algebra: the *conformal algebra*. A standard basis of this Lie algebra is given by the following generators

$$\begin{aligned} P_\mu &= -i\partial_\mu\,, & M_{\mu\nu} &= i(x_\mu\partial_\nu - x_\nu\partial_\mu)\,,\\ D &= -ix^\mu\partial_\mu\,, & K_\mu &= -i(2x_\mu x^\nu\partial_\nu - x^2\partial_\mu)\,. \end{aligned} \tag{2.6}$$

[3] Strictly speaking, finite conformal transformation are well defined on the conformal compactification of $\mathbb{R}^d$ (or $\mathbb{M}^d$), see [47] for more details.

[4] In fact, inversion can be obtained from parity by conjugation with $SO(d+1,1)$ transformations. Therefore, any parity-violating CFT also breaks inversion.

These generators obey the following commutation relations

$$\begin{aligned}
&[P_\mu, M_{\nu\rho}] = i\delta_{\mu\nu}P_\rho - i\delta_{\mu\rho}P_\nu\,,\\
&[M_{\mu\nu}, M_{\rho\sigma}] = i\delta_{\mu\rho}M_{\nu\sigma} - i\delta_{\nu\rho}M_{\mu\sigma} + i\delta_{\nu\sigma}M_{\mu\rho} - i\delta_{\mu\sigma}M_{\nu\rho}\,,\\
&[D, P_\mu] = iP_\mu\,, \qquad [D, K_\mu] = -iK_\mu\,,\\
&[K_\mu, M_{\nu\rho}] = i\delta_{\mu\nu}K_\rho - i\delta_{\mu\rho}K_\nu\,,\\
&[P_\mu, K_\nu] = -2i(\delta_{\mu\nu}D + M_{\mu\nu})\,,
\end{aligned} \tag{2.7}$$

and all the other commutators are vanishing. The first two lines are the commutation relation of the Poincaré algebra. Hence, the conformal algebra is an extension of the Poincaré algebra. An interesting observation is that P_μ, $K_{\mu\nu}$ and D form a closed subalgebra. Therefore, it is in principle possible for a theory to be invariant only under this subalgebra generated by Poincaré generators and dilatations, breaking special conformal transformations. Understanding the conditions under which a theory can be scale invariant but not fully conformally invariant is a problem that has been extensively studied. For relevant works on this topic, including recent developments, see [48–51]. To see that the algebra (2.7) is isomorphic to $\mathfrak{so}(d+1,1)$, one can define

$$\begin{aligned}
&L_{\mu,\nu} = M_{\mu\nu}\,, \qquad && L_{-1,\mu} = \frac{P_\mu - K_\mu}{2}\,,\\
&L_{0,\mu} = \frac{P_\mu + K_\mu}{2}\,, \qquad && L_{-1,0} = D\,,
\end{aligned} \tag{2.8}$$

with $L_{AB} = -L_{BA}$, and check that these generators indeed satisfy the desired commutation relations.

2.1.3 Representation theory

In a QFT that is invariant under conformal symmetry, it is natural to expect that the algebra (2.7) is realised as an operator algebra acting on the Hilbert space of the theory. This raises the problem of determining the possible infinite-dimensional representations of the conformal algebra (which must also be unitary in Minkowskian theories). One approach is to exploit the fact that the conformal algebra is $\mathfrak{so}(d+1,1)$ by considering its action on an "extended" space $\mathbb{M}^{d+2}$ rather than the physical space $\mathbb{R}^d$. In this higher-dimensional setting, conformal transformations act linearly, leading to the embedding space formalism [52–54].

Alternatively, it is possible to tackle this problem directly. For a conformal transformation $g \in SO(d+1,1)$ that acts as $x \overset{g}{\mapsto} x'(x)$, one expects that there is an operator U_g that implements this transformation at the level of the Hilbert space. The operator U_g also acts

naturally on the local operators of the theory $\mathcal{O}^a(x)$ by conjugation. Assuming that there is an invariant vacuum $|0\rangle$, one expects that [5]

$$U_g \mathcal{O}^a(x) U_g^{-1} = T_g^{ab}(x') \mathcal{O}^b(x') \,. \tag{2.9}$$

The above equation essentially means that, since a conformal transformation relates the points x and x', a state created by acting with $\mathcal{O}^a(x)$ on the vacuum $|0\rangle$ should equivalently be expressible as a linear combination of states created by acting with $\mathcal{O}^b(x')$ on $|0\rangle$. Moreover, at the level of correlators, Ward identities impose the following symmetry condition [55]

$$\begin{aligned} &\langle \mathcal{O}_1^{a_1}(x_1) \dots \mathcal{O}_n^{a_n}(x_n) \rangle = \\ &\qquad = T_g^{a_1 b_1}(x_1') \dots T_g^{a_n b_n}(x_n') \, \langle \mathcal{O}_1^{b_1}(x_1') \dots \mathcal{O}_n^{b_n}(x_n') \rangle \,, \end{aligned} \tag{2.10}$$

for distinct points $x_1, \dots, x_n$.
To find out what are the possible matrices $T_g^{ab}(x)$ in (2.9), it is convenient to look at the little group of conformal transformations that preserves the origin $x = 0$. The method is analogous to the one commonly used to construct representations of the Poincaré group (see for example [56]). At the level of the algebra, such transformations are $M_{\mu\nu}$, D, and K_μ. The action of conformal transformation on operators inserted at an arbitrary point x can then be recovered using the fact that translations act as

$$e^{ix^\mu P_\mu} \mathcal{O}^a(0) e^{-ix^\mu P_\mu} = \mathcal{O}^a(x) \,, \tag{2.11}$$

together with the commutation relations (2.7). It is natural to pick a basis of local operators $\mathcal{O}^a(0)$ that diagonalise the dilatation operator

$$[D, \mathcal{O}^a(0)] = i\Delta_{\mathcal{O}} \mathcal{O}^a(0) \,, \tag{2.12}$$

where $\Delta_{\mathcal{O}}$ is some real number called *conformal dimension*. The eigenvalue needs to be imaginary to ensure the correct action of the dilatation operator, as it will become clear at the end of the construction (for example, in (2.16)).
By using the commutation relations (2.7), it is easy to see that the operator $K_\mu \mathcal{O}^a(0)$ has conformal dimension $\Delta_{\mathcal{O}} - 1$. Therefore, by repeatedly acting with $K_{\mu_1}, \dots, K_{\mu_n}$, one could obtain an operator with arbitrarily low conformal dimension. Since in physically relevant theories conformal dimensions are always bounded from below, this process

[5] Clearly, for a Lorentzian theory, the operator U_g must also be unitary to ensure a consistent probabilistic interpretation. However, this requirement does not apply in the Euclidean case. In fact, in the statistical physics interpretation of Euclidean field theory, there is no intrinsic notion of an inner product. See also the discussion in Section 2.1.5.

must terminate at some point. Hence, there must exist operators such that

$$[K_\mu, \mathcal{O}^a(0)] = 0\,. \tag{2.13}$$

Such operators are called *primary operators*.[6] From a primary operator, one can define a tower of *descendant operators* with increasing conformal dimensions by acting with momentum generators. For example, for a primary $\mathcal{O}(0)$ of dimension $\Delta_\mathcal{O}$, the descendant operator $P_{\mu_1} \dots P_{\mu_n}\mathcal{O}(0)$ has dimension $\Delta_\mathcal{O} + n$.
Without loss of generality, one can also assume that primary operators $\mathcal{O}^a(0)$ transform in an irreducible representation of the Lorentz group generated by $M_{\mu\nu}$. That is to say

$$[M_{\mu\nu}, \mathcal{O}^a(0)] = (S_{\mu\nu})^{ab}\,\mathcal{O}^b(0)\,. \tag{2.14}$$

Once the conformal dimension and the representation with respect to the Lorentz group of a primary operator $\mathcal{O}^a(0)$ inserted at the origin is known, (2.11) can be used to determine the action of the full conformal algebra on $\mathcal{O}^a(x)$. The result is

$$\begin{aligned}
&[P_\mu, \mathcal{O}^a(x)] = -i\partial_\mu \mathcal{O}^a(x)\,,\\
&[M_{\mu\nu}, \mathcal{O}^a(x)] = \big(i(-x_\mu\partial_\nu + x_\nu\partial_\mu)\delta^{ab} + (S_{\mu\nu})^{ab}\big)\mathcal{O}^b(x)\,,\\
&[D, \mathcal{O}^a(x)] = i(x^\mu\partial_\mu + \Delta_\mathcal{O})\mathcal{O}^a(x)\,,\\
&[K_\mu, \mathcal{O}^a(x)] = -\big(i(2x_\mu\Delta_\mathcal{O} + 2x_\mu x^\nu\partial_\nu - x^2\partial_\mu)\delta^{ab} + 2x^\nu(S_{\nu\mu})^{ab}\big)\mathcal{O}^b(x)\,.
\end{aligned} \tag{2.15}$$

Finally, by exponentiating the action of the infinitesimal transformations, one finds that of finite conformal transformations. This is a tedious but in principle straightforward computation. For example, in the case of a scalar primary operator $\mathcal{O}(x)$, one finds

$$U_g\mathcal{O}(x)U_g^{-1} = \left|\frac{\partial x'}{\partial x}\right|^{\frac{\Delta_\mathcal{O}}{d}} \mathcal{O}(x')\,, \tag{2.16}$$

where $|\partial x'/\partial x|$ is the determinant of the Jacobian of the conformal transformation $x \mapsto x'$. Similarly, it is possible to derive transformation laws for tensors or spinors, and for descendant operators as well.

2.1.4 Correlators and Ward identities

Once transformation rules of primary operators such as (2.16) are known, they can be used to impose constraints on the correlators of the theory trough Ward identities (2.10). For example, Ward identities coming from translational and scale invariance can be used to show that

[6] In two-dimensional CFTs these operators are called *quasi-primaries*.

one-point functions of primary operators are always vanishing, unless the operator has conformal dimension $\Delta = 0$. In general, in a CFT the only operator with vanishing dimension is the identity operator.

For two-point functions of scalar primary operators, Poincaré and scale invariance impose that the correlator must take the form

$$\langle \mathcal{O}_1(x_1)\mathcal{O}_2(x_2)\rangle = \frac{\mathcal{N}_{\mathcal{O}_1\mathcal{O}_2}}{|x_1 - x_2|^{\Delta_1+\Delta_2}}\,, \tag{2.17}$$

where Δ_1 and Δ_2 are the conformal dimensions of the operators. Furthermore, the Ward identity for special conformal transformations impose that either $\Delta_1 = \Delta_2$ or the correlator is vanishing. By choosing a suitable basis of primary operators and normalising them, it is possible to conclude that

$$\langle \mathcal{O}_1(x_1)\mathcal{O}_2(x_2)\rangle = \frac{\delta_{\mathcal{O}_1\mathcal{O}_2}}{|x_1 - x_2|^{2\Delta_1}}\,. \tag{2.18}$$

It is worth noting that the vanishing of two-point functions of primaries with different dimensions can serve as an indication of full conformal invariance in scale-invariant theories [57].

In the case of three-point functions of three scalar primaries, exploiting all the Ward identities still yields a completely fixed kinematics

$$\langle \mathcal{O}_1(x_1)\mathcal{O}_2(x_2)\mathcal{O}_3(x_3)\rangle = \frac{\lambda_{\mathcal{O}_1\mathcal{O}_2\mathcal{O}_3}}{x_{12}^{\Delta_1+\Delta_2-\Delta_3} x_{13}^{\Delta_1+\Delta_3-\Delta_2} x_{23}^{\Delta_2+\Delta_3-\Delta_1}}\,, \tag{2.19}$$

where $x_{ij} = |x_i - x_j|$. The coefficient $\lambda_{\mathcal{O}_1\mathcal{O}_2\mathcal{O}_3}$ is physical, since the freedom in the normalisation of operators has already been used in (2.18).

Starting from four-point functions, Ward identities do not completely fix the kinematics of the correlator. The main reason is that with four points x_1, x_2, x_3, and x_4, it is possible to construct the *conformal cross-ratios*

$$u = \frac{x_{12}^2\, x_{34}^2}{x_{13}^2\, x_{24}^2}\,, \qquad v = \frac{x_{14}^2\, x_{23}^2}{x_{13}^2\, x_{24}^2}\,. \tag{2.20}$$

These cross-ratios are invariant under the action of the full conformal group. In the case of four scalar primaries, the most general form of the four-point function is

$$\langle \mathcal{O}_1(x_1)\mathcal{O}_2(x_2)\mathcal{O}_3(x_3)\mathcal{O}_4(x_4)\rangle = \frac{F(u,v)}{\prod_{i<j} x_{ij}^{\Delta_i+\Delta_j-\Sigma_k\Delta_k/3}}\,, \tag{2.21}$$

where $F(u,v)$ is an arbitrary function.

Similar statements apply to correlators of primaries that belong to other representations of the Lorentz group. Again, two-point functions are completely fixed, three-point functions are fixed up to a finite number of physical coefficients, and four-point functions depend non-trivially on conformal cross ratios. For more details see [52]. For example, for normalised identical spin-one operators one has

$$\langle \mathcal{O}^\mu(x_1)\mathcal{O}_\nu(x_2)\rangle = \frac{I^\mu_\nu(x_1-x_2)}{x_{12}^{\Delta_\mathcal{O}}}\,, \tag{2.22}$$

where $I^\mu_\nu(x_1-x_2) = \delta^\mu_\nu - 2x^\mu x_\nu/x^2$. An interesting point is that in CFTs conserved operators typically have protected conformal dimensions. For example, for a conserved current $\partial_\mu J^\mu(x) = 0$, (2.22) can be used to show that $\Delta_J = d-1$. Similarly, for the conserved stress-energy tensor $\partial_\mu T^{\mu\nu}(x) = 0$, one finds that $\Delta_T = d$. Note that this is also expected from dimensional analysis, since T^{00} has the physical interpretation of an energy density. A final remark is that, while conformal invariance uniquely determines the two-point function of the stress-energy tensor, the correlator still carries physical information in the form of a real constant. This is because the stress-energy tensor is a physical quantity, leaving no freedom in its normalisation.

2.1.5 Radial quantisation

So far, the discussion has focused on operators without specifying the relevant Hilbert space on which they act. In the quantisation of Poincaré-invariant theories defined on $\mathbb{M}^d$, the standard approach is to assign a Poincaré-invariant vacuum state $|0\rangle$ and construct an Hilbert space by acting on it with local operators.[7] Moreover, invariance under time translations gives rise to a one-parameter family of unitary time evolution operators $U(t) = e^{iHt}$ which can be used to evolve local operators according to

$$\mathcal{O}(t,x) = U(t-t')\mathcal{O}(t',x)U^{-1}(t-t')\,. \tag{2.23}$$

A key assumption is that states created by acting on the vacuum with the algebra of local operators at any fixed time t can be used to span the entire Hilbert space of the theory.[8] To specify the inner product, it is sufficient to declare all the local operators to be Hermitian

[7] More generally, one can also consider states created by the action of non-local operators. This is precisely what occurs in the case of defects, which will be explored in Section 2.2.

[8] Strictly speaking, this picture is somewhat naive. To construct well-defined states, quantum operators need to be smeared. However, in interacting theories, smearing only across space rather than spacetime may not be sufficient [58]. Nonetheless, this viewpoint provides a useful operational intuition for the present discussion.

$\mathcal{O}(t,x) = \mathcal{O}^\dagger(t,x)$, and the vacuum to be unit-normalised $\langle 0|0\rangle = 1$. The correlators of the theory are defined as time-ordered vacuum expectation values of local operators. For example, a two-point function is defined as

$$\begin{aligned}&\langle \mathcal{O}(t,x)\mathcal{O}'(t',x')\rangle = \\ &\quad = \theta(t-t')\langle 0|\mathcal{O}(t,x)\mathcal{O}'(t',x')|0\rangle + \big((t,x)\leftrightarrow(t',x')\big)\,.\end{aligned} \tag{2.24}$$

Note that this construction relies on choosing a foliation of $\mathbb{M}^d$ into fixed-time slices along a preferred time direction.

The framework of interest in this thesis is Euclidean CFTs. In this setting, it is natural to choose a different foliation, as there is no preferred time direction. One possible choice is to use a radial coordinate centred at the origin to foliate $\mathbb{R}^d$ into spheres $\mathbb{S}^{d-1}_r$ of increasing radii labelled by $r \in \mathbb{R}_+$, although this is not the only option. Note that the choice of the origin is somewhat arbitrary, just as the choice of a time direction in Minkowski space is arbitrary due to invariance under Lorentz boosts. The dilatation operator D provides a one-parameter family of operators such that

$$e^{i\lambda D}\mathcal{O}(x)e^{-i\lambda D} = \mathcal{O}(e^\lambda x)\,. \tag{2.25}$$

As before, it is assumed that states created by operators $\mathcal{O}(x)$ at any fixed radius $|x| = r$ acting on the vacuum span the entire Hilbert space. Correlators of the theory are defined as radially-ordered vacuum expectation values. The example of the two-point function is

$$\langle \mathcal{O}(x)\mathcal{O}'(x')\rangle = \theta(|x|-|x'|)\langle 0|\mathcal{O}(x)\mathcal{O}'(x')|0\rangle + (x\leftrightarrow x')\,. \tag{2.26}$$

Once again, specifying an inner product requires a notion of adjointness. This step is not essential in Euclidean CFTs, as it is not needed in their statistical physics interpretation. However, in some cases, such a product can still be defined, leading to interesting consequences. Assuming the existence of an inner product, one naturally expects that $D^\dagger = -D$, since its spectrum is purely imaginary.[9] Then, by taking the adjoint of (2.25) while sending $\lambda \to -\lambda$, it follows that

$$e^{i\lambda D}\mathcal{O}^\dagger(x)e^{-i\lambda D} = \mathcal{O}^\dagger(e^{-\lambda}x)\,. \tag{2.27}$$

[9] Although this choice may seem forced, there are some subtleties. In Lorentzian CFTs, the dilatation operator is Hermitian $D = D^\dagger$, even if its spectrum is imaginary. This phenomenon is related to the fact that the states $\mathcal{O}(0)|0\rangle$ are not normalisable [59]. A more careful analysis of this issue requires a precise definition of "spectrum" and the distinction between (essentially) self-adjoint operators and more general symmetric operators (see also [60]).

Therefore, the condition $\mathcal{O}^\dagger(x) = \mathcal{O}(x)$ cannot hold for any x. Instead, one can consistently take $\mathcal{O}^\dagger(x) = \mathcal{O}(\mathcal{I}(x))$, where $\mathcal{I}(x) = x/|x|^2$ denotes the inversion.[10] This also suggests that $P_\mu^\dagger = K_\mu$, since translations and special conformal transformations are conjugates under inversion. By requiring compatibility of the adjoint operation with the conformal algebra (2.7), one finds

$$D = -D^\dagger\,, \quad P_\mu^\dagger = K_\mu\,, \quad M_{\mu\nu}^\dagger = M_{\mu\nu}\,. \tag{2.28}$$

Theories for which an inner product satisfying (2.28) exists are said to be *reflection positive*.[11]

A key consequence of reflection positivity is the existence of *unitarity bounds*. These bounds constrain the possible values of the conformal dimensions of primary operators in different representations of the conformal group. They are derived by requiring the positivity of the norm of states of the form

$$|\psi\rangle = (\alpha P_\mu + \beta_{\mu\nu} P_\mu P_\nu + \dots)\mathcal{O}^a(0)|0\rangle\,. \tag{2.29}$$

For scalar operators, the unitarity bounds are

$$\begin{aligned} &\Delta_\mathcal{O} = 0 \quad \text{iff} \quad \mathcal{O} = \mathbb{1}\,, \\ &\Delta_\mathcal{O} \geqslant \frac{d-2}{2}\,. \end{aligned} \tag{2.30}$$

For spin-ℓ tensors, the bound is

$$\Delta_{\mathcal{O}_\ell} \geqslant d + \ell - 2\,. \tag{2.31}$$

Additionally, unitarity bounds impose constraints on three-point function coefficients. For example, one can show that the three-point function coefficient $\lambda_{\mathcal{O}_1\mathcal{O}_2\mathcal{O}_\ell}$ between two scalar primaries $\mathcal{O}_1$, $\mathcal{O}_2$, and a spin-ℓ tensor $\mathcal{O}_\ell$, must be real [61].

2.1.6 The operator product expansion

As mentioned in Section 2.1.5, a natural basis for the Hilbert space of states in the CFT is given by

$$\{\mathcal{O}_1(x_1)\dots\mathcal{O}_n(x_n)|0\rangle\}\,, \tag{2.32}$$

[10] More generally, one can choose $\mathcal{O}^\dagger(x) = \mathcal{O}(\alpha\mathcal{I}(x))$ for any nonzero constant α. This choice, however, can be undone by a dilatation.

[11] The choice of the name "reflection positivity" becomes more clear by doing a conformal transformation to cylindrical coordinates via $r = e^\tau$. The inversion $r \to 1/r$ becomes a reflection $\tau \to -\tau$. In this case, the statement of reflection positivity becomes exactly the Wick rotated version of unitarity for Lorentzian theories.

where $\mathcal{O}_k$ are either primary operators or their descendants, and with $|x_1| = \cdots = |x_n| = r$ for any positive r. It is interesting to consider the limit $r \to 0$, as the sphere $\mathbb{S}^{d-1}_r$ collapses to a single point. Since products of local operators at coincident points are generally ill-defined, it is reasonable to assume that the Hilbert space is fully spanned by the states

$$\{\mathcal{O}(0)|0\rangle\}\,. \tag{2.33}$$

In other words, by acting with the dilatation operator, products of operators as in (2.32) can be reduced to products of operators supported on an arbitrarily small sphere centered at the origin. As the radius of this sphere shrinks to zero, the resulting product is expected to define a local operator at $x = 0$. Then a natural assumption is that the algebra of local operators at the origin is complete, allowing it to generate all possible local operators constructed in this way. This establishes a connection between local operators inserted at the origin and states in the Hilbert space. This relationship is known as the *state-operator correspondence*. More precisely, it defines a one-to-one correspondence between primary operators $\mathcal{O}$ and states $|\Delta\rangle$ that are annihilated by the generator K_μ (referred to as primary states):

$$\begin{aligned} &[K_\mu, \mathcal{O}(x)] = 0 \quad \leftrightarrow \quad K_\mu|\Delta_\mathcal{O}\rangle = 0\,, \\ &|\Delta_\mathcal{O}\rangle = \mathcal{O}(0)|0\rangle\,, \quad D|\Delta_\mathcal{O}\rangle = i\Delta_\mathcal{O}|\Delta_\mathcal{O}\rangle\,. \end{aligned} \tag{2.34}$$

This correspondence extends naturally to descendant operators and their associated "descendant states".

The most important consequence of the state-operator correspondence is that it allows to prove the existence of a convergent operator product expansion (OPE). In a generic QFT, the product of two operators, in the limit where they approach each other, can be approximated by an (infinite) linear combination of local operators inserted at their midpoint. In a CFT, this idea can be formalised by reinterpreting it in terms of states. Consider two scalar operators, $\mathcal{O}_1$ and $\mathcal{O}_2$. A state can be defined by acting with these operators on the vacuum

$$|\psi_x\rangle = \mathcal{O}_1(x)\mathcal{O}_2(0)|0\rangle\,. \tag{2.35}$$

The state $|\psi_x\rangle$ can be expressed as sum over the basis given in (2.33)

$$|\psi_x\rangle \;=\; \sum_{\mathcal{O}\ \text{primaries}} C_\mathcal{O}(x,\partial_y)\mathcal{O}(y)\big|_{y=0}\,|0\rangle\,, \tag{2.36}$$

where $C_\mathcal{O}(x,\partial_y)$ is a polynomial in ∂_y that accounts for descendant states. The sum in (2.36) is convergent with respect to the usual ℓ^2

norm of Hilbert spaces. The expansion can be reformulated as a statement about operators

$$\mathcal{O}_1(x)\mathcal{O}_2(0) \;=\; \sum_{\mathcal{O}\ \text{primaries}} C_{\mathcal{O}}(x,\partial_y)\mathcal{O}(y)\big|_{y=0}\,. \tag{2.37}$$

The OPE in (2.37) is convergent when inserted into any correlation function, provided that no other operators are inserted at points x_k with $|x_k| < |x|$. The operators $\mathcal{O}$ appearing in the sum in (2.37) are said to be *exchanged* in the OPE between $\mathcal{O}_1$ and $\mathcal{O}_2$. An analogous OPE can be derived by expanding around a different point, with convergence inside correlation functions guaranteed, as long as no other operator insertions are closer to the expansion point than the two primaries. For more details about OPE convergence, see [62,63]. The coefficients $C_{\mathcal{O}}(x,\partial_y)$ are fully determined by requiring consistency with the conformal algebra in (2.7). For instance, in the case under consideration, it can be shown that for an exchanged scalar primary $\mathcal{O}'$, the coefficient $C_{\mathcal{O}'}(x,\partial_y)$ is given by

$$C_{\mathcal{O}'}(x,\partial_y) = \frac{\lambda_{\mathcal{O}_1\mathcal{O}_2\mathcal{O}'}}{|x|^{\Delta_{\mathcal{O}_1}+\Delta_{\mathcal{O}_2}-\Delta_{\mathcal{O}'}}}\left(1+\tfrac{\Delta_{\mathcal{O}_1}-\Delta_{\mathcal{O}_2}+\Delta_{\mathcal{O}'}}{2\Delta_{\mathcal{O}'}}x^\mu\partial_\mu+\dots\right)\,, \tag{2.38}$$

where the coefficient in the numerator matches the one in the three-point function in (2.19).

In general, the complete information required to reconstruct all the OPE coefficients between two primaries is encoded in the set of exchanged operators (along with the labels of their conformal representations) and the three-point function coefficients between the two primaries and the exchanged operators. For this reason, three-point function coefficients are often referred to as OPE coefficients. The key point is that, by repeatedly applying OPEs, it is possible to reduce any correlator of a CFT to infinite sums over two- and three-point functions. Once the conformal dimension (and spin) of each primary operator in a CFT is known, along with all the three-point function coefficients, the coefficients and terms of these sums are fully determined, at least in principle. Therefore, the complete information needed to reconstruct all correlators of local operators in a CFT is

$$\{(\mathcal{O},\Delta_{\mathcal{O}},\ell)\,,\ \lambda_{\mathcal{O}_1\mathcal{O}_2\mathcal{O}_3}\}\,. \tag{2.39}$$

This set is called *CFT data*.

2.1.7 The conformal bootstrap

The CFT data in (2.39) is not arbitrary. On the contrary, it must satisfy an infinite set of complicated constraints. For instance, OPEs

must be associative. In other words, given an n-point function, there are multiple ways to apply the OPE between pairs of operators to reduce it to sums of known terms. Clearly, the results of all such computations must agree. Other constraints, in addition to the associativity of the OPE, include the existence of special operators with protected dimensions (such as the stress-energy tensor in local theories and conserved currents for internal symmetries) and unitarity bounds for reflection-positive theories. In particular, in the case of $d = 2$, the enhanced infinite-dimensional conformal symmetry, together with unitarity, was successfully used to solve and classify a specific family of two-dimensional CFTs: the minimal models [1]. Although the situation is very different in CFTs with $d \geqslant 3$, one can still hope that constraints imposed by symmetry and consistency can be leveraged to extract useful information using methods that are similar in spirit. This idea leads to the *conformal bootstrap*, a programme designed to exploit these constraints to classify and compute the possible sets of consistent CFT data. A fundamental feature of this approach is that it does not rely on a Lagrangian formulation and is inherently non-perturbative.

To illustrate the central idea of the conformal bootstrap, consider the example of the four-point function of four identical scalar primaries $\mathcal{O}$. This correlator is given by (2.21), and since all the operators have the same conformal dimension it can be rewritten as

$$\langle \mathcal{O}(x_1)\mathcal{O}(x_2)\mathcal{O}(x_3)\mathcal{O}(x_4)\rangle = \frac{G(u,v)}{x_{12}^{2\Delta_\mathcal{O}} x_{34}^{2\Delta_\mathcal{O}}} \,. \tag{2.40}$$

Using the OPE (2.37) between the operators $\mathcal{O}(x_1)$ and $\mathcal{O}(x_2)$, and between $\mathcal{O}(x_3)$ and $\mathcal{O}(x_4)$, one obtains

$$G(u,v) = \sum_{\Delta',\ell'} \lambda^2_{\mathcal{O}\mathcal{O}\mathcal{O}'} \, G_{\Delta',\ell'}(u,v) \,, \tag{2.41}$$

where the sum runs over the exchanged primary operators $\mathcal{O}'$, which are labeled by their conformal dimension Δ' and spin ℓ'. The functions $G_{\Delta',\ell'}(u,v)$ are called *conformal blocks* and are given by

$$G_{\Delta',\ell'}(u,v) = x_{12}^{2\Delta_\mathcal{O}} x_{34}^{2\Delta_\mathcal{O}} C_{\Delta',\ell'}(x_{12},\partial_2) C_{\Delta',\ell'}(x_{34},\partial_4) \langle \mathcal{O}'(x_2)\mathcal{O}'(x_4)\rangle \,. \tag{2.42}$$

These blocks are entirely determined by conformal symmetry and are independent of the specific theory. They can be computed directly by exploiting the fact that they are eigenfunctions of the quadratic Casimir operator of the conformal algebra [2, 64, 65]. For $d = 1$ or even d, they are known in closed form. Otherwise, they can be expressed as

infinite sums whose coefficients satisfy a recursion relation [66].

An important observation is that in (2.40), one can exchange $\mathcal{O}(x_1)$ and $\mathcal{O}(x_3)$ since operators inside correlation functions are radially ordered and therefore always commute. In practice, this corresponds to swapping x_1 and x_3, which, at the level of the cross-ratios (2.20), amounts to exchanging u and v. As a result, the function $G(u, v)$ must satisfy the *crossing symmetry* condition

$$v^{\Delta_\mathcal{O}} G(u, v) = u^{\Delta_\mathcal{O}} G(v, u) \,. \tag{2.43}$$

By combining crossing symmetry (2.43) with the conformal block decomposition (2.41), one obtains the *bootstrap equations*

$$\sum_{\Delta', \ell'} \lambda^2_{\mathcal{O}\mathcal{O}\mathcal{O}'} \left(v^{\Delta_\mathcal{O}} G_{\Delta', \ell'}(u, v) - u^{\Delta_\mathcal{O}} G_{\Delta', \ell'}(v, u) \right) = 0 \,. \tag{2.44}$$

A crucial property is that the expansion coefficients $\lambda^2_{\mathcal{O}\mathcal{O}\mathcal{O}'}$ are always positive in reflection-positive CFTs. This plays a key role in the application of numerical techniques to analyse solutions to these equations. The bootstrap equations are often represented pictorially as follows

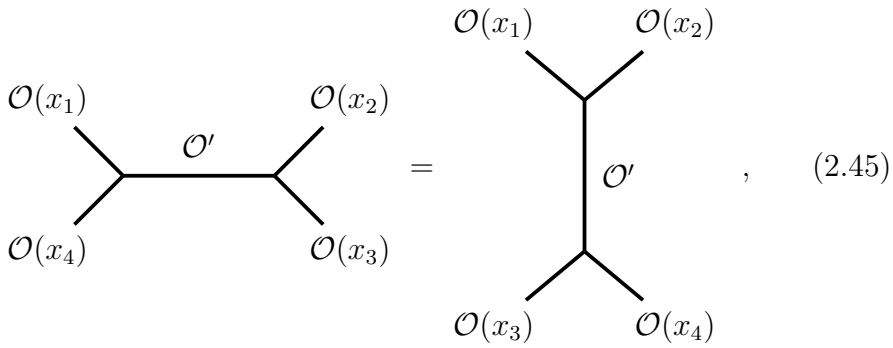

, (2.45)

where merging lines indicate that an OPE has been applied, and summation over the exchanged operators $\mathcal{O}'$ is implied. These equations constitute an infinite-dimensional nonlinear system that the CFT data must satisfy. Similar equations can be derived by considering non-identical operators as well as operators transforming under different representations of the conformal group. Moreover, one can extend this approach to correlators with $n \geqslant 4$ operator insertions.

The primary goal of the conformal bootstrap is to leverage the constraints imposed by the bootstrap equations (2.44) and their analogues to extract information about the CFT data. A major breakthrough in this direction came from the realisation that numerical techniques could be applied to the bootstrap equations to derive strong bounds on the

conformal dimensions of the lightest operators of the theory, without requiring an exact analytic solution [3]. This is the essence of the *numerical bootstrap*, which has led to remarkable non-perturbative results for strongly-coupled CFTs, with the prototypical example being the $3d$ Ising CFT [7–9]. For a detailed review of this topic, see [61]. Another important line of research has emerged from studying the analytic continuation of the bootstrap equations to Lorentzian signature. This has led to the development of powerful analytic techniques for extracting information about the CFT data. These techniques include taking specific kinematic limits [4, 5] or employing more refined methods such as inversion formulae or dispersion relations [6, 67, 68]. Collectively, these methods are referred to as *analytic bootstrap*. For a comprehensive review of these techniques, see [69].

As a final remark, it is important to note that, while the focus of this section has been on the study of correlators of local operators, these are not the only interesting observables in CFTs. For instance, correlators involving extended objects, such as line and surface operators, boundaries, and interfaces, are also of primary importance for a complete understanding of CFTs. This will be the main topic of Section 2.2.

2.2 Conformal defects

Extended operators, commonly referred to as *defects*, are essential objects in the study of QFTs, with a wide range of applications in both theoretical and phenomenological contexts. In statistical physics, they are used to describe inhomogeneous systems by modelling impurities, boundaries, and interfaces. From a more fundamental perspective, defects serve as probes of QFTs, offering new ways to analyse their structure. In particular, they give rise to novel observables, such as defect correlation functions and entropy-like quantities, which can help towards the characterisation and classification of these theories. A prototypical example of a defect is the Wilson line in gauge theories, whose expectation value serves as an order parameter for detecting confinement, a phase that is not easily characterised by conventional local observables [10]. More generally, defects are powerful tools for exploring dualities, renormalisation group flows, and (generalised) symmetries of QFTs. A notable case is the distinction between $SU(N)$ and $SU(N)/\mathbb{Z}_N$ pure Yang-Mills theories. The former possesses a global electric $\mathbb{Z}_N$ one-form symmetry, which is absent in the latter [13]. However, this difference cannot be detected by correlators of local operators alone; to distinguish between these theories, one must consider Wilson

lines.

This thesis focuses on *conformal defects*. In a CFT, defects can be understood as extended operators embedded within the theory, explicitly breaking conformal symmetry. A defect is called *conformal* if a "large" (in a sense that will be clarified shortly) subgroup of the conformal group leaves it invariant. This residual symmetry subgroup must also stabilise the submanifold on which the defect is supported. In CFTs on flat space, such submanifolds are typically either linear or spherical. Conformal defects are of great interest for several reasons. On the one hand, they can be studied using a theoretical framework analogous to that of CFTs, as introduced in Section 2.1. On the other hand, they have applications across various areas of physics. Many such applications arise in statistical physics: line defects describe point-like impurities in quantum statistical systems at criticality, boundaries capture finite-size effects, and interfaces model domain walls. Other examples can be found in high-energy theory: generalisations of straight or circular Wilson loops in superconformal gauge theories (both supersymmetric and non-supersymmetric) are conformal line defects. CFTs with boundaries provide an exact world-sheet description of D-branes in open string theory. CFTs with boundaries also admits an interesting holographic description [70]. Finally, CFTs with boundaries have also applications in the context of entanglement entropy, where they provide useful insights [71].

In this section, conformal defects are introduced according to the standard treatment in the literature. The aim is both to establish notation and to ensure self-containment. References to key articles and reviews are provided throughout.

2.2.1 Defect conformal symmetry

A conformal defect is an extended object that breaks the conformal group down to a non-trivial subgroup. A typical example is a CFT on a d-dimensional flat space, with a defect supported on a linear p-dimensional subspace. It is natural to choose coordinates such that $x = (x_\parallel, x_\perp) \in \mathbb{R}^d$, where $x_\parallel = (x_1, \dots, x_p)$ and $x_\perp = (x_{p+1}, \dots, x_d)$, with the defect $\mathcal{D}$ supported on $\{x : x_\perp = 0\}$. It is also useful to define the defect co-dimension $q = d - p$. First, any conformal transformation that does not preserve the defect's support is necessarily broken. Translations along the orthogonal directions $P_{p+1}, \dots, P_d$, are clearly broken, and the same applies to the orthogonal special conformal transformations $K_{p+1}, \dots, K_d$, as can be easily verified from (2.4). Rotations that mix orthogonal and parallel directions are also broken. The re-

maining translations, special conformal transformations, rotations, and the dilatation preserve the linear subspace defined by $x_\perp = 0$. It can be shown that the subgroup formed by these transformations is

$$SO(p+1,1) \times SO(q) \subset SO(d+1,1) \tag{2.46}$$

This group is the direct product of the conformal transformations on the p-dimensional defect and rotations around the defect, and it is usually referred to as the *defect conformal group* . One can verify that a spherical defect leads to the same pattern of symmetry breaking. The inversion in (6.31) also preserves the defect's support.[12]

A *conformal defect* is an extended operator that is invariant under the full defect conformal group, as given in (2.46). More precisely, if $T_a^{\mathcal{D}}$ are the operators that generate the representation of the defect conformal algebra $\mathfrak{so}(p+1,1) \oplus \mathfrak{so}(q)$ in the CFT's Hilbert space, a defect $\mathcal{D}$ is conformal provided that

$$[T_a^{\mathcal{D}}, \mathcal{D}] = 0\,, \quad \forall a\,. \tag{2.47}$$

The insertion of a conformal defect $\mathcal{D}$ modifies correlators of local operators, defining what is known as a *defect CFT* (dCFT). More generally, a dCFT is any theory whose correlation functions respect the spacetime symmetries of the defect conformal group. These correlators can be studied using techniques similar to those employed for an ordinary CFT (sometimes referred to as a homogeneous CFT) introduced in Section 2.1. The main concepts will be summarised in the following sections. Key references include the seminal articles [17, 72]; for a review of the main topics, see also [73].

As a side note, the term "conformal defect" is sometimes also used for extended operators that preserve a smaller subgroup than the one in (2.46). For example, by fusing two conformal defects, one can construct a new defect that breaks part of the transverse $SO(q)$ symmetry [74]. Nevertheless, such defects still share many properties with their "maximally symmetric" counterparts. Another example where the transverse $SO(q)$ symmetry is broken is provided by several superconformal line defects in superconformal field theories [75].

2.2.2 Correlators in the defect theory

In a dCFT, the defect conformal group imposes strong constraints on the correlators of local operators through Ward identities, much like in

[12] As mentioned earlier, the symmetries of a CFT may or may not include inversion. Even if they do, inversion may still be broken by the defect.

homogeneous CFTs. Before exploring these constraints, it is important to clarify what constitutes a local operator in a dCFT. Local operators fall into two categories: *bulk operators* and *defect operators*.

Bulk operators are those inserted at points a finite, non-zero distance from the defect (the term "bulk" refers to the region defined by $x_\perp \neq 0$). For instance, when dCFT correlators are defined as expectation values of the CFT in the presence of an extended operator, bulk operators correspond to the usual local operators of the CFT. Such operators are not defined at points lying on the defect due to short-distance singularities that typically arise in QFT when operators approach one another. In this case, bulk operators are organised into representations of the full conformal group $SO(d+1,1)$, and they are labelled by the conformal dimension Δ and spin ℓ. The situation differs slightly for monodromy defects, which will not be examined in this thesis.[13]

Defect operators, on the other hand, can only be inserted on the defect itself. They should be viewed as local modifications of the defect. They can also be constructed by renormalising the singularities that arise when a bulk operator approaches the defect. However, the resulting defect operator is not unique, as different renormalisation procedures may lead to different operators. Defect operators are classified according to representations of the defect conformal group $SO(p+1,1) \times SO(q)$. They are divided into *defect primaries* and *defect descendants*, and the former are characterised by the *defect conformal dimension* $\hat{\Delta}$ and *parallel spin* $\hat{\ell}$, which specify their representation under the p-dimensional conformal group, as well as the *transverse spin* s, which specifies their representation under $SO(q)$.[14]

Throughout this thesis, symbols with a hat are used exclusively to denote defect objects (such as observables, operators, quantum numbers, *etc*), while unhatted symbols refer to bulk objects. In terms of bulk, parallel, and transverse coordinates, $x = (x_\parallel, x_\perp)$ and $x = (\tau, x_\perp)$ are used interchangeably. Moreover, Greek indices run over all coordinates, *i.e.* $\mu = 1, \ldots, d$, while Latin indices are restricted to the orthogonal coordinates, *i.e.* $i = p+1, \ldots, d$. For example, $\mathcal{O}(x)$ is a bulk operator, whereas $\hat{\mathcal{O}}(x_\parallel)$ or $\hat{\mathcal{O}}(\tau)$ are defect operators.

[13] For completeness, a monodromy defect can be understood as the conformal boundary of a topological domain wall in a theory with a non-trivial internal symmetry group [76]. Each time a bulk operator crosses the topological domain wall, it transforms under a non-trivial element of the internal symmetry group. Thus, from an intuitive perspective, bulk operators are not necessarily ordinary local operators of the CFT but can also include local operators attached to a topological line ending on the domain wall.

[14] Note that for $p = 1$ there is no parallel spin $\hat{\ell}$, whereas for $q = 1$ there is no transverse spin s.

When the conformal defect is implemented by an extended operator $\mathcal{D}$, correlators are defined as normalised CFT expectation values

$$\langle \mathcal{O}_1(x_1) \dots \hat{\mathcal{O}}_n(\tau_n) \rangle_{\mathcal{D}} = \frac{\langle \mathcal{O}_1(x_1) \dots \hat{\mathcal{O}}_n(\tau_n) \mathcal{D} \rangle}{\langle \mathcal{D} \rangle} , \tag{2.48}$$

where the defect operators $\hat{\mathcal{O}}_k$ are either defined through a specific renormalisation procedure or are interpreted as local modifications of the defect $\mathcal{D}$. Correlators in (2.48) are normalised such that the identity operator has a unit expectation value, *i.e.* $\langle \mathbb{1} \rangle_{\mathcal{D}} = 1$. Since both the CFT vacuum and the defect $\mathcal{D}$ are invariant under the action of the defect conformal group, the defect correlator must satisfy Ward identities similar to those introduced in Section 2.1.3, but only for the unbroken symmetries. More generally, correlators in a dCFT are required to satisfy these Ward identities. Another property of defect correlators is that if only bulk operators are inserted, and they are sufficiently far from the defect, the correlator approaches that of the homogeneous CFT

$$\lim_{|(x_k)_\perp| \to \infty} \langle \mathcal{O}(x_1) \dots \mathcal{O}(x_n) \rangle_{\mathcal{D}} \to \langle \mathcal{O}(x_1) \dots \mathcal{O}(x_n) \rangle . \tag{2.49}$$

This can be interpreted as a defect analogue of the cluster decomposition principle.

One can follow the same approach as in Section 2.1.4 and use Ward identities to constrain correlators. First, correlators involving only defect operators are identical to those of a p-dimensional CFT, due to the $SO(p+1,1)$ conformal symmetry. From the perspective of defect operators, the $SO(q)$ symmetry acts as an internal symmetry. Therefore, once defect operators are properly normalised,[15] their two-, three-, and four-point functions take the same form as those in (2.18), (2.19), and (2.21), respectively, with dimensions and three-point function coefficients replaced by their hatted counterparts, $\hat{\Delta}_{\hat{\mathcal{O}}}$ and $\hat{\lambda}_{\hat{\mathcal{O}}_1 \hat{\mathcal{O}}_2 \hat{\mathcal{O}}_3}$.

The first difference from the case of homogeneous CFTs is that one-point functions of bulk operators are not necessarily zero. In fact, for a scalar operator Ward identities are satisfied as long as

$$\langle \mathcal{O}(x) \rangle_{\mathcal{D}} = \frac{a_{\mathcal{O}}}{|x_\perp|^{\Delta_{\mathcal{O}}}} , \tag{2.50}$$

[15] Some operators, such as the Displacement and Tilt operators introduced later in Section 2.2.3, cannot be freely normalised. In fact, as will be shown, their normalisation is already fixed by the bulk.

Since the operators are already normalised such that their two-point function approaches the one in (2.18) when they are far from the defect, the constant $a_{\mathcal{O}}$ contains physical information about the theory.

Operators with non-zero spin can also have a non-vanishing one-point function. For example, for a spin-two bulk operator, one has

$$\langle \mathcal{O}_{\mu\nu}(x)\rangle_{\mathcal{D}} = \frac{a_{\mathcal{O}}}{|x_\perp|^{\Delta_{\mathcal{O}}}}\left(J_{\mu\nu}(x) - \frac{q-1}{d}\delta_{\mu\nu}\right), \tag{2.51}$$

where

$$J_{ij}(x) = \delta_{ij} - \frac{x_i x_j}{|x_\perp|^2}, \tag{2.52}$$

and $J_{\mu\nu} = 0$ if any of the indices are parallel. For a co-dimension-one defect, *i.e.* $q = 1$, it is clear that the correlator vanishes identically. Moreover, (2.51) is consistent with the conservation condition $\partial^\mu \langle \mathcal{O}_{\mu\nu}(x)\rangle_{\mathcal{D}} = 0$ when $\Delta_{\mathcal{O}} = d$, which holds for a conserved spin-two current. Therefore, the stress-energy tensor for a dCFT with co-dimension $q \geqslant 2$ can have a non-zero one-point function.

Another interesting correlator is that between a bulk operator and a defect operator. For simplicity, consider the correlator between a bulk scalar $\mathcal{O}$ and a defect operator $\hat{\mathcal{O}}_s$, where the defect operator has transverse spin s and no parallel spin. Ward identities constrain this correlator to take the following form

$$\langle \mathcal{O}(x)\hat{\mathcal{O}}_s(0)\rangle_{\mathcal{D}} = \frac{b_{\mathcal{O}\hat{\mathcal{O}}}\ \hat{x}_\perp^s}{|x_\perp|^{\Delta_{\mathcal{O}}-\hat{\Delta}_{\hat{\mathcal{O}}}}|x|^{2\hat{\Delta}_{\hat{\mathcal{O}}}}}, \tag{2.53}$$

where $\hat{x}_\perp^s$ represents the only allowed traceless symmetric $SO(q)$ tensor structure:

$$\frac{x_{i_1}\dots x_{i_s}}{|x_\perp|^s} - (\text{traces}). \tag{2.54}$$

Since the normalisation of both defect and bulk operators has already been fixed, the coefficient $b_{\mathcal{O}\hat{\mathcal{O}}}$ is physically relevant.

As in the case of homogeneous CFTs discussed in Section 2.1.4, when more operator insertions are considered, the kinematics of correlators is no longer fixed, as it becomes possible to construct invariant cross-ratios. In a dCFT, this occurs in the case of the two-point function of two bulk operators. In fact, with two bulk points x ans y, it is possible to construct the *defect cross-ratios* z and $\bar{z}$ defined by

$$\frac{(1-z)(1-\bar{z})}{\sqrt{z\bar{z}}} = \frac{(x-y)^2}{|x_\perp||y_\perp|}, \qquad \frac{z+\bar{z}}{2\sqrt{z\bar{z}}} = \frac{x_\perp \cdot y_\perp}{|x_\perp||y_\perp|}. \tag{2.55}$$

These cross-ratios are invariant under the action of the defect conformal group. There is also a geometric interpretation of these cross-ratios: one can use conformal transformations that preserve the defect to place the two bulk points on a plane orthogonal to the defect and then move one of them to $(1,0)$ on this plane. In Euclidean signature, z and $\bar{z}$ are the complex coordinates for the second point on this plane. It is also useful to introduce radial coordinates r and w on the orthogonal plane, given by

$$z = rw, \quad \bar{z} = \frac{r}{w}\,. \tag{2.56}$$

In Euclidean signature, z and $\bar{z}$ are clearly complex conjugates of each other. Lorentzian signature can be accessed by allowing z and $\bar{z}$ to be independent real coordinates. In the special case of a boundary, it is straightforward to see from the second equation in (2.55) that there is only one independent cross-ratio, as $z = \bar{z} = r$.

The two-point function of two bulk scalars can be written in terms of an arbitrary function of the two defect cross-ratios

$$\langle \mathcal{O}_1(x)\mathcal{O}_2(y)\rangle_{\mathcal{D}} = \frac{F(z,\bar{z})}{|x_\perp|^{\Delta_{\mathcal{O}_1}}|y_\perp|^{\Delta_{\mathcal{O}_2}}}\,. \tag{2.57}$$

Further details on the kinematics of correlators in a dCFT can be found in [17, 72, 21, 23].

2.2.3 Displacement and Tilt operators

In a dCFT, there is a canonical operator associated with the explicit breaking of translational symmetries in the directions orthogonal to the defect: the *displacement operator* $\hat{D}^i$ [16]. This operator measures the non-conservation of the currents associated with the orthogonal translational symmetries, *i.e.* the orthogonal components of the stress-energy tensor

$$\partial^\mu T_{\mu i}(0, x_\perp) = -\hat{D}_i(0)\delta^{d-1}(x_\perp)\,. \tag{2.58}$$

The displacement operator is a primary operator and transforms as a vector under the $SO(q)$ symmetry, as can be seen in (3.87) (for $q = 1$, it is a scalar). Since the stress-energy tensor has conformal dimension $\Delta_T = d$, it follows from (3.87) that the displacement operator has protected dimension $\hat{\Delta}_{\hat{D}} = p + 1$. Importantly, this operator always exists in non-trivial dCFTs. Furthermore, the Ward identity in (3.87) fixes the normalisation of $\hat{D}^i$, which implies that the two-point function coefficient of the displacement operator contains physical information. The displacement operator also has a geometric interpretation: it measures the response of the partition function to an infinitesimal deformation

of the location of the defect. Additionally, there are interesting Ward identities that relate correlators with displacement insertions to those without. For more details see [17, 25].

A similar situation arises for internal symmetries of the homogeneous CFT that are broken by the presence of the defect. If the internal symmetry is broken to a subgroup $H \subset G$, there must be $(\dim G - \dim H)$ spin-one currents among the bulk operators, each corresponding to a broken generator. The conservation of these currents is spoiled by the defect

$$\partial^\mu J^a_\mu(0, x_\perp) = \kappa \hat{T}^a(0)\delta^{d-1}(x_\perp)\,, \tag{2.59}$$

where κ is a dimensionless constant that sets the normalisation of $\hat{T}^a$. The operators $\hat{T}^a$ are primary operators and are referred to as *tilt operators* [77,32].[16] According to (2.59), they have protected dimension $\hat{\Delta}_{\hat{T}} = p$. Interestingly, these operators are exactly marginal on the defect, hence they generate deformations of the dCFT that form a *defect conformal manifold*, which is isomorphic to the coset manifold G/H [78].

2.2.4 The defect OPE

In a dCFT, bulk operators can be brought close together and expanded using the same OPE as the one of the homogeneous theory (2.37). This OPE is usually referred to as the *bulk-to-bulk OPE*. Convergence is guaranteed in any disk that contains the two operators, provided it is not intersected by any other operator or by the defect. A similar OPE, called *defect-to-defect OPE*, also holds for any two defect operators, since defect operators form a p-dimensional CFT.

However, in a dCFT, a novel expansion is possible: a bulk operator can be brought close to the defect and expanded as a sum of defect operators. For a scalar bulk operator, this expansion, known as the *bulk-to-defect OPE*, takes the following form

$$\mathcal{O}(x) \;=\; \sum_{\hat{\mathcal{O}} \text{ primaries}} b_{\mathcal{O}\hat{\mathcal{O}}}\, \frac{\hat{x}_\perp^s}{|x_\perp|^{\Delta_\mathcal{O} - \hat{\Delta}_{\hat{\mathcal{O}}}}} \left(\hat{\mathcal{O}}_s(x_\parallel) + \text{descendants}\right), \tag{2.60}$$

where one can check that the coefficients match those of the bulk-to-defect two-point function (2.53) through an analysis similar to that in Section 2.1.6. The structure of the descendant terms, which are omitted in (2.60) for convenience, is entirely determined by defect conformal

[16] If the bulk current is conserved up to a descendant defect operator (which can be interpreted as a total derivative), it can be shown that the symmetry is not broken. In this case, symmetry charges can be exchanged between the bulk and the defect.

symmetry and is independent of the specific theory.

The three OPEs described in this section are all that is needed, in principle, to compute any correlator in the dCFT, as correlators with a large number of insertions can be expressed as infinite sums over correlators whose kinematics are completely determined. The complete information required to reconstruct all correlators in the dCFT consists of all bulk data (2.39), together with the following set

$$\{a_{\mathcal{O}}\,, b_{\mathcal{O}\hat{\mathcal{O}}}\,, (\hat{\mathcal{O}}, \hat{\Delta}_{\hat{\mathcal{O}}}, \hat{\ell}, s),\ \hat{\lambda}_{\hat{\mathcal{O}}_1\hat{\mathcal{O}}_2\hat{\mathcal{O}}_3}\}\,. \tag{2.61}$$

This set is known as the *defect data* and describes how the homogeneous CFT "interacts" with the conformal defect.

2.2.5 The defect conformal bootstrap

The defect data also needs to satisfy stringent constraints, much like the homogeneous CFT data. The main constraint once again arises from OPE associativity, as the same correlators can be expanded in different ways. This can be illustrated with the example of the bulk two-point function of two identical scalar primaries in the presence of a defect. From (2.53), it reads

$$\langle \mathcal{O}(x)\mathcal{O}(y)\rangle_{\mathcal{D}} = \frac{F(z,\bar{z})}{|x_\perp|^{\Delta_{\mathcal{O}}}|y_\perp|^{\Delta_{\mathcal{O}}}}\,. \tag{2.62}$$

The first way to expand this correlator is to take the OPE between the two bulk operators, and the result is a weighted sum over one-point function coefficients

$$F(z,\bar{z}) = \left(\frac{\sqrt{z\bar{z}}}{(1-z)(1-\bar{z})}\right)^{\Delta_{\mathcal{O}}} \sum_{\Delta',\ell'} \lambda_{\mathcal{O}\mathcal{O}\mathcal{O}'}\, a_{\mathcal{O}'} f_{\Delta',\ell'}(z,\bar{z}), \tag{2.63}$$

where the sum runs over exchanged primaries $\mathcal{O}'$, and the functions $f_{\Delta,\ell}(z,\bar{z})$, which encode the contributions from all descendants, are known as *bulk conformal blocks*. These functions are not generally known in closed form, but they are fully determined by defect conformal symmetry and they can be expressed as double infinite sums over hypergeometric functions [79]. These expansions are provided in Appendix A.

Alternatively, one can expand both bulk operators using the defect OPE and then take the expectation value. This leads to the following expansion

$$F(z,\bar{z}) = \sum_{\hat{\Delta},s} b^2_{\hat{\Delta},s}\, \hat{f}_{\hat{\Delta},s}(z,\bar{z})\,, \tag{2.64}$$

where the sum runs over defect primaries $\hat{\mathcal{O}}$, characterised by their dimension $\hat{\Delta}$ and transverse spin s. In the expansion (2.64), only operators with zero longitudinal spin contribute, as the two-point function of a bulk scalar and a defect operator with nonzero longitudinal spin ($\hat{\ell} \neq 0$) always vanishes. The functions $\hat{f}_{\hat{\Delta},s}(z,\bar{z})$ are known as *defect conformal blocks*. They can be explicitly computed by solving a Casimir eigenvalue equation [17] and they are given in Appendix A.

As in the homogeneous case discussed in Section 2.1.7, the two expansions (2.63) and (2.64) must be consistent with each other. This leads to the *defect bootstrap equations*, which can be pictorially represented as

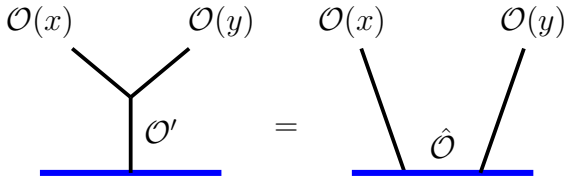

, (2.65)

where the blue line represents the defect $\mathcal{D}$. Similar equations can be derived for different bulk operators or for the three-point function involving two bulk operators and a defect operator. The constraints imposed by the defect bootstrap equations in (2.65), along with analogous equations, can be used to extract information about the dCFT data (2.61).

This leads to the formulation of the *defect bootstrap programme*, which aims to determine the set of all possible defect data (2.61) that consistently describe a defect embedded in a bulk theory characterised by a given set of CFT data (2.39). In general, this is an extremely challenging problem. The idea was first explored in the context of boundary CFTs, where the situation is somewhat simplified by the fact that there is only one independent defect cross-ratio. Both numerical and analytical approaches are possible.

On the numerical side, a straightforward generalisation of the conventional approach to the numerical bootstrap for CFTs (see the references in Section 2.1.7) is not feasible, as the coefficients in (2.63) are not generally positive, even for reflection-positive theories. Instead, an alternative method, originally developed for homogeneous CFTs [80,81], can also be applied to the study of boundary CFTs [15,82].

The analytic approach was similarly first developed for boundary CFTs [14,19,20]. In this case, the analytical techniques initially used to study homogeneous CFTs have been successfully generalised to dCFTs with

defects in arbitrary dimensions, leading to the development of both Lorentzian inversion formulae [18, 22] and dispersion relations [26, 27]. These methods are reviewed in Section 4.1 before being applied to specific instances of line defects in the $O(N)$ model.

2.3 RG flows and conformal fixed points

CFTs were introduced in Section 2.1 as QFTs whose spacetime symmetries are governed by the conformal group, and a formalism was presented to explore the consequences of such a powerful symmetry. However, it is natural to ask which QFTs can exhibit conformal symmetry and what physical situations these theories describe.

First of all, a CFT must be a scale-invariant theory, thus it cannot contain any dimensionful constants. Naively, as a first attempt, one could try to construct a scale-invariant QFT by introducing an action that involves only interactions with dimensionless couplings. However, this is not sufficient, as scales can often be dynamically generated in QFTs due to dimensional transmutation. This phenomenon is captured by the beta function

$$g_a \to g_a(\mu)\,, \quad \beta_{g_a}(g_b) = \mu \frac{dg_a}{d\mu}\,, \tag{2.66}$$

where μ is a mass scale that must be introduced to define the quantum theory, and g_a are the coupling constants of the theory, which acquire a non-trivial dependence on this scale. If any beta function is not identically zero, scale invariance is broken at the quantum level. This is the case for Yang-Mills theories, which are classically scale-invariant, but they break this symmetry through quantum corrections. A notable exception is $\mathcal{N} = 4$ Super Yang-Mills (SYM), where the large amount of supersymmetry ensures the vanishing of the beta function [83].

When the coupling constants of a QFT (2.66) exhibit a non-trivial dependence on the scale μ, the theory is said to undergo a *renormalisation group flow* (RG flow). In practice, all observables of the theory, such as correlation functions of local operators, also depend on the scale μ. It is interesting to consider the behaviour of the coupling constants (2.66) in the limit $\mu \to 0$, also known as the *infrared* (IR) limit. In the simple case of a single coupling constant, it can be shown that in the IR limit, either $g(\mu) \to \pm\infty$ or the coupling approaches a constant value, $g(\mu) \to g_*$, satisfying $\beta_g(g_*) = 0$ [84]. A similar statement holds in the *ultraviolet* (UV) limit, $\mu \to \infty$. More generally, this behaviour is also expected in the presence of multiple couplings: in the IR or

UV limits, the couplings either converge to a finite value that is a zero of the beta function, or they flow to infinity. When in the IR (UV) limit all couplings flow to finite values where all the beta functions vanish, the theory is said to flow to an IR (UV) *fixed point*. Indeed, the beta functions (2.66) define an autonomous system in the "time" $t = \log \mu$, whose fixed points correspond precisely to their zeros. At these fixed points, correlators are ensured to be scale-invariant by the Callan-Symanzik equation, which governs the RG flow. For a review of these topics see [84, 85]. An equivalent perspective is to consider correlators in the limit where the operators are inserted at large separations. These correlators exactly match those of the IR fixed point of the theory, as a dilation of the insertion points can be reformulated in terms of an inverse dilation of the energy scale.

Remarkably, correlators at the fixed points of RG flows in unitary, Poincaré-invariant theories are usually not only scale-invariant but they also exhibit an enhancement of spacetime symmetries to the full conformal group. This has been proven for two-dimensional QFTs [86, 48], and it has been argued to hold in $d = 4$ dimensions as well [50]. Fixed points where this occurs are said to be conformal. This fact provides an extremely useful tool for constructing examples of CFTs: it is often sufficient to construct an RG flow and look at its fixed points when they exist. In practice, one can begin with a free theory that does not have any dimensionful constants, which admits a description in terms of a classical action. This free theory is considered as a UV fixed point. To this action, S_{free}, one can add a local interaction in the following way [17]

$$S_{\text{free}} + \mu^{d-\Delta_{\mathcal{O}}} g \int d^d x \, \mathcal{O}(x) \,, \tag{2.67}$$

where $\mathcal{O}(x)$ is a composite operator with classical dimension $\Delta_{\mathcal{O}}$ constructed from fields of the free theory, and μ is a mass scale that must be introduced for dimensional reasons. If $\Delta_{\mathcal{O}} < d$, the operator $\mathcal{O}$ is said to be *relevant*, and it defines an RG flow with the free theory as its UV fixed point. Indeed, for small values of g, one has $\beta_g \sim (d - \Delta_{\mathcal{O}})g$, which implies that

$$g(\mu) \sim g_0 \left(\frac{\mu}{\mu_0} \right)^{\Delta_{\mathcal{O}} - d} , \tag{2.68}$$

leading to $g(\mu) \to 0$ in the UV limit as $\mu \to \infty$. One then needs to search for real solutions to $\beta_g(g_*) = 0$ other than $g = 0$. Such solutions indicate the presence of a non-trivial IR fixed point. The logic can also be reversed: starting from an IR free theory, one can

[17] More generally, one can add several interactions, each one with its own coupling constant.

add an interaction defined by an *irrelevant* operator with $\Delta_{\mathcal{O}} > d$, and search for non-trivial UV fixed points.

2.3.1 Defect RG flows

A similar strategy can be employed to construct dCFTs. Suppose one has successfully identified an IR conformal fixed point along an RG flow, triggered by the bulk action S_{bulk} given in (2.67). In addition to that, one can introduce another relevant interaction localised on a linear subspace of dimension p, which explicitly breaks Poincaré symmetry. However, this breaking occurs in a way that is, in principle, compatible with defect conformal symmetry

$$S_{\text{bulk}} + \mu^{p-\hat{\Delta}_{\hat{\mathcal{O}}}} h \int_{\mathcal{D}} d^p\tau \, \hat{\mathcal{O}}(\tau) \,, \tag{2.69}$$

where $\mathcal{D}$ is the p-dimensional support of the defect, and $\hat{\mathcal{O}}(\tau)$ is a composite operator with classical dimension $\hat{\Delta}_{\hat{\mathcal{O}}}$. In this case, as indicated by the exponent in (2.69), the operator is relevant if $\hat{\Delta}_{\hat{\mathcal{O}}} < p$. As with usual RG flows, the two couplings g and h will run with the scale μ, and both will become very small in the UV limit. This allows the use of standard perturbation theory to study this flow, known as *defect RG* flow, at least in the vicinity of the UV fixed point. First, correlators of operators that are far from the defect will not be affected by the new defect interaction. Consequently, the renormalisation of the *bulk coupling* g is independent of the *defect coupling* h. As a result, the beta function β_g will remain the same as it would without the defect interaction, and it will still have the same zero, g_*, as discussed in Section 2.3. On the other hand, the renormalisation of the defect coupling will depend on the bulk physics, hence the defect beta function will depend non-trivially on both bulk and defect couplings: $\beta_h = \beta_h(g, h)$. To have an IR fixed point in the defect RG flow, there must exist a real value h_* such that $\beta_h(g_*, h_*) = 0$. If an enhancement of spacetime symmetry similar to that discussed in Section 2.3 also occurs here, the correlators evaluated at this fixed point will correspond to those of a dCFT.

Defects obtained in this way are often called *order defects*. It is also possible to construct conformal defects by imposing boundary conditions in the path integral that are compatible with defect conformal symmetry. Such defects are known as *disorder defects*. Notable examples of disorder conformal defects include 't Hooft lines (when they are conformal) and monodromy defects. These defects will not be examined in this thesis.

A slightly more general way to obtain a defect RG flow is to couple a d-dimensional theory with a p-dimensional theory that lives on a linear subspace and allows them to interact. The theories do not need to be free, and the analysis is similar to that carried out in the previous case. In this scenario, standard perturbation theory cannot be applied to study the defect RG flow; however, conformal perturbation theory can be used instead.

Finally, it is important to note that many properties of standard RG flows also hold for defect RG flows. A particularly notable one is the irreversibility property: this essentially states that it is not possible to start from a CFT (or dCFT) and, through a series of (defect) RG flows, end up in the same CFT (or dCFT) one initially started with. From an intuitive perspective, each time a flow is followed from a UV theory to an IR theory, information about the short-distance behaviour of the theory is lost. This loss of information should be characterised by a quantity that monotonically decreases along the flow. This property has been proven for unitary homogeneous CFTs in various dimensions by identifying such a monotonic observable [86–88]. In the case of dCFTs, similar proofs have been established for line and surface defect RG flows.

For a line defect, the monotonically decreasing quantity is known as the *defect entropy* [24]. To define it, one must first introduce the g-function

$$\log g(\mu R) = \log \frac{Z_{\mathcal{D}_R}}{Z_0} \,, \tag{2.70}$$

where Z_0 and $Z_{\mathcal{D}_R}$ are the partition functions of the QFT and of the QFT with a circular defect $\mathcal{D}_R$ of radius R inserted, respectively. The function $g(\mu R)$ is essentially the expectation value of the defect $\mathcal{D}_R$ in the QFT, which depends non-trivially on the radius R. The g-function turns out to be scheme dependent due to possible cosmological constant counterterms of the form $\mu \int_{\mathcal{D}_R} d\tau$, which are linear in R. In $d > 2$, this is the only possible source of scheme dependence.[18] One can therefore define the scheme-independent defect entropy as

$$s(\mu R) = \left(1 - R\frac{\partial}{\partial R}\right) \log g(\mu R) \,. \tag{2.71}$$

Finally, it can be shown that $\frac{d}{d\mu} s(\mu R) < 0$ for reflection-positive theories, leading to the result

$$s_{UV} > s_{IR} \,. \tag{2.72}$$

[18] The result still holds for $d = 2$, modulo some additional technical details [24].

It is important to note that, for the computation of defect entropy, the defect must be defined on a circle rather than a straight line. Although the two configurations are conformally equivalent in a CFT, their expectation values differ due to the presence of a conformal anomaly [89].

For a surface defect, one can define the *defect free energy*

$$\mathcal{F}(\mu R) = \log \frac{Z_{\mathcal{D}_R}}{Z_0}\,, \tag{2.73}$$

where in this case $Z_{\mathcal{D}_R}$ is the partition function of the QFT with a spherical defect of radius R. It can be shown that at conformal fixed points, the defect free energy takes the form

$$\mathcal{F}(\mu R)\big|_{\text{dCFT}} = a_1 + a_2(\mu R)^2 - \frac{b}{3}\log(\mu R)\,, \tag{2.74}$$

where the coefficients a_1 and a_2 are scheme dependent, whereas b is universal. The coefficient b is related to the Weyl anomaly coefficient. Specifically, for a two-dimensional defect, the Weyl anomaly takes the form

$$T^{\mu}_{\ \mu}\Big|_{\text{defect}} = -\frac{1}{24\pi}\left(b\,\mathcal{R}_\Sigma + d_1\,K^{\mu}_{ab}K^{ab}_{\mu} - d_2\,W_{ab}{}^{ab}\right), \tag{2.75}$$

where $\mathcal{R}_\Sigma$ is the 2d Euler density, K^{μ}_{ab} is the traceless extrinsic curvature, and $W_{ab}{}^{ab}$ is the trace of the induced Weyl tensor on the surface Σ. The coefficient b decreases when flowing from a UV dCFT to an IR dCFT through a defect RG flow [16]

$$b_{UV} > b_{IR}\,. \tag{2.76}$$

Note that b is only defined at conformal fixed points, as (2.74) does not hold away from them. However, it is possible to define a function along the entire defect RG flow that coincides with b at fixed points and can be argued to decrease along the flow, although no non-perturbative proof has been found [90].

Chapter 3

The critical O(N) model and its defects

3.1 The critical O(N) model

A representative example of a CFT in $d > 2$ dimensions is the *critical* $O(N)$ *model*. One way to realise the critical $O(N)$ model as a CFT is to use the procedure outlined in Section 2.3: one can deform the four-dimensional free theory of N massless scalar fields by a quartic $O(N)$-invariant interaction and then follow the RG flow to the IR fixed point, as it will be explained in detail in Section 3.1.1. The most significant physical applications of these CFTs are in condensed matter physics, where they describe the universality classes of second-order phase transitions in various statistical systems. Notable examples include the Ising model for $N = 1$, the XY model and the helium superfluid transition for $N = 2$, and Heisenberg model and isotropic magnets for $N = 3$.

To illustrate this point, consider the Ising model, which is defined by the Hamiltonian

$$H_{\text{Ising}} = -J \sum_{\langle ij \rangle} \sigma_i \sigma_j - h \sum_i \sigma_i \,, \tag{3.1}$$

where the variables σ_i live on a lattice $\mathbb{Z}^d$ and take values ± 1. The first sum runs over nearest neighbours, and $J > 0$ is a positive constant. Given the Hamiltonian (3.1), the partition function can be defined as a function of the inverse temperature $\beta = 1/T$

$$Z(\beta) = \sum_{[\sigma]} e^{-\beta H[\sigma]} \,, \tag{3.2}$$

where the sum runs over all possible configurations of σ_i. Observables are given by functionals over the configuration space $\mathcal{O}[\sigma]$, and their

expectation value is defined by the normalised weighted sum

$$\langle \mathcal{O} \rangle_\beta = \frac{1}{Z(\beta)} \sum_{[\sigma]} \mathcal{O}[\sigma] e^{-\beta H[\sigma]} \,. \tag{3.3}$$

For $d = 1$, the Ising model does not exhibit any phase transition. For $d > 1$, the situation is more interesting, as the system develops a non-trivial phase diagram. In the plane of thermodynamic variables (β, h), there is a line of first-order phase transitions at $h = 0$ for $\beta > \beta_c$. This line terminates at the critical point $(\beta, h) = (\beta_c, 0)$, where a second-order phase transition occurs. In fact, one can show that the connected two-point function

$$G_\beta(n) = \langle \sigma_0 \sigma_{n\hat{e}} \rangle_\beta - \langle \sigma_0 \rangle_\beta \langle \sigma_{n\hat{e}} \rangle_\beta \,, \tag{3.4}$$

decays exponentially fast for $h = 0$ and $\beta < \beta_c$, where $\hat{e} \in \mathbb{Z}^d$ is a unit vector. However, the *correlation length*, defined as

$$\xi(\beta) = -\lim_{n \to \infty} \frac{n}{\log G_\beta(n)} \,, \tag{3.5}$$

diverges in the limit $\beta \to \beta_c$. A divergent correlation length is the hallmark of a second-order phase transition. At the critical temperature β_c, two-point functions at large distances decay as power laws, and correlators exhibit scale invariance due to the absence of a finite correlation length ξ. In the case of the Ising model (3.1), correlators at the critical temperature β_c and at large distances coincide with those of an Euclidean CFT known as the Ising CFT. In $d = 2$, the Ising model is exactly solvable [91], and the corresponding critical CFT belongs to the class of unitary minimal models [1]. For $d > 4$, the Ising CFT has long been known to be Gaussian [92,93]. A rigorous proof of Gaussianity for the Ising CFT in $d = 4$ was established more recently [94]. In $d = 3$, the Ising CFT is non-trivial, and its critical exponents (which are directly related to the conformal dimensions) are not known in closed analytic form. Various estimates of these exponents have been obtained through Monte Carlo simulations, the conformal bootstrap, and extrapolation from perturbation theory, see [95] for a comprehensive collection of results. Similar statements hold for the $O(N)$-symmetric generalisation of the Ising model.

The Lorentzian version of the $d = 3$ Ising CFT also has interesting applications. It describes phase transitions in quantum statistical systems in $2 + 1$ dimensions, and, in the large N limit, it has also been conjectured to be the holographic dual of a higher-spin Vasiliev gravity theory on AdS_4 [96].

3.1.1 The field theory description

The $O(N)$ model also admits a continuum description in terms of N scalar fields ϕ_a, with $a = 1, \ldots, N$. This is formulated through the Ginzburg-Landau action

$$S = \int d^d x \left(\frac{1}{2} (\partial_\mu \phi_a)^2 + \frac{m_0^2}{2} \phi_a \phi_a + \frac{\lambda_0}{4!} (\phi_a \phi_a)^2 \right), \tag{3.6}$$

which is manifestly $O(N)$ symmetric. For $N = 1$, it can be shown that the action (3.6) captures the long-range behaviour of the Ising model (3.1) near the critical temperature, provided that $m_0^2 \propto (\beta - \beta_c)$ (see [97] for a review).

To study the $O(N)$ model at criticality, the physical mass must be tuned to zero: $m^2_{\text{phys}} = 0$. As mentioned in Section 3.1, the most physically relevant dimension is $d = 3$. However, in this case, the quartic interaction term $(\phi_a \phi_a)^2$ is strongly relevant, making the study of the IR behaviour of the theory particularly challenging, as the theory becomes strongly coupled.

A possible solution to this problem is to use perturbation theory to obtain an asymptotic series for certain observables, followed by resummation techniques to extrapolate the results to strong coupling. For a fixed finite value of N, this can be done in two ways. One approach is to work directly in $d = 3$ (for example, using cutoff regularisation), while keeping a general mass term in (3.6), and only later tuning to the critical point [98]. Alternatively, one can work in $d = 4 - \varepsilon$ dimensions, treating ε as a small positive parameter and using dimensional regularisation. In this approach, the mass term can be omitted from the beginning, and the theory remains weakly-coupled, as the quartic interaction is only weakly relevant [99]. This allows observables to be computed as series expansions around $\varepsilon = 0$, which must then be extrapolated to $\varepsilon = 1$. The latter method, known as the *ε-expansion*, is the most widely used and will be employed extensively throughout this thesis. For a review of methods and results see [100]. Another important possibility is to work at fixed value of the dimension d, but in the limit $N \to \infty$. In this case, it is possible to develop a perturbative expansion in powers of $1/N$. The main advantage of this approach is that it allows to gain some analytical control over the dimension d, with the information extracted from this expansion being complementary to that obtained from the ε-expansion. For a review of the large-N limit, see [101]. Finally, it has recently been shown that it is also possible to use a "long-range" perturbation theory, in which both d and N can take arbitrary values. Instead, the expansion is taken in a new pa-

rameter that continuously connects the critical $O(N)$ CFT to a theory of non-local generalised free fields (GFF) [102]. This provides a third expansion, complementary to both the ε- and the large-N expansions. Some aspects of this long-range expansion are discussed in Chapter 6.

As it was anticipated, the focus of this thesis is mostly on the ε-expansion. Returning to the action (3.6), one can set $d = 4 - \varepsilon$. Since $d < 4$, the interaction becomes relevant and it triggers a renormalisation group flow. This flow can be studied perturbatively in λ_0. To renormalise the theory, dimensional regularisation and the minimal subtraction (MS) scheme will be used. The beta function of the renormalised coupling constant λ at two loops is given by

$$\beta(\lambda) = \mu \frac{d\lambda}{d\mu} = -\varepsilon\lambda + \frac{N+8}{48\pi^2}\lambda^2 - \frac{3N+14}{768\pi^4}\lambda^3 + \mathrm{O}(\lambda^4)\,, \tag{3.7}$$

where μ is the mass scale introduced in the renormalisation process. This flow admits the well known IR Wilson-Fisher fixed point [99], which describes a conformal field theory. This fixed point corresponds to the non-trivial zero of the beta function (3.7)

$$\lambda_* = \frac{48\pi^2}{N+8}\varepsilon + \frac{144\pi^2}{(N+8)^3}(3N+14)\varepsilon^2 + \mathrm{O}(\varepsilon^3)\,. \tag{3.8}$$

In the perturbative setup, the operators of this CFT are simply the renormalised versions of the local operators constructed using the bare fields. For example, the renormalised field $\phi_a(x)$ is given by

$$\phi_a(x) = Z_\phi \cdot (\phi_0)_a(x)\,, \tag{3.9}$$

where $(\phi_0)_a$ is the bare field and, in this case, the wavefunction renormalisation factor Z_ϕ is just a constant, as there is no operator mixing. The wavefunction renormalisation can be computed by imposing the finiteness of the correlators. In particular, at one loop, it is readily found that

$$Z_\phi(\lambda) = 1 + \mathrm{O}(\lambda^2)\,. \tag{3.10}$$

From the wavefunction renormalisation, the anomalous dimension of the field ϕ_a can be extracted as follows

$$\gamma_\phi(\lambda) = -\mu \frac{d\log Z_\phi}{d\mu} = -\beta(\lambda)\frac{d\log Z_\phi}{d\lambda} = 0 + \mathrm{O}(\lambda^2)\,. \tag{3.11}$$

The conformal dimension Δ_ϕ of the operator ϕ_a is [95]

$$\Delta_\phi = \frac{d-2}{2} + \gamma_\phi(\lambda_*) = 1 - \frac{\varepsilon}{2} + \mathrm{O}(\varepsilon^2)\,. \tag{3.12}$$

Note that, at this order, the conformal dimension exactly coincides with the engineering dimension of the bare field, as the anomalous dimension vanishes. The two-point function of the fundamental fields at the IR fixed point is given by

$$\langle \phi_a(x_1)\phi_b(x_2)\rangle = \frac{\mathcal{N}_\phi^2\,\delta_{ab}}{|x_1-x_2|^{2\Delta_\phi}}\,, \tag{3.13}$$

where the normalisation constant is

$$\mathcal{N}_\phi^2 = \frac{\Gamma\big(1-\frac{\varepsilon}{2}\big)}{4\pi^{2-\frac{\varepsilon}{2}}} + \mathrm{O}(\varepsilon^2)\,. \tag{3.14}$$

An important family of primary operators in this CFT, which will play a crucial role in the following sections, are the *twist-two* operators. The *twist* of a local operator $\mathcal{O}_{\Delta,\mu_1\ldots\mu_\ell}(x)$ with dimension Δ and spin ℓ is defined as $\tau = \Delta - \ell$. Twist-two operators are those with $\tau = 2 + \mathrm{O}(\varepsilon)$, and in the perturbative setup, they correspond to operators constructed from two fundamental fields ϕ_a. For $\ell \geqslant 1$, they can be interpreted as the renormalised versions of weakly broken higher-spin currents that are conserved in the UV free theory. Their explicit form, derived in [103], is given by

$$\begin{aligned} J^\alpha_{\mu_1\ldots\mu_\ell}(x) &= \mathcal{N}_\ell^R\, P^\alpha_{ab} \sum_{n=0}^{\ell} c_{\ell\,n}\, \partial_{\{\mu_1}\ldots\partial_{\mu_{\ell-n}}\phi_a\, \partial_{\mu_{\ell-n+1}}\ldots\partial_{\mu_\ell\}}\phi_b(x)\,, \\ c_{\ell\,n} &= \frac{(-1)^n}{n!\,(\ell-n)!\,\Gamma(n+\frac{d}{2}-1)\Gamma(\ell-n+\frac{d}{2}-1)}\,, \end{aligned} \tag{3.15}$$

where the brackets $\{\cdot\}$ denote traceless symmetrisation, and P^α_{ab} is a projector onto an irreducible representation R of $O(N)$, labelled by the index $\alpha = 1,\ldots,\dim R$. Since it involves only two indices, R can be either the singlet S, the symmetric traceless representation T, or the antisymmetric representation A. Moreover, from the structure of the coefficients $c_{\ell\,n}$, one can easily verify that for even (odd) ℓ, the sum in (3.15) is (anti-)symmetric in the indices a and b, implying that it is non-vanishing only for the representations S and T (A).
The factor $\mathcal{N}_\ell^R$ ensures that the two-point function of $J^\alpha_{\mu_1\ldots\mu_\ell}(x)$ is correctly normalised. The linear combination in (3.15) guarantees that these operators form a diagonal basis with respect to the dilatation operator, making them primary operators of the CFT.
In the spin $\ell = 0$ case, there are two such operators

$$\phi^2(x) = \mathcal{N}_0^S \phi_a\phi_a(x), \quad T_{ab}(x) = \tfrac{1}{2}\mathcal{N}_0^T\big(\phi_a\phi_b - \tfrac{\delta_{ab}}{N}\phi_c\phi_c\big)(x)\,. \tag{3.16}$$

Their anomalous dimensions appear at first order in ε and are given by

$$\gamma_{S,0} = \frac{N+2}{N+8}\varepsilon + \mathrm{O}(\varepsilon^2)\,, \quad \gamma_{T,0} = \frac{2}{N+8}\varepsilon + \mathrm{O}(\varepsilon^2)\,. \tag{3.17}$$

On the other hand, for spin $\ell \geqslant 1$, it can be shown (see *e.g.* [103]) that all anomalous dimensions vanish at first order in ε, and only appear at second order

$$\gamma_{R,\ell} = 0 + \mathrm{O}(\varepsilon^2), \quad \forall\, \ell \geqslant 1. \tag{3.18}$$

This fact will be crucial in Section 4.2, as bulk anomalous dimensions serve as the key input data required for the defect analytic bootstrap.

3.2 The localised magnetic field

A natural extension of this theory is obtained by turning on a magnetic field along a line, thus breaking the $O(N)$ symmetry down to $O(N-1)$ along the defect. This line defect, known as the *localised magnetic field*, can be effectively realised on a lattice and has been studied through Monte Carlo simulations in [28, 104]. Experimental applications are also conceivable, either in quantum simulators [105] or in a mixture of two liquids with a colloidal impurity [106, 107, 104]. Therefore, it is important to make predictions for the defect data of this critical system. Field-theoretical studies of certain observables, either in the large-N limit or via the ε-expansion, are available in [108, 109, 32]. In particular, [32] provides new results for certain observables in the ε-expansion, as well as a well-defined strategy for investigating the large-N regime, yielding consistent results across both expansions. In another study, this defect with $N = 3$ was examined using numerical bootstrap techniques to analyse the four-point function of defect operators [110]. Section 4.2 will show how the defect analytic bootstrap can be applied to this model to extract new results, following [26].

The localised magnetic field can be realised in the ε-expansion trough a perturbative defect RG flow by adding a weakly relevant defect interaction to the action (3.6)

$$S_{\mathcal{D}} = h_0 \int d\tau\, |\dot{x}(\tau)| \phi_1(x(\tau))\,, \tag{3.19}$$

where $x(\tau)$ describes a line defect $\mathcal{D}$ as the real parameter τ varies, and h_0 is the defect coupling constant. In particular, the case where $\mathcal{D}$ is a straight line (or equivalently, a circle) will be considered. This perturbation explicitly breaks the $O(N)$ global symmetry of the model down to $O(N-1)$. For the free theory in four dimensions, this perturbation provides a simple example of a conformal defect, as the operator ϕ has dimension exactly one, and h_0 is a defect marginal parameter [111]. As the system moves away from four dimensions, the bulk theory flows to the Wilson-Fisher fixed point, and the operator ϕ induces a weakly relevant defect deformation (the bulk dimension is $4-\varepsilon$, but the defect

dimension remains fixed at one). Therefore, this perturbation, along with the quartic interaction, triggers a renormalisation group flow in the two coupling constants. This joint flow can be studied using standard diagrammatic techniques without the need for a perturbative expansion in h_0, since any diagram contributing to a correlator at a fixed order in λ will involve an insertion of h_0 only up to a finite power. Thus, h_0 is not considered a small coupling constant.

To renormalise the theory, one possible approach is to define a renormalised defect coupling by $h_0 = \mu^{\frac{\varepsilon}{2}} Z_h h$, and require that the counterterms introduced by $Z_h = \sum_{i,j,k} c_{i,j,k} h^i \lambda^j / \varepsilon^k$ precisely cancel all the divergences in the one-point function of the renormalised bulk field $\langle \phi_1(x) \rangle_{\mathcal{D}}$. The relevant diagrams for this computation are

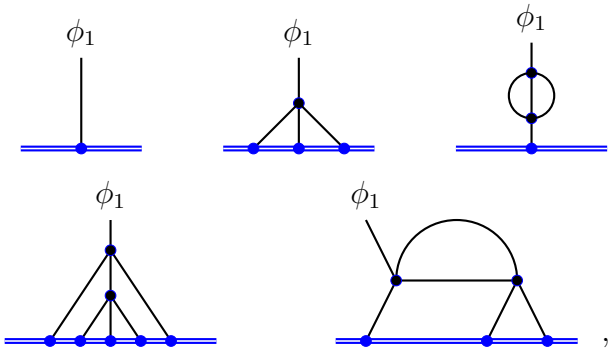

(3.20)

where the blue line represents the defect $\mathcal{D}$, the black lines represent free propagators, and the dots indicate defect and bulk interactions. Once Z_h has been determined, the beta function is obtained by requiring that the bare coupling is independent of the renormalisation scale, *i.e.* $\frac{d}{d\mu} h_0 = 0$. The result is [109, 32]

$$\beta_h = -\frac{\varepsilon h}{2} + \frac{\lambda h^3}{96\pi^2} + \frac{\lambda^2}{(4\pi)^4}\left(\frac{N+2}{36}h - \frac{N+8}{36}h^3 - \frac{h^5}{12}\right) + \mathrm{O}(\lambda^3)\,. \quad (3.21)$$

From (3.21) it follows that this flow admits an IR fixed point at $\lambda = \lambda_*$ and at the following value of the renormalised defect coupling constant [109, 32] [1]

$$h_* = \sqrt{N+8} + \frac{4N^2 + 45N + 170}{4(N+8)^{\frac{3}{2}}}\,\varepsilon + \mathrm{O}(\varepsilon^2)\,. \quad (3.22)$$

The defect perturbation explicitly breaks the conformal symmetry group $SO(d+1,1)$ of the system at the fixed point. Since the defect $\mathcal{D}$ is

[1] As noted in [32], to calculate the value of h_* to first order in ε, perturbations up to two loops must be considered. However, for the purpose of computing observables of the dCFT, the parameter of expansion is ε, and therefore results are not truncated at one or two loops, but rather at order one in ε.

chosen to be a straight line, the system remains invariant under the defect symmetry group $SO(2,1) \times SO(d-1)$, which is generated by conformal transformations on the line and rotations around the defect $\mathcal{D}$. This implies that the fixed point under consideration can be described by a (line) dCFT.

One of the simplest observables in this dCFT is the coefficient of the one-point function of the fundamental field $\phi_a(x)$, which was used to renormalise the theory

$$\langle \phi_a(x) \rangle_{\mathcal{D}} = \delta_{a1} \frac{\mathcal{N}_\phi \, a_\phi}{|x_\perp|^{\Delta_\phi}} \,, \tag{3.23}$$

with

$$a_\phi^2 = \frac{N+8}{4} + \frac{(N^2 - 3N + (N+8)^2 \log(4) - 22)}{8(N+8)} \, \varepsilon + \mathrm{O}(\varepsilon^2) \,. \tag{3.24}$$

An interesting fact is that the first non-trivial term in (3.24) can be computed through a semiclassical analysis by using the equation of motion (EOM) of the bulk fields and assuming a symmetry-breaking pattern $O(N) \to O(N-1)$, without the need to compute any Feynman diagrams or even formulate a defect action [37]. This is shown in Section 3.4.2.

As explained in Section 2.2.3, there are protected defect operators associated with the breaking of the $O(N)$ internal symmetry by the defect. The bulk currents associated with the broken generators are

$$J^\mu_{1\hat{a}}(x) = \phi_1 \partial^\mu \phi_{\hat{a}}(x) - \phi_{\hat{a}} \partial^\mu \phi_1(x) \,, \tag{3.25}$$

where $\hat{a} = 2, \ldots, N$ is an $O(N-1)$ index. The corrected Ward identity for these currents is

$$\partial_\mu J^\mu_{1\hat{a}}(0, x_\perp) = h_0 \, \hat{\phi}_{\hat{a}}(0) \delta^{d-1}(x_\perp) \,. \tag{3.26}$$

The $N-1$ tilt operators $\hat{\phi}_{\hat{a}}$ have protected dimension $\hat{\Delta}_{\hat{\phi}_{\hat{a}}} = 1$ [32]. These tilt operators provide exactly marginal deformations on the defect, which can be used to navigate the defect conformal manifold $O(N)/O(N-1) \cong \mathbb{S}_N$ [78].

Similarly, there is a displacement operator arising from the non-conservation of the stress-energy tensor in the directions perpendicular to the defect

$$\hat{D}_i(\tau) \sim \partial_i \hat{\phi}_1(\tau) \,, \tag{3.27}$$

with protected dimension $\hat{\Delta}_{\hat{D}} = 2$.

3.2.1 The bulk two-point function

A particularly interesting correlator in the localised magnetic field is the bulk two-point function of two fundamental fields, as it contains significant dynamical information about the dCFT. Conformal and global symmetries constrain this correlator to take the following form

$$\langle \phi_a(x)\phi_b(y)\rangle_{\mathcal{D}} = \frac{F_1(z,\bar{z})\delta_{ab} + F_2(z,\bar{z})\delta_{a1}\delta_{b1}}{|x_\perp|^{\Delta_\phi}|y_\perp|^{\Delta_\phi}}\,, \tag{3.28}$$

where the defect cross-ratios z and $\bar{z}$ have already been defined in (2.55). To obtain the block decompositions of the functions $F_1(z,\bar{z})$ and $F_2(z,\bar{z})$, it is convenient to first refine the OPE expansions in order to explicitly account for the structure of the internal symmetry of the theory.

For the bulk channel, the OPE of two operators transforming under the representations R_1 and R_2 of the internal symmetry group must contain exchanged operators in an irreducible representation that appears in the Clebsch-Gordan decomposition of $R_1 \otimes R_2$. In the case of the present model, for two fundamental scalar fields, the OPE can be written symbolically as

$$\phi_a(x)\phi_b(y) = \sum_{\Delta,\ell,R} \lambda^{ab\,\alpha}_{\phi\phi\mathcal{O}}\, |x-y|^{\Delta-2\Delta_\phi} \left(\mathcal{O}^{\alpha}_{\Delta,\ell}(y) + \text{descendants}\right), \tag{3.29}$$

where Δ_ϕ is the conformal dimension of the field ϕ. The conformal dimension and spin of the exchanged primary operator $\mathcal{O}^{\alpha}_{\Delta,\ell}$ are labelled by Δ and ℓ, respectively, and R denotes the $O(N)$ irreducible representations contained in the tensor product $V \otimes V$ of two vector representations V, *i.e.* the singlet S, the symmetric traceless T, and the antisymmetric A. The index α runs over $\alpha = 1, \ldots, \dim R$. In (3.29), spacetime indices have been suppressed. Since this is an OPE between scalar operators, only operators in even spin-ℓ traceless symmetric representations of $SO(d)$ can appear in the decomposition. The tensor structure of the three-point function coefficients $\lambda^{ab}_{\phi\phi\mathcal{O}_R}$ can be easily written down for $R = S, T, A$ as

$$\begin{aligned} &\lambda^{ab}_{\phi\phi\mathcal{O}_S} = \lambda_{\phi\phi\mathcal{O}_S}\delta^{ab}\,, \quad \lambda^{ab\,(cd)}_{\phi\phi\mathcal{O}_T} = \lambda_{\phi\phi\mathcal{O}_T}\left(\delta^a_{(c}\delta^b_{d)} - \tfrac{1}{N}\delta^{ab}\delta_{cd}\right)\,, \\ &\lambda^{ab\,[cd]}_{\phi\phi\mathcal{O}_A} = \lambda_{\phi\phi\mathcal{O}_A}\delta^a_{[c}\delta^b_{d]}\,, \end{aligned} \tag{3.30}$$

where the (anti-)symmetrization is taken with weight 1/2.

On the other hand, the operators appearing in the defect OPE will be organised into $O(N-1)$ representations, since the $O(N)$ symmetry is

explicitly broken by the defect. In general, if the symmetry group G is broken down to a subgroup H by the defect, and if a bulk operator belongs to the representation R of G, the operators exchanged in the defect OPE must transform in irreducible representations contained within the branching rule of the restricted representation $R^{(G)} \to R^{(H)}$. Therefore, the OPE can be written as

$$\phi_a(x) = \sum_{\hat{\Delta},s,R} b^{a\,\alpha}_{\phi\hat{\mathcal{O}}} |x_\perp|^{\hat{\Delta}-\Delta_\phi} \left(\hat{\mathcal{O}}^{\alpha}_{\hat{\Delta},s}(x_\parallel) + \text{descendants} \right), \tag{3.31}$$

where $\hat{\Delta}$ and s are the conformal dimension and the transverse spin of the defect operator $\hat{\mathcal{O}}^{\alpha}_{\hat{\Delta},s}$, respectively. Since $\phi_a(x)$ is a scalar, the operators exchanged in this OPE do not carry longitudinal spin. From the branching rule $V^{O(N)} \to S^{O(N-1)} \oplus V^{O(N-1)}$, it is immediately evident that the only allowed representations R are the singlet S and the vector V of $O(N-1)$. For these two representations, the tensor structures of the bulk-defect two-point function coefficients $b^{a\,\alpha}_{\phi\hat{\mathcal{O}}}$ are

$$b^{a}_{\phi\hat{\mathcal{O}}_S} = b_{S,\hat{\Delta},s}\delta^{a1}\,, \qquad b^{a\,\hat{b}}_{\phi\hat{\mathcal{O}}_V} = b_{V,\hat{\Delta},s}\delta^{a\hat{b}}\,, \tag{3.32}$$

where $\hat{b} = 2,\dots,N$, and δ^{a1} and $\delta^{a\hat{b}}$ are projectors from the representation space of $V^{O(N)}$ to those of $S^{O(N-1)}$ and $V^{O(N-1)}$, respectively.

These two different OPE decompositions lead to two distinct conformal block expansions. The first is the bulk block expansion. To analyse this, it is convenient to rewrite the bulk two-point function as

$$\langle \phi_a(x)\phi_b(y)\rangle_{\mathcal{D}} = \frac{F_S(z,\bar{z})\delta_{ab} + F_T(z,\bar{z})\left(\delta_{a1}\delta_{b1} - \frac{1}{N}\delta_{ab}\right)}{|x_\perp|^{\Delta_\phi}|y_\perp|^{\Delta_\phi}}\,, \tag{3.33}$$

where $F_S(z,\bar{z})$ and $F_T(z,\bar{z})$ are linear combinations of the functions $F_1(z,\bar{z})$ and $F_2(z,\bar{z})$ introduced in (3.28) (see (A.7)). This bulk channel decomposition is given by

$$\begin{aligned} &F_S(z,\bar{z})\delta_{ab} + F_T(z,\bar{z})\left(\delta_{a1}\delta_{b1} - \tfrac{1}{N}\delta_{ab}\right) = \\ &\quad = \left(\frac{\sqrt{z\bar{z}}}{(1-z)(1-\bar{z})}\right)^{\Delta_\phi} \sum_{\substack{\Delta,\ell \\ R=S,T}} \lambda^{ab\,\alpha}_{\phi\phi\mathcal{O}}\, a^{\alpha}_{\mathcal{O}}\, f_{\Delta,\ell}(z,\bar{z})\,, \end{aligned} \tag{3.34}$$

where the explicit form of the bulk conformal blocks $f_{\Delta,\ell}(z,\bar{z})$ was derived in [79] and is provided in Appendix A. It is important to note that the only bulk operators that can have a non-vanishing one-point function are those for which the identity operator appears as an exchanged operator in their defect OPE. Therefore, the allowed tensor structures

for the coefficients $a_{\mathcal{O}}^{\alpha}$ are obtained by projecting $O(N)$ representations onto the singlet $S^{O(N-1)}$. It immediately follows that operators in antisymmetric representations have a zero one-point function. For this reason, the sum in (3.34) is taken only over the singlet S and the symmetric traceless T representations of $O(N)$. The tensor structures of the one-point functions for $R = T, S$ are

$$a_{\mathcal{O}_S}\,, \quad a_{\mathcal{O}_T}^{(ab)} = a_{\mathcal{O}_T}\left(\delta^{a1}\delta^{b1} - \tfrac{1}{N}\delta^{ab}\right)\,. \tag{3.35}$$

Inserting (3.30) and (3.35) into (3.34) yields the following block decompositions

$$\begin{aligned} F_S(z,\bar{z}) &= \left(\frac{\sqrt{z\bar{z}}}{(1-z)(1-\bar{z})}\right)^{\Delta_\phi} \sum_{\Delta,\ell} \lambda_{\phi\phi\mathcal{O}_S} a_{\mathcal{O}_S} f_{\Delta,\ell}(z,\bar{z})\,, \\ F_T(z,\bar{z}) &= \left(\frac{\sqrt{z\bar{z}}}{(1-z)(1-\bar{z})}\right)^{\Delta_\phi} \sum_{\Delta,\ell} \lambda_{\phi\phi\mathcal{O}_T} a_{\mathcal{O}_T} f_{\Delta,\ell}(z,\bar{z})\,. \end{aligned} \tag{3.36}$$

In a similar manner, for the defect channel, it is useful to rewrite the bulk two-point function as follows

$$\langle \phi_a(x)\phi_b(y)\rangle_{\mathcal{D}} = \frac{\hat{F}_S(z,\bar{z})\delta_{a1}\delta_{b1} + \hat{F}_V(z,\bar{z})\,(\delta_{ab} - \delta_{a1}\delta_{b1})}{|x_\perp|^{\Delta_\phi}|y_\perp|^{\Delta_\phi}}\,, \tag{3.37}$$

where, once again, $\hat{F}_S(z,\bar{z})$ and $\hat{F}_V(z,\bar{z})$ are linear combinations of $F_1(z,\bar{z})$ and $F_2(z,\bar{z})$ as given in (A.7). The defect channel decomposition is

$$\hat{F}_S(z,\bar{z})\delta_{a1}\delta_{b1} + \hat{F}_V(z,\bar{z})\,(\delta_{ab} - \delta_{a1}\delta_{b1}) = \sum_{\substack{\hat{\Delta},s \\ R=S,V}} b_{\phi\hat{\mathcal{O}}}^{a\,\alpha} b_{\phi\hat{\mathcal{O}}}^{b\,\alpha}\, \hat{f}_{\hat{\Delta},s}(z,\bar{z})\,, \tag{3.38}$$

where the explicit form of the defect conformal blocks $\hat{f}_{\hat{\Delta},s}(z,\bar{z})$ is given in Appendix A. Using (3.32) one gets

$$\begin{aligned} \hat{F}_S(z,\bar{z}) &= \sum_{\hat{\Delta},s} b^2_{S,\hat{\Delta},s} \hat{f}_{\hat{\Delta},s}\,, \\ \hat{F}_V(z,\bar{z}) &= \sum_{\hat{\Delta},s} b^2_{V,\hat{\Delta},s} \hat{f}_{\hat{\Delta},s}\,. \end{aligned} \tag{3.39}$$

Everything stated so far applies at the non-perturbative level. However, further insights can be gained by examining the interplay between the block expansions (3.36) and (3.39) and the perturbative series. For example, consider the three-point function coefficients $\lambda_{\phi\phi\mathcal{O}}$. If the operator $\mathcal{O}$ is composed of an even number $2(k+1)$ of fundamental

fields, a straightforward diagrammatic argument immediately implies that this coefficient is at least of order k in ε.[2] In particular, at the first order in ε, only operators with $k = 0$ or $k = 1$ will contribute to the bulk block expansion of the functions $F_S(z, \bar{z})$ and $F_T(z, \bar{z})$. Moreover, only the anomalous dimensions of operators with $k = 0$ are relevant at this order, as only the classical dimensions of operators with $k = 1$ will contribute to the expansions. These kind of arguments will play a central role in Section 4.2, where the two block decompositions (3.36) and (3.39) will be used to extract defect data in the ε-expansion in an extremely efficient way through the defect analytic bootstrap.

3.3 The magnetic impurity

Another interesting line defect is the *magnetic impurity*, which can be constructed in the critical $O(3)$ model. Magnetic impurities were originally introduced in [29, 30] with the aim of modelling a doped two-dimensional anti-ferromagnet at the quantum critical point. More recently, there has been a renewed interest for these defects. In [112], they were analysed at large N with the long-term goal of understanding the interplay between symmetry protected topological phases and quantum criticality, whereas [33] found a semiclassical description for this defect in the limit of large spin. In [113], it was also noted how these defects emerge in a specific scaling limit of superconformal Wilson lines in $\mathcal{N} = 4$ SYM theory. In Section 4.3, the defect analytic bootstrap will be applied to investigate this model, as presented in [35].

Following [33], the line defect is represented by an extended operator, given by the trace of the following path-ordered exponential

$$\mathcal{D}_j(u, v) = \mathcal{P}\text{exp}\left(\frac{\zeta_0}{\sqrt{\kappa}}\int_u^v d\tau\, \phi^a(\tau) T_a\right), \tag{3.40}$$

where the factor

$$\kappa = \frac{\Gamma\left(\frac{d}{2}\right)}{2\pi^{d/2}(d-2)}, \tag{3.41}$$

is introduced for future convenience.
For compactness, $\phi_a(\tau) \equiv \phi_a(\tau, 0, \ldots, 0)$ is used. The focus will primarily be on the infinite defect $\mathcal{D}_j \equiv \mathcal{D}_j(-\infty, \infty)$, although occasionally it will be useful to consider the finite version given by (3.40). The matrices T^a form a spin-j representation of $\mathfrak{su}(2)$, or equivalently, they are

[2] In the case of an odd $2k + 1$ number, the coefficient simply vanishes due to representation theory reasons.

$(2j+1)\times(2j+1)$ matrices.[3] The matrices are normalised such that the commutation relations and Casimir operator satisfy

$$[T^a, T^b] = i\epsilon^{abc}T^c\,, \qquad T_aT_a = j(j+1)\,. \tag{3.42}$$

The defect $\mathrm{Tr}\mathcal{D}_j$ manifestly preserves the connected component of the $O(3)$ global symmetry, and consequently, it can be realised on the lattice by inserting a spin-j impurity that interacts with other lattice sites through $SU(2)$-preserving interactions.[4] The coupling ζ_0 is marginally irrelevant in four dimensions, but it becomes relevant for $d<4$, causing the system to flow to a non-trivial interacting dCFT in IR. Interestingly, this dCFT remains perturbatively non-trivial even when the bulk is tuned to the free-theory point $\lambda_0 = 0$. However, it will be shown in Section 4.3 using non-perturbative arguments that such a dCFT for the free bulk theory does not exist at the value $\varepsilon = 1$, or equivalently, $d = 3$.

3.3.1 Defect β-function for free and interacting bulks

For the magnetic impurities of interest, the β-function has been computed up to two loops in [114,115]. The procedure, as usual, is to select a specific observable and renormalise the coupling ζ_0 so that the result is UV-finite. Since the focus is on the UV behaviour of the theory for the purposes of renormalisation, a finite line defect $\tau \in [u,v]$ can be considered. The UV-finiteness condition is imposed on the vertex operator

$$\mathcal{V}(x) = \frac{\mathrm{Tr}\left\langle \phi_a(x)T^a\,\mathcal{D}_j(u,v)\right\rangle}{\mathrm{Tr}\left\langle \mathcal{D}_j(u,v)\right\rangle}\,, \tag{3.43}$$

where $\phi_a(x)T^a$ is inserted in the trace, but it is placed in a point x in the bulk.

Free bulk

Consider the case of a free bulk, where the bulk operator $\phi_a(x)$ does not renormalise. In this scenario, all the divergences in (3.43) can be

[3] Note that the Lie algebra isomorphism $\mathfrak{su}(2) \cong \mathfrak{so}(3)$ is what allows the construction of this defect. A straightforward generalisation of this defect for the $O(N)$ vector model is not possible; however, an analogous defect can be constructed for bulk scalars in the adjoint representation of $O(N)$. The defect action (3.40) also admits different representations which can lead to interesting generalisations, as it is explained in Appendix A of [37].

[4] Strictly speaking, in the definition of the defect, the trace is taken over the representations of $SU(2)$ rather than $O(3)$, in order to allow for half-integer values of j. At the level of the algebra, this distinction makes no difference. This subtlety will be ignored in the following, as it does not affect the results.

attributed to the renormalisation of the coupling ζ_0. The details of the computation are provided in Appendix B.2. Only the final result is presented here, which has been computed for the first time up to order ζ^7 in [35]. In the MS scheme, the relationship between the bare and renormalised coupling is given by

$$\zeta_0 = \mu^{\varepsilon/2}\zeta\left(1+\frac{\zeta^2}{\varepsilon}-\frac{\zeta^4}{2\varepsilon}+\frac{3\zeta^4}{2\varepsilon^2}+\frac{\zeta^6}{3\varepsilon}\left(2-\pi^2\left(j(j+1)-\frac{1}{3}\right)\right)\right.$$
$$\left.-\frac{11\zeta^6}{6\varepsilon^2}+\frac{5\zeta^6}{2\varepsilon^3}+\mathrm{O}(\zeta^8)\right). \tag{3.44}$$

From the usual condition that the bare coupling does not depend on the renormalisation scale μ, namely $d\zeta_0/d\mu = 0$, one extracts the beta function

$$\beta_\zeta = -\frac{\varepsilon}{2}\zeta+\zeta^3-\zeta^5+\left(2-\pi^2\left(j(j+1)-\frac{1}{3}\right)\right)\zeta^7+\dots \tag{3.45}$$

An interesting observation is that, starting at $\mathrm{O}(\zeta^7)$, the β-function depends on the spin j. This presents an obstacle towards the resummation of the perturbative series, even for the case of a free bulk. However, for large spin j, a double-scaling limit can be taken in which $\zeta \to 0$, $j \to \infty$, and $\zeta^2 j$ is kept fixed. The β-function in this limit was computed in [33], and the result of [35] presented in this section is in perfect agreement for large j. The fixed point equation $\beta(\zeta) = 0$ can be solved perturbatively in ε, leading to a defect fixed point for

$$\zeta_*^2 = \frac{\varepsilon}{2}+\frac{\varepsilon^2}{4}+\left(j(j+1)-\frac{1}{3}\right)\frac{\pi^2\varepsilon^3}{8}+\mathrm{O}(\varepsilon^4). \tag{3.46}$$

For $\varepsilon > 0$, a non-trivial fixed point exists, even though the bulk is free. The existence of this fixed point in three dimensions, *i.e.* for $\varepsilon \to 1$, was questioned in [33] based on a large spin analysis. In Section 4.3, it will be demonstrated that this fixed point is, in fact, trivial.

Interacting bulk

For an interacting bulk, pushing the calculation to higher orders in perturbation theory is more challenging due to the presence of diagrams with quartic bulk interactions. In the case of the interacting bulk, it is found (see appendix B.2.6) that

$$\zeta_0 = \mu^{\varepsilon/2}\zeta\left(1+\frac{\zeta^2}{\varepsilon}-\frac{\zeta^4}{2\varepsilon}+\frac{3\zeta^4}{2\varepsilon^2}+\frac{5\,\lambda^2}{72(4\pi)^4\varepsilon}+\frac{\left(j(j+1)-\frac{1}{3}\right)\zeta^2\lambda}{48\varepsilon}+\dots\right). \tag{3.47}$$

From this it is possible to extract the β-function [29, 30, 116]

$$\beta_\zeta = -\frac{\varepsilon}{2}\zeta + \zeta^3 - \zeta^5 + \frac{5}{36}\frac{\zeta\lambda^2}{(4\pi)^4} + \left(j(j+1) - \frac{1}{3}\right)\frac{\zeta^3\lambda}{24} + \dots \quad (3.48)$$

After setting the bulk coupling to the fixed-point value λ_*, one can solve perturbatively the equation $\beta_\zeta(\zeta_*, \lambda_*) = 0$, finding

$$\zeta_*^2 = \frac{\varepsilon}{2} + \varepsilon^2\left(\frac{29}{121} - \frac{\pi^2}{11}\left(j(j+1) - \frac{1}{3}\right)\right) + \mathrm{O}(\varepsilon^3)\,. \quad (3.49)$$

Notice that in the interacting theory, the dependence on j appears already at order ε^2. Moreover, it is also noteworthy that, both in the free and interacting bulk cases, the defect coupling constants at the fixed point, as given in (3.46) and (3.49), are perturbatively small. In contrast, in the case of the localised magnetic field discussed in Section 3.2, this was not the case, as can be seen in (3.22).

When the bulk and defect couplings are tuned to their fixed-point values, an interacting dCFT is obtained. While the bulk spectrum remains clearly unaffected by the presence of the defect, it is of interest to explore in greater detail how to characterise the defect operators. This is addressed in Section 3.3.3.

3.3.2 Correlators and discrete symmetries

In equation (3.40), the line defect is introduced through the path-ordering operation. Explicitly, this corresponds to the definition

$$\mathcal{D}_j(u,v) = \sum_{n=0}^{\infty}\frac{\zeta_0^n}{\kappa^{\frac{n}{2}}}\int_{u<\tau_1<\dots<\tau_n<v} d\tau_1\dots d\tau_n\;\phi_{a_1}(\tau_1)\dots\phi_{a_n}(\tau_n)\,T^{a_1}\dots T^{a_n}\,. \quad (3.50)$$

In particular, (3.50) allows to map correlators of the defect theory to those of the homogeneous theory. The simplest correlation functions in the presence of $\mathcal{D}_j$ involve insertions of bulk operators as follows

$$\langle \mathcal{O}_1(x_1)\dots\mathcal{O}_n(x_n)\rangle_{\mathcal{D}_j} = \frac{\langle \mathcal{O}_1(x_1)\dots\mathcal{O}_n(x_n)\,\mathrm{Tr}\,\mathcal{D}_j\rangle}{\langle\,\mathrm{Tr}\,\mathcal{D}_j\rangle}\,, \quad (3.51)$$

where recall that $\mathcal{D}_j = \mathcal{D}_j(-\infty,\infty)$ is the infinite length defect.

However, this is not the most general possibility. In fact, one can define operators $\hat{\mathcal{O}}(\tau)$ that live on top of the defect. As will become evident in Section 3.3.3, defect operators in this model can, in principle, be matrix-valued (with matrices having the same dimension as the

generators T^a). Therefore, for the most general correlators of defect operators, the path-ordering must be sliced as follows

$$\begin{aligned}\langle \hat{\mathcal{O}}_1(\tau_1)\dots\hat{\mathcal{O}}_n(\tau_n)\rangle_{\mathcal{D}_j} &= \\ &= \frac{\langle \mathrm{Tr}\left[\mathcal{D}_j(-\infty,\tau_1)\hat{\mathcal{O}}(\tau_1)\mathcal{D}_j(\tau_1,\tau_2)\hat{\mathcal{O}}(\tau_2)\dots\hat{\mathcal{O}}(\tau_n)\mathcal{D}_j(\tau_n,\infty)\right]\rangle}{\langle\,\mathrm{Tr}\,\mathcal{D}_j\rangle}\,.\end{aligned} \tag{3.52}$$

Note that defect operators are not necessarily matrix-valued. For example, with a single fundamental field ϕ one can build two distinct operators

$$\hat{\mathcal{O}}_1^a(\tau) = \phi^a(\tau,0,\dots)\,, \qquad \hat{\mathcal{O}}_2(\tau) = \phi^a(\tau,0,\dots)T_a\,. \tag{3.53}$$

When $\hat{\mathcal{O}}_1^a$ is inserted into correlation functions, it can be factored outside the trace, whereas $\hat{\mathcal{O}}_2$ is a matrix and thus interacts non-trivially with the trace. Many examples of defect operators are provided in Section 3.3.3.

An important point when dealing with defect correlators, is that they depend on the coordinate of a defect operator $\hat{\mathcal{O}}(\tau)$ also through the endpoints of the neighbouring defect operators $\mathcal{D}_j(\cdot,\tau)$ and $\mathcal{D}_j(\tau,\cdot)$, as it is clear by looking at the right hand side of (3.52). For this reason, it is convenient to introduce a defect covariant derivative

$$\mathcal{D}_j(u,\tau)\,D_\tau\hat{\mathcal{O}}(\tau)\,\mathcal{D}_j(\tau,v) \equiv \frac{d}{d\tau}\big(\mathcal{D}_j(u,\tau)\,\hat{\mathcal{O}}(\tau)\,\mathcal{D}_j(\tau,v)\big), \tag{3.54}$$

From this one readily finds

$$D_\tau\hat{\mathcal{O}}(\tau) = \partial_\tau\hat{\mathcal{O}}(\tau) + \frac{\zeta_0}{\sqrt{\kappa}}\phi^a(\tau)\big[T_a,\hat{\mathcal{O}}(\tau)\big]\,. \tag{3.55}$$

This covariant derivative is really analogous to the one introduced in the case of Wilson lines (see *e.g.* [117]).

Finally, it is possible to consider correlators that contain a mix of bulk and defect operators, and their correlators are given by the obvious generalisation of (3.51) and (3.52).

Once correlators have been properly defined, it is interesting to look at which discrete symmetries are preserved by the defect, because they imply selection rules, and they also help in the classification of defect operators. The bulk theory, both in the free and in the interacting case, is invariant under time reversal symmetry [5] and under a global

[5] In the context of defects, the inversion of the defect coordinate is also known as $\mathcal{S}$-parity [118, 76].

$\mathbb{Z}_2$ symmetry

$$\begin{aligned} T_t &: \phi^a(\tau, x_\perp) \mapsto \phi^a(-\tau, x_\perp)\,, \\ T_{\mathbb{Z}_2} &: \phi^a(\tau, x_\perp) \mapsto -\phi^a(\tau, x_\perp)\,. \end{aligned} \tag{3.56}$$

By a symmetry of the defect theory, one usually means that the correlators in the left hand side of (3.51) are invariant under the action of the symmetry generators. A sufficient condition for this to happen is that the generator of a symmetry of the homogeneous theory also leaves invariant the trace of the defect operator $\operatorname{Tr}\mathcal{D}_j$. This is exactly what happens to the $SU(2)$ global symmetry. On the contrary, the generators $T_{\mathbb{Z}_2}$ and T_t clearly modify the defect. It is straightforward to see that the net effect of $T_{\mathbb{Z}_2}$ is to change the sign of the defect coupling constant [112]

$$T_{\mathbb{Z}_2}\,\mathcal{D}_j^{\zeta} = \mathcal{D}_j^{-\zeta}\,, \tag{3.57}$$

where $\mathcal{D}_j^{\zeta}$ is the defect extended operator with coupling constant ζ. On the other hand, T_t flips the signs of the arguments of all the fields in (3.50). However, by a convenient change of integration variables and name redefinitions, this is equivalent to reversing the order of the generators inside the trace. For generators of representations of $\mathfrak{su}(2)$, the following relation holds [6]

$$\operatorname{Tr}\left(T^{a_n}\dots T^{a_1}\right) = (-1)^n \operatorname{Tr}\left(T^{a_1}\dots T^{a_n}\right)\,. \tag{3.58}$$

From this it follows that also T_t is tantamount to a change in the sign of the defect coupling constant

$$T_t\,\operatorname{Tr}\mathcal{D}_j^{\zeta} = \operatorname{Tr}\mathcal{D}_j^{-\zeta}\,. \tag{3.59}$$

At this point one can define a modified time reversal symmetry for the defect theory by asking that the fundamental fields are odd under this symmetry

$$\bar{T}_t = T_{\mathbb{Z}_2}\circ T_t : \phi^a(\tau, x_\perp) \mapsto -\phi^a(-\tau, x_\perp)\,. \tag{3.60}$$

Now, $\bar{T}_t$ is both a symmetry of the homogeneous theory and leaves $\operatorname{Tr}\mathcal{D}_j^{\zeta}$ invariant (it changes the sign of ζ twice). Therefore, it is also a symmetry of the defect theory. To obtain useful selection rules, it is necessary to understand how this symmetry acts on defect operators. This will be briefly discussed in section 3.3.3, after a general understanding of the defect operators in this model has been established.

[6] This is due to the facts that the generators T^a are taken to be Hermitean and that the $\mathfrak{su}(2)$ representation given by the complex conjugated generators $(T^a)^*$ is equivalent to the original one, so that $(T^a)^T = P\,T^a\,P^{-1}$ for some matrix P.

3.3.3 The defect spectrum

In this section, the spectrum of operators living on top of the magnetic impurity defect is studied, following the analysis presented in [35]. The motivation is that, for the efficient application of bootstrap techniques, it is helpful to know what defect operators can contribute to different OPE decompositions. It is useful to start from the free-bulk theory, because the spectrum is simpler and Ward identities protect several defect operators. When the bulk interaction is introduced in the ε-expansion, the dimension of these operators is modified by additional terms proportional to powers of λ_*, which is perturbatively small. This approach allows to understand the perturbative definition of these operators, which is surprisingly non-trivial in certain cases. This, in turn, provides insight into how to list all possible defect operators within perturbation theory.

The defect spin operator

As pointed out in [33], an interesting Ward identity is obtained by considering the shift of the fields $\phi_a(x) \to \phi_a(x) + c_a$ for some constants c_a. This is a symmetry of the free-bulk theory without the defect. The Noether currents for these symmetries are $J_a^\mu(x) = -\partial^\mu \phi_a(x)$, and their conservation is equivalent to the equations of motion since $0 = \partial_\mu J_a^\mu(x) = -\Box \phi_a(x)$. The defect interaction breaks explicitly the shift symmetry, so the conservation equation is modified by a term localised on the defect

$$\partial_\mu J^{\mu\, a}(0, x_\perp) = -\frac{\zeta_0}{\sqrt{\kappa}}\, \hat{S}_0^a(0)\, \delta^{d-1}(x_\perp)\,, \tag{3.61}$$

where the minus sign is introduced for future convenience. Note that the bulk fundamental fields ϕ_a do not renormalise since the bulk is free. Introducing renormalisation factors such that $\hat{S}_0^a = Z_{\hat{S}}\, \hat{S}^a$ and $\zeta_0 = \mu^{\frac{\varepsilon}{2}} Z_\zeta\, \zeta$, then it follows that in the MS scheme

$$Z_{\hat{S}} = Z_\zeta^{-1}\,, \tag{3.62}$$

at all orders in perturbation theory, since the right hand side of (3.61) must be finite. In particular, (3.61) holds even when renormalised quantities are substituted for the bare ones.[7] The operator $\hat{S}_a$, responsible for the symmetry breaking, is a defect primary operator at the fixed point and is referred to as the *defect spin* operator. As discussed

[7] More precisely, for renormalised quantities, one would have $\partial_\mu J^{\mu\, a}(0, x_\perp) = -\frac{\mu^{\frac{\varepsilon}{2}} \zeta}{\sqrt{\kappa}}\, \hat{S}^a(0)\, \delta^{d-1}(x_\perp)$. In this thesis, the scale factor μ is often set to one, as is customary in the CFT literature, since the correlation functions at the fixed point depend on μ in a trivial way.

in [33], the above Ward identities protect its dimension, which is given by $\hat{\Delta}_{\hat{S}} = \varepsilon/2$.[8] The explicit form of the defect spin operator $\hat{S}_a$ in the perturbative setup can be derived via the Schwinger-Dyson equations. To do this, it is convenient to think of the defect as contributing an extra term to the full action $S = S_{\text{bulk}} + S_{\text{defect}}$, where

$$S_{\text{defect}} = -\log \operatorname{Tr} \mathcal{D}_j \,. \tag{3.63}$$

Inside correlation functions it must hold

$$\begin{aligned} \Box\phi_a(\tau, x_\perp) &= \frac{\delta S_{\text{defect}}}{\delta\phi_a(\tau, x_\perp)} = \\ &= -\frac{\zeta_0}{\sqrt{\kappa}}\,\delta^{d-1}(x_\perp)\frac{\operatorname{Tr}\big(\mathcal{D}_j(-\infty,\tau)\,T_a\,\mathcal{D}_j(\tau,\infty)\big)}{\operatorname{Tr}\mathcal{D}_j}\,. \end{aligned} \tag{3.64}$$

Therefore, comparing with (3.61) one finds that correlators involving a defect spin operator $\hat{S}_0^a(\tau)$ inserted at a point τ lying on the defect satisfy

$$\begin{aligned} \langle \mathcal{O}_1(x_1)\ldots\hat{S}_0^a(\tau)\ldots\mathcal{O}_n(x_n)\rangle_{\mathcal{D}_j} = \\ = -\langle \mathcal{O}_1(x_1)\ldots T^a(\tau)\ldots\mathcal{O}_n(x_n)\rangle_{\mathcal{D}_j}\,, \end{aligned} \tag{3.65}$$

where the right hand side has to be interpreted in the same sense as (3.52). In the following, this relation is written as

$$\hat{S}_a(\tau) = -Z_{\hat{S}}^{-1}\,T_a(\tau)\,. \tag{3.66}$$

In this sense, the $\hat{S}_a$ operators in perturbation theory are just normal matrices which acquire an anomalous dimension once they are inserted into the defect.[9]

Another notable consequence of (3.61) is that it can be rewritten as

$$\Box\phi_a(0, x_\perp) = \frac{\zeta}{\sqrt{\kappa}}\,\hat{S}_a(0)\,\delta^{d-1}(x_\perp)\,, \tag{3.67}$$

and this equation can be easily inverted

$$\phi_a(0, x_\perp) = \sqrt{\kappa}\,\zeta\int d\tau\,\frac{\hat{S}_a(\tau)}{\left(|x_\perp|^2+\tau^2\right)^{1-\frac{\varepsilon}{2}}} + \phi_a^{\text{free}}(0, x_\perp)\,, \tag{3.68}$$

[8] This result can also be derived using diagrammatic methods, as originally shown in [29].

[9] Similar non trivial constant operators have already appeared in the literature, see for example [119, 120]. In the present case, this unfamiliar situation could be avoided by considering an equivalent representation of the defect in terms of one dimensional fermions. From that point of view $\hat{S}_a$ can be realised as a regular fermion bilinear operator.

where ϕ_a^{free} represents a free field that does not interact with the defect. In particular, correlators involving fundamental fields and their orthogonal derivatives (both in the bulk and on the defect) can be reduced to defect integrals of correlators involving $\hat{S}_a$ (not necessarily at the fixed point), as it will be demonstrated in the following (see *e.g.* (3.84) and (3.109)).

It is important to understand what are the conformal descendants of the operator $\hat{S}_a$ at the fixed point. Such descendants are obtained by acting with the defect covariant derivative defined in (3.55). In the case of the $\hat{S}_a$ operator, one gets

$$D_\tau \hat{S}^a(\tau) = -i\frac{\zeta_0}{\sqrt{\kappa}}\epsilon^{abc}\phi_b T_c(\tau)\,, \tag{3.69}$$

where the generator on the right hand side has to be inserted inside the path ordering, similarly to (3.65). This example illustrates that, in this setup, determining whether an operator is primary can be challenging. Although (3.69) contains no ∂_τ derivatives, it is, in fact, a descendant.

Once the bulk quartic interaction is turned on, the shift symmetry is explicitly broken in the bulk, hence the above analysis does not apply. Nevertheless, it still makes sense to consider the $\hat{S}_a$ operators defined by (3.65). The dimension of these operators is no longer protected, and since it is classically vanishing, one has

$$\hat{\Delta}_{\hat{S}} = \left(\beta_\zeta \frac{\partial \log Z_{\hat{S}}}{\partial \zeta} + \beta_\lambda \frac{\partial \log Z_{\hat{S}}}{\partial \lambda}\right)\Big|_{\zeta_*,\lambda_*}\,, \tag{3.70}$$

where now $Z_{\hat{S}}$ depends also on the bulk coupling constant λ. Interestingly, up to two loops in perturbation theory $Z_{\hat{S}}$ does not receive any divergent corrections from the bulk interaction.[10] Therefore, in the interacting case one can still write

$$Z_{\hat{S}} = \left(Z_\zeta|_{\lambda=0}\right)^{-1} + \mathrm{O}(\zeta^2\lambda^2, \zeta^4\lambda)\,, \tag{3.71}$$

This is sufficient to compute the first correction to the dimension $\Delta_{\hat{S}}$ using only the result for the β-function in the interacting case, without

[10] One way to see this is noting that diagrammatically no propagator can be attached to the operator $\hat{S}_a$, since in the definition (3.66) there are no fundamental fields. This implies that any contribution that involves both the defect and the bulk interaction either comes from a correction to bulk propagators and is at least of order $\mathrm{O}(\zeta^2\lambda^2)$, or has at least four internal legs attached to the defect and is at least of order $\mathrm{O}(\zeta^4\lambda)$.

having to do any further diagrammatic computation [29]

$$\begin{aligned}\hat{\Delta}_{\hat{S}} &= \beta_\zeta \frac{\partial \log Z_{\hat{S}}}{\partial \zeta}\bigg|_{\zeta_*,\lambda_*} + \mathrm{O}(\varepsilon^3) = \\ &= \frac{\varepsilon}{2} - \varepsilon^2\left(\frac{5}{484} + \frac{\pi^2}{11}\left(j(j+1) - \frac{1}{3}\right)\right) + \mathrm{O}(\varepsilon^3)\,.\end{aligned} \tag{3.72}$$

Correlators of defect spin operators in perturbation theory

Once the explicit form of the defect spin operator in perturbation theory is known, it is possible to evaluate correlators using standard diagrammatic techniques. This section is devoted to the computation of the two-point function $\langle \hat{S}_a(\tau_1)\hat{S}_b(\tau_2)\rangle_{\mathcal{D}_j}$ at two loops, both in the free and interacting bulk cases. The overall normalisation of the two-point function in free theory has a physical meaning, since the normalisation of $\hat{S}$ is fixed by its definition (3.61), and in fact this normalisation will be useful later.

Neglecting the renormalisation factors for the moment, this two-point function is the expectation value of the defect with generators T_a and T_b inserted at τ_1 and τ_2, respectively. Since in (3.52) one needs to divide by the defect expectation value, traces can be normalised by dividing by $2j+1$, which is the classical expectation value. Moreover, it is convenient to define the "connected part" of a diagram as what remains after one subtracts all contributions that are products of lower order diagrams, or pieces that contain "defect bubbles". Using this terminology, the defect correlator is the sum of all connected diagrams.

The leading order term is given by the following diagram

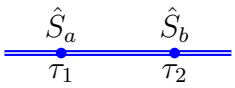

(3.73)

where the blue line represents the defect and the blue points indicate that a generator has to be inserted into the trace. Since there are no lower order diagrams, this diagram is already connected, and it gives

$$I_c^{(0)}(\tau_1,\tau_2) = \frac{1}{2j+1}\mathrm{Tr}\,(T_a T_b) = \frac{j(j+1)}{3}\delta_{ab}. \tag{3.74}$$

At one loop there are only two diagrams contributing to the connected term (all other diagrams exactly factor into an order zero diagram times a piece of a one-loop bubble and they have to be subtracted)

(3.75)

where the additional blue points indicate interactions with a generator insertion and the black line represents a free propagator. In $d = 4 - \varepsilon$ dimensions the free propagator reads

$$\langle \phi_a(x_1)\phi_b(x_2)\rangle\big|_{\lambda=0} = \frac{\kappa\,\delta_{ab}}{|x_1 - x_2|^{2-\varepsilon}}\,, \tag{3.76}$$

where κ was defined in equation (3.41). The interactions have to be integrated along the defect, but without crossing any other generator insertions. These two diagrams have the same color factor, given by

$$I^{(1)} \sim \frac{1}{2j+1}\mathrm{Tr}\,(T_c T_a T_c T_b) = \frac{j(j+1)(j(j+1)-1)}{3}\,\delta_{ab}\,. \tag{3.77}$$

From these diagrams, one still needs to subtract the product of the order zero diagram times pieces of one-loop "defect bubbles", which have the same kinematical integral but color factor given by

$$I_c^{(0)} \times \text{bubbles}^{(1)} \sim \frac{1}{(2j+1)^2}\mathrm{Tr}\,(T_a T_b)\ \mathrm{Tr}\,(T_c T_c) = \frac{j^2(j+1)^2}{3}\,\delta_{ab}\,. \tag{3.78}$$

Therefore, one gets

$$\begin{aligned} I_c^{(1)}(\tau_1,\tau_2) = -\zeta_0^2\frac{j(j+1)}{3}\delta_{ab}\Bigg(&\int\limits_{-\infty<\tau<\tau_1<\tau'<\tau_2} \frac{d\tau\,d\tau'}{|\tau-\tau'|^{2-\varepsilon}} \\ &+ \int\limits_{\tau_1<\tau<\tau_2<\tau'<+\infty} \frac{d\tau\,d\tau'}{|\tau-\tau'|^{2-\varepsilon}}\Bigg)\,. \end{aligned} \tag{3.79}$$

After performing the trivial integrals, one finds

$$I_c^{(1)}(\tau_1,\tau_2) = -\frac{2\,\zeta_0^2\,j(j+1)}{3(1-\varepsilon)\varepsilon}|\tau_1-\tau_2|^{\varepsilon}\,\delta_{ab}\,. \tag{3.80}$$

As expected, this contribution has a pole for $\varepsilon \to 0$, since this computation is for the bare two-point function At the next order, there are many diagrams that contribute to this two-point function, but the computation goes on in a similar way, and it is carried out explicitly in Appendix B.2.7. It is interesting to note that the same diagrams contribute to the free and interacting bulk cases. The reason is that, at the order under consideration, the only new diagram in the interacting case would be a mass correction to the bulk propagator, which is set to zero. Once all the diagrams are evaluated, one introduces the wave-function renormalisation coefficient $Z_{\hat{S}}$ and rewrites the bare coupling constant in terms of the renormalised one, while keeping in mind that

$Z_{\hat{S}} = Z_\zeta^{-1}$. Then, imposing finiteness of $Z_{\hat{S}}^{-2}\langle \hat{S}_0^a(\tau_1)\hat{S}_0^b(\tau_2)\rangle_{\mathcal{D}_j}$ at this order in the coupling constant yields

$$Z_{\hat{S}} = 1 - \frac{\zeta^2}{\varepsilon} - \frac{\zeta^4}{2\varepsilon^2} + \frac{\zeta^4}{2\varepsilon} + \mathrm{O}(\zeta^6). \tag{3.81}$$

Putting everything together, the renormalised two-point function evaluated at the free bulk fixed point (3.46) is

$$\langle \hat{S}_a(\tau_1)\hat{S}_b(\tau_2)\rangle_{\mathcal{D}_j} = \frac{\mathcal{N}_{\hat{S}}}{|\tau_1-\tau_2|^{2\hat{\Delta}_{\hat{S}}}} \cdot \frac{\delta_{ab}}{3}\,, \tag{3.82}$$

where $\hat{\Delta}_{\hat{S}} = \varepsilon/2$ and

$$\mathcal{N}_{\hat{S}} = j(j+1)\left(1 - \varepsilon + \varepsilon^2 \frac{12+\pi^2}{24}\right) + \mathrm{O}(\varepsilon^3)\,. \tag{3.83}$$

Clearly, by conformal symmetry and by the fact that $\hat{S}_a$ is protected, one already knows that (3.82) holds at the non-perturbative level. The above computation is nevertheless necessary to determine the constant $\mathcal{N}_{\hat{S}}$.[11]

This result, along with (3.68), can be used to compute the bulk-to-defect two-point function between ϕ^a and $\hat{S}^b$

$$\langle \phi^a(0,x_\perp)\hat{S}^b(0)\rangle_{\mathcal{D}_j} = \sqrt{\kappa}\,\zeta \int d\tau \frac{\langle \hat{S}^a(\tau)\hat{S}^b(0)\rangle_{\mathcal{D}_j}}{(\tau^2+|x_\perp|^2)^{1-\frac{\varepsilon}{2}}}\,, \tag{3.84}$$

which is exact in the free-bulk theory.[12] Using (3.82), solving the integral and evaluating at the fixed point yields

$$\begin{aligned}\langle \phi^a(0,x_\perp)\hat{S}^b(0)\rangle_{\mathcal{D}_j} &= \\ &= \frac{\delta^{ab}}{3\,|x_\perp|} \cdot \frac{\sqrt{\kappa}\,\zeta_*\,\mathcal{N}_{\hat{S}}\,\sqrt{\pi}\,\Gamma\left(\frac{1-\varepsilon}{2}\right)}{\Gamma\left(1-\frac{\varepsilon}{2}\right)} \equiv \frac{\delta^{ab}}{3\,|x_\perp|}\, b_{\phi\hat{S}}\,.\end{aligned} \tag{3.85}$$

Interestingly, the above correlator contains a factor $\Gamma\left(\frac{1-\varepsilon}{2}\right)$ that diverges in the $\varepsilon \to 1$ limit. At this stage, it is still unclear whether the divergence could be cured by the ε-dependent term $\zeta_*\mathcal{N}_{\hat{S}}$. Nevertheless, this should be taken as a hint that the theory is sick for $\varepsilon = 1$, *i.e.* in three dimensions, as it will be proved in Section 4.3.

[11] Note that the normalization of $\hat{S}_a$ is already fixed from the bulk through the Ward identity (3.67).

[12] As long as one is interested in computing the correlator at the fixed point, it is enough to evaluate it with vanishing parallel distance between the operators. The kinematics is already fixed by conformal symmetry.

When the bulk interaction is turned on, using (3.49) and (3.72) one obtains

$$\mathcal{N}_{\hat{S}} = j(j+1)\left(1-\varepsilon+\varepsilon^2\left(\frac{1512-55\pi^2}{2904}+\frac{2\pi^2 j(j+1)}{11}\right)\right)+\mathrm{O}(\varepsilon^3)\,. \tag{3.86}$$

The displacement operator and the defect stress-energy tensor

In a similar way, one can consider the Ward identity given by the translational invariance of the bulk theory, as outlined in 2.2.3. The defect explicitly breaks this symmetry and the conservation of the bulk stress-energy tensor is also modified by a term localised on the defect [24, 17]

$$\partial_\mu T^{\mu\nu}(0,x_\perp) = -\left(\delta_i^\nu \hat{D}^i(0) + \partial_\tau x^\nu(0)\,\partial_\tau \hat{T}_{\mathcal{D}_j}(0)\right)\delta^{d-1}(x_\perp)\,, \tag{3.87}$$

where $x^\nu(\tau)$ is the embedding function that describes the defect and τ is the coordinate that parametrises the line. $\hat{D}^i$ and $\hat{T}_{\mathcal{D}_j}$ are two defect operators, each of which will be discussed below.

$\hat{D}^i$ is called the *displacement* operator and it is a primary operator. By the above Ward identity, it has protected dimension $\hat{\Delta}_D = 2$. The explicit expression for the bare displacement operator can be derived by considering the variation of the action with respect to $x^i(\tau)$

$$\hat{D}^i_0(x(\tau)) = \frac{1}{|\dot{x}(\tau)|}\frac{\delta S_{\text{defect}}}{\delta x_i(\tau)}. \tag{3.88}$$

Computing this functional derivative and at the end evaluating at unit speed parametrization of the flat defect one finds [13]

$$\hat{D}^i_0(\tau) = \frac{\zeta_0}{\sqrt{\kappa}}\partial^i\phi_a(\tau)\,\frac{\mathrm{Tr}\big(\mathcal{D}_j(-\infty,\tau)\,T_a\,\mathcal{D}_j(\tau,\infty)\big)}{\mathrm{Tr}\;\mathcal{D}_j}\,. \tag{3.89}$$

In terms of correlators, the bare displacement operator inserted at a point τ lying on the defect satisfies

$$\begin{aligned}\langle \mathcal{O}_1(x_1)\ldots\hat{D}^i_0(\tau)\ldots\mathcal{O}_n(x_n)\rangle_{\mathcal{D}_j} = \\ = \frac{\zeta_0}{\sqrt{\kappa}}\,\langle \mathcal{O}_1(x_1)\ldots\partial^i\phi^a(\tau)T_a\ldots\mathcal{O}_n(x_n)\rangle_{\mathcal{D}_j}\,.\end{aligned} \tag{3.90}$$

This will just be rewritten as

$$\hat{D}_i(\tau) \sim \partial_i\phi^a T_a(\tau)\,. \tag{3.91}$$

[13] Note that one needs to first reintroduce the arc length element $|\dot{x}(\tau)|$ in the integral of the defect action (3.63) since a generic variation of the embedding spoils the unit speed parametrisation.

Note that this analysis holds regardless of whether the bulk is interacting or not, since the bulk stress-energy tensor is nevertheless conserved.

The other operator that appears in the Ward identity (3.87) is the *defect stress-energy tensor* $\hat{T}_{\mathcal{D}_j}$. By the Ward identity, it has protected dimension $\hat{\Delta}_{\hat{T}_{\mathcal{D}_j}} = 1$. The existence of such operator breaks conformal invariance on the line defect, therefore it must vanish at the fixed point. In this model, the defect stress-energy tensor reads [14]

$$\hat{T}_{\mathcal{D}_j}(\tau) = \frac{\beta_\zeta}{\sqrt{\kappa}} \hat{\Phi}(\tau)\,, \tag{3.92}$$

where for future convenience it is defined $\hat{\Phi}(\tau) = \phi_a T^a(\tau)$.[15] Using the definition of conformal dimension $\mu \frac{\partial \hat{\mathcal{O}}}{\partial \mu} = -\hat{\Delta}_{\hat{\mathcal{O}}} \hat{\mathcal{O}}$ and the fact that $\hat{T}_{\mathcal{D}_j}$ is protected, it follows

$$\hat{\Delta}_{\hat{\Phi}} = 1 + \frac{\partial \beta_\zeta}{\partial \zeta} + \frac{\beta_\lambda}{\beta_\zeta} \frac{\partial \beta_\zeta}{\partial \lambda}\,. \tag{3.93}$$

This formula is exact and holds both for the case of free and interacting bulk theories. A consequence of the last equation and the definition of the anomalous dimension of $\hat{\Phi}$ in terms of the wavefunction renormalisation of the operator is that in free theory

$$Z_{\hat{\Phi}} = -\frac{2\beta_\zeta}{\varepsilon\, \zeta\, Z_\zeta}\,. \tag{3.94}$$

Finally, using the expression for the beta function in the free bulk theory (3.45) and the value of ζ at the critical point, one obtains the conformal dimension of the defect operator $\hat{\Phi}$

$$\hat{\Delta}_{\hat{\Phi}} = 1 + \varepsilon - \frac{\varepsilon^2}{2} + \frac{\varepsilon^3}{2}\left(1 - \pi^2\left(j\,(j+1) - \frac{1}{3}\right)\right) + \mathrm{O}(\varepsilon^4)\,. \tag{3.95}$$

One can do the same in the interacting case, where

$$\hat{\Delta}_{\hat{\Phi}} = 1 + \varepsilon - \varepsilon^2\left(\frac{257}{484} - \frac{4\pi^2}{11}\left(j(j+1) - \frac{1}{3}\right)\right) + \mathrm{O}(\varepsilon^3)\,. \tag{3.96}$$

[14] For a generic line defect with a Lagrangian of the form $\mathcal{L}_{\text{defect}} = g\hat{\mathcal{O}}$, the defect stress tensor reads $\hat{T} = \beta_g \hat{\mathcal{O}}$. This follows from the more general result $\partial_\nu T^\nu_\mu x^\mu = \beta_i \frac{\partial \mathcal{L}}{\partial g_i}$, which is a consequence of Noether's theorem applied to the renormalized Lagrangian in the case of scale transformations.

[15] Here and in the rest of this paper it is assumed that defect operators with generator insertions have to be interpreted in the sense of (3.65) and (3.89).

Correlators of $\hat{\Phi}$

The one-loop two-point function of $\hat{\Phi}$ is computed here, both in the free bulk and interacting bulk cases. This computation, besides providing a sanity check of the arguments of the previous section, it also shows how correlators of operators composed both of generators insertions and of fundamental fields are evaluated in practice.

At tree level there is only one diagram

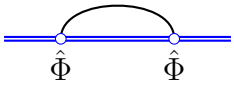

$$= \; j(j+1)\,\frac{\kappa}{|\tau_1-\tau_2|^{2-\varepsilon}}\,. \tag{3.97}$$

At one loop one finds two kind of connected diagrams: the two operators can be either connected by a free bulk propagator, or they interact with the defect. Note that even in the interacting bulk case there are no other diagrams, since bulk interactions contribute only at the next order. The first kind of diagrams are

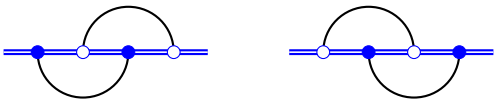

(3.98)

the computation of these integrals is analogous to the one for the operators $\hat{S}_a$ of (3.75), with the only difference that now everything is multiplied by a free propagator. The result is

$$I_1^{(1)}(\tau_1,\tau_2) = -\frac{\zeta_0^2\, j(j+1)\Gamma\left(2-\frac{\varepsilon}{2}\right)}{\pi^{2-\frac{\varepsilon}{2}}(2-\varepsilon)(1-\varepsilon)\,\varepsilon\,|\tau_1-\tau_2|^{2-2\varepsilon}}\,. \tag{3.99}$$

The other diagrams are those where the two operators interact with the defect. There are twelve of them and they come with two different color structures: eight diagrams with $\mathrm{Tr}\,(T_aT_aT_bT_b) \sim j^2(j+1)^2$ and the remaining four with $\mathrm{Tr}\,(T_aT_aT_bT_b) \sim j(j+1)(j^2+j-1)$. The sum of all the diagrams contains a piece proportional to $j^2(j+1)^2$ which is a sum of the ordered integral of two propagators over all possible orders, hence giving $\kappa^2 \int d\sigma_1\,|\sigma_1-\tau_1|^{-2+\varepsilon} \int d\sigma_2\,|\sigma_2-\tau_2|^{-2+\varepsilon}$ which vanishes in the chosen regularisation. Hence one is left with the evaluation of the

following four diagrams

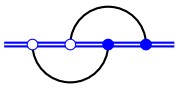

$$= -\frac{\zeta_0^2\, j(j+1)\,\Gamma\left(2-2\varepsilon\right)\Gamma\left(1-\frac{\varepsilon}{2}\right)\Gamma\left(\varepsilon\right)}{4\pi^{2-\frac{\varepsilon}{2}}(1-\varepsilon)\Gamma\left(2-\varepsilon\right)\,|\tau_1-\tau_2|^{2-2\varepsilon}}\,,$$

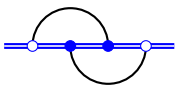

$$= -\frac{\zeta_0^2\, j(j+1)\,\Gamma\left(1-\frac{\varepsilon}{2}\right)\left(\Gamma\left(\varepsilon\right)^2-\Gamma\left(2\varepsilon-1\right)\right)}{8\pi^{2-\frac{\varepsilon}{2}}(1-\varepsilon)^3\Gamma\left(-2+2\varepsilon\right)\,|\tau_1-\tau_2|^{2-2\varepsilon}}\,,$$

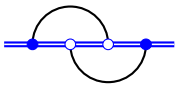

$$= -\frac{\zeta_0^2\, j(j+1)\,\Gamma\left(1-\frac{\varepsilon}{2}\right)}{4\pi^{2-\frac{\varepsilon}{2}}(1-\varepsilon)^2\,|\tau_1-\tau_2|^{2-2\varepsilon}}\,,$$

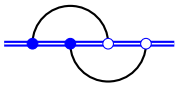

$$= -\frac{\zeta_0^2\, j(j+1)\,\Gamma\left(2-2\varepsilon\right)\Gamma\left(1-\frac{\varepsilon}{2}\right)\Gamma\left(\varepsilon\right)}{4\pi^{2-\frac{\varepsilon}{2}}(1-\varepsilon)\Gamma\left(2-\varepsilon\right)\,|\tau_1-\tau_2|^{2-2\varepsilon}}\,. \tag{3.100}$$

Summing all the contributions, introducing the wavefunction renormalisation coefficient $Z_{\hat\Phi}$ and imposing finiteness of $Z_{\hat\Phi}^{-2}\langle\hat\Phi(\tau_1)\hat\Phi(\tau_2)\rangle_{\mathcal{D}_j}$ at one loop, one gets

$$\begin{aligned} Z_{\hat\Phi} &= 1-\frac{3\,\zeta^2}{\varepsilon}+\mathrm{O}\left(\zeta^4,\zeta^2\lambda,\lambda^2\right)\,,\\ \gamma_{\hat\Phi}|_{\zeta_*,\lambda_*} &= \beta_\zeta\frac{\partial\log Z_{\hat\Phi}}{\partial\zeta}\bigg|_{\zeta_*,\lambda_*}+\mathrm{O}(\varepsilon^2)=\frac{3}{2}\,\varepsilon+\mathrm{O}(\varepsilon^2)\,. \end{aligned} \tag{3.101}$$

The renormalised two-point function evaluated at the fixed point is

$$\langle\hat\Phi(\tau_1)\hat\Phi(\tau_2)\rangle_{\mathcal{D}_j}=\frac{\mathcal{N}_{\hat\Phi}}{|\tau_1-\tau_2|^{\hat\Delta_{\hat\Phi}}}\,, \tag{3.102}$$

where both in the free bulk and in the interacting bulk case

$$\begin{aligned} \mathcal{N}_{\hat\Phi} &= \frac{j(j+1)}{4\pi^2}\left(1+\varepsilon\left(-2+\frac{\gamma_E}{2}+\frac{\log\pi}{2}\right)\right)+\mathrm{O}(\varepsilon^2)\,,\\ \hat\Delta_{\hat\Phi} &= 1+\varepsilon+\mathrm{O}(\varepsilon^2)\,. \end{aligned} \tag{3.103}$$

General defect operators

The defect spin and the displacement operators arose as defect corrections to Ward identities. It is natural to ask whether there are other defect operators with protected dimensions that can be obtained in this way. In particular, in the bulk-free theory there exists an infinite tower of conserved higher spin currents (3.15).[16] Their dimension (in the free theory) is $\Delta_{J_{s+1}}=s+1-\varepsilon$. From the modified Ward identity

$$\partial^\nu J^{ab}_{\nu\mu_1\ldots\mu_s}(0,x_\perp)=\frac{\zeta_0}{\sqrt{\kappa}}\,\hat J^{ab}_{\mu_1\ldots\mu_s}(0)\,\delta^{d-1}(x_\perp)\,, \tag{3.104}$$

[16] For $s=0$, up to an antisymmetric tensor one just gets the Noether current associated to the $SU(2)$ global symmetry: $J^a_\mu\sim\epsilon^{abc}\phi_b\partial_\mu\phi_c$, which is conserved also in the defect theory.

one immediately finds a tower of defect operators that at the fixed point have protected dimension $\hat{\Delta}_{\hat{J}_s} = s + 1 \in \mathbb{N}$. Their explicit form can be determined by a computation analogous to the one of the defect spin operator. In equation (3.104), one gets defect primary operators only when all the free spatial indices are taken to be orthogonal to the defect, since derivatives parallel to the defect give rise to descendants. Therefore, it is enough to consider $\hat{J}^{ab}_{i_1\dots i_s}$, which clearly has orthogonal spin s. As for color indices, it is convenient to think in terms of $\mathfrak{so}(3)$ rather than $\mathfrak{su}(2)$. For even s, the two color indices must be in the antisymmetric representations; this is equivalent to the vector representation $\hat{J}^{a}_{i_1\dots i_s}$. For odd s, the representations can be the traceless symmetric $\hat{J}^{\{ab\}}_{i_1\dots i_s}$ and the singlet $\hat{J}_{i_1\dots i_s}$. Like in the case of the defect spin operators, when the bulk interaction is turned on, these higher spin currents are weakly broken and their dimensions will get corrections starting at second order in ε.

It is possible to obtain more information on the defect spectrum by looking at Ward identities for particular correlators. Following [121], consider the bulk-to-defect two-point function of ϕ and $\hat{\phi}$, which by conformal symmetry must take the form

$$\langle \phi_a(0, x_\perp)\hat{\phi}_b(0)\rangle_{\mathcal{D}_j} = \frac{b_{\phi\hat{\phi}}}{|x_\perp|^{\Delta_\phi - \hat{\Delta}_{\hat{\phi}}}|x_\perp|^{2\hat{\Delta}_{\hat{\phi}}}}\delta_{ab}\,. \tag{3.105}$$

Specialising to the free-bulk case and acting with the Laplacian $\Box_x$ at a point away from the defect x, one finds

$$\begin{aligned} 0 &= \langle \Box\phi_a(0, x)\hat{\phi}_b(0)\rangle_{\mathcal{D}_j} \\ &= (\hat{\Delta}_{\hat{\phi}} + \Delta_\phi - 1)(\hat{\Delta}_{\hat{\phi}} - \Delta_\phi)\frac{b_{\phi\hat{\phi}}}{|x_\perp|^{\Delta_\phi - \hat{\Delta}_{\hat{\phi}}+2}|x_\perp|^{2\hat{\Delta}_{\hat{\phi}}}}\delta_{ab}\,, \end{aligned} \tag{3.106}$$

and since from an immediate tree-level diagram computation one knows that $\hat{\Delta}_{\hat{\phi}} = 1 + \mathrm{O}(\varepsilon)$ and that $b_{\phi\hat{\phi}} \neq 0$, it must be that $\hat{\Delta}_{\hat{\phi}} = \Delta_\phi$ holds at the non-perturbative level. The same argument can be applied to the transverse spin-s operators $\hat{\mathcal{O}}^{a}_{i_1\dots i_s} \sim \partial_{i_1}\dots\partial_{i_s}\hat{\phi}^a$. One readily finds that their exact dimension is $\hat{\Delta}_s = \Delta_\phi + s$. Again, those dimensions will receive correction in the interacting bulk case, starting always at second order in ε.

In this Section, it has been shown that in this theory there are some defect operators such as the defect spin and the displacement operator that include in their definition the insertion of a generator T_a, and thus are matrix-valued. This suggests that a generic local defect operator is a $2j + 1 \times 2j + 1$ Hermitian matrix, with entries that are composite

operators made of fundamental fields and their derivatives. Their correlators are given by (3.52). Clearly, when the matrix is proportional to the identity, one recovers the case of operators that can be factored outside the trace of the path-ordering, such as the fundamental fields $\hat{\phi}_a$. In order to be able to construct and identify all the possible defect operators, it is useful to choose a convenient basis for the space of these matrices.

In the simplest situation where $j = \frac{1}{2}$, *i.e.* in the fundamental representation of $\mathfrak{su}(2)$, the three generators together with the identity span the whole real vector space of 2×2 Hermitian matrices. In particular, a defect operator with an arbitrary Hermitian matrix insertion in the defect can be decomposed into operators with insertions that are at most linear in the generators T^a. For the more general case of spin $j > \frac{1}{2}$ representations, the space of possible Hermitian matrix insertions has real dimension $(2j+1)^2$. This space can be spanned by taking Hermitian combinations of products of the generators T^a. A natural choice of basis is given by the totally symmetrised traceless product of generators [17]

$$T^{\{a_1} \dots T^{a_k\}}, \quad k = 0, \dots, 2j\,. \tag{3.107}$$

In particular, there are $4j(j+1)$ primary defect operators defined by the basis elements

$$\hat{S}^{\{a_1 \dots a_k\}}(x) \equiv T^{\{a_1} \dots T^{a_k\}}(x)\,, \quad k \geqslant 1\,, \tag{3.108}$$

inserted in the path-ordered exponential, without any fundamental field insertion. These operators are expected to be among the lightest operators of the theory, since their classical dimension is zero. Moreover, there cannot be any mixing between them for representation theory reasons. For operators composed also of powers of the fundamental fields and their derivatives, it still makes sense to organise operators according to their color index structure. However, in general there will be several operators in the same representation and with the same classical dimension, so that one should worry about their mixing. Finally, it is important to pay attention to the fact that defect descendants are given by the defect covariant derivative (3.55) and not by the ordinary one. As an example, as was found out in (3.69), the defect operator defined by $\epsilon^{abc}\phi_b T_c(\tau)$ is not a new primary, but it is a descendant.

[17] To show that these symmetrised traceless products constitute a basis, note that they are $\sum_{k=0}^{2j}(2k+1) = (2j+1)^2$ and that they are orthogonal with respect to the trace inner product.

Correlators of $\hat{\phi}_a$ and $\hat{\mathcal{O}}^a_{i_1\dots i_s}$

Among the defect operators discussed, there are some interesting exact relations that hold between correlators when the bulk is free. As an example, consider the defect operator $\hat{\phi}_a$, which corresponds to the fundamental field placed on the defect. By using the analogue of (3.68) for $\hat{\phi}_a$ (*i.e.* when $x \perp\!\!\!= 0$), its two-point function can be computed in terms of that of the defect spin operator

$$\begin{aligned}\langle\hat{\phi}_a(\tau_1)\hat{\phi}_b(\tau_2)\rangle_{\mathcal{D}_j} = &\frac{\kappa\, j(j+1)\,\delta_{ab}}{3\,|\tau_1-\tau_2|^{2-\varepsilon}}\\ &+\kappa\,\zeta^2\int d\sigma_1\int d\sigma_2\,\frac{\langle\hat{S}(\sigma_1)\hat{S}(\sigma_2)\rangle_{\mathcal{D}_j}}{\left(|\tau_1-\sigma_1|\,|\tau_2-\sigma_2|\right)^{2-\varepsilon}}\,,\end{aligned} \tag{3.109}$$

which holds at all orders in perturbation theory. In particular, evaluating at the fixed point one gets

$$\begin{aligned}\langle\hat{\phi}_a(\tau_1)\hat{\phi}_b(\tau_2)\rangle_{\mathcal{D}_j} = &\frac{\delta_{ab}}{3\,|\tau_1-\tau_2|^{2-\varepsilon}}\Bigg(\kappa\, j(j+1)\\ &-\frac{\zeta_*^2\,\mathcal{N}_{\hat{S}}\,\Gamma(1-\varepsilon)\,\Gamma\left(\frac{\varepsilon-1}{2}\right)\sin\left(\frac{\pi\varepsilon}{2}\right)}{2^{2-\varepsilon}\,\pi^{\frac{3-\varepsilon}{2}}}\Bigg)\,.\end{aligned} \tag{3.110}$$

From this, it follows that $\hat{\phi}_a$ has a vanishing anomalous dimension, as it was previously argued through Ward identities. Similarly, one can do the same for the two-point function of one operator in the bulk and one placed on the defect. At the fixed point one finds

$$\begin{aligned}\langle\phi_a(0,x_\perp)\hat{\phi}_b(\tau)\rangle_{\mathcal{D}_j} = &\frac{\delta_{ab}}{3\,\left(|x_\perp|^2+\tau^2\right)^{1-\frac{\varepsilon}{2}}}\Bigg(\kappa\, j(j+1)\\ &-\frac{\zeta_*^2\,\mathcal{N}_{\hat{S}}\,\Gamma(1-\frac{\varepsilon}{2})\tan\left(\frac{\pi\varepsilon}{2}\right)}{\pi^{1-\frac{\varepsilon}{2}}(\varepsilon-1)}\Bigg)\,.\end{aligned} \tag{3.111}$$

Note that the above two-point function depends only on the four-dimensional distance between the bulk field and the defect field because they have exactly the same conformal dimension. The same argument applies to correlators involving $\hat{\mathcal{O}}^a_{i_1\dots i_s} \sim \partial_{i_1}\dots\partial_{i_s}\hat{\phi}^a$, in which case one only need to take orthogonal derivatives in (3.68) before setting $x_\perp = 0$. Finally, one could do the same to get the two-point function of two bulk fields, as it will be shown in Section 4.3.3.

Obviously, in the interacting bulk case there will be corrections to the correlators (3.110) and (3.111) starting at order ε^2.

Time-reversal symmetry for defect operators

At this point, it is possible to extend the discussion of time-reversal symmetry to generic defect operators. Their parity under this symmetry will be an useful tool to classify such operators. It is clear that defect operators without any insertions, *i.e.* those composed only of fundamental fields and their derivatives, behave just like bulk operators under this symmetries. On the other hand, the very same argument used in Section 3.3.2 can be repeated in the presence of operators with insertions into the defect. A careful analysis shows that the effect of T_t on generator insertions is $T_t : T^a(\tau) \mapsto -T^a(-\tau)$. Since $T_{\mathbb{Z}_2}$ does not act on generators, it follows that also T^a is odd under $\bar{T}_t$. This can also be seen, for example, by the Ward identity

$$\Box\phi_a(0, x_\perp) = \frac{\zeta_0}{\sqrt{\kappa}}\, \hat{S}_a(0)\, \delta^{d-1}(x_\perp)\,. \tag{3.112}$$

When there are more than just one generator inserted at the same point (only for $j \geqslant 1$), an analogue analysis shows that the effect of time reversal is not only a factor (-1) for each generator, but also an inversion in the order of the insertions. For this reason, it is convenient to express insertions in the basis given in (3.107). Indeed one can clearly see that this basis is diagonal under time reversal, and that $\bar{T}_t : T_{\{a_1} \dots T_{a_k\}}(\tau) \mapsto (-1)^k\, T_{\{a_1} \dots T_{a_k\}}(-\tau)$.

This symmetry imposes useful constraints on correlators. For example, sometimes it can be used to lift some degeneracies, since two defect operators with different parities must have vanishing two-point function at the non-perturbative level. The same holds for the two-point function of a bulk operator and a defect operator, giving useful selection rules for the coefficients of the defect block expansion (2.64). Finally, one must be careful that this conclusion does not generalise to correlators with more defect operators. In fact, in the case of one-dimensional defects, the three-point function of three defect operators can be antisymmetric [121].[18] For example, one can check that $\langle \hat{S}_a(\tau_1)\hat{S}_b(\tau_2)\hat{S}_c(\tau_3)\rangle \propto i\epsilon_{abc}$.

Classification of low-lying defect operators

All the information about the low-lying spectrum of the defect obtained so far through various tools is conveniently summarised here. Defect operators are classified according to their transverse spin s, their $\mathfrak{su}(2)$

[18] Indeed given any two points on an ordered straight line it is possible to invert their order through a special conformal transformation that preserves the line. But the same cannot be done for three points.

representation (characterised by the dimension of the representation), their parity under the time reversal symmetry $\bar{T}_t$, and their classical dimension. It is important to note that some of these operators only exist for sufficiently high values of j, where j specifies the $\mathfrak{su}(2)$-representation of the generators T_a in the definition of the defect (3.40).

Obtaining a complete list of defect operators at twist zero is straightforward.[19] At twist one, it is sufficient to construct all the possible composite operators using only one fundamental field ϕ_a, an arbitrary number of generators T_a and orthogonal derivatives ∂_i. Then one needs to decompose them into irreducible representations of $\mathfrak{su}(2)$. Finally, since the defect covariant derivative increases the twist by one, one needs to exclude all the descendants of the twist-zero primaries. Clearly, it is in principle possible to continue the classification by considering higher twist operators, which can be constructed by using an arbitrary number of fundamental fields and also orthogonal Laplacians $\Box_\perp$. Again, one needs to exclude all the descendants of lower-twist primaries. The number of primary operators grows combinatorially with the defect twist.

Table 3.1 lists all the defect twist-zero and defect twist-one primary operators, along with their quantum numbers and scaling dimensions at the fixed point (for both the free bulk and interacting bulk cases). Table 3.2 presents the explicit definitions of these operators in perturbation theory.

[19] Recall that the defect twist $\hat{\tau}$ of a defect operator with dimension $\hat{\Delta}$ and orthogonal spin s is defined as $\hat{\tau} \equiv \hat{\Delta} - s$.

$\hat{\mathcal{O}}$	s	$\dim R_{\mathfrak{su}(2)}$	$\bar{T}_t$	$\hat{\Delta}_{\hat{\mathcal{O}}}\big\vert_{\lambda=0}$	$\hat{\Delta}_{\hat{\mathcal{O}}}\big\vert_{\lambda_*}$
$\hat{S}^a$	0	3	$-$	$\frac{\varepsilon}{2}$	(3.72)
$\hat{S}^{\{a_1\dots a_k\}}$	0	$2k+1$	$(-)^k$	$\mathrm{O}(\varepsilon)$	$\mathrm{O}(\varepsilon)$
$\hat{\phi}^a$	0	3	$-$	$1-\frac{\varepsilon}{2}$	$1-\frac{\varepsilon}{2}+\mathrm{O}(\varepsilon^2)$
$\hat{\Phi}$	0	1	$+$	(3.95)	(3.96)
$\hat{D}_i$	1	1	$+$	2	2
$\hat{J}^a_{i_1\dots i_s}$	s	3	$+$	$s+1$	$s+1+\mathrm{O}(\varepsilon^2)$
$\hat{J}^{\{ab\}}_{i_1\dots i_s}$	s	5	$+$	$s+1$	$s+1+\mathrm{O}(\varepsilon^2)$
$\hat{J}_{i_1\dots i_s}$	s	1	$+$	$s+1$	$s+1+\mathrm{O}(\varepsilon^2)$
$\hat{\mathcal{O}}^a_{i_1\dots i_s}$	s	3	$-$	$s+1-\frac{\varepsilon}{2}$	$s+1-\frac{\varepsilon}{2}+\mathrm{O}(\varepsilon^2)$
$\hat{U}^{\{a_1\dots a_k\}}_{i_1\dots i_s}$	s	$2k+1$	$(-)^k$	$s+1+\mathrm{O}(\varepsilon)$	$s+1+\mathrm{O}(\varepsilon)$
$\hat{V}^{\{a_1\dots a_k\}}_{i_1\dots i_s}$	s	$2k+1$	$(-)^k$	$s+1+\mathrm{O}(\varepsilon)$	$s+1+\mathrm{O}(\varepsilon)$
$\hat{W}^{\{a_1\dots a_k\}}_{i_1\dots i_s}$	s	$2k+1$	$(-)^{k+1}$	$s+1+\mathrm{O}(\varepsilon)$	$s+1+\mathrm{O}(\varepsilon)$

Table 3.1: Defect twist-zero and twist-one primary operators with their quantum numbers and scaling dimensions.

Operator	Perturbative definition	Existence
$\hat{S}^a$	T^a	
$\hat{S}^{\{a_1\dots a_k\}}$	$T^{\{a_1}\dots T^{a_k\}}$	$2\leqslant k\leqslant 2j$
$\hat{\phi}^a$	ϕ^a	
$\hat{\Phi}$	$\phi^a T_a$	
$\hat{D}_i$	$\partial_i\phi^a T_a$	
$\hat{J}^a_{i_1\dots i_s}$	$\epsilon^{abc}\partial_{i_1}\dots\partial_{i_s}\phi_b T_c$	even s, $s\geqslant 2$
$\hat{J}^{\{ab\}}_{i_1\dots i_s}$	$\partial_{i_1}\dots\partial_{i_s}\phi^{\{a}T^{b\}}$	odd s, $s\geqslant 1$
$\hat{J}_{i_1\dots i_s}$	$\partial_{i_1}\dots\partial_{i_s}\phi^a T_a$	odd s, $s\geqslant 3$
$\hat{\mathcal{O}}^a_{i_1\dots i_s}$	$\partial_{i_1}\dots\partial_{i_s}\phi^a$	$s\geqslant 1$
$\hat{U}^{\{a_1\dots a_k\}}_{i_1\dots i_s}$	$\partial_{i_1}\dots\partial_{i_s}\phi_b T^{\{b}T^{a_1}\dots T^{a_k\}}$	$1\leqslant k\leqslant 2j-1, s\geqslant 0$
$\hat{V}^{\{a_1\dots a_k\}}_{i_1\dots i_s}$	$\partial_{i_1}\dots\partial_{i_s}\phi^{\{a_1}T^{a_2}\dots T^{a_k\}}$	$3-\delta_{0,s}\leqslant k\leqslant 2j+1, s\geqslant 0$
$\hat{W}^{\{a_1\dots a_k\}}_{i_1\dots i_s}$	$\partial_{i_1}\dots\partial_{i_s}\phi^b\epsilon^{bc\{a_1}T^cT^{a_2}\dots T^{a_k\}}$	$2\leqslant k\leqslant 2j, s\geqslant 1$

Table 3.2: Schematic perturbative definition of defect twist-zero and twist-one operators.

Note that for some of these operators the form is just schematic. Indeed, beyond tree level mixing among operators sharing the same quantum numbers can occur, and an orthogonalisation with respect to the two-point functions must be performed. For example, the explicit form of the operator $\hat{U}^a = \text{“}\phi_b T^{\{b}T^{a\}}\text{”}$ is correct only at tree-level, and at higher loops one must make sure that this operator is orthogonalised with respect to $\hat{\phi}_a$.

Further results about defect operators, their dimensions and coefficients of their correlators will be obtained in Section 4.3 trough analytic bootstrap techniques.

3.4 Other defects in the critical O(N) model

In Sections 3.2 and 3.3, two important examples of line defects for the critical $O(N)$ model have been introduced. These defects will be analysed in detail in Chapter 4 using the defect analytic bootstrap.

For completeness, this section briefly presents some additional examples of defects for the $O(N)$ critical model. First, defects that can be constructed and studied using perturbative techniques such as those used for the localised magnetic field and the magnetic impurity are considered in Section 3.4.1. Then, in Section 3.4.2, the scenario in which the defect coupling is strongly relevant is outlined. In this case, dCFTs observables are beyond the reach of the usual perturbative approach, and alternative techniques needs to be employed. The problem of studying “strongly-coupled” defects will also be addressed from different perspectives in Chapter 5 and Section 6.2.3.

3.4.1 Weakly-coupled defects

As explained in Section 2.3.1, defect fixed point are obtained by imposing that the beta function for the defect coupling is vanishing. To understand better the behaviour of these solutions, it is convenient to have a closer look at the condition that the defect coupling h_* at the fixed point must satisfy. For a defect interaction of the schematic form $h \int d^p\tau \mathcal{O}(\tau)$, using dimensional regularisation the condition is

$$0 = \beta_h(h_*, \lambda_*) = -(p - \Delta_{\mathcal{O}})\, h_* + \sum_{n\geqslant 2} c_{0,n} h_*^n + \lambda_* \sum_{m\geqslant 2} c_{1,m} h_*^m + \mathrm{O}(\lambda_*^2)\,, \tag{3.113}$$

where the first term is the classical contribution to the beta function, and quantum corrections are organised in powers of h and λ given by the coefficients $c_{k,n}$, which are pure numbers in the MS scheme. Recall

that $\lambda_* \sim \varepsilon$, as given in (3.8), and $\Delta_{\mathcal{O}}$ is the conformal dimension of $\mathcal{O}$ at the bulk fixed point. Note that the truncation of higher-order terms in λ_* in equation (3.113) is justified only if h_* is at most of order $\mathrm{O}(\varepsilon^0)$. There are two possibilities:

- $h_* \sim \mathrm{O}(\varepsilon^0)$, as in the case of the localised magnetic field. This scenario is more complicated and it should be analysed on a case-by-case basis. In general, since h_* is not small, one can expand perturbatively only in the bulk coupling λ, and h must be treated exactly. If the series in powers of h in (3.113) truncates at any given order in λ, as in the case of the localised magnetic field, perturbation theory could still be applied.

- $h_* \sim \mathrm{O}(\varepsilon^a)$ for $a > 0$ (not necessarily integer), as in the case of the magnetic impurity. From (3.113) and the fact that $\lambda_* \sim \varepsilon$, it follows that a solution is only possible if $p - \Delta_{\mathcal{O}} \sim \alpha\varepsilon$ for some (ε-independent) coefficient α. Furthermore, there must be a non-zero coefficient $c_{0,k}$ for some minimal value of $k \geqslant 2$. This, in turn, implies that $h_* \sim \varepsilon^{\frac{1}{k-1}}$. The theory can then be treated perturbatively in both the defect and bulk couplings in a regime where $\lambda \sim h^{k-1}$.

From the above analysis, it follows that there is a simple recipe to find weakly-coupled defect fixed points: one needs to find a bulk operator $\mathcal{O}$ that is weakly relevant, *i.e.* $p - \Delta_{\mathcal{O}} \sim \alpha\varepsilon$ with $\alpha > 0$, as this is a necessary condition.[20] Then one can just compute a finite number of Feynmnan diagrams to get the beta function and look for real solutions h_* of (3.113).

For $p = 1$, the only deformations one can consider are those linear in the field ϕ_a, which are exactly those considered in 3.2 and 3.3.

The surface defect

For $p = 2$, an interesting deformation is given by the following defect action

$$S_{\mathcal{D}} = \frac{h_{ab}}{2} \int d^2\tau \, \phi_a \phi_b \,, \tag{3.114}$$

where h_{ab} is a symmetric tensor. This action yields weakly coupled defect fixed points for different tensor structures h_{ab} that have been

[20] More generally, it is possible to couple the bulk theory to a defect theory, as it is done in the context of free bulk theories in [122]. See also the construction of non-local defects in Section 6.2.1. Instead, here only deformations that can be constructed using the operators of the bulk theory are considered.

studied at one loop in [123–125] and at two loops in [36].[21] An interesting point is that for $\varepsilon = 1$ the bulk becomes three-dimensional, and therefore the defect given in (3.114) should describe a boundary or an interface.

Following [36], the two-loop beta-function is

$$\begin{aligned}\beta_{ab} = -\varepsilon h_{ab} + h_{ac}h_{bc} + \lambda[2h_{ab} + h_{cc}\delta_{ab} - 2(2h_{ac}h_{bc} + h_{ab}h_{cc})] \\ - \frac{1}{6}\lambda^2[(N+10)h_{ab} + 4h_{cc}\delta_{ab}]\,.\end{aligned} \tag{3.115}$$

Terms of order λh^2 can be directly computed using results of Section 5.1.2, specifically (5.22).[22] Terms of order $\lambda^2 h$ can be computed using a trick discussed in [126]; since they are linear in h, they can be easily obtained from the dimensions of corresponding operators in the bulk theory (at the trivial defect).

In the $O(N)$ symmetric case $h_{ab} = \delta_{ab}h$, the beta function simplifies to

$$\beta_h = -\varepsilon h + h^2 + \lambda(N+2)h(1-2h) - \frac{5}{6}\lambda^2(N+2)h\,. \tag{3.116}$$

This result was also computed in [127]. The beta function (3.4.1) admits a real fixed point for any value of N, where correlators describe a dCFT. At this fixed point, one can compute several observables. For example, the dimension of $\hat{\phi}^2$ at the fixed point is

$$\hat{\Delta}_{\hat{\phi}^2} = 2 + \frac{\partial\beta_h}{\partial h}\Big|_{\lambda_*,h_*} = 2 + \frac{6\varepsilon}{N+8} - \frac{(N+2)(13N+44)\,\varepsilon^2}{2(N+8)^3} + \mathrm{O}(\varepsilon^3)\,. \tag{3.117}$$

In the similar context of the ϕ^2 deformation integrated on a boundary, the extrapolation from the two-loop result [128] was already very close to the result of the numerical boundary bootstrap [15]. One can expect a similar behaviour here. Indeed, for example by setting $N = 1$ one finds that the Padé approximants at $\varepsilon = 1$ are already relatively close to each other

$$\hat{\Delta}_{\hat{\phi}^2}[2/0] \approx 2.55\,, \qquad \hat{\Delta}_{\hat{\phi}^2}[1/1] \approx 2.57\,. \tag{3.118}$$

In [129] it was proposed that at $\varepsilon = 1$ this fixed point describes an interface between two copies of the $O(N)$ CFT with Dirichlet boundary conditions. However, a singlet primary operator with dimension given by (3.118) should be absent in such a dCFT (this is again known

[21] In [123, 125] one can find also a large-N analysis of the same defect.

[22] In fact, these results are a secondary outcome of the analysis of *transdimensional defects* presented in [36].

from the results of the numerical boundary bootstrap [15]). Numerical evidence presented in [127] suggests that the operator $\hat{\phi}^2$ factorises into two different copies of the boundary operator $\partial_\perp \hat{\phi}$. Indeed one can check that $\Delta_{\hat{\phi}^2} \approx 2\Delta_{\partial_\perp \hat{\phi}}$.

One can also allow for symmetry-breaking patterns, where h_{ab} is not proportional to δ_{ab}. Without loss of generality, one can assume that h_{ab} is diagonal. A real fixed point is found for some symmetry-breaking patterns of the form $O(N) \to O(m) \times O(n)$ with $m+n=N$ [123]. In this case, h_{ab} has m eigenvalues of value h_m and n eigenvalues of value h_n. The two couplings h_m and h_n have their own beta-function that follow directly from (3.115). At two loops one finds [36]

$$\beta_{h_m} = -\varepsilon h_m + h_m^2 + \lambda[(m+2)h_m + nh_n - 2(m+2)h_m^2 - 2nh_m h_n] - \lambda^2[\tfrac{1}{2}h_m(5m+n+10) + 2nh_n]\,, \tag{3.119}$$

$$\beta_{h_n} = -\varepsilon h_n + h_n^2 + \lambda[(n+2)h_n + mh_m - 2(n+2)h_n^2 - 2mh_m h_n] - \lambda^2[\tfrac{1}{2}h_n(m+5n+10) + 2mh_m]\,. \tag{3.120}$$

Zeroes of these beta functions at the $O(N)$ bulk fixed point, where $\lambda = \frac{1}{N+8}\varepsilon + \frac{3(3N+14)}{(N+8)^3}\varepsilon^2$, are found by substituting $h_m = h_m^{(1)}\varepsilon + h_m^{(2)}\varepsilon^2$ and similarly for h_n into (3.119), (3.120), and solving the resulting equations order by order in ε. At leading order this yields two fixed points, given by

$$h_{m,\pm}^{(1)} = \frac{m+3 \pm \sqrt{9-mn}}{m+n+8}\,, \qquad h_{n,\pm}^{(1)} = \frac{n+3 \mp \sqrt{9-mn}}{m+n+8}\,. \tag{3.121}$$

The expressions for $h_{m,\pm}^{(2)}, h_{n,\pm}^{(2)}$ and the analogue of (3.117) are easy to work out but too complicated to present here.

Due to the square root $\sqrt{9-mn}$, these fixed points exist only for $mn \leqslant 9$. This inequality is saturated for integer m,n when $m=1, n=9$ and when $m=n=3$ where, without loss of generality, it is assumed that $m \leqslant n$. For these values of m,n the two fixed points collide and they move off to the complex plane for $mn > 9$. This collision point is corrected at next-to-leading order in ε, and a standard analysis following [130] shows that the critical n for which the two fixed points collide is given by

$$n_c = \frac{9}{m} - \frac{3(m^2-22m+9)}{2m(m^2+8m+9)}\varepsilon + \mathrm{O}(\varepsilon^2)\,. \tag{3.122}$$

For $m = 1$ this becomes $9+\varepsilon$ and for $m = 3$ it becomes $3+\frac{4}{7}\varepsilon$. In both cases the collision point lies above 9 and 3, respectively, which renders the fixed points at $m = 1, n = 9$ and $m = n = 3$ unitary. Nevertheless, the ε expansion that has been used so far breaks down and an expansion of h_m, h_n involving half-integer powers of ε is necessary to describe them. For $m = 1, n = 9$ one finds the two fixed points

$$h_{m=1,\pm} = \tfrac{2}{3}\varepsilon \pm \tfrac{1}{18}\varepsilon^{3/2} + \mathrm{O}(\varepsilon^2)\,, \qquad h_{n=9,\pm} = \tfrac{2}{9}\varepsilon \mp \tfrac{1}{18}\varepsilon^{3/2} + \mathrm{O}(\varepsilon^2)\,, \tag{3.123}$$

and for $m = n = 3$

$$h_{m=3,\pm} = \tfrac{3}{7}\varepsilon \pm \tfrac{\sqrt{21}}{49}\varepsilon^{3/2} + \mathrm{O}(\varepsilon^2)\,, \qquad h_{n=3,\pm} = \tfrac{3}{7}\varepsilon \mp \tfrac{\sqrt{21}}{49}\varepsilon^{3/2} + \mathrm{O}(\varepsilon^2)\,. \tag{3.124}$$

Note that in the $m = n = 3$ case the defect symmetry at leading order is $O(3)^2 \rtimes \mathbb{Z}_2$, but this is broken to $O(3)^2$ at next-to-leading order.

The cubic defect

If $p = 3$, it is possible to consider the deformation given by the following defect action

$$S_{\mathcal{D}} = \int d^{3-\varepsilon}\tau \left(\frac{h_1}{2}\phi_1\phi_a\phi_a + \frac{h_2}{3!}\phi_1^3\right)\,. \tag{3.125}$$

This action explicitly breaks the $O(N)$ symmetry down to $O(N-1)$. The action (3.125) was considered in [131], where it was found that, for an interface, a real fixed point exists for $N < N_{\text{crit}} \approx 7$, whereas for $N > 4$, IR stable fixed points with purely imaginary defect couplings appear. For a boundary, real fixed points exist for any value of N. This defect will not be further analysed in this thesis, although, in principle, a variety of methods and results from the following chapters could be generalised to this model.

3.4.2 Strongly-coupled defects

In the previous sections, defects have been realised as fixed points of defect RG flows triggered by interactions that are classically marginal. However, strongly relevant interactions might as well originate a defect RG flow that ends in an IR fixed point. The latter case is in general more difficult to study, since the defect coupling is usually not perturbatively small. One way to get around this problem is to look for non-trivial saddle points of the path integral that respects the defect-conformal symmetry group. Perturbation theory around these new saddles can then be used to compute quantum corrections for various observables.

To illustrate this idea, one can consider the local $O(N)$ model, whose action is

$$S_{\text{bulk}} = \int d^d x \left(\frac{1}{2} (\partial \phi_a)^2 + \frac{\lambda_0}{4!} (\phi_a)^2 \right) . \tag{3.126}$$

One can add an interaction localised on a p-dimensional defect

$$S_D = h_0 \int d^p \tau \ \phi_1 . \tag{3.127}$$

When $d = 4 - \varepsilon$ and $p = 1$, the interaction is marginally relevant and one can therefore use standard diagrammatic techniques to compute observables [109, 32]. In the more general case, the beta-function for the defect coupling reads

$$\beta_h = -(p - \Delta_\phi)\, h + \mathrm{O}(\lambda) , \tag{3.128}$$

with $\Delta_\phi = (d-2)/2$. If $d = 4-\varepsilon$ (but with p generic), the bulk coupling constant undergoes a "short" RG flow from the Gaussian fixed point to the Wilson-Fisher fixed point. At any scale μ the following inequality holds

$$0 \leqslant \lambda(\mu) \leqslant \lambda_* = \frac{48\pi^2}{N+8}\, \varepsilon + \mathrm{O}(\varepsilon^2) , \tag{3.129}$$

and in the IR limit one has $\lim_{\mu \to 0} \lambda(\mu) = \lambda_*$. Using this bound, one can solve (3.128) for $h(\mu)$

$$h(\mu) = h(\mu_0) \left(\frac{\mu}{\mu_0} \right)^{-(p-\Delta_\phi)+\mathrm{O}(\varepsilon)} . \tag{3.130}$$

It is now evident that if $p - \Delta_\phi \gg \varepsilon$, then $h(\mu)$ rapidly flows to infinity in the IR limit, while $\lambda(\mu)$ is still perturbatively small. This new phase of the theory should correspond to a non-trivial saddle point of the path integral. The saddle point is described by a classical profile $\phi^a_{\text{cl}}(x)$ that satisfies the classical equations of motion. One can formulate an *ansatz* that respects all the symmetries of the problem

$$\phi^a_{\text{cl}}(x) = \delta_{a1} \frac{\mathcal{N}_\phi\, a_{\text{cl}}}{|x_\perp|^{\Delta_{\text{cl}}}} . \tag{3.131}$$

The equations of motion yield

$$\Box \phi^a_{\text{cl}}(x) = \frac{\mathcal{N}_\phi\, a_{\text{cl}}}{|x_\perp|^{\Delta_{\text{cl}}+2}} \left(\Delta_{\text{cl}} \left(\Delta_{\text{cl}} + p + \varepsilon - 2 \right) \right) \delta_{a1} = \frac{\lambda_0}{3!} \frac{\mathcal{N}_\phi^3\, {a_{\text{cl}}}^3}{|x_\perp|^{3\Delta_{\text{cl}}}}\, \delta_{a1} . \tag{3.132}$$

This is readily solved

$$\Delta_{\text{cl}} = 1 , \quad \mathcal{N}_\phi^2\, {a_{\text{cl}}}^2 = \frac{6}{\lambda_0} (p + \varepsilon - 1) . \tag{3.133}$$

The two solutions for $a_{\rm cl}$ are associated to the $\mathbb{Z}_2$ symmetry $\phi_a \to -\phi_a$, which is explicitly broken by the defect. In the following, the focus will be on the solution $a_{\rm cl} > 0$. To compute observables, one can expand the bulk action around this new saddle point

$$\phi^a(x) = \phi^a_{\rm cl}(x) + \delta\phi^a(x)\,, \quad S'[\delta\phi^a] = S_{\rm bulk}[\phi^a_{\rm cl} + \delta\phi^a] - S_{\rm bulk}[\phi^a_{\rm cl}]\,, \tag{3.134}$$

and then use standard diagrammatic techniques with the new action $S'[\delta\phi^a]$.[23] Note that $\phi^a_{\rm cl}(x)$ plays the role of a classical external source in this new action.

For some simple observables, the semiclassical analysis is sufficient to determine their value at the IR fixed point at leading order. For instance, for the order parameter one has

$$\langle\phi^a(x)\rangle = \phi^a_{\rm cl}(x) + \langle\delta\phi^a(x)\rangle\,, \tag{3.135}$$

where the second term at the IR fixed point is of order $\varepsilon^{\frac{1}{2}}$ and is therefore subleading. Moreover, conformal symmetry imposes

$$\langle\phi^a(x)\rangle = \delta_{a1}\frac{\mathcal{N}_\phi\, a_\phi}{|x_\perp|^{\Delta_\phi}}\,. \tag{3.136}$$

From this it follows that at the IR fixed point

$${a_\phi}^2 = {a_{\rm cl}}^2(1 + \mathrm{O}(\varepsilon)) = \frac{24\pi^2}{\lambda_*}\,(p-1) + \mathrm{O}(\varepsilon^0)\,. \tag{3.137}$$

For the boundary case $p = 3 - \varepsilon$, this is indeed the correct value of the coefficient of the one-point function [132].

Note that for $p = 1$ the classical contribution is vanishing as expected, since in that case the defect interaction is classically marginal. Interestingly, the equations of motion toghether with conformal symmetry can still be used to find the coefficient of the one-point function at leading order. Indeed, from the original action S it is evident that $\langle\phi^a\phi^b\phi^b\rangle = \langle\phi^a\rangle\langle\phi^b\rangle\langle\phi^b\rangle + \mathrm{O}(\lambda)$. Assuming the form of the one-point function at the fixed point (3.136), the expectation value of the equation of motion then gives [24]

$${a_\phi}^2 = \frac{N+8}{4} + \mathrm{O}(\varepsilon)\,, \tag{3.138}$$

[23] In this realisation, the presence of the defect is imposed trough the *ansatz* (3.131) instead of an explicit defect term in the action.

[24] Note that this is not equivalent as taking $p = 1$ in (3.133) and expanding. Indeed to get the correct result one need Δ_ϕ instead of $\Delta_{\rm cl}$, together with the fact that at order $O(\varepsilon)$ the operator ϕ has no anomalous dimension.

which agrees with the result of (3.24) computed with Feynman diagrams.

More details about this method are given in Section 6.2.3, where it will be applied to the localised magnetic field for the long-range $O(N)$ model, following [37].

Chapter 4

Analytic bootstrap for line defects in the O(N) model

4.1 Lorentzian inversion formulae and dispersion relation

As outlined in Section 2.2.5, the defect data must satisfy a complicated set of constraints in order to be consistent with the bulk CFT. The goal of the defect bootstrap programme is to use these constraints to extract information about the defect data, starting from the bulk data. The main tools for defect bootstrap in its analytic form are presented in this section: the *Lorentzian inversion formulae* and the *dispersion relation*. Once these tools have been introduced, they will be applied in Sections 4.2 and 4.3 to derive as much information as possible about the localised magnetic field and the magnetic impurity in the ε-expansion, introduced in Sections 3.2 and 3.3, respectively.

The first Lorentzian inversion formula was introduced to study homogeneous CFTs analytically [6]. It is an integral formula which reconstructs the OPE data of any CFT from the double discontinuity of four-point functions. In favourable situations, the double discontinuity receives contributions only from very few operators and the inversion formula can extract from it an infinite amount of CFT data [133, 134].

For the defect case, there are two analogous formulae. A defect inversion formula was derived in [18] and allows to extract the defect channel

CFT data from a single discontinuity of the bulk two-point function

$$b(\hat{\Delta},s)=\int_0^1\frac{dz}{2z}z^{-\frac{\hat{\tau}}{2}}\int_1^{\frac{1}{z}}\frac{d\bar{z}}{2\pi i}\frac{(1-z\bar{z})(\bar{z}-z)}{\bar{z}^{\frac{\hat{\Delta}+s}{2}+2}}{}_2F_1\Big(s+1,2-\frac{q}{2},\frac{q}{2}+s,\frac{z}{\bar{z}}\Big)$$
$$ {}_2F_1\left(1-\hat{\Delta},1-\frac{p}{2},1+\frac{p}{2}-\hat{\Delta},z\bar{z}\right)\mathrm{Disc}\,F(z,\bar{z})\,, \tag{4.1}$$

where $\hat{\tau}$ is the *transverse twist* defined by $\hat{\tau}=\hat{\Delta}-s$, and $F(z,\bar{z})$ is related to the bulk two-point function as in (2.57). The coefficient function $b(\hat{\Delta},s)$ has simple poles for $\hat{\Delta}$ equal to the dimensions of exchanged operators and residues given by the defect OPE coefficients $b^2_{\hat{\Delta},s}$. Therefore, $b(\hat{\Delta},s)$ contains all the CFT data of the exchanged defect operators. The crucial ingredient of this inversion formula is the discontinuity

$$\mathrm{Disc}F(z,\bar{z})=F(z,\bar{z}+i\varepsilon)-F(z,\bar{z}-i\varepsilon)\,, \tag{4.2}$$

where $F(z,\bar{z}+i\varepsilon)$ and $F(z,\bar{z}-i\varepsilon)$ indicate that $\bar{z}$ should be taken above or below the branch cut at $\bar{z}=1$, leaving z fixed. The defect inversion formula was derived in [18] through a contour deformation argument, which is justified only if the integrand vanishes sufficiently fast for large w, or equivalently for $w\to 0$ since the correlator is symmetric under $w\leftrightarrow\frac{1}{w}$. More precisely, this implies that the formula (4.1) is valid for transverse spin $s>s_*$ if

$$F(r,w)\sim w^{-s_*}\,,\qquad w\to 0\,. \tag{4.3}$$

This implies that, in general, the inversion formula may fail to capture contributions to the CFT data from low-spin operators. Currently, no upper bound has been established for the value of s_*; however, it can be stated with certainty that s_* cannot universally be lower than zero (in other words, the Lorentzian inversion formula cannot be expected to work for spin-zero operators in the case of an arbitrary line defect). A simple way to motivate this statement is that, in general, multiple defects can be constructed for the same bulk theory. For instance, in the case of the $O(N)$ critical model with $N=3$, at least the localised magnetic field and the magnetic impurity exist. For both of these cases, the discontinuity of the correlator at first order is identical, as it depends solely on bulk CFT data. However, the defect CFT data differ due to low-spin ambiguities.

There is also a bulk inversion formula, which allows to extract the bulk

OPE data from a double discontinuity [22]. The formula reads [1]

$$\begin{aligned} c(\Delta,\ell) &= c^t(\Delta,\ell) + (-1)^\ell c^u(\Delta,\ell), \\ c^t(\Delta,\ell) &= \frac{\kappa_{\Delta+\ell}}{2}\int_0^1 d^2z\ \mu(z,\bar z)\ f_{\ell+d-1,\Delta-d+1}(z,\bar z) \\ &\qquad \text{dDisc}\left(\left(\frac{(1-z)(1-\bar z)}{\sqrt{z\bar z}}\right)^{\Delta_\phi} F(z,\bar z)\right), \end{aligned} \tag{4.4}$$

with

$$\begin{aligned} \kappa_{\Delta+\ell} &= \frac{\Gamma(\frac{\Delta+\ell}{2})^4}{2\pi^2\Gamma(\Delta+\ell)\Gamma(\Delta+\ell-1)}, \\ \mu(z,\bar z) &= \frac{|z-\bar z|^{d-p-2}|1-z\bar z|^p}{(1-z)^d(1-\bar z)^d}, \end{aligned} \tag{4.5}$$

and where $f_{\Delta,\ell}(z,\bar z)$ are the bulk blocks. The u-channel term is the same with the two external bulk operators exchanged. In this case, the coefficient function $c(\Delta,\ell)$ has poles corresponding to the dimensions of the operators that are exchanged in the bulk OPE and corresponding residues given by the product of bulk three-point functions and one-point functions, $\lambda_{\phi\phi\mathcal{O}}a_{\mathcal{O}}$. The input of the formula is the double discontinuity defined by

$$\text{dDisc}F(z,\bar z) = F(z,\bar z) - \frac{1}{2}F^{\circlearrowleft}(z,\bar z) - \frac{1}{2}F^{\circlearrowright}(z,\bar z), \tag{4.6}$$

where this time the functions $F^{\circlearrowleft}(z,\bar z)$ and $F^{\circlearrowright}(z,\bar z)$ are obtained by taking the analytic continuation around the point $\bar z = 0$, leaving z fixed. Just like the defect inversion formula, the bulk inversion formula might fail for low spins [22]. More precisely, the formula is valid for spins $\ell > \ell_*$ where

$$\left(\frac{(w-r)(1-wr)}{rw}\right)^{\Delta_\phi} F(r,w) \lesssim w^{1-\ell_*}, \qquad w\to 0. \tag{4.7}$$

The two Lorentzian inversion formulae allow to extract the defect CFT data of the theory from certain discontinuities of the two-point functions. Therefore, these discontinuities contain all the information that is necessary to reconstruct the full correlator. This is made explicit in the dispersion relation, a formula that computes the full correlator directly from a discontinuity [68]. In the case of defect CFTs, the dispersion relation reads [26, 27]

$$F(r,w) = \int_0^r \frac{dw'}{2\pi i}\left(\frac{1}{w'-w} + \frac{1}{w'-\frac{1}{w}} - \frac{1}{w'}\right)\text{Disc}F(r,w'), \tag{4.8}$$

[1] Compared to [22], the bulk inversion formula is rewritten for $\left(\frac{(1-z)(1-\bar z)}{\sqrt{z\bar z}}\right)^{\Delta_\phi} F(z,\bar z)$ instead of $F(z,\bar z)$, in order to use a more conventional definition of the double discontinuity.

where Disc $F(r,w)$ is the discontinuity through the cut running from $w=0$ to $w=r$. From the definition of the variable w, it follows that $\text{Disc}F(r,w) = -\text{Disc}F(z,\bar{z})$, as defined in (4.2). Just like the defect inversion formula (4.1), this dispersion relation is derived from Cauchy's theorem by deforming the contour around the singularities and dropping the contributions at infinity. This contour deformation argument misses terms that are given by low spin conformal blocks, which give contributions at infinity. If one knows the behaviour of the correlator for $w \to 0$ (or equivalently for $|w| \to \infty$) (4.3), one can take into account these terms by introducing a prefactor in front of the correlator

$$\tilde{F}(r,w) = \left(\frac{r}{(w-r)(\frac{1}{w}-r)}\right)^{s_*+1} F(r,w)\,. \tag{4.9}$$

By construction, $\tilde{F}(r,w)$ goes like w^{-1} at large w and therefore one can safely ignore the contribution at infinity and reconstruct this rescaled correlator from (4.8). From the point of view of the original correlator, this implies an improved dispersion relation

$$\begin{aligned}\frac{F(r,w)}{(w-r)^{s_*+1}(\frac{1}{w}-r)^{s_*+1}} = \int_0^r \frac{dw'}{2\pi i}\left(\frac{1}{w'-w}+\frac{1}{w'-\frac{1}{w}}-\frac{1}{w'}\right)\\ \text{Disc}\left(\frac{F(r,w')}{(w'-r)^{s_*+1}(\frac{1}{w'}-r)^{s_*+1}}\right)\,.\end{aligned} \tag{4.10}$$

In the following, the formulae introduced in this section will be applied to the ε-expansion of correlators in the critical $O(N)$ model.

4.2 Analytic bootstrap for the localised magnetic field

This section applies the techniques introduced in Section 4.1 to study the localised magnetic field in the ε-expansion. First, the tree-level case is considered in Section 4.2.1 as a warm-up. Then, in Section 4.2.2, the same methods are used to extract an infinite amount of new defect data at one loop, following [34]. A similar analysis can be found in [135].

4.2.1 Tree level

At leading order in the ε-expansion, the correlator contains two terms: the free correlator without the defect which contributes to F_1 in (3.28) and the square of the one-point function (3.23) which gives the leading contribution to F_2.[2] In particular, the perturbative expansion of a_ϕ in

[2]The defect coupling at the fixed point is not perturbatively small, hence the one-point function of local operators are not suppressed in the ε-expansion.

(3.23) reads [109, 32]

$$a_\phi^2 = \frac{N+8}{4} + \varepsilon \frac{(N^2 - 3N + (N+8)^2 \log(4) - 22)}{8(N+8)} + \mathrm{O}(\varepsilon^2)\,, \quad (4.11)$$

and the leading-order contribution to the two-point function is

$$F_1^{(0)}(r,w) = \frac{rw}{(r-w)(rw-1)}\,, \qquad F_2^{(0)}(r,w) = a_\phi^{2\,(0)}\,. \quad (4.12)$$

Each of these two terms has a simple interpretation in one of the two channels. The free correlator $F_1^{(0)}$ corresponds to the exchange of the identity operator in the bulk channel, while the squared one-point function is associated to the exchange of the defect identity in the defect channel. On the other hand, as usual, to reproduce the identity in a given channel, an infinite tower of operators is needed in the crossed one. The CFT data of these exchanged operators will now be reviewed.

Using the linear combinations in (A.7), one can rewrite (4.12) in terms of F_S and F_T introduced in (3.33)

$$\begin{aligned} F_S^{(0)}(r,w) &= \frac{a_\phi^{2\,(0)}}{N} + \frac{rw}{(r-w)(rw-1)}\,, \\ F_T^{(0)}(r,w) &= a_\phi^{2\,(0)}\,. \end{aligned} \quad (4.13)$$

From this expression, it is obvious that the bulk identity contributes only to the singlet exchange. On the other hand, the constant term $a_\phi^{2\,(0)}$ can be reproduced by the exchange of two infinite towers of twist-two spin-ℓ operators of the schematic form [3]

$$[\phi^2]_{S,0,\ell} = \phi^a \partial_{\mu_1} ... \partial_{\mu_\ell} \phi_a\,, \quad [\phi^a \phi^b]_{T,0,\ell} = \phi^{(a} \partial_{\mu_1} ... \partial_{\mu_\ell} \phi^{b)} - \text{trace}\,. \quad (4.14)$$

Their CFT data can be extracted simply by comparing (4.13) with the block expansion (3.36) or from the Lorentzian inversion formula (4.4) using [4]

$$\begin{aligned} \mathrm{dDisc}\left(\left(\frac{(1-z)(1-\bar{z})}{\sqrt{z\bar{z}}}\right)^{\Delta_\phi} F_S^{(0)}(z,\bar{z})\right) &= 2\frac{a_\phi^{2\,(0)}}{N}\frac{(1-z)(1-\bar{z})}{\sqrt{z\bar{z}}}\,, \\ \mathrm{dDisc}\left(\left(\frac{(1-z)(1-\bar{z})}{\sqrt{z\bar{z}}}\right)^{\Delta_\phi} F_T^{(0)}(z,\bar{z})\right) &= 2a_\phi^{2\,(0)}\frac{(1-z)(1-\bar{z})}{\sqrt{z\bar{z}}}\,. \end{aligned} \quad (4.15)$$

[3] This symbolic notation is used to indicate the number of derivatives associated with a given twist-two primary operator.

[4] As mentioned in Section 4.1, the Lorentzian inversion formula does not work for low spins and in this case it does not reproduce the contribution of the bulk identity. Nevertheless, it still reproduces correctly all the defect CFT data of the twist-two operators.

The result is [5] [22]

$$\begin{aligned}
&\Delta^{(0)}_{S,0,\ell} = \Delta^{(0)}_{T,0,\ell} = 2\Delta_\phi + \ell\,, \\
&a\lambda^{(0)}_{T,k,\ell} = a\lambda^{(0)}_{S,k,\ell}\; N = \delta_{k,0}\; a_\phi^{2\,(0)}\, \frac{2^{-\ell}\Gamma\left(\frac{\ell+1}{2}\right)^3}{\pi\Gamma\left(\frac{\ell}{2}+1\right)\Gamma\left(\ell+\frac{1}{2}\right)}\,,
\end{aligned} \tag{4.16}$$

where the spin ℓ is even. The labels for the operators, which will remain unchanged at order ε, are now discussed. The index k is used to label the classical twist $\tau^{(0)} = \Delta^{(0)} - \ell$, specifically $k = \frac{\tau^{(0)}}{2} - \Delta_\phi$. At this order, only two families of operators appear in the bulk OPE: the identity and the twist-two operators ($k = 0$). Moreover, for the case $k = 0$, it is known that there is a single primary operator for each spin ℓ. This is no longer the case for higher values of k, where degeneracies may arise. As a result, the notation will not distinguish between degenerate operators; however, this will not be necessary for the current analysis.

Moving on to the defect channel, one has

$$\begin{aligned}
\hat{F}^{(0)}_S(r,w) &= a_\phi^{2\,(0)} + \frac{rw}{(r-w)(rw-1)}\,, \\
\hat{F}^{(0)}_V(r,w) &= \frac{rw}{(r-w)(rw-1)}\,,
\end{aligned} \tag{4.17}$$

where again the defect identity only enters the singlet channel, while the bulk identity is reproduced by two infinite towers of defect operators of the schematic form

$$[\phi]_{S,0,s} = \partial_\perp^s \hat{\phi}\,, \qquad [\phi^{\hat{a}}]_{V,0,s} = \partial_\perp^s \hat{\phi}^{\hat{a}}\,. \tag{4.18}$$

These operators have transverse spin s and transverse twist $\hat{\tau} = \hat{\Delta} - s = 1$. As before, one can compare (4.17) with the block expansion (3.39) or use the inversion formula (4.1) with [6]

$$\begin{aligned}
\mathrm{Disc}\hat{F}^{(0)}_S(r,w) &= 2\pi i\left(\frac{rw}{1-rw}\right)\delta(r-w)\,, \\
\mathrm{Disc}\hat{F}^{(0)}_V(r,w) &= 2\pi i\left(\frac{rw}{1-rw}\right)\delta(r-w)\,.
\end{aligned} \tag{4.19}$$

The result is [18, 17]

$$\begin{aligned}
\hat{\Delta}^{(0)}_{S,0,s} &= \hat{\Delta}^{(0)}_{V,0,s} = 1 + s\,, \\
\hat{b}^{2(0)}_{S,m,s} &= \hat{b}^{2(0)}_{V,m,s} = \delta_{m,0}\,.
\end{aligned} \tag{4.20}$$

[5] The twist-two operators have the same dimensions in both channel at tree level, however they are distinct operators and have different anomalous dimensions and OPE coefficients.

[6] Also in this case the Lorentzian inversion formula fails to reproduce the contribution of the identity.

As in the bulk case, an additional label m is used for the classical transverse twist, defined as $m = \frac{\hat{\tau}^{(0)}-1}{2}$. In this case, only twist-one operators ($m = 0$) appear in the OPE, as expected from the equation of motion of the bulk field [18].

4.2.2 One loop

As previously remarked, the idea behind the defect analytic bootstrap is to use information from the bulk theory to compute correlators in the presence of the defect. In particular, the discontinuity relevant to the dispersion relation (4.8) is controlled by the bulk block expansion. Hence, one needs to analyse the operators appearing in the perturbative expansion of (3.36). The bulk channel CFT data can be perturbatively expanded as follows

$$\begin{aligned} \Delta &= \Delta^{(0)} + \varepsilon\, \gamma^{(1)} + \mathrm{O}(\varepsilon^2)\,, \\ \lambda_{\phi\phi\Delta} a_\Delta &= a\lambda^{(0)} + \varepsilon\, a\lambda^{(1)} + \mathrm{O}(\varepsilon^2)\,. \end{aligned} \tag{4.21}$$

More precisely, operators that appeared at tree level, namely twist-two operators, enter in the one-loop OPE with their anomalous dimensions

$$\Delta_{S/T,0,\ell} = 2\Delta_\phi + \ell + \varepsilon\gamma^{(1)}_{S/T,0,\ell} + \mathrm{O}(\varepsilon^2)\,, \tag{4.22}$$

which are known from previous work on the $O(N)$ model without defects (see for example [95] and references therein)

$$\gamma^{(1)}_{S,0,\ell} = \frac{N+2}{N+8}\delta_{0,\ell}\,, \qquad \gamma^{(1)}_{T,0,\ell} = \frac{2}{N+8}\delta_{0,\ell}\,. \tag{4.23}$$

Notice the crucial fact that only the spin-zero operator of each representation has a non-vanishing anomalous dimension at one loop. This will be extremely important for the computation of the discontinuity.

The second contribution one needs to consider originates from the anomalous dimension of the external operator ϕ_a

$$\Delta_\phi = 1 - \frac{\varepsilon}{2} + \varepsilon\gamma^{(1)}_\phi + \mathrm{O}(\varepsilon^2)\,, \tag{4.24}$$

which gives a correction to the bulk identity contribution

$$\begin{aligned} \left(\frac{rw}{(r-w)(rw-1)}\right)^{\Delta_\phi} &= \frac{rw}{(r-w)(rw-1)}\Bigg(1+ \\ &+ \varepsilon\left(\gamma^{(1)}_\phi - \frac{1}{2}\right)\log\left(\frac{rw}{(1-rw)(w-r)}\right) + \mathrm{O}(\varepsilon^2)\Bigg)\,. \end{aligned} \tag{4.25}$$

Specifically, the anomalous dimension $\gamma_\phi^{(1)}$ is well-known to be vanishing at one loop, *i.e.* $\gamma_\phi^{(1)} = 0$, but clearly this does not kill the contribution (4.25).

In principle, one can also have operators with higher twist, which appear in the OPE with their classical dimensions

$$\Delta_{S/T,k,\ell} = 2\Delta_\phi + 2k + \ell + \mathrm{O}(\varepsilon)\,, \qquad k > 0\,. \tag{4.26}$$

In particular, only operators with twist up to 4 are expected, since the bulk OPE coefficients of higher-twist operators are of order ε^2 [136,137]. Nevertheless, while there is a single family of operators with twist two, *i.e.* a single primary operator for each spin, starting from twist four there can be degenaracies which cannot be lifted by studying a single correlator. Luckily, these operators do not contribute to the discontinuity in (4.8) so this is not an issue to reconstruct the full correlator. Further discussion on this matter will be provided in Section 4.2.3.

All in all, the one-loop bulk block expansion for the singlet reads

$$\begin{aligned} F_S^{(1)}(r,w) = &-\frac{rw}{2(1-rw)(w-r)}\log\left(\frac{rw}{(1-rw)(w-r)}\right)+ \\ &+\frac{rw}{2(1-rw)}a\lambda^{(0)}_{S,0,0}\gamma^{(1)}_{S,0,0}\left(\tilde{f}_{2,0}(r,w)\log(w-r)+\partial_\Delta\tilde{f}_{2,0}(r,w)\right)+ \\ &+\sum_{k=0}^{1}\sum_{\ell}\ \frac{rw}{1-rw}a\lambda^{(1)}_{S,k,\ell}(w-r)^k\tilde{f}_{2+2k+\ell,\ell}(r,w)\,, \end{aligned} \tag{4.27}$$

where $\tilde{f}_{\Delta,\ell}(r,w) = (w-r)^{\frac{-\Delta+\ell}{2}} f_{\Delta,\ell}$, with $f_{\Delta,\ell}$ given in (A.2). For the symmetric traceless part one has

$$\begin{aligned} F_T^{(1)}(r,w) = &\frac{rw}{2(1-rw)}a\lambda^{(0)}_{T,0,0}\gamma^{(1)}_{T,0,0}\Big(\tilde{f}_{2,0}(r,w)\log(w-r) \\ &+\partial_\Delta\tilde{f}_{2,0}(r,w)\Big)+\sum_{k=0}^{1}\sum_{\ell}\frac{rw}{1-rw}a\lambda^{(1)}_{T,k,\ell}(w-r)^k\tilde{f}_{2+2k+\ell,\ell}(r,w)\,. \end{aligned} \tag{4.28}$$

One can consider an analogous expansion for the defect channel CFT data

$$\begin{aligned} \hat{\Delta} &= \hat{\Delta}^{(0)} + \varepsilon\,\hat{\gamma}^{(1)} + \mathrm{O}(\varepsilon^2)\,, \\ \hat{b} &= \hat{b}^{(0)} + \varepsilon\,\hat{b}^{(1)} + \mathrm{O}(\varepsilon^2)\,. \end{aligned} \tag{4.29}$$

As before, operators with transverse twist one, which already appeared at tree level, enter the block expansion with their anomalous dimension

$$\hat{\Delta}_{S/V,0,s} = 1 + s + \varepsilon\, \hat{\gamma}^{(1)}_{S/T,0,s} + \mathrm{O}(\varepsilon^2)\,, \tag{4.30}$$

while higher-twist operators contribute with their classical dimensions

$$\hat{\Delta}_{S/V,m,s} = 1 + 2m + s + \mathrm{O}(\varepsilon)\,, \qquad m > 0\,. \tag{4.31}$$

n particular, at one loop, only operators with transverse twist one, *i.e.*, $m = 0$, are expected, since higher-twist defect operators have bulk-to-defect couplings $\hat{b}$ of order ε, hence their squared coefficients are at least of order ε^2. This expectation is later confirmed by the inversion formula. The defect block expansions at one loop are given by

$$\begin{aligned}
\hat{F}^{(1)}_S(r,w) &= a_\phi^{2\,(1)} + \sum_s \hat{b}^{2(1)}_{S,0,s} \hat{f}_{1+s,s}(r,w) + \hat{b}^{2(0)}_{S,0,s} \hat{\gamma}^{(1)}_{S,0,s} \partial_{\hat{\Delta}} \hat{f}_{1+s,s}(r,w)\,,\\
\hat{F}^{(1)}_V(r,w) &= \sum_s \hat{b}^{2(1)}_{V,0,s} \hat{f}_{1+s,s}(r,w) + \hat{b}^{2(0)}_{V,0,s} \hat{\gamma}^{(1)}_{V,0,s} \partial_{\hat{\Delta}} \hat{f}_{1+s,s}(r,w)\,.
\end{aligned} \tag{4.32}$$

In the following section, the full one-loop correlator is computed using the dispersion relation, after which the results for the defect CFT data are presented.

4.2.3 The full result

The dispersion relation (4.8) can be used to compute the full correlator at one loop, provided the correlator behaves sufficiently well for $w \to 0$, as discussed in (4.3). Specifically, following [34], it is assumed that after subtracting the defect identity (which corresponds to the one-loop correction to the squared one-point function a_ϕ^2), the remaining part of the correlator vanishes as $w \to 0$, *i.e.* that $s_* < 0$ in (4.3). This assumption was verified by comparing the non-trivial part of the full correlator, obtained from the dispersion relation (4.35), with the numerical integration of the result from Feynman diagrams presented in Appendix B.1.3. Perfect agreement was found between the two results.

The main ingredient of the dispersion relation is the discontinuity (4.2). The discontinuity can be computed term by term in the bulk-channel block expansion. It is convenient to consider the singlet and traceless contribution separately. Starting from the singlet representation, one can see from (4.27) that the discontinuity at first order in the ε-expansion is given only by the logarithmic terms, because the blocks $\tilde{f}_{\Delta,\ell}(r,w)$ and their derivatives, evaluated at the tree-level dimensions

(4.16), are regular at $w = r$. Crucially, these terms are proportional to tree-level data and one-loop anomalous dimensions. Notice that (4.23), combined with (4.27), implies that the one-loop discontinuity of the singlet is just given by two terms: one is the correction to the bulk identity from the engineering dimension of the external field and the other one is proportional to a single bulk block. Using

$$\text{Disc}(\log(w-r)) = 2\pi i\,, \tag{4.33}$$

and the explicit form of the bulk blocks as a series expansion (A.2) one finds

$$\begin{aligned}\text{Disc}F_S^{(1)}(r,w) = -\pi i\frac{(rw)}{(r-w)(rw-1)}+\\ +\frac{N+2}{8N}\frac{4\pi\sqrt{rw}\left(F\left(\sin^{-1}\left(\sqrt{r}\sqrt{\frac{r-w}{1-rw}}\right)|\frac{(rw-1)^2}{(r-w)^2}\right)-F\left(\sin^{-1}\left(\frac{\sqrt{\frac{r-w}{1-rw}}}{\sqrt{r}}\right)|\frac{(rw-1)^2}{(r-w)^2}\right)\right)}{r-w}\,,\end{aligned} \tag{4.34}$$

where $F(x\,|\,k)$ represents the incomplete elliptic integral of the first kind. It is important to note that this contribution comes from a single operator in the bulk expansion, namely the operator of twist two and spin zero, ϕ^2, whose anomalous dimension, given in (4.23), is the only input required. The complex form of the function (4.34) arises from the bulk conformal block $\tilde{f}_{2,0}$, which is a particular case of the more complicated expression in (A.2).

The first term in (4.34) trivially reproduces the correction to the bulk identity (4.25), as expected. The second contribution is considerably more complicated, and the corresponding integral in the dispersion relation could not be solved in terms of simple functions. However, the result can be obtained either as a series expansion or as a derivative of a special function. The explicit computation is provided in (B.1.1). Ultimately, the result is

$$\begin{aligned}F^{(1)}(r,w)_{S,\,\text{not id}} &= \frac{N+2}{8N}\sum_{m=0}^{\infty}\frac{2^{1-m}rw(1-r^2)^m G^{4,2}_{4,4}\left(\frac{4w}{wr^2-(w^2+1)r+w}\,\middle|\,\begin{matrix}0,0,\frac{m}{2},\frac{m+1}{2}\\ -\frac{1}{2},0,m,m\end{matrix}\right)}{(m!)(r^2(-w)+rw^2+r-w)} = \\ &= \frac{N+2}{8N}\frac{\partial}{\partial t}\left(\left(\frac{(r-w)(rw-1)}{(1+r)^2w}\right)^t\frac{4r}{(1+r)^2(2t+1)}\times\right.\\ &\qquad\left.\times F^{112}_{101}\left(\begin{matrix}1+t:\frac{1}{2};\frac{1}{2}+t,1;\\ \frac{3}{2}+t:-;1+t;\end{matrix}\quad\left(\frac{1-r}{1+r}\right)^2,\frac{(r-w)(rw-1)}{(1+r)^2w}\right)\right)\Bigg|_{t=0}\\ &\equiv\frac{N+2}{8N}I(r,w)\,,\end{aligned} \tag{4.35}$$

where the result is expressed in terms of an infinite sum of Meijer G-functions $G^{4,2}_{4,4}$ or a derivative of a Kampè de Fèriet function F^{112}_{101} [138], whose definitions are given in Appendix B.1.1. In the last line of (4.35) the function $I(r,w)$ is defined for later convenience. Putting all together and adding back the contribution of the defect identity, the singlet contribution reads

$$F_S^{(1)}(r,w) = \frac{a_\phi^{2\,(1)}}{N} - \left(\frac{rw}{2(1-rw)(w-r)}\right)\log\left(\frac{rw}{(1-rw)(w-r)}\right) + \frac{N+2}{8N} I(r,w)\,. \tag{4.36}$$

One can follow the same argument for the symmetric traceless part, the only difference is that the bulk identity contribution is absent and the overall factor changes because of the OPE data (4.16) and (4.23). The discontinuity reads

$$\begin{aligned} \text{Disc}F_T^{(1)}(r,w) &= 2\pi i\left(\frac{rw}{2(1-rw)}\right) a\lambda^{(0)}_{T,0,0}\gamma^{(1)}_{T,0,0}\tilde{f}_{2,0}(r,w) = \\ &= \frac{\pi\sqrt{rw}\left(F\left(\sin^{-1}\left(\sqrt{r}\sqrt{\frac{r-w}{1-rw}}\right)|\frac{(rw-1)^2}{(r-w)^2}\right) - F\left(\sin^{-1}\left(\frac{\sqrt{\frac{r-w}{1-rw}}}{\sqrt{r}}\right)|\frac{(rw-1)^2}{(r-w)^2}\right)\right)}{r-w}\,. \end{aligned} \tag{4.37}$$

At the end of the day one finds

$$F_T^{(1)}(r,w) = a_\phi^{2\,(1)} + \frac{1}{4} I(r,w)\,. \tag{4.38}$$

Using the combinations in (A.7) one can rewrite the results in terms of the functions $\hat{F}_S$ and $\hat{F}_T$ that are natural in the defect channel as

$$\begin{aligned} \hat{F}_S^{(1)}(r,w) &= a_\phi^{2\,(1)} - \left(\tfrac{rw}{2(1-rw)(w-r)}\right)\log\left(\tfrac{rw}{(1-rw)(w-r)}\right) + \tfrac{3}{8} I(r,w)\,, \\ \hat{F}_V^{(1)}(r,w) &= -\left(\tfrac{rw}{2(1-rw)(w-r)}\right)\log\left(\tfrac{rw}{(1-rw)(w-r)}\right) + \tfrac{1}{8} I(r,w)\,. \end{aligned} \tag{4.39}$$

The computation of the defect CFT data, which appear in the two channels, will now be addressed.

Defect channel data

In principle, the defect CFT data in the defect channel could be extracted by plugging the discontinuity into the defect inversion formula (4.1), under the same assumptions as for the dispersion relation, namely that no low-spin contributions, other than the defect identity, are missing. However, as is typically the case, solving the integral to determine

the full coefficient function $b(\hat{\Delta}, s)$ is challenging. For this reason, the approach of [6], specialised to the case of defects in [18], is followed. A small z expansion is performed in the inversion formula, and the integral is then computed for each term in the expansion. Expanding the defect inversion integral at small z, one obtains

$$\begin{aligned} b(\hat{\Delta}, s) &= \int_0^1 \frac{dz}{2z} z^{-\frac{\hat{\tau}}{2}} \sum_{m=0} z^m \sum_{k=-m}^{m} c_{m,k}(\hat{\Delta}, s) B(z, \beta + 2k)\,, \\ B(z, \beta) &= \int_1^\infty \frac{d\bar{z}}{2\pi i} \bar{z}^{-\frac{\beta}{2}-1}\, \mathrm{Disc}\hat{F}_{S,V}(z, \bar{z})\,, \end{aligned} \tag{4.40}$$

where $\beta = \hat{\Delta} + s = \hat{\tau} + 2s$ and where $c_{m,k}(\hat{\Delta}, s)$ are the coefficients obtained from the small z expansion of the integrand of (4.1). Notice that a term proportional to z^α in the small z expansion reproduces the contribution of twist 2α in the coefficient function $b(\hat{\Delta}, s)$, because the last integral is

$$\int_0^1 dz\, \frac{z^{-\frac{\hat{\tau}}{2}}}{2z} z^\alpha = -\frac{1}{\hat{\tau} - 2\alpha}\,. \tag{4.41}$$

The computation of the coefficient is explicitly shown only for the leading order in the small z expansion, which allows for the extraction of the CFT data for transverse twist equal to 1. Results for higher orders are provided without detailed computation, as the expressions become increasingly complicated.

Starting from (4.34) and (4.37) and performing the linear combinations (A.7), one obtains

$$\begin{aligned} \mathrm{Disc}\hat{F}_S^{(1)}(r, w) &= -\frac{\pi i (rw)}{(r-w)(rw-1)} \\ &\quad + \frac{3\pi\sqrt{rw}\left(F\left(\sin^{-1}\left(\sqrt{r}\sqrt{\frac{r-w}{1-rw}}\right)|\frac{(rw-1)^2}{(r-w)^2}\right) - F\left(\sin^{-1}\left(\frac{\sqrt{\frac{r-w}{1-rw}}}{\sqrt{r}}\right)|\frac{(rw-1)^2}{(r-w)^2}\right)\right)}{2(r-w)}\,, \\ \mathrm{Disc}\hat{F}_V^{(1)}(r, w) &= -\frac{\pi i (rw)}{(r-w)(rw-1)} \\ &\quad + \frac{\pi\sqrt{rw}\left(F\left(\sin^{-1}\left(\sqrt{r}\sqrt{\frac{r-w}{1-rw}}\right)|\frac{(rw-1)^2}{(r-w)^2}\right) - F\left(\sin^{-1}\left(\frac{\sqrt{\frac{r-w}{1-rw}}}{\sqrt{r}}\right)|\frac{(rw-1)^2}{(r-w)^2}\right)\right)}{2(r-w)}\,. \end{aligned} \tag{4.42}$$

One can see that in both the singlet and the vector defect representations there are two contributions in the discontinuity.[7] The first one

[7] Notice that in both channels the discontinuity does not depend on N, therefore the only data in the defect OPE that will depend on N will be the defect identity correction, which is missed by the inversion formula.

comes from the the bulk identity operator. This contribution was already considered in [18] for a generic value of Δ_ϕ and it gives

$$B(z,\beta)_{\text{id}} = \frac{\sin(\pi\Delta_\phi)\Gamma(1-\Delta_\phi)\left(-\frac{\sqrt{z}}{z-1}\right)^{\Delta_\phi}\Gamma\left(\frac{\beta+\Delta_\phi}{2}\right)}{\pi\Gamma\left(\frac{1}{2}(\beta-\Delta_\phi+2)\right)}\,. \tag{4.43}$$

Expanding in ε and selecting the first order gives

$$\begin{aligned} B(z,\beta)^{(1)}_{\text{id}} &= \frac{\sqrt{z}\left(\psi^{(0)}\left(\frac{\beta+1}{2}\right)+\log\left(-\frac{\sqrt{z}}{z-1}\right)+\gamma\right)}{2(z-1)} = \\ &= \frac{1}{4}\sqrt{z}\left(-2\psi^{(0)}\left(\frac{1+\beta}{2}\right)-\log(z)-2\gamma\right)+\mathrm{O}(z^{\frac{3}{2}})\,, \end{aligned} \tag{4.44}$$

where $\psi^{(0)}(z)$ is the digamma function. This result has to be combined with the second contribution in equation (4.42), which can be expanded as

$$\begin{aligned} \mathrm{Disc}\hat{F}_S(z,\bar{z})_{\text{not id}} &= \frac{3}{4}i\pi\sqrt{z}\Bigg(\log(z) \\ &\qquad +\log(\bar{z})-4\log\left(\frac{2\sqrt{\bar{z}}}{\sqrt{\bar{z}}+1}\right)\Bigg)+\mathrm{O}(z^{\frac{3}{2}})\,, \\ \mathrm{Disc}\hat{F}_V(z,\bar{z})_{\text{not id}} &= \frac{1}{4}i\pi\sqrt{z}\Bigg(\log(z) \\ &\qquad +\log(\bar{z})-4\log\left(\frac{2\sqrt{\bar{z}}}{\sqrt{\bar{z}}+1}\right)\Bigg)+\mathrm{O}(z^{\frac{3}{2}})\,. \end{aligned} \tag{4.45}$$

Inserting these discontinuities into (4.40) one finds

$$\begin{aligned} B_S(z,\beta)_{\text{not id}} &= \frac{3\sqrt{z}\left(2(\beta+1)-2(\beta-1)\beta\left(\psi^{(0)}\left(\frac{\beta}{2}\right)+\gamma\right)+(\beta-1)\beta\left(2H_{\frac{\beta-3}{2}}+\log(z)\right)\right)}{4(\beta-1)\beta^2}\,, \\ B_V(z,\beta)_{\text{not id}} &= \frac{\sqrt{z}\left(2(\beta+1)-2(\beta-1)\beta\left(\psi^{(0)}\left(\frac{\beta}{2}\right)+\gamma\right)+(\beta-1)\beta\left(2H_{\frac{\beta-3}{2}}+\log(z)\right)\right)}{4(\beta-1)\beta^2}\,. \end{aligned} \tag{4.46}$$

where H_z are harmonic numbers. Combining both contributions (4.44) and (4.46) in (4.40) it follows that

$$\begin{aligned} B_S(\hat{\Delta},s) &\sim \frac{s-1}{(2s+1)(\hat{\tau}-1)^2}+\frac{2(s-1)H_s+3H_{s+\frac{1}{2}}}{2(2s+1)(\hat{\tau}-1)}\,, \\ b_V(\hat{\Delta},s) &\sim \frac{s}{(2s+1)(\hat{\tau}-1)^2}+\frac{(2s+1)\left(2sH_s+H_{s-\frac{1}{2}}\right)+2}{2(2s+1)^2(\hat{\tau}-1)}\,. \end{aligned} \tag{4.47}$$

The appearance of double poles signals the presence of anomalous dimensions, indeed

$$b(\hat{\Delta}, s) \sim \frac{\hat{b}^{(0)} + \varepsilon \hat{b}^{(1)}}{\hat{\tau}^{(0)} + \varepsilon \hat{\gamma}^{(1)} - 1} = \frac{\hat{b}^{(1)}}{\hat{\tau}^{(0)} - 1} - \frac{\hat{b}^{(0)} \hat{\gamma}^{(1)}}{(\hat{\tau}^{(0)} - 1)^2}. \tag{4.48}$$

Comparing with (4.47), one finds the one-loop defect data

$$\begin{aligned} \hat{\gamma}^{(1)}_{S,0,s} &= \frac{1-s}{(2s+1)}\,, \qquad \hat{b}^{2(1)}_{S,0,s} = \frac{-2(s-1)H_s - 3H_{s+\frac{1}{2}}}{2(2s+1)}\,, \\ \hat{\gamma}^{(1)}_{V,0,s} &= -\frac{s}{(2s+1)}\,, \quad \hat{b}^{2(1)}_{V,0,s} = -\frac{(2s+1)\left(2sH_s + H_{s-\frac{1}{2}}\right) + 2}{2(2s+1)^2}\,. \end{aligned} \tag{4.49}$$

Several sanity checks can be performed on these results. First of all, one can check that $\hat{\gamma}^{(1)}_{S,0,1} = 0$, *i.e.* the presence of the displacement operator in the defect OPE of the fundamental field, introduced in (3.27). In this case, the displacement operator must have dimension two and orthogonal spin one and it must be a singlet under internal symmetries. The only candidate in this case is the operator $\partial_\perp \hat{\phi}^1$ which is indeed associated to the vanishing anomalous dimension $\hat{\gamma}^{(1)}_{S,0,1}$.

Another universal protected operator is the tilt operator (3.26). This vector has dimension one and orthogonal spin zero, *i.e.* it is given precisely by $\hat{\phi}^{\hat{i}}$, the $N-1$ scalars that are not involved in the construction of the defect. Correspondingly, one finds $\hat{\gamma}^{(1)}_{V,0,0} = 0$.

For other defect operators some results are already available in the literature. The anomalous dimensions for the spin-zero singlet, *i.e.* $\hat{\phi}^1$ and the spin-one vector operators, *i.e.* $\partial_\perp \hat{\phi}^{\hat{i}}$, have been computed in equations (3.19) and (3.52) of [32], and they agree with the results of this section. More generally, the leading-twist contribution to the defect anomalous dimensions from the inversion of a single bulk scalar operator of arbitrary dimension Δ was computed in (3.53) of [18]. The perturbative expansion of that result again perfectly matches the ones obtained here. The results for the bulk-to-defect couplings are new defect data that follows from this analysis.

As already mentioned, the one-loop result contains information about the anomalous dimensions of operators that already appeared at tree level. Nevertheless, by keeping more terms in the small-z expansion (4.40) and (4.45), one can also extract the bulk-to-defect couplings for higher-twist operators. As one could have guessed from a diagrammatic argument and as was anticipated in (4.32), it turns out that all higher-

twist coefficients are zero at this order in perturbation theory

$$\hat{b}^{2(1)}_{S,m,s} = \hat{b}^{2(1)}_{V,m,s} = 0\,, \quad m > 0\,, \tag{4.50}$$

Therefore the only non zero OPE data in the defect channel are (4.49) and the defect identity at one loop (4.11).

Bulk channel data

Finally, one can extract the bulk data using the bulk inversion formula (4.4). The bulk anomalous dimensions are well-known and reproducing them is just a consistency check for the validity of this procedure. On the other hand, the product $a\lambda^{(1)}$ depends on the defect through the one-point function a, providing new predictions for all operators that are not affected by perturbative degeneracies (specifically, all twist-two operators and the first two operators in the twist-four family).

In order to use the formula (4.4), one needs to analyse the behaviour of $\left(\frac{(1-z)(1-\bar{z})}{\sqrt{z\bar{z}}}\right)^{\Delta_\phi} F(z,\bar{z})$ for $w \to 0$, according to (4.7).[8] In this case, one can see that $\ell_* = 2$ by expanding the results of the dispersion relation (4.36) and (4.38) around $w = 0$ and comparing with (4.7). Therefore, the inversion formula will work for $\ell > 2$. Since the integral in (4.4) is too hard, it is possible to use the same strategy that was used in the case of the defect inversion. One can expand the integrand around $z = 1$ and compute the coefficient term by term in the expansion. Namely, using [22]

$$\begin{aligned}
c^t(\Delta,\ell) &= \int_0^1 \frac{dz}{2} \sum_{m=0} (1-z)^{m-1+\frac{\Delta-\ell}{2}} \sum_{k=-m}^{m} B_{m,k}(\Delta,\ell) C^t(z, \Delta+\ell+2k)\,,\\
C^t(z,\beta) &= \kappa_\beta \int_0^z \frac{d\bar{z}}{(1-\bar{z})^2} k_\beta(1-\bar{z})\, \mathrm{dDisc}\left(\left(\frac{(1-z)(1-\bar{z})}{\sqrt{z\bar{z}}}\right)^{\Delta_\phi} F(z,\bar{z})\right),\\
k_\beta(z) &= z^{\frac{\beta}{2}}\, {}_2F_1\left(\frac{\beta}{2},\frac{\beta}{2},\beta,z\right), \qquad \kappa_\beta = \frac{\Gamma\left(\frac{\beta}{2}\right)^3}{2\pi^2\Gamma(\beta)\Gamma(\beta-1)}\,,
\end{aligned} \tag{4.51}$$

where $B_{m,k}(\Delta,\ell)$ are coefficients that can be fixed by expanding the

[8] Notice that for the bulk inversion one needs to consider an extra factor in front of the correlator $F(r,w)$. For this reason, the behaviour at small w is different from the one discussed in the defect inversion section.

kernel in (4.4) and comparing with (4.51), *i.e.*

$$\begin{aligned}&(1-z)(1-\bar{z})^2(1-z)^{\frac{\Delta-l}{2}}\mu(z,\bar{z})f^{HS}_{d+l-1,-d+\Delta+1}=\\&=\sum_m(1-z)^m\sum_{k=-m}^{m}\frac{\kappa_{\Delta+2k+l}}{\kappa_{\Delta+l}}B_{m,k}(\Delta,\ell)k_{\Delta+\ell+2k}(1-\bar{z})\,.\end{aligned}\tag{4.52}$$

Just like in the defect case, a given term in the series expansion around $z=1$ (4.51) reproduces the contribution of a given twist to the coefficient. One can compute the double discontinuity at order ε by taking the expressions for the full correlator (4.36) and (4.38), multiplying by $\frac{(1-z)(1-\bar{z})}{\sqrt{z\bar{z}}}$ and expanding in $z=1$. Every term in the expansion of the non trivial part of the correlator $\frac{(1-z)(1-\bar{z})}{\sqrt{z\bar{z}}}I(r,w)$ contains only integer powers of $\bar{z}$. Therefore, this part of the correlator does not contribute to the double discontinuity. The same applies for the contribution from the correction to the bulk identity. In other words, the only contributions to the double discontinuity of both representations at one loop are the terms proportional to the defect identity, $a_\phi^{2\,(1)}\frac{(1-z)(1-\bar{z})}{\sqrt{z\bar{z}}}$. However, the one-loop coefficient (4.51) will also receive a contribution from the tree-level double discontinuity, since it contains factors that depend on Δ_ϕ and d, which will give terms of order ε when combined with the order zero double discontinuity (4.15). In particular, both $C^t(z,\beta)$ and $B_{m,k}(\Delta,\ell)$ depend on ε through Δ_ϕ and d. All in all, the discontinuities are

$$\begin{aligned}&\text{dDisc}\left(\left(\tfrac{(1-z)(1-\bar{z})}{\sqrt{z\bar{z}}}\right)^{\Delta_\phi}F_S(r,w)\right)=\\&\qquad=\left(\frac{a_\phi^{2\,(0)}}{N}+\varepsilon\frac{a_\phi^{2\,(1)}}{N}\right)2\sin^2\left(\frac{\pi\Delta_\phi}{2}\right)\left(\frac{(1-z)(1-\bar{z})}{\sqrt{z\bar{z}}}\right)^{\Delta_\phi},\\&\text{dDisc}\left(\left(\tfrac{(1-z)(1-\bar{z})}{\sqrt{z\bar{z}}}\right)^{\Delta_\phi}F_T(r,w)\right)=\\&\qquad=\left(a_\phi^{2\,(0)}+\varepsilon a_\phi^{2\,(1)}\right)2\sin^2\left(\frac{\pi\Delta_\phi}{2}\right)\left(\frac{(1-z)(1-\bar{z})}{\sqrt{z\bar{z}}}\right)^{\Delta_\phi}.\end{aligned}\tag{4.53}$$

The first few contributions to $C^t(z,\beta)$ in the $z=1$ expansion in the appendix (B.8), for both representations. Plugging those expressions in (4.51), using (4.11) and expanding at first order in ε, one can find the one-loop coefficients $c^t_{S/T}(\Delta,\ell)$. Since the external operators are identical, the u-channel contribution $c^u_{S/T}(\Delta,\ell)$ is the same. At the end of the day, one can extract the one-loop bulk OPE data for both

representations

$$
\begin{aligned}
a\lambda^{(1)}_{T,0,\ell} &= -\frac{2^{-\ell-5}\Gamma\left(\frac{\ell}{2}+\frac{1}{2}\right)^3}{\pi\Gamma\left(\frac{\ell}{2}+1\right)\Gamma\left(\ell+\frac{1}{2}\right)}\Big(-32a_\phi^{2\,(0)}H_{\frac{\ell}{2}-\frac{1}{2}}+35a_\phi^{2\,(0)}H_{\ell-\frac{1}{2}} \\
&+19a_\phi^{2\,(0)}\psi^{(0)}(\ell)-38a_\phi^{2\,(0)}\psi^{(0)}(2\ell)-19\gamma a_\phi^{2\,(0)}+6a_\phi^{2\,(0)}\log 2+32a_\phi^{2\,(1)}\Big)\,, \\
a\lambda^{(1)}_{T,1,\ell} &= -\frac{a_\phi^{2\,(0)}2^{-\ell-3}\Gamma\left(\frac{\ell+1}{2}\right)\Gamma\left(\frac{\ell+3}{2}\right)^2}{\pi\Gamma\left(\frac{\ell}{2}+2\right)\Gamma\left(\ell+\frac{3}{2}\right)}\,, \\
a\lambda^{(1)}_{S,0,\ell} &= \frac{1}{N}\lambda^{(1)}_{T,0,\ell}\,, \\
a\lambda^{(1)}_{S,1,\ell} &= \frac{1}{N}\lambda^{(1)}_{T,1,\ell}\,.
\end{aligned}
\tag{4.54}
$$

The anomalous dimensions are all zero for $\ell > 0$, as it was already known. During this calculation, $C^t(z,\beta)$ was also computed and (4.51) to higher order in the $z = 1$ expansion to extract the coefficients and anomalous dimensions of higher-twist operators and checked that they turn out to be zero. The data at low spin have to be computed in a different way, because the inversion formula does not converge in that case. For example, one can compute the missing data by expanding the full results (4.36) and (4.38) in series and comparing it to the bulk OPE expansion. Although the inversion formula was expected to fail at spin $\ell = 0, 2$, it turns out that the only data that are missed by the inversion formula are the coefficients of the twist-two operators with $\ell = 0$ (3.34). One finds

$$
\begin{aligned}
a\lambda^{(1)}_{T,0,0} &= a_\phi^{2\,(1)} - \frac{1}{2} - \frac{\log(2)}{2}\,, \\
a\lambda^{(1)}_{S,0,0} &= -\frac{-4a_\phi^{2\,(1)} + N + N\log(2) + 2 + \log(4)}{4N}\,.
\end{aligned}
\tag{4.55}
$$

As another non-trivial check of these results at twist 4 at low spin, it is possible to follow an alternative route to derive the coefficient of the operator ϕ^4, namely $a\lambda^{(1)}_{S/T,1,0}$, and compare with the result from the inversion formula. For the sake of simplicity, it is convenient to set $N = 1$ and therefore consider only the singlet representation. From the two-point function of the operator ϕ^2 at tree level one can extract the bulk CFT data. Just like in the case of the two-point function of ϕ, the tree-level correlator has a contribution from the squared one-point function and from the bulk identity with dimension $\Delta_{\phi^2} = 2 + \mathrm{O}(\varepsilon)$,

namely

$$F^{(0)}(r,w) = a^{2\,(0)}_{\phi^2} + a^{2\,(0)}_{\phi} \frac{rw}{(r-w)(rw-1)} + \left(\frac{rw}{(r-w)(rw-1)}\right)^2 . \tag{4.56}$$

A family of double-twist operators with twist 4 enters in the bulk spectrum at this order. In particular, one can extract the coefficient of the spin zero double twist $a\lambda^{(0)}_{\phi^2\phi^2\phi^4} = a^{(0)}_{\phi^4}\lambda^{(0)}_{\phi^2\phi^2\phi^4}$ from the bulk expansion. Since the squared three-point coefficients $\lambda^{2\,(0)}_{\phi^2\phi^2\phi^4}$ are known from previous work on the theory without defects [95], one can immediately derive an expression for the squared one-point function $a^{2\,(0)}_{\phi^4}$ from $a\lambda^{(0)}_{\phi^2\phi^2\phi^4}$. Multiplying this expression and the known squared one-loop OPE coefficients $\lambda^{2\,(1)}_{\phi\phi\phi^4}$, one can compute the square of the ϕ^4 coefficient $a^{2\,(0)}_{\phi^4}\lambda^{2\,(1)}_{\phi\phi\phi^4} = a\lambda^{2(1)}_{S,1,\ell}$, where the fact that $\lambda^{2\,(0)}_{\phi\phi\phi^4} = 0$ was used. The results obtained from this analysis match with what was expected from (4.54). Obviously, this reasoning can be extended to any N. Considering other correlators is not only useful to check results but also to solve the mixing problem. Indeed, starting at spin $\ell = 2$, the twist-four operators suffer from degeneracies, namely there are multiple operators that have the same classical scaling dimensions and therefore are indistinguishable from the bootstrap perspective. For this reason, the data found at twist four (4.54) has to be interpreted as an average over all degenerate twist-four operators for a given spin. In order to lift the degeneracy, one should in principle compare the results from different correlators.

4.3 Analytic bootstrap for the magnetic impurity

This section presents a bootstrap analysis similar to that of the localised magnetic fields, applied to the $O(3)$ magnetic impurity, following the approach in [35]. The analysis is conducted separately for the case of a free bulk, discussed in 4.3.1, and for the case of an interacting bulk, presented in 4.3.2. Finally, in 4.3.3, perturbative computations are carried out, and the results are compared with those obtained using bootstrap techniques. As it will be shown, the results are in perfect agreement.

The observables of interest are the two-point functions of ϕ_a and ϕ^2 at

the conformal fixed point, which can be written as

$$\begin{aligned}\langle\phi_a(x)\phi_b(y)\rangle_{\mathcal{D}_j} &= \frac{\delta_{ab}F_{\phi\phi}(r,w)}{|x_\perp|^{\Delta_\phi}|y_\perp|^{\Delta_\phi}}\,,\\ \langle\phi^2(x)\phi^2(y)\rangle_{\mathcal{D}_j} &= \frac{F_{\phi^2\phi^2}(r,w)}{|x_\perp|^{\Delta_{\phi^2}}|y_\perp|^{\Delta_{\phi^2}}}\,.\end{aligned} \tag{4.57}$$

Here r and w are the two defect cross-ratios expressed in radial coordinates (2.56). Note that throughout this section all the operators are unit-normalised, a convention that differs from Section 3.3. After computing these correlators, the bulk and defect CFT data are extracted by expanding the correlators, using either the bulk block expansion [9]

$$F_{\phi\phi}(r,w) = \xi^{-\Delta_\phi}\sum_{\mathcal{O}}\lambda_{\phi\phi\mathcal{O}}\,a_{\mathcal{O}}\,f_{\Delta,\ell}(r,w)\,,\quad \xi = \frac{(1-rw)(w-r)}{rw}\,, \tag{4.58}$$

or the defect block expansion

$$F_{\phi\phi}(r,w) = \sum_{\hat{\mathcal{O}}} b^2_{\phi\hat{\mathcal{O}}}\,\hat{f}_{\hat{\Delta},s}(r,w)\,. \tag{4.59}$$

Once again, for definitions and conventions, see Appendix A.

4.3.1 Free bulk

Bootstrap of $\langle\phi\phi\rangle$

The first observable that is studied is the two-point function of the order parameter ϕ_a. Since the bulk theory is free, the bulk OPE of ϕ_a contains only the identity and the twist-two operators defined in (3.15), [10] namely

$$\phi_a\times\phi_a = \mathbb{1} + \sum_\ell J_\ell\,, \tag{4.60}$$

with

$$\Delta_\ell = 2\Delta_\phi + \ell,\quad \Delta_\phi = 1 - \frac{\varepsilon}{2}\,. \tag{4.61}$$

Note that only operators in the singlet representation can appear in the OPE in (4.60). Is is useful to define the shorthand notation $c_{\mathcal{O}} =$

[9] The following expressions for $F_{\phi\phi}(r,w)$ are presented, but analogous results apply to $F_{\phi^2\phi^2}$.

[10] Intuitively, the reason why only twist-two operators appear in free theory is the following: since there are no interactions, only operators with two ϕ's appear in the OPE, namely $\phi\times\phi\sim\phi\partial_{\mu_1}\ldots\partial_{\mu_\ell}\Box^n\phi$. Those are exactly the twist-two operators. However, because of the equation of motion $\Box\phi=0$, only the $n=0$ family of twist-two operators contributes. More rigorously, one should compute the four-point function of free fields ϕ_a, and observe that its block expansion contains only twist-two operators.

$\lambda_{\phi\phi\mathcal{O}} a_{\mathcal{O}}$. All the (defect) CFT data can be expanded in ε with obvious notation, for example

$$c_\ell = c_\ell^{(0)} + \varepsilon c_\ell^{(1)} + \dots \,. \tag{4.62}$$

Here $c_\ell^{(0)}$ might itself be of order $\mathrm{O}(\varepsilon^n)$, and in fact, in the examples below $c^{(0)} \sim \mathrm{O}(\varepsilon)$. The first step is to compute the discontinuity of $F_{\phi\phi}$, which is given by the sum of the discontinuities of the bulk blocks associated to the bulk OPE expansion 4.60. An analogous argument to the one used for the localised magnetic field in Section 4.2.3 shows that the discontinuity of twist-two operators is proportional to their anomalous dimension. Since in free theory twist-two operators do not have anomalous dimension, the discontinuity only receives a contribution from the identity operator

$$\mathrm{Disc} F_{\phi\phi} = \mathrm{Disc}\ \xi^{-\Delta_\phi} = 2i \sin(\pi\Delta_\phi)(-\xi)^{-\Delta_\phi} \,. \tag{4.63}$$

Notice that this equation is correct to all orders ε, and not only at leading order. Using the dispersion relation (4.8), and adding a low-spin ambiguity as explained in Section 4.1, one obtains

$$F_{\phi\phi}(r,w) = \xi^{-\Delta_\phi} + \text{low-spin ambiguity} \,. \tag{4.64}$$

To resolve the low-spin ambiguity, the results from Section 3.3.3 on the operators that can appear in the defect channel can be used. As shown there, the equation of motion $\Box\phi_a = 0$ imposes constraints on the dimensions of the defect operators that couple to it. In particular, following [121], from

$$\Box\langle\phi_a(x)\hat{\mathcal{O}}_b(\tau)\rangle = 0 \,, \tag{4.65}$$

it can be inferred that two families of operators exist:

- Modes $\hat{\mathcal{O}}^a_{0,s} \sim (\partial_\perp)^s \phi^a$ with $s \geqslant 0$ and $\hat{\Delta}_{0,s} = \Delta_\phi + s = 1 - \varepsilon/2 + s$.
- An operator $\hat{S}^a$, with $s = 0$ and $\hat{\Delta} = \varepsilon/2$.[11] This is precisely the defect spin operator of Section 3.3.3, defined in (3.65).

It is a known fact that the defect-channel expansion of the term $\xi^{-\Delta_\phi}$ contains the $\hat{\mathcal{O}}^a_{0,s}$ operators [18], but it does not include any operator with the quantum numbers of $\hat{S}^a$. Therefore, it must be that the dispersion relation fails to reproduce the contribution for spin $s = 0$, and therefore one needs to correct all possible $s = 0$ operators. The result is that the most general ansatz for the correlator is

$$F_{\phi\phi}(r,w) = \xi^{-\Delta_\phi} + k_1 \hat{f}_{1-\varepsilon/2,0}(r,w) + k_2 \hat{f}_{\varepsilon/2,0}(r,w) \,, \tag{4.66}$$

[11] More generally, one would find spinning operators with $\hat{\Delta} = \varepsilon/2 - s$, but they break unitarity for $s > 0$.

where the extra terms are the defect blocks associated with the low-spin ambiguities. The coefficients k_1 and k_2 are not arbitrary. The reason is that for arbitrary k_1 and k_2, it is generically not possible to expand (4.66) in the bulk channel. To be more precise, consider changing from radial coordinates (r, w) to lightcone coordinates $(z, \bar{z})$, defined in (2.55). In this coordinate system, one can see that the expansion of (4.66) around $|1-z| \ll |1-\bar{z}| \ll 1$ contains spurious powers $(1-z)^n(1-\bar{z})^{-m}$ for $m \geqslant 2$, and spurious logarithms $\log(1-\bar{z})$ which are not accompanied by $\log(1-z)$. These terms are incompatible with an expansion in terms of bulk-channel conformal blocks, and therefore one must choose the relative size of k_1 and k_2 to make sure they are absent. After carrying out this procedure, one finds that the free correlator is

$$F_{\phi\phi}(r, w) = \xi^{-\Delta_\phi} + c_{\phi^2} J_\varepsilon(r)\,, \tag{4.67}$$

where [12]

$$J_\varepsilon(r) = \frac{\Gamma\left(\frac{1-\varepsilon}{2}\right)}{\sqrt{\pi}\Gamma\left(\frac{2-\varepsilon}{2}\right)} \hat{f}_{\varepsilon/2,0}(r, w) + \frac{\Gamma\left(\frac{\varepsilon-1}{2}\right)}{\sqrt{\pi}\Gamma\left(\frac{\varepsilon}{2}\right)} \hat{f}_{1-\varepsilon/2,0}(r, w)\,. \tag{4.68}$$

It should be emphasised that this correlation function is exact to all orders in ε. However, it depends on a single parameter, c_{ϕ^2}, which cannot be determined by the bootstrap. Since (4.67) is exact in ε, it is possible to explore the properties of the fixed point in three dimensions by setting $\varepsilon = 1$. Despite the presence of divergent factors in (4.68), it can be verified that $J_\varepsilon(r)$ remains finite in the limit $\varepsilon \to 1$. This leaves two possibilities: either $c_{\phi^2}\big|\varepsilon = 1 = 0$, or $c_{\phi^2}\big|_{\varepsilon=1} \neq 0$. In the first case, $F_{\phi\phi}$ is just a free correlator. This is sufficient to show that ϕ satisfies the free-field equations of motion, and therefore all its correlators are those of the free theory. Instead, if $c_{\phi^2}\big|_{\varepsilon=1}$ is a finite non-zero number, one can try to expand the correlator in the defect channel by taking $r \ll 1$. However, this expansion contains terms with factors of $\log r$ that cannot be reproduced by the defect blocks. Therefore, this correlator does not obey the defect bootstrap equation. The inevitable conclusion is that in three dimensions and for a free bulk there is no non-trivial magnetic impurity [35].

For $0 < \varepsilon < 1$, instead, the function $J_\varepsilon(r)$ is a truncated solution of crossing,[13] because it has sensible bulk and defect expansions on its own, and it involves finitely many transverse spins (in this case, $s = 0$

[12] Note that this function does not depend on w because it is a sum of two $s = 0$ blocks (A.6).

[13] This is an analogue of the solutions of crossing with finite support in spin of [139], which play an important role in the ε-expansion bootstrap for four-point functions [136, 137, 140–142].

only).

As an interesting exercise, from the full two-point function one can still extract the CFT data for $\varepsilon < 1$ in both OPE channels as a function of c_{ϕ^2}. From the above discussion, the defect expansion takes the form

$$F_{\phi\phi}(r,w) = b^2_{\phi\hat{\mathcal{O}}_{0,0}} \hat{f}_{1-\varepsilon/2,0}(r,w) + b^2_{\phi\hat{S}} \hat{f}_{\varepsilon/2,0}(r,w) + \sum_{s=1}^{\infty} b^2_{\phi\hat{\mathcal{O}}_{0,s}} \hat{f}_{\Delta_\phi+s,s}(r,w)\,. \tag{4.69}$$

Using the formula for conformal blocks (A.6), it is not hard to extract the CFT data

$$\begin{aligned} b^2_{\phi\hat{\mathcal{O}}_{0,0}} &= 1 + \frac{\Gamma\left(\frac{\varepsilon-1}{2}\right)}{\sqrt{\pi}\Gamma\left(\frac{\varepsilon}{2}\right)} c_{\phi^2}\,, \qquad b^2_{\phi\hat{S}} = \frac{\Gamma\left(\frac{1-\varepsilon}{2}\right)}{\sqrt{\pi}\Gamma\left(\frac{2-\varepsilon}{2}\right)} c_{\phi^2}\,, \\ b^2_{\phi\hat{\mathcal{O}}_{0,s}} &= \frac{2^s(\Delta_\phi)_s}{s!}\,. \end{aligned} \tag{4.70}$$

Similarly, using the formulas for the bulk blocks (A.2) one finds the expansion

$$F_{\phi\phi}(r,w) = \xi^{-\Delta_\phi} + \xi^{-\Delta_\phi} \sum_{\ell=0}^{\infty} \lambda_{\phi\phi J_\ell} a_{J_\ell} f_{2\Delta_\phi+\ell,\ell}(r,w)\,. \tag{4.71}$$

The bulk expansion contains only twist-two operators, as expect in the bulk-free theory. Here $\lambda_{\phi\phi J_\ell}$ are thee-point OPE coefficients of the $O(3)$ model at the free fixed point, which are known exactly

$$\lambda_{\phi\phi J_\ell} = \sqrt{\frac{2}{3}} \frac{2^{\frac{\ell}{2}}(\Delta_\phi)_\ell}{\sqrt{\ell!(2\Delta_\phi+\ell-1)_\ell}}\,. \tag{4.72}$$

As a result, from the block expansion (4.71), one gets a prediction for all the one-point functions of twist-two operators:

$$a_{\phi^2} = \sqrt{\frac{3}{2}}\, c_{\phi^2}\,, \quad a_{J_\ell} = \frac{(1-\varepsilon)_\ell \left(\frac{\ell-\varepsilon+2}{2}\right)_{\frac{\ell}{2}} \sqrt{\ell!(\ell-\varepsilon+1)_\ell}}{2^{5\ell/2}\left(\frac{\ell}{2}!\right)^2 \left(\frac{\ell-\varepsilon+1}{2}\right)_{\frac{\ell}{2}} \left(1-\frac{\varepsilon}{2}\right)_\ell} a_{\phi^2}\,. \tag{4.73}$$

The particular case $\ell = 2$ corresponds to the stress tensor $a_{J_2} \sim \langle T_{\mu\nu}\rangle_{\mathcal{D}_j}$.[14] This has been conjectured to be positive [18], hence in bulk-free theory it should be $a_{\phi^2} > 0$.

[14] In the $\mathcal{N} = 4$ SYM literature this observable is usually called the Bremsstrahlung function.

At the end of the day, the two-point function of ϕ and the CFT data are entirely fixed by the bootstrap analysis up to an undetermined constant, which corresponds to the value of the one-point function a_{ϕ^2} of the unit-normalised ϕ^2 operator at the critical point. This will be computed to order $\mathrm{O}(\varepsilon^3)$ in equation (4.113) below.

Bootstrap of $\langle\phi^2\phi^2\rangle$

A second observable that can be considered is the two-point function of ϕ^2. Once again the bulk OPE is known exactly

$$\phi^2 \times \phi^2 = \mathbb{1} + \sum_{\ell} J_\ell + \sum_{n>1}\sum_{\ell} \mathcal{O}_{n,\ell}\,, \tag{4.74}$$

where

$$\mathcal{O}_{n,\ell} \sim \phi^a \Box^n \partial_{\mu_1} \dots \partial_{\mu_\ell} \phi_a\,, \tag{4.75}$$

with

$$\Delta_{n,\ell} = 2\Delta_{\phi^2} + 2n + \ell, \quad \Delta_{\phi^2} = 2\Delta_\phi = 2 - \varepsilon\,. \tag{4.76}$$

The bulk expansion reads

$$\begin{aligned} F_{\phi^2\phi^2}(r,w) = \xi^{-2\Delta_\phi} + \xi^{-2\Delta_\phi} \sum_{\ell=0}^{\infty} \lambda_{\phi^2\phi^2 J_\ell} a_{J_\ell} f_{2\Delta_\phi+\ell,\ell} \\ + \xi^{-2\Delta_\phi} \sum_{n,\ell=0}^{\infty} c_{n,\ell} f_{4\Delta_\phi+\ell+2n,\ell}\,. \end{aligned} \tag{4.77}$$

In this case, the discontinuity receives contributions from the identity and J_ℓ operators, but it kills all of the $\mathcal{O}_{n,l}$ operators. To compute the discontinuity of the J_ℓ operators, notice that although $\xi^{-2\Delta_\phi} f_{2\Delta_\phi+\ell,\ell}(r,w)$ has a branch cut, the combination $\xi^{-\Delta_\phi} f_{2\Delta_\phi+\ell,\ell}(r,w)$ does not have a discontinuity, see (A.2). As a result, the discontinuity reads

$$\begin{aligned} \mathrm{Disc} F_{\phi^2\phi^2}(r,w) =& \mathrm{Disc}\left(\xi^{-2\Delta_\phi}\right) \\ &+ \sum_{\ell=0}^{\infty} \lambda_{\phi^2\phi^2\mathcal{J}_\ell} a_{\mathcal{J}_\ell} \xi^{-\Delta_\phi} f_{2\Delta_\phi+\ell,\ell}(r,w) \mathrm{Disc}\left(\xi^{-\Delta_\phi}\right). \end{aligned} \tag{4.78}$$

Furthermore, one can easily check that in free theory $\lambda_{\phi^2\phi^2 J_\ell} = 2\lambda_{\phi\phi J_\ell}$. Therefore, the sum that appears in the discontinuity gives the same result as in the $\langle\phi\phi\rangle_{\mathcal{D}_j}$ correlator, up to a factor of 2. Hence one has

$$\mathrm{Disc} F_{\phi^2\phi^2}(r,w) = \mathrm{Disc}\left(\xi^{-2\Delta_\phi}\right) + 2c_{\phi^2} J_\varepsilon(r) \mathrm{Disc}\left(\xi^{-\Delta_\phi}\right). \tag{4.79}$$

Both terms get mapped to themselves by the dispersion relation (4.8) because they are of the form $\xi^\alpha f(r)$, and the dispersion relation only involves w. There is an obvious spin $s = 0$ contribution from the defect identity $a^2_{\phi^2}$ that is missed by the dispersion relation. In principle there could be other low-spin ambiguities. Contrary to the previous case, there does not seem to be any Ward identity that constrains the form of the low spin ambiguities in $\langle\phi^2\phi^2\rangle_{\mathcal{D}_j}$. Therefore, the conclusion of the bootstrap analysis is

$$F_{\phi^2\phi^2}(r,w) = \xi^{-2\Delta_\phi} + 2c_{\phi^2}\xi^{-\Delta_\phi} J_\varepsilon(r) + a^2_{\phi^2} + \text{low-spin ambiguity}\,. \tag{4.80}$$

From the diagrammatic computation in Section 4.3.3, it will be shown that at next-to-leading order there is indeed an extra term which corresponds to the contribution of the operator $\hat{\Phi}$ and that of an infinite family of integer-twist operators with transverse spin $s = 0$. This means that the bootstrap result is not complete, but it can still be used to extract defect CFT data with $s > 0$. For further details on the low spin contribution see the discussion around (4.126). In the defect channel two families of operators are found

$$F_{\phi^2\phi^2}(r,w) = \sum_{n,s=0}^{\infty} \left(b^2_{\phi\hat{\mathcal{O}}_{n,s}}\, \hat{f}_{\hat{\Delta}_{n,s},s} + b^2_{\phi\hat{J}_{n,s}}\, \hat{f}_{\hat{\Delta}_{\hat{J}_{n,s}},s} \right). \tag{4.81}$$

The first family of operators has the interpretation $\hat{\mathcal{O}}_{n,s} \sim (\partial_\perp)^s \Box^n \phi^2$, with

$$\hat{\Delta}_{s,n} = 2\Delta_\phi + s + 2n\,, \tag{4.82}$$

$$b^2_{\phi\hat{\mathcal{O}}_{n,s}} = c_{\phi^2} \frac{2^s \left(\frac{3}{2}\right)_{n-1} \Gamma\left(\frac{\varepsilon-1}{2}\right) \left(1-\frac{\varepsilon}{2}\right)_n^2 \left(n-\frac{\varepsilon}{2}+1\right)_s (n+s-\varepsilon+2)_n}{\sqrt{\pi}\, n!\, \Gamma\left(\frac{\varepsilon}{2}\right) (n+s)! \left(\frac{3}{2}-\frac{\varepsilon}{2}\right)_n \left(n+s-\frac{\varepsilon}{2}+1\right)_n} + \frac{2^s \left(1-\frac{\varepsilon}{2}\right)_n (2-\varepsilon)_{2n+s}}{n!(n+s)! \left(n+s-\frac{\varepsilon}{2}+1\right)_n}\,, \tag{4.83}$$

whereas the second family is $\hat{J}_{n,s} \sim (\partial_\perp)^s \Box^n \phi^a T_a$, with

$$\hat{\Delta}_{\hat{J}_{n,s}} = 1 + s + 2n\,, \tag{4.84}$$

$$b^2_{\phi\hat{J}_{n,s}} = c_{\phi^2} \frac{2^s (-4)^n \left(\frac{3}{2}\right)_{n-1} \Gamma\left(\frac{1-\varepsilon}{2}\right) (2n+s)! \left(\frac{\varepsilon}{2}\right)_n \left(-n-\frac{\varepsilon}{2}+1\right)_{2n+s}}{\sqrt{\pi}\, n!\, \Gamma\left(1-\frac{\varepsilon}{2}\right) ((n+s)!)^2 (\varepsilon)_{2n} \left(n+s+\frac{\varepsilon}{2}\right)_n}\,. \tag{4.85}$$

Note that these results are only valid for $s > 0$ due to low-spin ambiguities. Notice that the operators $\hat{J}_{n,s}$ have integer scaling dimension. In

particular, the operators $\hat{J}_{0,s}$ are related to the higher spin symmetries in the free bulk theory which are broken by the defect, as it can be seen from the Ward identity (3.104). Finally, since low s ambiguities potentially contribute to all data in the bulk OPE, it is not possible extract any meaningful observable in that channel.

4.3.2 Interacting bulk

Bootstrap of $\langle\phi\phi\rangle$

In this section, the case in which the bulk theory is the $O(3)$ model at the Wilson-Fisher fixed point in $d = 4 - \varepsilon$ dimensions is considered, restricting to the first non-trivial order in the perturbative expansion at small ε. The observable of interest is again the two-point function of the order parameter ϕ_a, namely

$$\langle\phi_a(x)\phi_a(y)\rangle_{\mathcal{D}_j} = \frac{F_{\phi\phi}(r,w)}{|x_\perp|^{\Delta_\phi}|y_\perp|^{\Delta_\phi}}\,. \tag{4.86}$$

The same correlator was computed in presence of a different line defect using the analytic bootstrap in Section 4.2 [34, 135]. It turns out that the computation in the present case is very similar. The reason is very simple: the discontinuity is computed by expanding the two-point function in bulk blocks and evaluating the discontinuity of each block. At first order in perturbation theory, the discontinuity of a block is proportional to the anomalous dimension of the corresponding bulk operator, which is independent of the defect. Finally, it turns out that in the $O(3)$ model all the operators that appear in the $\phi \times \phi$ OPE at order ε have vanishing anomalous dimensions, except for one operator. More precisely, the bulk OPE is

$$\phi_a \times \phi_a = \mathbb{1} + \sum_\ell J_\ell + \sum_{n>1}\sum_\ell \mathcal{O}_{n,\ell}\,, \tag{4.87}$$

where, for the leading twist family [95, 143]

$$\begin{aligned}\Delta_\ell &= 2\Delta_\phi + \ell + \varepsilon\frac{5}{11}\delta_{\ell,0} + \mathrm{O}(\varepsilon^2)\,,\\ \Delta_\phi &= 1 - \frac{\varepsilon}{2} + \mathrm{O}(\varepsilon^2)\,,\end{aligned} \tag{4.88}$$

and

$$\begin{aligned}\lambda_{\phi\phi J_\ell} &= \lambda^{(0)}_{\phi\phi J_\ell} + \varepsilon\lambda^{(1)}_{\phi\phi J_\ell} + \varepsilon^2\lambda^{(2)}_{\phi\phi J_\ell} + \mathrm{O}(\varepsilon^3)\,,\\ a_{J_\ell} &= a^{(0)}_{J_\ell} + \varepsilon a^{(1)}_{J_\ell} + \varepsilon^2 a^{(2)}_{J_\ell} + \mathrm{O}\left(\varepsilon^3\right)\,.\end{aligned} \tag{4.89}$$

For higher-twist operators, one has

$$\begin{aligned}\Delta_{n,\ell} &= 2\Delta_\phi + 2n + \ell + \varepsilon\gamma^{(1)}_{n,\ell} + \mathrm{O}(\varepsilon^2)\,,\\ \lambda_{\phi\phi\mathcal{O}_{n,\ell}} &= \varepsilon\lambda^{(1)}_{\phi\phi\mathcal{O}_{n,\ell}} + \varepsilon^2\lambda^{(2)}_{\phi\phi\mathcal{O}_{n,\ell}} + \mathrm{O}(\varepsilon^3)\,.\end{aligned} \tag{4.90}$$

Therefore only the bulk identity and ϕ^2 operators contribute to the discontinuity. All the other operators do not contribute at the order considered, since their anomalous dimensions or OPE coefficients are higher order. At the end of the day, the discontinuity reads

$$\mathrm{Disc}F_{\phi\phi}(r,w) = \mathrm{Disc}\xi^{-\Delta_\phi} + \varepsilon^2\frac{5\pi i}{11}\lambda^{(0)}_{\phi\phi\phi^2}a^{(1)}_{\phi^2}\xi^{-1}f_{2,0}(r,w) + \mathrm{O}(\varepsilon^3)\,. \tag{4.91}$$

A comment is in order: the one-point coefficient a_{ϕ^2} which appears in the discontinuity cannot be determined by the bootstrap but, at leading order, coincides with the tree-level free theory result [33], and in particular it turns out that $a_{\phi^2} \sim \varepsilon$. Therefore, the non-trivial correction to the discontinuity starts at order ε^2. The discontinuity (4.91) is the same that was found in [135, 34], up to a different factor in front of the non-trivial term, which depends on the specific defect through the one-point function coefficient a_{ϕ^2}. The other coefficient $\lambda_{\phi\phi\phi^2}$ does not depend on the defect, just like the anomalous dimensions of bulk operators, and has the value [144, 136, 137]

$$\lambda_{\phi\phi\phi^2} = \sqrt{\frac{2}{3}}\left(1 - \varepsilon\frac{5}{22}\right) + \mathrm{O}(\varepsilon^2)\,. \tag{4.92}$$

In particular, at leading order $\lambda^{(0)}_{\phi\phi\phi^2} = \sqrt{\frac{2}{3}}$. The discontinuity and the result of the dispersion relation can both be evaluated explicitly in terms of special functions. It turns out that the result of the dispersion relation is

$$F_{\phi\phi}(r,w) = \xi^{-\Delta_\phi} + \varepsilon^2\sqrt{\frac{2}{3}}\frac{5a^{(1)}_{\phi^2}}{11}H(r,w) + \text{low spin} + \mathrm{O}(\varepsilon^3)\,, \tag{4.93}$$

where $H(r,w)$ can be conveniently expressed as

$$H(r,w) = \xi^{-1}\left(\partial_\Delta - 1 - \log 2\right)f_{2,0}(r,w)\,, \tag{4.94}$$

where as always $f_{2,0}(r,w)$ is a bulk block. This function can also be represented in a variety of different ways which are better suited for explicit evaluation or the extraction of the CFT data, for example as a multivariable hypergeometric function. As in the free bulk case, the result of the dispersion relation may miss low spin contributions. For example, in the free theory discussed in Section 4.3.1, one had to add

by hand a truncated solution to crossing $J_\varepsilon(r)$ to the correlator. It is convenient to expand this function perturbatively in ε

$$J_\varepsilon(r) = 1 + \frac{\varepsilon}{2}\log\frac{4r}{(1+r)^2} + \mathrm{O}(\varepsilon^2)\,. \tag{4.95}$$

A similar correction can be expected in the present case. The goal here is to see if it is possible to find more general truncated solutions to be added to the final interacting correlator. To be able to make progress, it is convenient to make the simplifying assumption that only the defect twist-one family contributes. This assumption is motivated by the fact that this is what happens in the free bulk case (and in a variety of other perturbative setups) and one expects the defect spectra in the free and interacting case to be perturbatively close to each other. Provided the assumption is true, the most general ansatz for the ambiguity is

$$\begin{aligned} F_{\text{amb}}(r,w) = (q_0 + r_0\partial_{\hat{\Delta}})\,\hat{f}_{0,0} + (q_1 + r_1\partial_{\hat{\Delta}})\,\hat{f}_{1,0} \\ + \sum_{s=1}^{s_*}(q_{s+1} + r_{s+1}\partial_{\hat{\Delta}})\hat{f}_{s+1,s}\,, \end{aligned} \tag{4.96}$$

where q and r are arbitrary constants. For any finite $s_* \in \mathbb{N}$, the conformal blocks in this sum can be written as polylogarithms using `HypExp` [145,146]. For example, the lowest lying ones take a very simple form

$$\begin{aligned} &\hat{f}_{0,0}(r,w) = 1\,, \quad \partial_{\hat{\Delta}}\hat{f}_{0,0}(r,w) = \log\frac{r}{1-r^2}\,, \\ &\hat{f}_{1,0}(r,w) = \tanh^{-1} r\,, \quad \ldots \end{aligned} \tag{4.97}$$

Given the ansatz (4.96), one can attempt to expand it in the bulk channel, but generically this is not possible. The reason can be seen more easily by changing from radial coordinates (r,w) to lightcone coordinates $(z,\bar{z})$, defined in (2.55). In this coordinate system, one can see that the expansion of (4.96) around $|1-z| \ll |1-\bar{z}| \ll 1$ contains spurious powers $(1-z)^n(1-\bar{z})^{-m}$ for $m \geqslant 2$, and spurious logarithms $\log(1-\bar{z})$ which are not accompanied by $\log(1-z)$. These terms are incompatible with an expansion in terms of bulk-channel conformal blocks (A.2), since the latter are symmetric in z and $\bar{z}$. Therefore, demanding they vanish puts non-trivial constraints on the ansatz. Although a general proof has not been found, by experimenting with low values $s_* \leqslant 5$, it is possible to conclude that the most general truncated solution is

$$\begin{aligned} F_{\text{amb}}(r,w) = q_0\hat{f}_{0,0}(r,w) + r_0\left(\partial_{\hat{\Delta}}\hat{f}_{0,0}(r,w) - 2\hat{f}_{1,0}(r,w)\right) = \\ = q_0 + r_0\log\frac{r}{(1+r)^2}\,. \end{aligned} \tag{4.98}$$

Both equation (4.95) and (4.98) suggest that the ambiguities of interest are a constant and a logarithm. At the end of the day, the ansatz for the correlator can be expressed as

$$F_{\phi\phi}(r,w) = \xi^{-\Delta_\phi} + \varepsilon^2\sqrt{\frac{2}{3}}\frac{5a^{(1)}_{\phi^2}}{11}H(r,w) + q_0 + r_0\log\frac{r}{(1+r)^2} + \mathrm{O}(\varepsilon^3)\,. \tag{4.99}$$

The constants $a^{(1)}_{\phi^2}, q_0, r_0$ cannot be fixed from the bootstrap alone. However, it can be shown that they are not independent. One can fix r_0 in terms of $a^{(1)}_{\phi^2}$ by exploiting the analysis on the defect spectrum in Section 3.3.3. Indeed, the defect expansion has the same form as in the case of the free bulk

$$F_{\phi\phi}(r,w) = b^2_{\phi\hat{\mathcal{O}}_{0,0}}\hat{f}_{\hat{\Delta}_{0,0},0}(r,w) + b^2_{\phi\hat{S}}\hat{f}_{\hat{\Delta}_{\hat{S}},0}(r,w) + \sum_{s=1}^{\infty} b^2_{\phi\hat{\mathcal{O}}_{0,s}}\hat{f}_{\Delta_\phi+s,s}(r,w)\,, \tag{4.100}$$

and in particular it contains the spin operator $\hat{S}^a$. As discussed in Section 3.3.3, while this operator has no longer protected dimension if the bulk is not free, one can see from the Ward identity that the correction to the anomalous dimension starts at order ε^2. Therefore, the leading dimension must coincide with the one in the free bulk case. This fixes $r_0 = \varepsilon\sqrt{\frac{2}{3}}\frac{a^{(1)}_{\phi^2}}{2}$. Finally, one can fix q_0 in terms of $\lambda_{\phi\phi\phi^2}a_{\phi^2}$ just by expanding the correlator in the bulk channel, namely

$$F(r,w) = \xi^{-\Delta_\phi} + c_{\phi^2}\xi^{-\Delta_\phi}f_{\Delta_{\phi^2},0} + \xi^{-\Delta_\phi}\sum_{\ell=2}^{\infty} c_\ell f_{2\Delta_\phi+\ell,\ell}\,, \tag{4.101}$$

where the general definition $c_{\mathcal{O}} = \lambda_{\phi\phi\mathcal{O}}a_{\mathcal{O}}$ has been used. By comparing with (4.99), it is possible to fix $q_0 = \lambda_{\phi\phi\phi^2}a_{\phi^2} + \varepsilon^2\sqrt{\frac{2}{3}}a^{(1)}_{\phi^2}\left(\frac{5}{11} + \frac{16}{11}\log 2\right)$. Therefore, at the end of the day the correlator and all the CFT data are fixed in terms of a single unknown one-point function coefficient a_{ϕ^2}, more precisely one finds

$$F(r,w) = b\xi^{-\Delta_\phi} + c_{\phi^2}\left(1 + \frac{\varepsilon}{2}\log\frac{4r}{(1+r)^2} + \varepsilon\,\frac{5}{11}\left(1+\log 2 + H(r,w)\right)\right) + \mathrm{O}(\varepsilon^3)\,, \tag{4.102}$$

where as always $c_{\phi^2} = \lambda_{\phi\phi\phi^2} a_{\phi^2} = \sqrt{\frac{2}{3}}(1-\varepsilon\frac{5}{22})\left(\varepsilon a^{(1)}_{\phi^2} + \varepsilon^2 a^{(2)}_{\phi^2}\right) + \mathrm{O}(\varepsilon^3)$. The CFT data for the defect spin operator reads

$$\hat{\Delta}_{\hat{S}} = \frac{\varepsilon}{2} + \mathrm{O}(\varepsilon^2)\,, \tag{4.103}$$

$$b^2_{\phi\hat{S}} = c_{\phi^2} + \varepsilon^2\sqrt{\frac{2}{3}}a^{(1)}_{\phi^2}\left(\frac{5}{11} + \frac{16}{11}\log 2\right) + \mathrm{O}(\varepsilon^3)\,. \tag{4.104}$$

Notice that from (4.102) one can extract the defect spin dimension up to $\mathrm{O}(\varepsilon)$ since $b_{\phi\hat{S}}$ is also $\mathrm{O}(\varepsilon)$. However, the correction of order $\mathrm{O}(\varepsilon^2)$ for $\hat{\Delta}_{\hat{S}}$ is known and it is reported it in (3.72). Moving on to the other operators in the defect channel, one see that for the operator $\hat{\mathcal{O}}_{0,0}$ the CFT data is

$$\hat{\Delta}_{0,0} = \Delta_\phi + \varepsilon^2\sqrt{\frac{2}{3}}\frac{10a^{(1)}_{\phi^2}}{11} + O(\varepsilon^3)\,, \tag{4.105}$$

$$b^2_{\phi\hat{\mathcal{O}}_{0,0}} = 1 - \varepsilon^2\sqrt{\frac{2}{3}}a^{(1)}_{\phi^2}\left(\frac{31}{11} - \frac{20}{11}\log 2\right) + O(\varepsilon^3)\,. \tag{4.106}$$

Finally, one finds a single infinite family of defect operators $\hat{\mathcal{O}}_{0,s}$ with

$$\hat{\Delta}_{0,s} = \Delta_\phi + s + \varepsilon^2\sqrt{\frac{2}{3}}\frac{5a^{(1)}_{\phi^2}}{11}\frac{1}{s+1/2} + \mathrm{O}(\varepsilon^3)\,, \tag{4.107}$$

$$b^2_{\phi\hat{\mathcal{O}}_{0,s}} = 2^s\left(\frac{(\Delta_\phi)_s}{s!} + \varepsilon^2\sqrt{\frac{2}{3}}\frac{5a^{(1)}_{\phi^2}}{11}\left(\frac{H_s - H_{s-1/2}}{s+1/2} - \frac{1}{(s+1/2)^2}\right) + \mathrm{O}(\varepsilon^3)\right). \tag{4.108}$$

In the bulk channel, there are the twist-two operators J_ℓ with

$$c_\ell = \frac{\Gamma\left(\frac{\ell+1}{2}\right)\Gamma(\ell+1)^2}{8^\ell\left(\frac{\ell}{2}!\right)^2\Gamma\left(\frac{\ell+2}{2}\right)\Gamma\left(\frac{2\ell+1}{2}\right)}\Bigg(c_{\phi^2} + \\ + \varepsilon^2\sqrt{\frac{2}{3}}a^{(1)}_{\phi^2}\left(\frac{5}{11}(1+\log 2) + \frac{1}{2}\left(H_{\frac{\ell}{2}} - H_{\frac{\ell-1}{2}} + H_{\ell-\frac{1}{2}} - 3H_\ell\right)\right) + \mathrm{O}(\varepsilon^3)\Bigg)\,. \tag{4.109}$$

Notice the absence of double-twist operators with twist higher than 2. This is consistent with the fact that [136, 143] $\lambda_{\phi\phi\mathcal{O}_{n,\ell}} \sim \varepsilon$ and $a_{\mathcal{O}_{n,\ell}} \sim \varepsilon^2$. The latter fact follows immediately by considering tree-level Feynman diagrams.

4.3.3 Diagrammatic computation

In this section, the diagrammatic computation for the correlators of the bulk fields ϕ_a and ϕ^2 is outlined and compared with the bootstrap results of Sections 4.3.1 and 4.3.2.

One-point function $\langle\phi^2\rangle$, free bulk

The first computation is for the one-point function of ϕ^2 in the free theory, which was already computed at next-to-leading order in [33]. This observable is not accessible by the bootstrap analysis, and indeed it is the only information needed to completely fix the two point function of ϕ. Since the bulk is free, there are two ways of doing the computation: one can exploit the Ward identity and write the bulk correlator in terms of an integrated defect correlator using (3.68), or perform a direct computation of the bulk correlator in terms of Feynman diagrams. In terms of the defect correlator, one has

$$\langle\phi^2(0,x_\perp)\rangle_{\mathcal{D}_j} = \kappa\,\zeta^2\int d\tau\int d\tau'\frac{\langle\hat{S}^a(\tau)\hat{S}^a(\tau')\rangle_{\mathcal{D}_j}}{(\tau^2+|x_\perp|^2)^{1-\frac{\varepsilon}{2}}(\tau'^2+|x_\perp|^2)^{1-\frac{\varepsilon}{2}}}\,. \tag{4.110}$$

At the fixed point, $\langle\hat{S}^a(\tau)\hat{S}^a(\tau')\rangle_{\mathcal{D}_j}$ is given by (3.82). By computing the integrals, one obtains [15]

$$\langle\phi^2(0,x_\perp)\rangle_{\mathcal{D}_j} = \frac{\kappa\,\zeta_*^2\mathcal{N}_{\hat{S}}}{|x_\perp|^{2-\varepsilon}}\frac{\pi^{3/2}\Gamma\left(\frac{1}{2}-\frac{\varepsilon}{2}\right)}{\Gamma\left(1-\frac{\varepsilon}{2}\right)} \equiv \frac{\mathcal{N}_{\phi^2}a_{\phi^2}}{|x_\perp|^{2-\varepsilon}}\,. \tag{4.111}$$

Here $\mathcal{N}_{\phi^2}$ is the normalisation of the two-point function, which according to conventions used is

$$\langle\phi^2(x)\phi^2(0)\rangle = \frac{\mathcal{N}_{\phi^2}^2}{|x|^{2\Delta_{\phi^2}}}\,,\qquad \mathcal{N}_{\phi^2}^2 = 6\kappa^2\,. \tag{4.112}$$

By plugging in the value of the coupling at the fixed point (3.46) and the normalisation constant $\mathcal{N}_{\hat{S}}$ in (3.83), one obtains [16]

$$a_{\phi^2} = \frac{\pi^2 j(j+1)\varepsilon}{2\sqrt{6}}\left(1+\varepsilon\frac{\log 4-1}{2} + \varepsilon^2\frac{2\pi^2 j(j+1)+(\log 4-2)\log 4}{8}\right)+\mathrm{O}(\varepsilon^4)\,. \tag{4.113}$$

This result has also been reproduced using Feynman diagrams.

[15] Notice that in the bootstrap computation in Sections 4.3.1 and 4.3.2 the operators to be unit-normalised, as is customary in the CFT literature. In the diagrammatic calculation, it is convenient to use a different normalisation, and this is why the one point function here has an extra factor compared to (2.50).

[16] This result for the one-point function at the fixed point, as presented in [35], differs from the one in equation (2.14) of [33] at order ε^2. This discrepancy may arise from the possibility that the authors of [33] employed the critical coupling at leading order rather than at next-to-leading order, potentially overlooking a contribution of order ε^2 in the one-point coefficient.

One-point function $\langle\phi^2\rangle$, interacting bulk

When bulk interactions are turned on, it is no longer particularly convenient to express the bulk correlator in terms of a defect one, since the Ward identity (3.61) gets corrected and the relation between the two correlators becomes more involved. Therefore, it is easier to compute the one-point function directly using Feynman diagrams. The diagrams that contribute to the one-point function $\langle\phi^2\rangle_{\mathcal{D}_j}$ up to order ε^2 are

$\langle\phi^2(0,x_\perp)\rangle_{\mathcal{D}_j}$ =

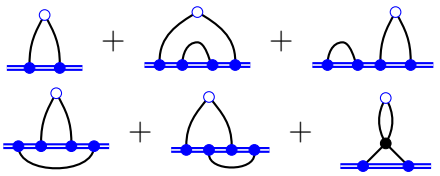

(4.114)

where in the last equation it is intended that one should consider also the specular version of diagrams (obtained by reversing the order of the insertion of all the defect interactions) such as the third and the fifth, and the black point represents the bulk interaction.

The diagrams without bulk interactions were already computed in the free bulk case in [33], but because of the shift in the critical coupling (3.49), they will give slightly different results in the interacting case. The only diagram with bulk interactions was computed in [32]. Details of the computation can be found in those papers. All in all one finds

$$a_{\phi^2} = \frac{\pi^2 j(j+1)\varepsilon}{2\sqrt{6}}\Bigg(1 - \frac{2\pi^2}{11}\Big(j(j+1) - \frac{1}{3}\Big)\varepsilon - \frac{181}{242}\varepsilon + \frac{6}{11}\varepsilon\log 2\Bigg) + \mathrm{O}(\varepsilon^3)\,. \tag{4.115}$$

Two-point function $\langle\phi\phi\rangle$, free bulk

Moving on to the two point function of the order parameter ϕ in a free bulk, it is possible to play the same trick as before and compute it in terms of an integrated defect two-point function. In particular, using (3.68), one has

$$\langle\phi_a(0,x_\perp)\phi_b(0,y_\perp)\rangle_{\mathcal{D}_j} = \kappa\,\zeta^2 \int d\tau \int d\tau' \frac{\langle\hat{S}_a(\tau)\hat{S}_b(\tau')\rangle_{\mathcal{D}_j}}{(\tau^2+|x_\perp|^2)^{1-\frac{\varepsilon}{2}}(\tau'^2+|y_\perp|^2)^{1-\frac{\varepsilon}{2}}} + \langle\phi_a^{\text{free}}(0,x_\perp)\phi_b^{\text{free}}(0,y_\perp)\rangle_{\mathcal{D}_j}\,. \tag{4.116}$$

At the fixed point, using (3.46) and (3.82), one finds

$$\begin{aligned}&\langle\phi_a(0,x_\perp)\phi_b(0,y_\perp)\rangle_{\mathcal{D}_j} = \\ &= \frac{\kappa\zeta_*^2\mathcal{N}_{\hat{S}}}{3}\int d\tau\int d\tau'\frac{\delta_{ab}}{|\tau-\tau'|^{2\hat{\Delta}_{\hat{s}}}(\tau^2+r^2)^{1-\frac{\varepsilon}{2}}(\tau'^2+1)^{1-\frac{\varepsilon}{2}}}+\frac{\mathcal{N}_\phi^2\delta_{ab}\xi^{-\Delta_\phi}}{|x_\perp|^{\Delta_\phi}|y_\perp|^{\Delta_\phi}} = \\ &\equiv \frac{\mathcal{N}_\phi^2\delta_{ab}F_{\phi\phi}(r,w)}{|x_\perp|^{\Delta_\phi}|y_\perp|^{\Delta_\phi}}\,,\end{aligned} \tag{4.117}$$

where symmetry was used to set the first operator at $x=(0,z,\bar{z},0,0,...)$ and the other one at $(0,1,0,0,...)$, and then everything was expressed in radial coordinates (2.56) in order to simplify the computation. The factor ξ was defined in (4.58), and $\mathcal{N}_\phi=\sqrt{\kappa}$. The integral can be solved in terms of hypergeometric functions and gives

$$\begin{aligned}F_{\phi\phi}(r,w) &= \xi^{-\Delta_\phi}+\frac{\zeta_*^2\mathcal{N}_{\hat{S}}}{3}\left(\frac{2\pi\tan\left(\frac{\pi\varepsilon}{2}\right)r^{1-\frac{\varepsilon}{2}}\,{}_2F_1\left(\frac{1}{2},1-\frac{\varepsilon}{2};\frac{3}{2}-\frac{\varepsilon}{2};r^2\right)}{\varepsilon-1}\right. \\ &\qquad\left.+\frac{\pi\,r^{\frac{\varepsilon}{2}}\Gamma\left(\frac{1}{2}-\frac{\varepsilon}{2}\right)^2\,{}_2F_1\left(\frac{1}{2},\frac{\varepsilon}{2};\frac{\varepsilon+1}{2};r^2\right)}{\Gamma\left(1-\frac{\varepsilon}{2}\right)^2}\right) = \\ &= \xi^{-\Delta_\phi}+\lambda_{\phi\phi\phi^2}\,a_{\phi^2}J_\varepsilon(r)\,,\end{aligned} \tag{4.118}$$

where the second line was obtained using the expression of the one-point function (4.111), the three-point function coefficient (4.72), and well known identities for the hypergeometric function. This result holds for all ε and perfectly matches the bootstrap prediction (4.67), in particular note that the non-trivial integral corresponds to $J_\varepsilon(r)$, the contribution of spin $s=0$ defect operators defined in (4.95).

Two-point function $\langle\phi\phi\rangle$, interacting bulk

When bulk interactions are turned on, it is convenient to use Feynman diagrams, since most of the diagrams have already been evaluated in [34, 135]. At order ε^2 one has

$\langle\phi_a\phi_a\rangle_{\mathcal{D}_j}$ = 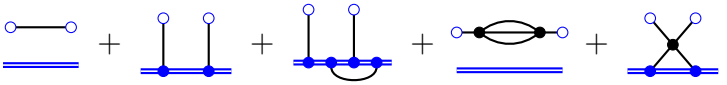 ,

(4.119)

where again also the contribution from the specular version of the third diagram is implied. The first two diagrams are the just the free propagator and the square of the one-point function of ϕ^a, which is zero. The

only non-trivial diagram is the last one, and it was already computed in [34, 135] in terms of the function $H(r,w)$ introduced in (4.94). All in all, one finds

$$F_{\phi\phi}(r,w) = \xi^{-\Delta_\phi} + c_{\phi^2}\left(1 + \frac{\varepsilon}{2}\log\frac{4r}{(1+r)^2} + \frac{5\varepsilon}{11}\big(1+\log 2 + H(r,w)\big)\right), \tag{4.120}$$

where as always $c_{\phi^2} = \lambda_{\phi\phi\phi^2} a_{\phi^2}$, with $\lambda_{\phi\phi\phi^2}$ given by (4.92) and a_{ϕ^2} by (4.115). This result perfectly matches the bootstrap prediction (4.102).

Two-point function $\langle\phi^2\phi^2\rangle$, free bulk

The two-point function of ϕ^2 in free theory can once again be computed in terms of defect correlators, namely

$$\begin{aligned}
&\langle\phi^2\phi^2\rangle_{\mathcal{D}_j} = \\
&= \kappa^2\,\zeta_*^4 \int d\tau_1 \int d\tau_2 \int d\tau_3 \int d\tau_4 \frac{\langle \hat{S}_a(\tau)\hat{S}^a(\tau_1)\hat{S}_b(\tau_2)\hat{S}^b(\tau_3)\rangle_{\mathcal{D}_j}}{({\tau_1}^2+r^2)^{1-\frac{\varepsilon}{2}}({\tau_2}^2+r^2)^{1-\frac{\varepsilon}{2}}({\tau_3}^2+1)^{1-\frac{\varepsilon}{2}}({\tau_4}^2+1)^{1-\frac{\varepsilon}{2}}} + \\
&+ 2\kappa\,\zeta_*^2 \int d\tau_1 \int d\tau_2 \frac{\langle\hat{S}^a(\tau_1)\hat{S}^b(\tau_2)\rangle_{\mathcal{D}_j}\langle\phi_a^{\text{free}}\phi_b^{\text{free}}\rangle_{\mathcal{D}_j}}{({\tau_1}^2+r^2)^{1-\frac{\varepsilon}{2}}({\tau_2}^2+1)^{1-\frac{\varepsilon}{2}}} + \langle\phi^2_{\text{free}}\phi^2_{\text{free}}\rangle_{\mathcal{D}_j} = \\
&= \kappa^2\,\zeta_*^4 \int d^4\tau \frac{\langle\hat{S}_a(\tau_1)\hat{S}^a(\tau_2)\hat{S}_b(\tau_3)\hat{S}^b(\tau_4)\rangle_{\mathcal{D}_j}}{({\tau_1}^2+r^2)^{1-\frac{\varepsilon}{2}}({\tau_2}^2+r^2)^{1-\frac{\varepsilon}{2}}({\tau_3}^2+1)^{1-\frac{\varepsilon}{2}}({\tau_4}^2+1)^{1-\frac{\varepsilon}{2}}} + \\
&+ \frac{1}{|x_\perp|^{\Delta_{\phi^2}}|y_\perp|^{\Delta_{\phi^2}}}\left(\xi^{-\Delta_{\phi^2}} + 2c_{\phi^2}\xi^{\Delta_\phi}J_\varepsilon(r)\right),
\end{aligned} \tag{4.121}$$

where the explicit dependence on the external coordinates of the free fields ϕ^{free} was suppressed and the results of the previous section were used in order to simplify the expression. Contrary to the previous cases, it is not possible to simplify the result further without expanding in ε. The reason is that the four-point function of defect operator is not completely fixed by conformal invariance and one cannot do the first integral without knowing its explicit expression.[17] The four-point function of $\hat{S}^a$ at tree-level is just given by traces of the generators T^a, just like the two point function. However, one should be careful about the order of the positions where the generators are inserted, which corresponds to step functions. This happens because, as explained in Section 3.3.3, the defect spin operator has to be interpreted as a

[17] The defect four-point function at the conformal fixed point can be expressed as $\langle\hat{S}_a(\tau_1)\hat{S}_a(\tau_2)\hat{S}_a(\tau_3)\hat{S}_a(\tau_4)\rangle_{\mathcal{D}_j} = \mathcal{N}_{\hat{S}}^2 f(z)/(\tau_{12}^{2\hat{\Delta}_{\hat{S}}}\tau_{34}^{2\hat{\Delta}_{\hat{S}}})$, where $f(z)$ is an arbitrary function of the conformal cross-ratio $z = \frac{\tau_{12}\tau_{34}}{\tau_{13}\tau_{24}}$.

generator inserted at a specific position in the path ordering. Therefore, it follows that

$$\begin{aligned}
&\langle \hat{S}_a(\tau_1)\hat{S}^a(\tau_2)\hat{S}_b(\tau_3)\hat{S}^b(\tau_4)\rangle_{\mathcal{D}_j} = \\
&= \frac{1}{2j+1}\big[\mathrm{Tr}\,(T_aT_aT_bT_b)\,(\theta_{1>2>3>4}+\text{cyclic perm.})+ \\
&+ \mathrm{Tr}\,(T_aT_bT_aT_b)\,(\theta_{1>3>2>4}+\theta_{1>4>2>3}+\text{cyclic perm.})\big]+\mathrm{O}(\varepsilon) = \\
&= j^2(j+1)^2\,(\theta_{1>2>3>4}+\theta_{1>3>2>4}+\theta_{1>4>2>3}+\text{cyclic perm.})+ \\
&- j(j+1)\,(\theta_{1>3>2>4}+\theta_{1>4>2>3}+\text{cyclic perm.})+\mathrm{O}(\varepsilon)\,,
\end{aligned} \tag{4.122}$$

where the order of the points is indicated by the theta functions. When this result is plugged into (4.121) and the symmetry of the integrand is used, the term that goes like $\sim j^2(j+1)^2$ reproduces the square of the one-point function. The other term reduces to

$$-\int_{\tau_1>\tau_3>\tau_2>\tau_4} d\tau^4\ ({\tau_1}^2+r^2)^{-1}({\tau_2}^2+r^2)^{-1}({\tau_3}^2+1)^{-1}({\tau_4}^2+1)^{-1} \equiv \frac{\pi^2}{2r^2}\,W(r)\,, \tag{4.123}$$

where $W(r)$ is given by

$$\begin{aligned}
W(r) = 2\mathrm{Li}_2\left(\frac{1-r}{2}\right) &-\mathrm{Li}_2(1-r)-\mathrm{Li}_2(-r)+ \\
&+\log(r+1)\log\left(\frac{r+1}{4r}\right)+\log^2 2\,.
\end{aligned} \tag{4.124}$$

At the end of the day, the two-point function reads

$$\langle\phi^2(0,x_\perp)\phi^2(0,y_\perp)\rangle_{\mathcal{D}_j} = \frac{\mathcal{N}_{\phi^2}^2\,F_{\phi^2\phi^2}(r,w)}{|x_\perp|^{\Delta_{\phi^2}}|y_\perp|^{\Delta_{\phi^2}}}\,, \tag{4.125}$$

where

$$\begin{aligned}
F_{\phi^2\phi^2}(r,w) = \xi^{-\Delta_{\phi^2}} + a_{\phi^2}^2 + 2c_{\phi^2}\xi^{\Delta_\phi}\left(1+\frac{\varepsilon}{2}\,\log\frac{4r}{(1+r)^2}\right)+ \\
-\frac{\pi^2 j(j+1)}{6}\varepsilon^2 W(r)+\mathrm{O}(\varepsilon^3)\,.
\end{aligned} \tag{4.126}$$

Comparing with the bootstrap result (4.80), one immediately sees that the two results coincide up to the term proportional to $W(r)$. Indeed the function $W(r)$ corresponds to a spin $s=0$ ambiguity, in the language of the bootstrap. It has a simple block expansion in the defect channel

$$W(r) = (2-4\log 2)\hat{f}_{1,0}(r) - 2\partial_{\hat{\Delta}}\hat{f}_{1,0}(r) + 4\sum_{n=2}^{\infty}\frac{(-1)^n(n-2)!}{n\left(\frac{3}{2}\right)_{n-2}}\,\hat{f}_{n,0}(r)\,. \tag{4.127}$$

Expanding (4.126) in the defect channel one finds that the lowest singlet operator, which can be identified with $\hat{\Phi}$, has

$$\hat{\Delta}_{\hat{\Phi}} = 1 + \varepsilon + \mathrm{O}(\varepsilon^2)\,. \tag{4.128}$$

This result matches with the expression computed from the beta function (3.95). One can also extract the bulk CFT data from (4.126), but the results are not particularly illuminating. Therefore, they are not presented here.

Two-point function $\langle\phi^2\phi^2\rangle$, interacting bulk

In the interacting case, the two-point function of ϕ^2 can only be computed using Feynman diagrams. At order ε^2, the relevant diagrams are

$\langle\phi^2(0,x_\perp)\phi^2(0,y_\perp)\rangle$ =

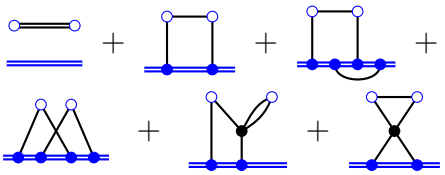

, (4.129)

where as before contributions from specular diagrams are implied. The first diagram stands for corrections to the propagator that come purely from bulk interactions. These have been computed long ago in the theory without the defect and generate corrections to the dimension of Δ_{ϕ^2} in the bulk identity term $\xi^{-\Delta_{\phi^2}}$. Those are not drawn explicitly to avoid cluttering. The only non-trivial diagram is the fifth, which can be computed in terms of $W(r)$ (4.123). All the other diagrams were already computed in [135]. The final result is

$$F_{\phi^2\phi^2}(r,w) = \xi^{-\Delta_{\phi^2}} + a_{\phi^2}^2 - \frac{\varepsilon^2\pi^2 j(j+1)}{6}W(r) + \frac{\pi^2 j(j+1)\varepsilon}{3\xi^{1-\frac{\varepsilon}{22}}}\Bigg(1+\varepsilon\log 2$$
$$+\frac{\varepsilon}{11}\Bigg(-\tfrac{118}{11} + 5H(r,w) - 2\pi^2\big(j(j+1)-\tfrac{1}{3}\big) + \tfrac{1}{2}\log\frac{4r}{(r+1)^2}\Bigg)\Bigg) + \mathrm{O}(\varepsilon^3)\,. \tag{4.130}$$

It would be difficult to compute this result using bootstrap methods, since the discontinuity would receive contributions from all the double-twist operators.

Chapter 5

Transdimensional defects

5.1 Transdimensional defects in the $O(N)$ model

The defects in the $O(N)$ model introduced in Chapter 3 within the framework of the ε-expansion always have either integer dimension or integer co-dimension. It is important to recall that the main idea behind the ε-expansion is to study a CFT in $d = 3$ dimensions by considering the CFT in $d = 4 - \varepsilon$ dimensions instead, where it is weakly coupled, and then extrapolating to $\varepsilon = 1$. When a defect is incorporated into this framework, having either integer dimension p or co-dimension q ensures that, when the bulk is extrapolated to some integer dimension, the defect will also be integer-dimensional, thus allowing for a physically meaningful interpretation. More generally, most defects considered in the literature, including those constructed in other CFTs, are either lines, surfaces, boundaries, or interfaces. However, in principle it is also possible to obtain an integer-dimensional defect in an integer-dimensional bulk by allowing both p and q to deviate from their original integer values, and then extrapolating to new values. The purpose of this chapter is to demonstrate that this more general perspective enables the construction of new and interesting defects by interpolating between different values of the defect dimension, as discussed in [36]. In this section, the focus is on the "p=2.01 defect in $d = 3.99$ dimensions" in the $O(N)$ model. In Section 5.2, another example is provided, considering a symmetry-breaking defect in the $O(N)$ model at large N whose dimension interpolates between $p = 1$ and $p = 2$ as the dimension of the bulk varies between $d = 4$ and $d = 6$.

5.1.1 Free $O(N)$ field theory

At first, one can consider a simple soluble example: the free scalar $O(N)$ theory in d dimensions. Its action is

$$S = \int d^d x \, \tfrac{1}{2} \partial^\mu \phi_a \partial_\mu \phi_a \,. \tag{5.1}$$

The action is deformed by the defect interaction terms

$$S_D = \tfrac{1}{2} (h_0)_{ab} \int d^p \tau \, (\delta_{ab} S + T_{ab}) \,, \tag{5.2}$$

where S and T_{ab} are the two primary operators that are quadratic in the fields,

$$S \equiv \frac{1}{N} \phi_a \phi_a \,, \qquad T_{ab} \equiv \phi_a \phi_b - \frac{\delta_{ab}}{N} \phi_c \phi_c \,, \tag{5.3}$$

and h_0 has mass dimension $p+2-d$. For simplicity, this section focuses on the $O(N)$-invariant defect.

For $d = 4 - \varepsilon < 4$ and $p = 2$, this deformation is weakly relevant and triggers a defect RG flow, as mentioned in 3.4.1. This flow can be studied exactly in ε, and for $\varepsilon = 1$ it reaches an IR fixed point that corresponds to the three-dimensional free scalar theory with an interface with Dirichlet boundary conditions [123–125]. If one instead takes $d = p = 3$, the action just defines a free massive scalar theory with mass $m^2 = h_0$. Here a third possibility is explored by setting $d = 4 - \varepsilon$ and $p = 2 + \delta$. The deformation is again weakly relevant and the defect flows to an IR fixed point. This defect RG flow can be studied in perturbation theory, where it is possible to resum diagrams at all orders. The analysis is essentially the same as in [123, 125], except that defect integrals have now to be performed in $p = 2 + \delta$ dimensions. A similar approach has been explored in the context of coupling theories across different dimensions [147].

More concretely, to renormalise the theory one sets $h_0 = \mu^{\varepsilon+\delta} Z_h h$, where Z_h is a renormalisation factor and h is the renormalised coupling. Then finiteness of the bulk one-point function $\langle \phi^2(x_\perp, x_\parallel) \rangle$ is imposed in the limit $\varepsilon, \delta \to 0$, where $x_\perp$ is the distance from the defect. The one-point function is given by the sum of the series of diagrams

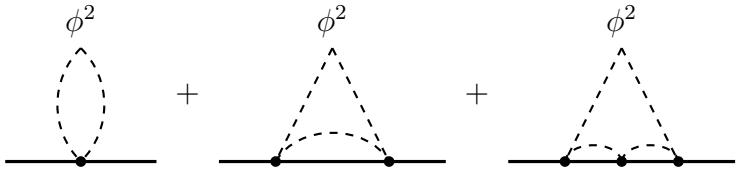

(5.4)

Here the solid line represents the p-dimensional defect and dashed lines are free propagators

$$G(x) = \frac{\mathcal{N}_\phi^2}{|x|^{d-2}}\,, \qquad \mathcal{N}_\phi^2 = \frac{\Gamma(d/2-1)}{4\pi^{d/2}}\,. \tag{5.5}$$

In the MS scheme,[1] finiteness of the sum in (5.4) is guaranteed at all orders provided that

$$Z_h = \frac{1}{1-h/(\varepsilon+\delta)}\,, \tag{5.6}$$

where $h \to 2\pi h$ has been rescaled. The exact beta-function is obtained by imposing $\mu\frac{d}{d\mu}h_0 = 0$; it reads

$$\beta_h = -(\varepsilon+\delta)h + h^2\,, \tag{5.7}$$

and admits a non-trivial IR fixed point for $h_* = \varepsilon + \delta$.

Since the action (5.1) is Gaussian, generic defect correlators can be obtained by Wick contractions, once the dimension of the defect operator $\hat\phi$, $\hat\Delta_{\hat\phi}$, and that of the defect operator $\partial_\perp\hat\phi$, $\hat\Delta_{\partial_\perp\hat\phi}$, are known. To determine the first, one can use that at the fixed point

$$\hat\Delta_{\hat S} = p + \frac{\partial\beta_h}{\partial h}\Big|_{h_*} = 2+\varepsilon+2\delta \qquad \Rightarrow \qquad \hat\Delta_{\hat\phi} = 1 + \frac{\varepsilon}{2} + \delta\,. \tag{5.8}$$

The operator $\partial_\perp\hat\phi$ does not get renormalised in this model, see Footnote 2, and its dimension is

$$\hat\Delta_{\partial_\perp\hat\phi} = 2 - \frac{\varepsilon}{2}\,. \tag{5.9}$$

The sum in (5.4) also determines the value of the one-point function of S at the bulk fixed point in the presence of the defect, see (B.76, B.77). To compute it one expands the result in powers of ε and δ which allows to guess the expression

$$\langle S(x_\perp, x_\parallel)\rangle = \frac{\mathcal{N}_S\, a_S}{|x_\perp|^{2\Delta_\phi}}\,, \quad \mathcal{N}_S = 2N\mathcal{N}_\phi^2\,, \quad a_S = -\frac{\sqrt{\pi}\,\Gamma\left(1+\frac{\varepsilon}{2}+\delta\right)}{2^{2+\delta}\Gamma\left(\frac{3+\delta}{2}\right)\Gamma\left(\frac{\varepsilon+\delta}{2}\right)}\,. \tag{5.10}$$

With these expressions at hand, one may consider different values of δ. For $\delta = 1-\varepsilon$ the defect is an interface and (5.8), (5.10) reproduce,

[1] In this case there are only poles in the variable $\varepsilon+\delta$, hence the MS scheme is unambiguous. In the interacting case, where the poles are different linear combinations of ε and δ, one needs to specify how the minimal subtraction should be performed.

for any ε, the values for the free scalar theory with Dirichlet boundary conditions [148]. The dimensions of both $\partial_\perp\hat{\phi}$ and $\hat{\phi}$ are $2-\varepsilon/2$ and further evidence that they are linearly dependent comes from the boundary operator product expansion (OPE) coefficients of these two operators [17]. At order ε^0 one has

$$\langle\phi(x)\hat{\phi}(\tau)\rangle = \frac{\mathcal{N}_\phi\mathcal{N}_{\hat{\phi}}b_{\phi,\hat{\phi}}}{|x_\perp|^{\Delta_\phi-\hat{\Delta}_{\hat{\phi}}}|x_\parallel-\tau|^{2\hat{\Delta}_{\hat{\phi}}}}\,,\quad b^2_{\phi,\hat{\phi}} = \frac{2^\delta\Gamma\left(1-\frac{\delta}{2}\right)\Gamma\left(\frac{1+\delta}{2}\right)}{\sqrt{\pi}}+\mathrm{O}(\varepsilon)\,, \tag{5.11}$$

where $\langle\hat{\phi}(0)\hat{\phi}(\tau)\rangle = \mathcal{N}^2_{\hat{\phi}}/|\tau|^{2\hat{\Delta}_{\hat{\phi}}}$, and similarly

$$b^2_{\phi,\partial_\perp\hat{\phi}} = \frac{2}{2-\delta}+\mathrm{O}(\varepsilon)\,. \tag{5.12}$$

This means that for $\varepsilon=0$ (and $\delta=1$), the boundary OPE coefficient for the unit normalised operator $\hat{\Phi}_+ = (\hat{\phi}+\partial_\perp\hat{\phi})/\sqrt{2}$ becomes $b^2_{\phi,\hat{\Phi}_+} = (b_{\phi,\hat{\phi}}+b_{\phi,\partial_\perp\hat{\phi}})^2/2 = 4$, which is the correct value for the boundary operator in the Dirichlet interface theory in $d=4$. Similarly, one can see that the operator $\hat{\Phi}_- = (\hat{\phi}-\partial_\perp\hat{\phi})/\sqrt{2}$ decouples. A similar statement should hold for $\varepsilon>0$.

As another example, one may attempt to construct a line defect via $\delta\to-1$. To keep the quadratic deformation relevant, one should make sure that $\varepsilon+\delta>0$. For the case of $\varepsilon=1$, one gets $\hat{\Delta}_{\hat{\phi}}=1/2$ from (5.8), which is the dimension of the bulk field, so this is the trivial defect with $h_*=0$. A similar result was obtained for $N=1$ in [121].

Next, for $\varepsilon,\delta\to1$ one gets a three-dimensional theory with $\hat{\Delta}_{\hat{\phi}}=5/2$, so a non-local theory of GFF. More generally, leaving $0<\varepsilon<1$ as a free parameter and looking only at defect correlators, one gets a continuous family of GFF theories with $2<\hat{\Delta}_{\hat{\phi}}<5/2$. This is similar in spirit to the defect description of the long-range Ising model discussed in Section 6.1. Another generalisation, starting with any theory near the critical dimension d_c, *i.e.* $d=d_c-\varepsilon$ and $p=d_c-2+\delta$ for some positive integer $d_c\geqslant2$, gives $\hat{\Delta}_{\hat{\phi}}=\frac{1}{2}(d_c+1)$ when $\varepsilon,\delta\to1$.

Finally, it is instructive to see what happens in the space-filling limit $p\to d$, *i.e.* $\delta\to2-\varepsilon$. Since in this limit there are no orthogonal directions ($|x_\perp|\to0$), the most one can do is push bulk operators to the defect by suitable rescalings. This procedure selects the lightest defect operator in the defect OPE. For example, in this limit the unit normalised operator $b^{-1}_{S,(\partial_\perp\hat{\phi})^2}|x_\perp|^{\Delta_S-\hat{\Delta}_{(\partial_\perp\hat{\phi})^2}}S(x)$ reduces to the defect operator $(\partial_\perp\hat{\phi})^2(x)$. Note that the dimensions of $\hat{\phi}$ and $\partial_\perp\hat{\phi}$ cross at

the interface value $\delta = 1 - \varepsilon$ and for $\delta > 1 - \varepsilon$ the latter becomes smaller. Crucially, for $\delta = 2 - \varepsilon$ the bulk one-point function coefficient a_S remains finite, whereas the defect OPE coefficient

$$b_{S,(\partial_\perp \hat{\phi})^2} = \frac{8N\pi^{\varepsilon}\Gamma\left(2-\frac{\varepsilon}{2}\right)^2}{(2-\varepsilon-\delta)^2}\,, \tag{5.13}$$

is divergent. Therefore, $\lim_{p\to d} a_S/b_{S,(\partial_\perp \hat{\phi})^2} = 0$, so that there are no non-zero one-point functions.

5.1.2 The interacting $O(N)$ model to all orders in the defect coupling

After studying the free theory, it is natural to consider the interacting $O(N)$ model with action

$$S = \int d^d x \left[\tfrac{1}{2}\partial^\mu \phi_a \partial_\mu \phi_a + \tfrac{1}{8}\lambda_0 \left(\phi_a \phi_a\right)^2\right]. \tag{5.14}$$

For $d = 4 - \varepsilon < 4$ the coupling triggers an RG flow. The one-loop beta function for λ (after rescaling $\lambda \to 16\pi^2\lambda$) is

$$\beta_\lambda = -\varepsilon\lambda + (N+8)\lambda^2 + \mathrm{O}(\lambda^3)\,. \tag{5.15}$$

This flow ends at the IR Wilson–Fisher fixed point at

$$\lambda_* = \frac{\varepsilon}{N+8} + \mathrm{O}(\varepsilon^2)\,. \tag{5.16}$$

The conformal dimensions of the S and T_{ab} operators in (5.3) are (see [100, 95] for a variety of methods and results)

$$\Delta_S = 2 - \frac{6}{N+8}\varepsilon + \mathrm{O}(\varepsilon^2)\,, \qquad \Delta_T = 2 - \frac{N+6}{N+8}\varepsilon + \mathrm{O}(\varepsilon^2)\,. \tag{5.17}$$

The defect action (5.2) then triggers a defect RG flow since the coupling $(h_0)_{ab}$ is relevant for any N provided that $p \gtrsim 2$.

Focusing again on the symmetry preserving defect with $(h_0)_{ab} = h_0\delta_{ab}$, the diagrams contributing to the one-point function $\langle S\rangle$ at first order in λ and at all orders in h are

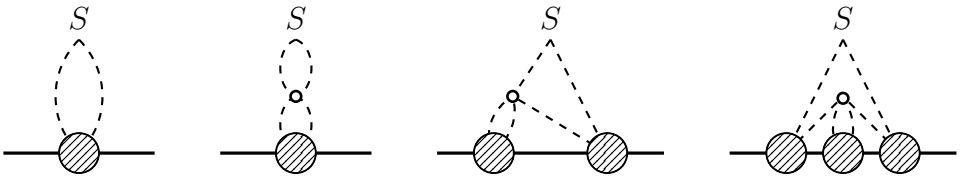

(5.18)

Here the bubbles represent contributions at all powers of h, or "hops" on the defect. They are first defined recursively as an effective defect-to-defect propagator

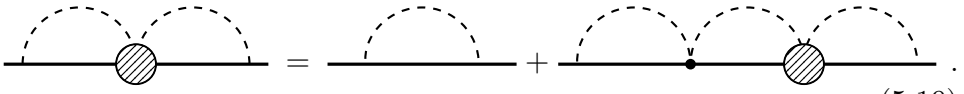

(5.19)

This is evaluated as an infinite sum in Appendix B.3, see (B.75). From this one defines the contraction with the bulk

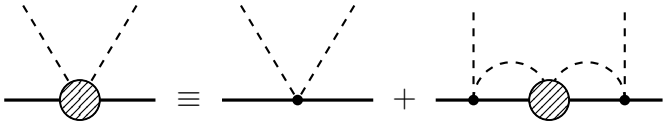

(5.20)

The expression for this is more complicated and it is difficult to compute it in closed form for arbitrary bulk endpoints. For the purpose of evaluating the divergences in the diagrams (5.18), one only needs it in two cases: with two coincident endpoints and with one endpoint close to the defect and the other far. These are written in (B.76) and (B.78-B.80).

At the end of the calculation of the divergences in (5.18), one can write the counterterm as an extra factor multiplying $Z_h\big|_{\lambda=0}$ of the free theory in (5.6) and its first terms are

$$Z_{h,\lambda} = Z_h\big|_{\lambda=0}\left(1+\lambda\,(N+2)\left(\frac{1}{\varepsilon}+\frac{h}{(\varepsilon+\delta)\,(2\varepsilon+\delta)}-\frac{2h}{2\varepsilon+\delta}+\cdots\right)\right)+\mathrm{O}(\lambda^2)\,. \tag{5.21}$$

As usual the relation between the bare and the renormalised coupling is $h_0 = \mu^{\varepsilon+\delta} Z_{h,\lambda}\, h$. Then imposing that h_0 does not depend on the scale μ, one gets the beta function

$$\beta_h = -(\varepsilon+\delta)h+h^2+\lambda\,(N+2)\left(h-2h^2+2h^3+\cdots\right)+\mathrm{O}(\lambda^2)\,, \tag{5.22}$$

with terms up to order λh^{11} written in (B.84). From this one can compute the fixed point coupling h_* (B.86) and the dimension of the defect operator $\hat{S}$ at the fixed point is

$$\hat{\Delta}_{\hat{S}} = p+\frac{\partial\beta_h}{\partial h}\Big|_{\lambda_*,h_*} = 2+2\delta+\varepsilon\left(\frac{6}{N+8}+\frac{N+2}{N+8}\,f(\delta)\right)+\mathrm{O}(\varepsilon^2)\,, \tag{5.23}$$

where the first ten terms in the expansion of $f(\delta)$ can be conveniently packaged as

$$f(\delta) = \frac{\delta-1}{\delta+1}+\frac{1}{1+2\delta}\exp\left(\zeta(3)\delta^3-\frac{9}{4}\zeta(4)\delta^4+\frac{9}{2}\zeta(5)\delta^5-\frac{135}{16}\zeta(6)\delta^6\right.$$
$$\left.+\frac{249}{16}\zeta(7)\delta^7-\frac{1827}{64}\zeta(8)\delta^8+\frac{2515}{48}\zeta(9)\delta^9-\frac{24687}{256}\zeta(10)\delta^{10}+\mathrm{O}(\delta^{11})\right). \tag{5.24}$$

While this is an economical way to write the answer, a pattern in the rational coefficients multiplying the zeta values has not been found, and the terms in the exponent do not decrease, so it does not provide a good indication of the analytic structure of $f(\delta)$. Instead, if one expands everything in a power series, the ratio of subsequent terms $f_k/f_{k+1} \xrightarrow{\sim} -2/3$. This indicates a pole and one can then repeat the analysis with the function $(\delta + 2/3)f(\delta)$, whose series suggests a further singularity at $\delta = -1$. Finally, the series of the function $(\delta + 1)(\delta + 2/3)f(\delta)$ is now quickly convergent for $|\delta| \leqslant 1$ and can be used to estimate both the value and the error of $f(1)$.[2] In this way, one finds

$$f(1) = 0.4999(3)\,. \tag{5.25}$$

An alternative approach is to use the Padé-conformal method (see [149] and references therein). In this case, the approximants up to the order that computed give $f(1) \approx 0.500\ldots$, where the given digits are completely stable. It is tempting to conclude that $f(1) = 1/2$, and this value will be used in what follows. See a graph of the function in Figure 5.1.

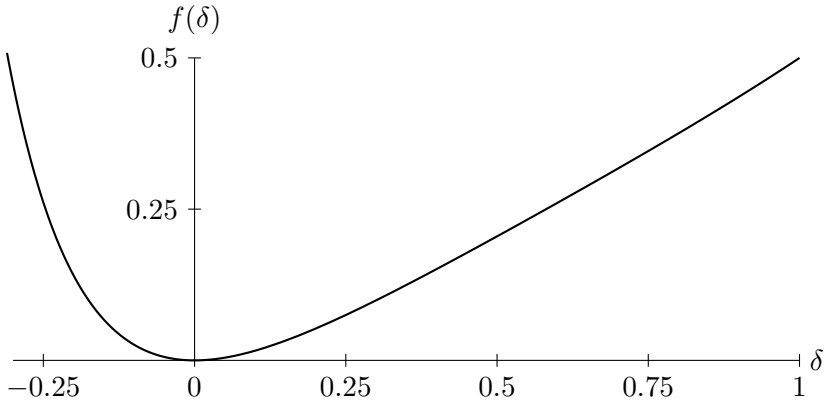

Figure 5.1: A graph of the function $f(\delta)$ in (5.24) that controls the dimension of $\hat{S}$.

With relatively little further effort one can compute the dimensions of $\hat{\phi}$ and $\partial_\perp\hat{\phi}$. The resulting expressions are easier and match the expansion of rational functions (B.90), (B.94), which is resummed to

$$\hat{\Delta}_{\hat{\phi}} = 1 + \delta + \frac{\varepsilon}{2} - \frac{N+2}{N+8}\,\frac{\varepsilon}{1+\delta} + \mathrm{O}(\varepsilon^2)\,, \tag{5.26}$$

$$\hat{\Delta}_{\partial_\perp\hat{\phi}} = 2 - \frac{\varepsilon}{2} - \frac{N+2}{N+8}\,\frac{\varepsilon\,\delta}{(2-\delta)(1+\delta)} + \mathrm{O}(\varepsilon^2)\,. \tag{5.27}$$

[2] A conservative way to estimate the error is to first observe that the ratios of consecutive coefficients of $g(\delta)$ are decreasing. Then the error can be computed as a geometric series starting with the last known coefficient and with rate given by the last known ratio.

At this point one can look at what happens for different values of δ. One obvious case is to set $\delta = 1 - \varepsilon$, where the defect becomes an interface. Collecting the results for the observables that have been computed, by using $f(1-\varepsilon) \approx f(1) + \mathrm{O}(\varepsilon) \approx \frac{1}{2} + \mathrm{O}(\varepsilon)$ one finds

$$\begin{aligned} \hat{\Delta}_{\hat{\phi}}\big|_{3-\varepsilon} &= 2 - \frac{N+5}{N+8}\varepsilon + \mathrm{O}(\varepsilon^2)\,, \quad \hat{\Delta}_{\hat{S}}\big|_{3-\varepsilon} = 4 - \frac{3}{2}\frac{N+6}{N+8}\varepsilon + \mathrm{O}(\varepsilon^2)\,, \\ \hat{\Delta}_{\partial_\perp\hat{\phi}}\big|_{3-\varepsilon} &= 2 - \frac{N+5}{N+8}\varepsilon + \mathrm{O}(\varepsilon^2)\,, \quad \hat{\Delta}_{\hat{D}}\big|_{3-\varepsilon} = 4 - \varepsilon\,, \end{aligned} \tag{5.28}$$

where $\hat{D} \sim \hat{\phi}_a \partial_\perp \hat{\phi}_a$ is the displacement operator, whose dimension is protected. Interestingly, the dimensions of $\hat{\phi}$ and $\partial_\perp\hat{\phi}$ coincide at first non-trivial order in ε, as they do in the free theory. Additionally, they both agree with the value of the boundary operator of the $O(N)$ model with Dirichlet boundary conditions (known also as the ordinary fixed point) [150,151,128]. Indeed, it was conjectured in [129] that the defect deformation under consideration should flow in $d = 3$ and $p = 2$ (so for $\varepsilon = 1$ and $\delta = 0$) to two disconnected copies of the ordinary fixed point in the IR. While this feature persists for $\varepsilon \neq 1$ and $p = d - 1$, according to (5.28) the dimensions of $\hat{S}$ and $\hat{D}$ do not match at order ε with $\hat{S}$ slightly lighter. This shows that the interface CFT limit of this transdimensional defect is not equivalent to two copies of the $O(N)$ model with Dirichlet boundary conditions, since in the latter case the lightest singlet defect operator is the displacement. It could still be that summing higher orders will lead to an identity at $\varepsilon = 1$.

Taking $\delta = -1$ to construct an $O(N)$ symmetric line defect is unsuccessful as all of (5.23), (5.26) and (5.27) diverge. This may be cured at higher orders in ε, but recall from Section 5.1.1 that in the free theory there is also no symmetry-preserving line defect at $\varepsilon = 1$.

Alternatively, for $\delta = 1$, the defect becomes three-dimensional. In this case, defect correlators immediately yield an example of a non-local CFT in three dimensions. Indeed, by looking at the sector of operators that are uncharged under the $SO(d-p)$ rotational symmetry around the defect, which is a global symmetry from the point of view of defect operators, one finds a CFT whose light spectrum is

$$\hat{\Delta}_{\hat{\phi}}\big|_{p=3} = 2 + \frac{3}{N+8}\varepsilon + \mathrm{O}(\varepsilon^2)\,, \qquad \hat{\Delta}_{\hat{S}}\big|_{p=3} = 4 + \frac{N+14}{2(N+8)}\varepsilon + \mathrm{O}(\varepsilon^2)\,. \tag{5.29}$$

Additionally, there are also sectors that are charged under $SO(d-p)$, where $d-p$ is generically non-integer, as investigated already in [152].

For instance, one has

$$\hat{\Delta}_{\partial_\perp \hat{\phi}}\big|_{p=3} = 2 - \frac{N+5}{N+8}\varepsilon + \mathrm{O}(\varepsilon^2)\,, \qquad \hat{\Delta}_{\hat{D}}\big|_{p=3} = 4\,. \tag{5.30}$$

These charged operators might be evanescent [153] for $\varepsilon = 1$. In fact, their correlators are necessarily proportional to contractions of projectors. For example, $\delta^{ij}\langle(\partial_i\phi)(\partial_j\phi)(\phi^2)\rangle \propto 1-\varepsilon$, which is vanishing for $\varepsilon = 1$.

For $\varepsilon \to 0$ and $\delta \to 1$ one recovers the free field results in Section 5.1.1, namely a three-dimensional GFF with $\hat{\Delta}_{\hat{\phi}} = 2$. In the free theory, tuning $\varepsilon \to 1$ leads to a GFF with $\hat{\Delta}_{\hat{\phi}} = 5/2$. In the interacting case here, turning on ε provides instead a continuous deformation of the three-dimensional GFF with $\hat{\Delta}_{\hat{\phi}} = 2$ into an interacting CFT. There is a vast literature on deformations of GFF, which can be obtained holographically [154] or through RG flows [155, 57, 156], yet this construction appears to be different. For example, in this deformation the dimension $\hat{\Delta}_{\hat{\phi}}$ depends non-trivially on ε as seen in (5.26). This clearly illustrates the point that transdimensional defects give new ways to define CFTs.

5.2 Large-N analysis for $4 < d < 6$

The large N limit of the interacting $O(N)$ model allows to treat the theory analytically in the space dimension d. (For reviews see [101,95].) In $d = 4+\varepsilon$ for $\varepsilon > 0$, the $O(N)$ model becomes an UV fixed point and it is natural to look for an alternative theory in which it is found as an IR fixed point. Such a theory would serve as the "UV completion" of the $O(N)$ model in $d = 5$. This question was discussed in great detail in [157–160], which found evidence that an $O(N)$ theory defined in $d = 6-\varepsilon$ may provide the desired UV completion, at least for sufficiently large N. The CFT in $d = 5$ has been studied also through bootstrap methods [161]. Generalisations to $d > 6$ were considered in [162–164].

The bulk action of the $O(N)$ model at large N is

$$S = \int d^d x \left(\tfrac{1}{2}\partial^\mu \phi_a \partial_\mu \phi_a + \frac{1}{2\sqrt{N}}\sigma\phi_a\phi_a\right), \tag{5.31}$$

where $\Delta_\phi = \frac{d-2}{2} + \mathrm{O}(N^{-1})$ and $\Delta_\sigma = 2 + \mathrm{O}(N^{-1})$. Co-dimension one defects for the large N vector model in $d = 3$ were studied in [129]. For $4 < d < 6$ one can look at surface defect with the action [123, 125]

$$S_{\mathcal{D}} = \int d^p\tau \left(g_0\,\phi_1(\tau) + h_0\,\sigma(\tau)\right), \tag{5.32}$$

and $p = 2$. It was shown there that, at leading order in ε, the symmetry preserving defect (with $g = 0$) in the $d = 6 - \varepsilon$ theory matches the symmetry-preserving surface defect of the $d = 4 + \varepsilon$ theory.

The symmetry-breaking defect was also studied in [123] in $d = 6 - \varepsilon$. To go beyond that requires transdimensional defects, as ϕ_1 is weakly relevant around $p = \frac{d-2}{2}$, which interpolates between a line defect in $d = 4$ and a surface defect in $d = 6$. Taking $p = \frac{d-2}{2} + \delta$ with small δ serving as a regulator, it is possible to use perturbation theory to compute observables at large N for all d. Away from $d \simeq 6$ one can consistently set $h_0 = 0$, as σ is irrelevant, but close to $d = 6$ it cannot be ignored and one returns to the ε expansion of [123], which could be generalised to allow corrections in δ.

If one takes $\delta = 2 - d/2$ or $\delta = 3 - d/2$, the defect again becomes a line or a surface for any value of d and requires high order analysis in δ, which will not be considered in this section. Instead, the focus is on large N analysis for small δ away from $d = 6$.

To renormalise the defect coupling g_0, it is convenient compute the order parameter $\langle \phi_1(x) \rangle$ as usual. At lowest non-trivial order, this is given by the diagrams

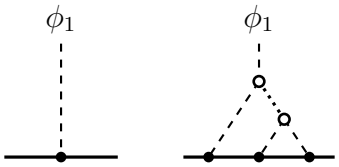

(5.33)

The dashed line is the ϕ_1 propagator as in (5.5), and the dotted line represents the propagator for the field σ

$$\langle \sigma(x)\sigma(y) \rangle = \frac{\mathcal{N}_\sigma^2}{|x-y|^4} + \mathrm{O}(N^{-1}), \quad \mathcal{N}_\sigma^2 = \frac{2^{d+2}\Gamma\left(\frac{d-1}{2}\right)\sin\left(\frac{\pi d}{2}\right)}{\pi^{3/2}\Gamma\left(\frac{d}{2}-2\right)}. \tag{5.34}$$

Setting $g_0 = \mu^\delta Z_g g$, one finds

$$Z_g = 1 + \frac{c\, g^2}{N\delta} + \mathrm{O}(N^{-2}), \qquad c = \frac{2^{d-3}\Gamma\left(\frac{d-1}{2}\right)\sin\left(\frac{\pi d}{4}\right)}{\pi^{3/2}\Gamma\left(\frac{d}{2}\right)}. \tag{5.35}$$

Note that at this order one does not need to take into account the wavefunction renormalisation of ϕ_1, since it is subleading in N. The beta function to order $1/N$ is

$$\beta_g = -\delta g + \frac{2cg^3}{N} + \mathrm{O}(N^{-2}), \tag{5.36}$$

and admits a fixed point for

$$g_*^2 = \frac{N\delta}{2c} + \mathrm{O}(\delta^2)\,. \tag{5.37}$$

At this fixed point,

$$\hat{\Delta}_{\hat{\phi}_1} = \frac{d}{2} - 1 + \delta + \frac{\partial \beta_g}{\partial g}\Big|_{g=g_*} = \frac{d}{2} - 1 + 3\delta + \mathrm{O}(N^{-1})\,. \tag{5.38}$$

At higher orders in δ one needs to include all the contributions from tree diagrams generalising the one on the right of (5.33). They contribute with terms like g^{2k+1}/N^k to β_g and they are needed to obtain a reliable result. The coefficient c (5.35) is negative for $4 < d < 6$, hence the fixed point value of the coupling is real when δ is negative and the fixed point is purely imaginary when δ is positive. In particular, for a line defect one has to take $\delta = (4-d)/2 < 0$, so a real fixed point is expected. On the other hand, for a surface defect one has to take $\delta = (6-d)/2 > 0$, which should give an imaginary fixed point.

The results obtained from this model can be checked against what can be obtained from the ε expansion. For $d = 4+\varepsilon$ and $\delta = -\varepsilon/2$, (5.38) gives $\hat{\Delta}_{\hat{\phi}_1} = 1 - \varepsilon + \mathrm{O}(N^{-1})$. This result is consistent with that derived for the symmetry-breaking line defect in $d = 4+\varepsilon$ [32].

Evaluating the one-point function of ϕ_1 at the fixed point yields

$$\langle \phi_1(x_\perp, x_\parallel)\rangle\big|_{g=g*} = \frac{\mathcal{N}_\phi\, a_\phi}{|x_\perp|^{\Delta_\phi}}\,, \qquad a_\phi^2 = \frac{\Gamma\left(\frac{d-2}{4}\right)^2 \Gamma\left(\frac{d}{2}\right)}{8\sin\left(\frac{\pi d}{4}\right)\Gamma(d-2)}\,\delta N + \mathrm{O}(N^0)\,, \tag{5.39}$$

with $\mathcal{N}_\phi$ given by (5.5). Expanding for $d = 4+\varepsilon$ and $\delta = -\varepsilon/2$ one finds

$$a_\phi^2 \sim \frac{N}{4} - \frac{N\varepsilon}{8}\,(1+\log 4) + \mathrm{O}(\varepsilon^2)\,, \tag{5.40}$$

which agrees with the large N behaviour of the result of Section 3.2 after a change in the sign of ε.

As mentioned, this solution is not valid around $d = 6-\varepsilon$, as the beta function of h contains the classical term $(3 - \frac{d}{2} - \delta)h$. For $3 - \frac{d}{2}$ close to zero, even if one tries to fine-tune $h = 0$, a non-trivial value of h would be dynamically generated along the RG flow. Unfortunately, it is difficult to perform explicit calculations analytic in d with $h_0 \neq 0$, due to the dimension of σ being close to 2 for all d. Of course one can perform such calculations for d close to 6, similarly to what has been done in $d = 4-\varepsilon$ in Section 5.1.2 above. Nevertheless, some

observables can still be computed thanks to the equation of motion. Indeed, at any fixed point one expects that in addition to a non-zero a_ϕ as in (5.39) one has

$$\langle \sigma(x_\perp, x_\parallel) \rangle = \frac{\mathcal{N}_\sigma \, a_\sigma}{|x_\perp|^2} \tag{5.41}$$

for some a_σ. Moreover, at leading order in $1/N$, one also expects that $\langle \sigma\phi_1 \rangle \sim \langle \sigma \rangle \langle \phi_1 \rangle$. Then the expectation value of the equation of motion of (5.31) yields

$$\begin{aligned} &\left(-\Box + \frac{\mathcal{N}_\sigma \, a_\sigma}{\sqrt{N}|x_\perp|^2} \right) \frac{1}{|x_\perp|^{\Delta_\phi}} = \\ &\qquad = \frac{1}{|x_\perp|^{\Delta_\phi+2}} \left(\Delta_\phi \left(\Delta_\phi + 2 + p - d \right) - \frac{\mathcal{N}_\sigma \, a_\sigma}{\sqrt{N}} \right) = 0 \, . \end{aligned} \tag{5.42}$$

For $p = d/2 - 1 + \delta$ the solution is

$$a_\sigma = \frac{1}{\mathcal{N}_\sigma} \frac{d-2}{2} \sqrt{N} \delta + \mathrm{O}(N^{-1/2}) \, . \tag{5.43}$$

One can now expand for $d = 6 - \varepsilon$ and $\delta = \varepsilon/2$ to find

$$a_\sigma \sim \frac{\sqrt{N\varepsilon}}{4\sqrt{6}} + \mathrm{O}(\varepsilon^{3/2}) \, , \tag{5.44}$$

which agrees with the large N behaviour of the result for the symmetry-breaking surface defect of [123].[3] In $d = 4 + \varepsilon$ the expansion of (5.43) also agrees with the results of Section 3.2.

[3] There is a typo in [123, Eq. (4.14)]; at leading order the correct behaviour in N is $h_* = -\sqrt{\pi N \varepsilon}/4\sqrt{6}$.

Chapter 6

The long-range O(N) model and its defects

6.1 The long range O(N) model

Another notable example of an interacting CFT is the *long-range $O(N)$ model*, which generalises the $O(N)$ model introduced in 3.1. More specifically, the long-range $O(N)$ model is not merely a single CFT, but rather a continuous family of non-local CFTs that features an interesting phase diagram and that includes the ordinary $O(N)$ model as one of its limiting cases.[1] This family of CFTs can be introduced either via a field theory framework or by looking the critical behaviour of a lattice model.

For $N = 1$, the corresponding lattice model is referred to as the *long-range Ising model*. It can be introduced in a similar way to the Ising model discussed in 3.1, though with a slightly different Hamiltonian

$$H_{\text{LRI}} = -J \sum_{i \neq j} \frac{\sigma_i \sigma_j}{|i-j|^{d+\sigma}} \,, \tag{6.1}$$

where $J > 0$, and the external magnetic field has been set to zero, since it plays no role in the following discussion. This model is called long-range because the interaction occurs not only between nearest neighbours but between all lattice sites, with the parameter σ governing the rate at which the interaction decays with distance. This model undergoes a second-order phase transition at a certain critical inverse temperature $\beta = \beta_c$. Depending on the value of the parameter σ, the critical exponents can be different from those of the Ising model [155, 165–167]. Such critical exponents describe a CFT.

[1] A non-local CFT is a theory in which there is no conserved stress-energy tensor, or equivalently, no spin-two operator with protected dimension $\Delta_T = d$.

The continuum model is introduced using the Ginzburg-Landau approach: at the critical temperature, the discrete model can be replaced by an interacting real massless scalar field with the following action

$$S = \frac{\mathcal{N}_\sigma}{2} \int d^d x d^d y \frac{\phi(x)\phi(y)}{|x-y|^{d+\sigma}} + \frac{\lambda_0}{4!} \int d^d x \, \phi(x)^4 \,, \tag{6.2}$$

with a normalisation constant $\mathcal{N}_\sigma$ fixed such that in momentum space the kinetic part of the action reads $\frac{1}{2}\int \frac{d^d p}{(2\pi)^p} |p|^\sigma \phi(-p)\phi(p)$. Such a normalisation is given by

$$\mathcal{N}_\sigma = \frac{2^\sigma \Gamma\left(\frac{d+\sigma}{2}\right)}{\pi^{\frac{d}{2}} \Gamma\left(-\frac{\sigma}{2}\right)} \,. \tag{6.3}$$

This continuum action will be referred to as the LRI model. The generalisation to the long-range $O(N)$ model is straightforward. One can promote ϕ to an $O(N)$ vector field, ϕ^a, where $a = 1, \ldots, N$, and contract the indices in the natural way

$$S = \frac{\mathcal{N}_\sigma}{2} \int d^d x d^d y \frac{\phi_a(x)\phi_a(y)}{|x-y|^{d+\sigma}} + \frac{\lambda_0}{4!} \int d^d x \left(\phi_a(x)\phi_a(x)\right)^2 \,. \tag{6.4}$$

The case $N = 1$ reduces to the LRI model (6.2).

The actions (6.2) and (6.4) are clearly non-local. More precisely, an action is *local* if it involves a single integral of the fields and their derivatives up to a finite order. In contrast, actions that depend on an infinite number of field derivatives or involve more than one integral are usually referred to as *non-local* (see [168] for a modern treatment of this subject). The non-local kinetic term can also be rewritten using the fractional Laplacian $\mathcal{L}_\sigma = (-\partial^2)^{\sigma/2}$, where σ is a real number. This operator acts on plane waves as $\mathcal{L}_\sigma e^{ipx} = |p|^\sigma e^{ipx}$, and in position space it is given by

$$\mathcal{L}_\sigma \phi(x) = \mathcal{N}_\sigma \int d^d y \frac{\phi(y)}{|x-y|^{d+\sigma}} \,. \tag{6.5}$$

Using this notation, the kinetic term becomes

$$S_{\text{kin}} = \frac{1}{2} \int d^d x \, \phi(x) \mathcal{L}_\sigma \phi(x) \,, \tag{6.6}$$

which leads to the following classical scaling dimension

$$\Delta_\phi = \frac{d-\sigma}{2} \,. \tag{6.7}$$

When $\sigma = 2$ the fractional Laplacian reduces to the usual Laplacian and the theory becomes the more familiar quartic theory that describes

the short-range Ising (SRI) model, as in (3.6).

As anticipated, the LRI has a rich phase space structure that depends on the value of σ [57, 169, 170]. This is illustrated in Figure 6.1:

- For $\sigma < d/2$, the quartic interaction is irrelevant, and the theory becomes free in the IR. In particular, it is a generalised free field (GFF) theory with Δ_ϕ given in (6.7).
- For $\sigma > \sigma_* = d - 2\Delta_\phi^{\text{SRI}}$, where Δ_ϕ^{SRI} is the conformal dimension of ϕ in the short-range Ising model, the critical theory reduces to the short-range Ising model.
- For $d/2 < \sigma < \sigma_*$, the critical theory is non-trivial and non-Gaussian. Indeed, the quartic interaction is relevant and drives the theory towards an IR fixed point, known as the LRI fixed point (see Figure 6.1).

Similar statements apply to the $O(N)$ generalisation of the LRI.

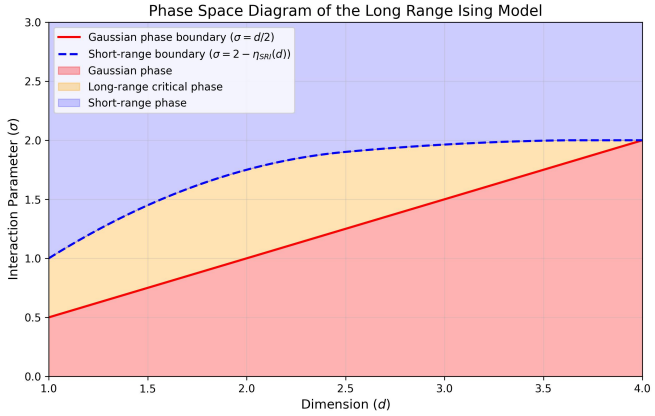

Figure 6.1: Phase space diagram for the long-range Ising model as a function of the dimension d and the parameter σ. The diagram shows the Gaussian phase ($\sigma \leqslant d/2$), the long-range critical phase ($d/2 < \sigma < 2 - \eta_{SRI}(d)$), and the short-range phase ($\sigma \geqslant 2 - \eta_{SRI}(d)$).

There is yet another way to get to the action in equation (6.2), where one interprets the LRI as a defect of dimension d embedded in a bulk space of (generically non-integer) dimension $d - \sigma + 2$. Specifically, if one considers a local massless field $\Phi(x, y)$ with action

$$S = \int d^d x \, d^{2-\sigma} y \left[(\partial_x \Phi)^2 + (\partial_y \Phi)^2 \right] + \int_{y=0} d^d x \, \Phi^4 \,, \tag{6.8}$$

then integrating out the bulk field $\Phi(x, y \neq 0)$ leads to a theory for $\phi(x) = \Phi(x, 0)$, which is identical to the LRI theory. This method is sometimes referred to as the Caffarelli-Silvestre trick [171]. In fact, this perspective is particularly useful for proving that the LRI exhibits enhanced conformal symmetry at the IR fixed point [57].

The free propagator of the long-range $O(N)$ model can be easily derived

$$G_{ab}(x) = \frac{2^{d-\sigma}\Gamma\left(\frac{d-\sigma}{2}\right)}{(4\pi)^{\frac{d}{2}}\Gamma\left(\frac{\sigma}{2}\right)} \frac{\delta_{ab}}{|x|^{d-\sigma}} = \frac{\mathcal{N}_\phi^2 \delta_{ab}}{|x|^{2\Delta_\phi}} . \tag{6.9}$$

To study the LRI fixed point perturbatively, the standard approach is to perform an ε-expansion near the crossover $\sigma = d/2$, as shown in Figure 6.1. However, it is also useful to introduce a second type of expansion close to the corner $d = 4$. For clarity and to set up the notation, both expansions are provided here.

- Setting $\sigma = \frac{d+\varepsilon}{2}$, the dimension of the field ϕ in equation (6.7) becomes $\Delta_\phi = \frac{d-\varepsilon}{4}$, so that the ϕ^4 interaction is weakly relevant, allowing for a perturbative expansion in ε. An important and interesting feature of this expansion is that it can be performed at a fixed d. The perturbative β-function for the λ coupling has a non-trivial zero, corresponding to an infrared (IR) fixed point. The standard ε-expansion procedure can then be used to compute observables at the perturbative fixed point, with the crucial difference that the field ϕ, being non-local, does not renormalize. This is the expansion that was first introduced in [155].

- Following the standard procedure, one can set $d = 4 - \hat{\varepsilon}$, while introducing an additional parameter κ such that $\sigma = 2 - \frac{(1-\kappa)\hat{\varepsilon}}{2}$. This new parameter defines a specific direction when moving away from the corner $d = 4$ in Figure 6.1. For $\kappa = 1$, one has $\sigma = 2$, and the action is local, corresponding to the ordinary short-range Ising (SRI) fixed point. The opposite limit is $\kappa = 0$, where $\sigma = d/2$, and one moves along the crossover to the Gaussian theories. All intermediate values $0 < \kappa < 1$ correspond to the LRI fixed points. A similar expansion has been considered in [172].

Note that in this chapter, and in this chapter only, it is necessary to distinguish between ε, which is a small parameter in $\sigma = \frac{d+\varepsilon}{2}$, and $\hat{\varepsilon}$, which is a small parameter in $d = 4-\hat{\varepsilon}$. Therefore, in order to compare the results from the ε-expansion in this chapter with those from other chapters, it is sometimes necessary to replace $\hat{\varepsilon}$ with ε. Unfortunately, this could not be easily avoided.

A large-N expansion is also possible [173], although it will not be considered in this work. The second expansion is particularly useful in Section 6.2.2, where the generalisation of the localised magnetic field to the long-range model will be considered. Here, the first expansion and the renormalisation procedure are briefly reviewed.

As mentioned earlier, the kinetic term of the action is non-local, and since renormalisation always introduces local counterterms, the field ϕ does not renormalise. This implies that all divergences must be cancelled by renormalising the coupling λ. One can express the renormalised coupling in terms of the bare coupling as $\lambda_0 = \mu^\varepsilon Z_\lambda \lambda$, where μ is a mass scale. The action is then written as

$$S = \frac{\mathcal{N}_\sigma}{2} \int d^d x d^d y \frac{\phi_a(x)\phi_a(y)}{|x-y|^{d+\sigma}} + \frac{Z_\lambda \lambda \mu^\varepsilon}{4!} \int d^d x \left(\phi_a(x)\phi_a(x)\right)^2 , \quad (6.10)$$

where Z_λ ensures the cancellation of all poles in ε in the correlators of ϕ. At two-loop order, in the MS scheme, one gets

$$Z_\lambda = 1 + \frac{\lambda(N+8)}{3(4\pi)^{\frac{d}{2}}\Gamma\left(\frac{d}{2}\right)\varepsilon} + \frac{\lambda^2}{9(4\pi)^d \Gamma\left(\frac{d}{2}\right)^2}\left(\frac{N+8}{\varepsilon^2} + \right.$$
$$\left. - \frac{(5N+22)\left(\psi\left(\frac{d}{2}\right) - 2\psi\left(\frac{d}{4}\right) - \gamma_E\right)}{\varepsilon}\right) + \mathrm{O}(\lambda^3) . \quad (6.11)$$

The beta function $\beta_\lambda = \mu \frac{\partial \lambda}{\partial \mu}$ is obtained by imposing $\mu \frac{d}{d\mu}\lambda_0 = 0$, and it is [155, 173]

$$\beta_\lambda = -\varepsilon\lambda + \frac{(N+8)\lambda^2}{3(4\pi)^{\frac{d}{2}}\Gamma\left(\frac{d}{2}\right)} - \frac{2(5N+22)(\psi\left(\frac{d}{2}\right) - 2\psi\left(\frac{d}{4}\right) - \gamma_E)\lambda^3}{9(4\pi)^d\Gamma\left(\frac{d}{2}\right)^2} + \mathrm{O}(\lambda^4) . \quad (6.12)$$

This beta function has a non-trivial zero, corresponding to a perturbative fixed point

$$\frac{\lambda_*}{\Gamma\left(\frac{d}{2}\right)(4\pi)^{\frac{d}{2}}} = \frac{3}{N+8}\varepsilon + \frac{6\,(5N+22)\left(\psi\left(\frac{d}{2}\right) - 2\psi\left(\frac{d}{4}\right) - \gamma_E\right)}{(N+8)^3}\varepsilon^2 + \mathrm{O}\left(\varepsilon^3\right) . \quad (6.13)$$

The conformal invariance of this long-range $O(N)$ fixed point can be ascertained by extending the arguments of [57] for the LRI model.

6.2 Defects in the long-range O(N) model

This section focuses on the construction of non-trivial conformal defects in the non-local $O(N)$ model introduced in 6.1, following the treatment

presented in [37]. As a secondary result, the existence of non-trivial defects in the specific case $\lambda = 0$, *i.e.* for GFF theories, is also discussed. Indeed, it has been shown that in integer dimensions less than four, free local theories do not admit any non-trivial defects [121], where trivial means Gaussian. It will be shown that, dropping the assumption of locality, it is possible to construct non-trivial conformal defects for GFF in three dimensions.

To begin, it is useful to consider the most straightforward examples of defect that can be constructed. The first type is obtained by integrating a power of one of the fields, ϕ^a, along a line, thereby breaking $O(N)$ symmetry down to $O(N-1)$. This is analogous to the localised magnetic field of Section 3.2. It will be explained why this construction does not lend itself easily to an expansion around $\sigma = d/2$ at fixed d, and two alternative strategies to overcome this challenge will be introduced: the *non-local* and the *semiclassical* construction of defects, presented in Sections 6.2.1 and 6.2.3, respectively.

Another simple defect is obtained by integrating the singlet $\phi_a\phi_a$ over a surface. The analogous defect for the local $O(N)$ model was introduced in 3.4. Similar considerations apply in this case as well.

It is useful to adopt a more systematic approach to the construction of defects. In the following, several methods will be summarised, each of which will be expanded on in the subsequent sections. The list is not intended to be exhaustive; in fact, the analogue of magnetic impurities or monodromy defects is not considered, as the focus is on the simplest constructions.

Local defects

The simplest approach to constructing defects is to integrate integer powers of the fields ϕ_a over a p-dimensional subspace. Thus, one can consider the action

$$S = S_{\text{bulk}} + h_0^{a_1\dots a_n} \int d^p\tau\, \phi_{a_1}(\tau)\dots\phi_{a_n}(\tau)\,, \tag{6.14}$$

where S_{bulk} is given by (6.4), and $h_0^{a_1\dots a_n}$ is a coupling constant. The usual strategy is to compute the beta function for the coupling h and look for perturbative fixed points in the ε-expansion. For the expansion to be reliable, one needs the coupling to be classically marginal, which requires $n\Delta_\phi = p$. Since the dimension of ϕ is determined by the bulk theory, one has

$$n = \frac{2p}{d-\sigma}\,. \tag{6.15}$$

At the crossover point $\sigma = d/2$, one finds $n = \frac{4p}{d}$, which, for $2 \leqslant d \leqslant 4$, is an integer only if $d = 2$ or $d = 4$. For this reason, this construction, unlike the case of the homogeneous long-range $O(N)$ model, requires consideration of the $\hat{\varepsilon}$-expansion around $d = 4$, and it is not possible to work at fixed d.

In Section 6.2.2, the $\hat{\varepsilon}$-expansion will be explored for the cases $p = n = 1$ (*i.e.* the long-range generalisation of the localised magnetic field (3.19), and $p = n = 2$ (*i.e.* the generalisation of the surface defects (3.114)).

Non-local defects

One of the main advantages of the non-local model is that it can be studied at fixed d. Therefore, It would be desirable to find a defect construction that is suitable for the ε-expansion near the crossover line $\sigma = d/2$. To achieve this, additional defect degrees of freedom with a non-local defect action are introduced , and they are coupled to the bulk via a local interaction. [2] For simplicity, consider the case $N = 1$. One can introduce an additional bosonic field $\hat{\psi}$ on the defect and consider the following class of actions

$$S = \int d^d x \left(\frac{1}{2} \phi \mathcal{L}_\sigma \phi + \frac{\lambda_0}{4!} \phi^4 \right) + \int d^p \tau \left(\frac{1}{2} \hat{\psi} \mathcal{L}_{\hat{\sigma}} \hat{\psi} + \frac{g_0}{2} \phi^a \hat{\psi}^b \right) , \quad (6.16)$$

where $\hat{\sigma} = p - 2\hat{\Delta}_{\hat{\psi}}$, and a and b are integers. By tuning the dimension $\hat{\Delta}_{\hat{\psi}}$ one can make the coupling g_0 to become classically marginal. This yields the condition

$$a\Delta_\phi + b\hat{\Delta}_{\hat{\psi}} \sim p \, , \quad (6.17)$$

where the relation holds up to a small regulator that must be introduced to cure the divergences of the theory. Near the crossover $\sigma = d/2$, one finds

$$\Delta_\phi \sim \frac{d}{4} \, , \qquad \hat{\Delta}_{\hat{\psi}} \sim \frac{4p - ad}{4b} \, . \quad (6.18)$$

Note that these dimensions will not receive quantum corrections as one moves away from the crossover, since both kinetic terms are non-local. To further constrain the allowed values of the exponents a and b, one can impose the unitarity condition

$$\hat{\Delta}_{\hat{\psi}} \geqslant \max \left(0, \frac{p-2}{2} \right) . \quad (6.19)$$

The valid choices of parameters for a unitary theory are summarised below for $3 \leqslant d \leqslant 4$:

[2] A similar construction can be found in [122], where free scalar theories are coupled to lower dimensional CFTs living on a defect.

- $\boldsymbol{p = 1}$: $a = 1$, any b
- $\boldsymbol{p = 2}$: $a = 1$ or 2, any b

Of course, having a classically marginal defect interaction is not sufficient to produce a non-trivial conformal defect in the IR. While the renormalisation of the coupling λ is unaffected by the presence of the defect, one must search for non-trivial fixed points of the coupling g by computing its beta function and looking for a non-trivial zero. Section 6.2.1 will be devoted to this analysis for specific cases with low values of a and b. In particular, it will be shown that these defects are admissible even in the case $\lambda = 0$, *i.e.* for GFF theory in $d = 3$.

Semiclassical defects

Another possible strategy for constructing conformal defects at fixed d in the long-range $O(N)$ model is to investigate the IR fixed points of defect RG flows triggered by strongly relevant interactions. In general, this is a challenging problem, as the defect couplings are not perturbatively small in this regime. However, in certain cases, it is possible to study a strongly coupled defect in a weakly coupled bulk theory by expanding the action around a classical configuration that corresponds to a saddle point of the path integral, as it was briefly discussed in 3.4.2. In this case, the classical configuration for the field $\phi(x)$ must be consistent with the constraints imposed by the defect conformal symmetry. For example, in the case of an $O(N)$ symmetry-breaking line, one must have

$$\phi^a_{\rm cl}(x) = \delta_{a1} \frac{\mathcal{N}_\phi \, a_{\rm cl}}{|x_\perp|^{\Delta_{\rm cl}}} \,. \tag{6.20}$$

The constants $a_{\rm cl}$ and $\Delta_{\rm cl}$ can be determined by solving the classical equations of motion. The semiclassical expansion

$$\phi^a(x) = \phi^a_{\rm cl}(x) + \delta\phi^a(x) \,, \tag{6.21}$$

leads to an action for the fluctuation $\delta\phi$, which can be used to compute quantum corrections to observables in the defect field theory. This method has been used to study the $O(N)$ model in the presence of a boundary in various regimes [174, 148, 132, 175], and was also considered for surface defects in [125].[3] However, some technical issues arise when one applies the same techniques to compute quantum corrections in defects with co-dimension $q = d - p \neq 1$. This construction is discussed in more details in Section 6.2.3.

[3] See also [176, 177] for a similar approach in the context of defects in $\mathcal{N} = 4$ super Yang-Mills.

An alternative approach for studying strongly coupled defects in weakly coupled bulks, is to use the transdimensional defects introduced in Chapter 5. By considering a non-integer dimensional defect where the interaction is weakly relevant, it may be possible to compute observables and then extrapolate the results to integer values of the defect dimension.

6.2.1 Non-local defects

In this section, the analysis of the non-local defects introduced in Section 6.2 is carried out, following [37]. The main goal is to compute the beta-function for the defect coupling g and identify non-trivial perturbative zeros in the ε-expansion at fixed d. The analysis focuses primarily on the free bulk case $\lambda = 0$, and on the LRI model, *i.e.* $N = 1$. However, most of the results can be straightforwardly generalised to arbitrary N. Since the construction of these defects is carried out at a fixed dimension d, this analysis also serves as a study of the existence of non-trivial defects in GFF theory across different dimensions. In particular, it will be shown that GFF theory in three dimensions admits non-trivial conformal defects. Additionally, it will also be shown that introducing the bulk interaction, in most cases, does not affect the leading-order results for the beta-function or the defect CFT data.

Before examining specific values of the exponents (a, b) in (6.16), it is first convenient to establish some general results that hold for all RG flows considered in this section. To begin, one needs to specify how the divergences are regulated. To do this, one introduces a regulator ε and then imposes that the defect interaction term in (6.16) is weakly relevant

$$a\Delta_\phi + b\hat{\Delta}_{\hat{\psi}} = p - \varepsilon\,. \tag{6.22}$$

When the bulk theory is free, this choice is sufficient to ensure that all correlators remain finite. In the case of an interacting bulk, one must also specify how to move away from the crossover at $\sigma = d/2$. As in Section 6.1, one can set $\varepsilon = 2\sigma - d$, where ε now regulates bulk integrals as well. This choice is not unique; one could have inserted an arbitrary coefficient in front of the ε in (6.22) (or, alternatively, use two independent regulators). However, as it will be shown, at leading order in ε only defect integrals contribute, and it is straightforward to generalise the results introducing an additional coefficient. With this choice, the relation between the bare and the renormalised defect coupling is

$$g_0 = \mu^\varepsilon Z_g g(\mu)\,, \tag{6.23}$$

and this can be used to compute the beta-function.

To compute the beta-function, one typically imposes that a given observable is finite by reabsorbing the divergences into the renormalisation constants. A commonly used observable for this purpose is the bulk one-point function of the field ϕ. However, in some models that are considered in this section, this one-point function involves tadpole integrals, which complicate the analysis.

Instead, it is more convenient to look at the defect two-point function of a special composite operator, $\hat{\mathcal{O}}_0 = \hat{\phi}^{a-1}\hat{\psi}^b$, which appears in the equation of motion for ϕ. Indeed, in the free bulk case one has

$$\mathcal{L}_\sigma \phi(0, x_\perp) = -\frac{g_0}{2} a\, \hat{\mathcal{O}}_0(0) \delta^{(d-p)}(x_\perp)\,. \tag{6.24}$$

Since the bulk field ϕ does not renormalise (due to its non-local kinetic term), the left-hand side of (6.24) remains unchanged under renormalisation. However, the right-hand side involves the renormalisation of the coupling $g_0 = \mu^\varepsilon Z_g g$ and the wavefunction renormalisation of the defect operator $\hat{\mathcal{O}}_0 = Z_{\hat{\mathcal{O}}}\hat{\mathcal{O}}$. This implies that in the MS scheme, these two quantities are related by the condition $Z_g Z_{\hat{\mathcal{O}}} = 1$. Therefore, the renormalisation of the coupling (and the corresponding beta function) can be derived from the wavefunction renormalisation of $\hat{\mathcal{O}}$. Indeed, at leading order, the wavefunction renormalisation is expected to take the form

$$Z_{\hat{\mathcal{O}}} = 1 - \frac{\alpha g^n}{\varepsilon} + \mathrm{O}\big(g^{n+1}\big)\,, \tag{6.25}$$

where n is an integer related to the values of a and b, and α is a real number. The renormalisation factor for the coupling is then given by

$$Z_g = 1 + \frac{\alpha g^n}{\varepsilon} + \mathrm{O}\big(g^{n+1}\big)\,, \tag{6.26}$$

and the beta function can be derived, as usual, by requiring that the bare coupling does not depend on the renormalisation mass scale, leading to

$$\beta_g = -\varepsilon g + \alpha n g^{n+1} + \mathrm{O}\big(g^{n+2}\big)\,. \tag{6.27}$$

The non-trivial zero of the beta function is $g_*^n = \varepsilon/(\alpha n) + \mathrm{O}(\varepsilon^2)$. For odd values of n this equation will always admit a real solution, while for even values of n the crucial requirement is that α is positive. At this fixed point, the equation of motion (6.24) implies that the operator $\hat{\mathcal{O}}$ is protected with dimension

$$\hat{\Delta}_{\hat{\mathcal{O}}} = p - \Delta_\phi\,. \tag{6.28}$$

This can also be checked by computing explicitly the anomalous dimension $\gamma_{\hat{\mathcal{O}}}$ which has the exact expression [4]

$$\gamma_{\hat{\mathcal{O}}} = \beta_g \frac{\partial \log Z_{\hat{\mathcal{O}}}}{\partial g} = \beta_g \frac{\partial \log Z_g^{-1}}{\partial g} = \varepsilon - \frac{\beta_g}{g}\,, \tag{6.29}$$

and the second term vanishes at the fixed point. Using also that $a\Delta_\phi + b\hat{\Delta}_{\hat{\psi}} = p - \varepsilon$, it follows that $\hat{\Delta}_{\hat{\mathcal{O}}} = (a-1)\Delta_\phi + b\hat{\Delta}_{\hat{\psi}} + \gamma_{\hat{\mathcal{O}}} = p - \Delta_\phi$, as expected. Therefore, one has

$$\langle \hat{\mathcal{O}}(\tau_1)\hat{\mathcal{O}}(\tau_2)\rangle = \frac{\mathcal{N}_{\hat{\mathcal{O}}}^2}{|\tau_1 - \tau_2|^{p-\Delta_\phi}}\,, \tag{6.30}$$

where $\mathcal{N}_{\hat{\mathcal{O}}}$ is a normalisation constant.

Furthermore, one can invert the equation of motion to express ϕ in terms of integrals of the operator $\hat{\mathcal{O}}$ on the defect. This allows to compute bulk correlators of ϕ by integrating defect correlators of $\hat{\mathcal{O}}$, without having to compute Feynman diagrams [35]. Indeed, by inverting (6.24), one finds

$$\phi\,(x) = -a\,\mathcal{N}_\sigma \frac{g_0}{2} \int d^p\tau \frac{\hat{\mathcal{O}}(\tau)}{(|x_\perp|^2 + |\tau|^2)^{\Delta_\phi}} + \phi_{\text{free}}(x)\,, \tag{6.31}$$

where ϕ_{free} is a free field, which does not interact with the defect. This can be used to compute the one-point function of ϕ^2

$$\begin{aligned}\langle \phi^2(x)\rangle &= g_0^2 \frac{a^2\mathcal{N}_\sigma^2\mathcal{N}_{\hat{\mathcal{O}}}^2}{4} \int \frac{d^p\tau_1\, d^p\tau_2}{(|x_\perp|^2 + |\tau_1|^2)^{\Delta_\phi}|\tau_1 - \tau_2|^{2(p-\Delta_\phi)}(|x_\perp|^2 + |\tau_2|^2)^{\Delta_\phi}} = \\ &= g_0^2 \frac{a^2\mathcal{N}_\sigma^2\,\mathcal{N}_{\hat{\mathcal{O}}}^2}{4}\, \frac{\pi^p \Gamma\left(\frac{p}{2}\right)\Gamma\left(\Delta_\phi - \frac{p}{2}\right)}{\Gamma\left(\Delta_\phi\right)(p-1)!}\, \frac{1}{|x_\perp|^{2\Delta_\phi}} = \frac{a_{\phi^2}\mathcal{N}_{\phi^2}}{|x_\perp|^{2\Delta_\phi}}\,,\end{aligned} \tag{6.32}$$

where $\mathcal{N}_{\phi^2} = 2\mathcal{N}_\phi^2$. The last step to compute a piece of defect CFT data is to evaluate this expression at the fixed point g_*. This will be done in a few specific cases below.

Similarly, one can compute the bulk-to-defect one-point functions of ϕ and $\hat{\mathcal{O}}$, as well as the bulk two-point function of ϕ. For example, consider the correlator $\langle\phi(x)\phi(y)\rangle$. Following [35], it is possible to exploit the residual conformal symmetry to set $x_\parallel = y_\parallel = 0$ and $x_\perp = (z, \bar{z}, 0, \ldots)$, $y_\perp = (0, 1, 0, \ldots)$. It is also convenient to define a radial

[4] A useful relation that can be used for this computation is $\beta_g = \frac{-\varepsilon g Z_g}{Z_g + g\partial_g Z_g}$.

coordinate by $z\bar{z} = r$. Using (6.31) it follows

$$\begin{aligned}&\langle\phi(0,x_\perp)\phi(0,y_\perp)\rangle = \\ &= g_0^2\frac{a^2\mathcal{N}_{2\Delta_\phi-d}^2\mathcal{N}_{\hat{\mathcal{O}}}^2}{4}\int\frac{d^p\tau_1\,d^p\tau_2}{(1+|\tau_1|^2)^{\Delta_\phi}|\tau_1-\tau_2|^{2(p-\Delta_\phi)}(r^2+|\tau_2|^2)^{\Delta_\phi}}+G(x-y)\,,\end{aligned} \tag{6.33}$$

where $G(x-y)$ is the free ϕ propagator. This integral can be computed exactly. By restoring the dependence on arbitrary x and y and evaluating at the fixed point, one gets

$$\begin{aligned}&\langle\phi(x)\phi(y)\rangle = \frac{\mathcal{N}_\phi^2\,F_{\phi\phi}(r)}{|x_\perp|^{\Delta_\phi}|y_\perp|^{\Delta_\phi}}\,,\\ &F_{\phi\phi}(r) = \xi^{-\Delta_\phi}+g_*^2\frac{a^2\mathcal{N}_\sigma^2\mathcal{N}_{\hat{\mathcal{O}}}^2}{4\mathcal{N}_\phi^2}\Bigg(\frac{\pi^{p+2}r^{p-\Delta_\phi}\,{}_2F_1\left(\frac{p}{2},p-\Delta_\phi;\frac{p}{2}-\Delta_\phi+1;r^2\right)}{\Gamma(\Delta_\phi)^2\sin^2\left(\pi(\frac{p}{2}-\Delta_\phi)\right)\Gamma\left(\frac{p}{2}-\Delta_\phi+1\right)^2}+\\ &\quad-\frac{2\pi^{p+1}r^{\Delta_\phi}\,{}_2F_1\left(\frac{p}{2},\Delta_\phi;1-\frac{p}{2}+\Delta_\phi;r^2\right)}{\Gamma(\Delta_\phi)(p-2\Delta_\phi)\sin\left(\pi(\frac{p}{2}-\Delta_\phi)\right)\Gamma(p-\Delta_\phi)}\Bigg)\,,\end{aligned} \tag{6.34}$$

where $\xi = (x-y)^2/(|x_\perp||y_\perp|)$ is a conformal cross-ratio. From (6.34) one can immediately read off the spectrum of the exchanged operators in the defect channel operator product expansion (OPE). The only primary operators are $(\partial_\perp)^s\phi$ with s integer and dimension $\hat{\Delta}_s = 1+s-\varepsilon/2$, and the operator $\hat{\mathcal{O}}$ with dimension $\Delta_{\hat{\mathcal{O}}} = p-\Delta_\phi$. one can also easily extract all the bulk-to-defect OPE coefficients for the operators exchanged in the defect channel, as well as the one-point function coefficients for the operators exchanged in the bulk channel, as showed in Section 4.3.

In the interacting bulk case, there are non-linear corrections to the left-hand side (6.24) and the above analysis does not apply. However, in the models considered in this section, corrections due to the bulk coupling only appear at next-to-leading order. As a result, the above results remain valid perturbatively at leading order in ε.

The wavefunction renormalisation $Z_{\hat{\mathcal{O}}}$ for some of the models discussed in Section 6.2 is now computed by examining the two-point function $\langle\hat{\mathcal{O}}\hat{\mathcal{O}}\rangle$ using Feynman diagrams. This approach enables the calculation of the beta function and the identification of perturbative fixed points. Specifically, the cases $(a,b) = (1,2)$, $(a,b) = (2,1)$, and $(a,b) = (2,2n)$ will be considered. Additionally, it will be demonstrated that for a line defect and $1/2 < \Delta_\phi < 1$, a real fixed point exists for arbitrary b.

Element	Rule
	ϕ propagator: $G(x-y)=\frac{\mathcal{N}_\phi^2}{\lvert x-y\rvert^{2\Delta_\phi}}$
	$\hat{\psi}$ propagator: $G(x-y)=\frac{\mathcal{N}_{\hat{\psi}}^2}{\lvert x-y\rvert^{2\Delta_{\hat{\psi}}}}$
	bulk ϕ^4 interaction $-\frac{\lambda_0}{4!}\int d^dx$, where x is the interaction point
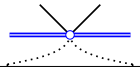	defect $\phi^a\hat{\psi}^b$ interaction $-\frac{g_0}{2}\int d^p\tau$, where τ is the interaction point on the defect

Table 6.1: Feynman rules for the non-local defect.

The conventions used for the Feynman diagrams throughout this chapter are here summarised. A blue line always represents a defect: a straight blue line corresponds to a linear defect (a line defect, a surface, etc.), while a blue circle represents a circular or (hyper)spherical defect. Solid black lines denote the field that is defined both in the bulk and on the defect (denoted by ϕ), whereas dotted lines represent a field defined only on the defect (denoted by $\hat{\psi}$). The following normalisation constants will be used

$$\mathcal{N}_\phi^2=\frac{\Gamma(\Delta_\phi)}{2^{d-2\Delta_\phi}\pi^{\frac{d}{2}}\,\Gamma\left(\frac{d}{2}-\Delta_\phi\right)}\,,\qquad \mathcal{N}_{\hat{\psi}}^2=\frac{\Gamma(\hat{\Delta}_{\hat{\psi}})}{2^{p-2\hat{\Delta}_{\hat{\psi}}}\pi^{\frac{p}{2}}\,\Gamma\left(\frac{p}{2}-\hat{\Delta}_{\hat{\psi}}\right)}\,. \tag{6.35}$$

Feynman rules are summarised in Table 6.1. Additionally, it is useful to define the following function [57]

$$w_\alpha^{(d)}=(4\pi)^{\frac{d}{2}}2^{-\alpha}\frac{\Gamma\left(\frac{d-\alpha}{2}\right)}{\Gamma\left(\frac{\alpha}{2}\right)}\,. \tag{6.36}$$

Defect with $(\mathbf{a},\mathbf{b})=(\mathbf{1},\mathbf{2})$

The first case under consideration is $(a,b)=(1,2)$. The free bulk case is considered first. The interaction term in (6.16) becomes $\frac{g_0}{2}\int d^p\tau\phi\hat{\psi}^2$. The operator $\hat{\mathcal{O}}$ in this case is $\hat{\mathcal{O}}=\hat{\psi}^2$. The bare two-point function $\langle\hat{\mathcal{O}}\hat{\mathcal{O}}\rangle$ at tree level is given by the following diagram

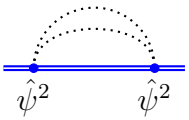

$$=\frac{2(\mathcal{N}_{\hat{\psi}}^2)^2}{|\tau|^{4\hat{\Delta}_{\hat{\psi}}}}\,. \tag{6.37}$$

At one loop, there are three diagrams, but only one turns out to be divergent. Since only $Z_{\hat{\mathcal{O}}}$ is needed, it suffices to consider this diagram

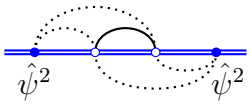

$$b = \\ = \mathcal{N}_\phi^2 \left(\mathcal{N}_{\hat{\psi}}^2\right)^4 g_0^2 \int \frac{d^p\tau_1\, d^p\tau_2}{\left(|\tau_1|\,|\tau_2|\,|\tau-\tau_1|\,|\tau-\tau_2|\right)^{2\hat{\Delta}_{\hat{\psi}}} |\tau_2-\tau_1|^{2\Delta_\phi}} \,. \tag{6.38}$$

The divergent part of this diagram can be easily extracted by analysing the limits $\tau_1, \tau_2 \to 0, \tau$

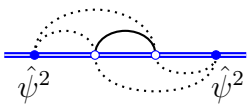

$$= \frac{\mathcal{N}_\phi^2 \left(\mathcal{N}_{\hat{\psi}}^2\right)^4 g_0^2}{|\tau|^{4\hat{\Delta}_{\hat{\psi}}}} \left(\frac{w^{(p)}_{2\Delta_\phi} w^{(p)}_{2\hat{\Delta}_{\hat{\psi}}}}{w^{(p)}_{2\Delta_\phi+2\hat{\Delta}_{\hat{\psi}}-p}} \frac{2\pi^{\frac{p}{2}}}{\Gamma\left(\frac{p}{2}\right)} \frac{1}{\varepsilon} + \mathrm{O}(\varepsilon^0) \right) . \tag{6.39}$$

This divergence must be cancelled by introducing the wavefunction renormalisation $Z_{\hat{\mathcal{O}}}$. Then, using (6.27), one can extract the beta function and the fixed point g_*

$$\begin{aligned} Z_{\hat{\mathcal{O}}} &= 1 + g^2 \frac{\Gamma\left(\frac{p}{2}-\Delta_\phi\right)}{2^{d+1}\pi^{\frac{d}{2}}\Gamma\left(\frac{p}{2}\right)\Gamma\left(\frac{d}{2}-\Delta_\phi\right)\varepsilon} + \mathrm{O}\left(g^4\right) , \\ \beta_g &= -\varepsilon g - \frac{\Gamma\left(\frac{p}{2}-\Delta_\phi\right)}{2^d\pi^{\frac{d}{2}}\Gamma\left(\frac{p}{2}\right)\Gamma\left(\frac{d}{2}-\Delta_\phi\right)} g^3 + \mathrm{O}(g^4) , \\ g_*^2 &= -\frac{2^d\pi^{\frac{d}{2}}\Gamma\left(\frac{p}{2}\right)\Gamma\left(\frac{d}{2}-\Delta_\phi\right)}{\Gamma\left(\frac{p}{2}-\Delta_\phi\right)} \varepsilon + \mathrm{O}(\varepsilon^2) . \end{aligned} \tag{6.40}$$

Notice that the fixed-point coupling g_* is not necessarily real. Interestingly, when $d = p + 2$, one has $g_*^2 > 0$ for any Δ_ϕ above the unitarity bound. In the general case, only certain ranges of Δ_ϕ yield a real fixed point.

Using (6.32), one can also extract the one-point function of ϕ^2

$$a_{\phi^2} = -\frac{9\,\Gamma\left(\frac{p}{2}\right)^2\Gamma\left(\Delta_\phi-\frac{p}{2}\right)\Gamma\left(\frac{p-\Delta_\phi}{2}\right)^2}{8\,\Gamma\left(\frac{\Delta_\phi}{2}\right)^2\Gamma\left(\frac{p}{2}-\Delta_\phi\right)(p-1)!} \varepsilon + \mathrm{O}\left(\varepsilon^2\right) . \tag{6.41}$$

In summary, the interaction term $\phi\hat{\psi}^2$ provides a non-trivial defect CFT for some values of p, d, and Δ_ϕ. Specifically, for $d = 3$ and $p = 1$, there is a perturbative fixed point at

$$g_*^2 = 2\pi^2\varepsilon + \mathrm{O}(\varepsilon^2) . \tag{6.42}$$

Notice that the bulk interaction here was not taken into account here; therefore, this is an explicit example of a non-trivial conformal defect in three-dimensional GFF theory. In this picture, Δ_ϕ is a free parameter.

One may also wonder what the effect of introducing the bulk interaction would be. One can easily see that this effect would only contribute at higher orders in ε for the beta function. However, in this case, Δ_ϕ is no longer a free parameter, because one must take $\Delta_\phi = (d-\varepsilon)/4$.[5] For $d = 3$, the fixed point with $p = 1$ is the only real one, since $p = 2$ yields a negative value for g_*^2.

Defect with $(\mathbf{a}, \mathbf{b}) = (\mathbf{2}, \mathbf{1})$

The second case analysed is $(a, b) = (2, 1)$, with interaction term $\frac{g_0}{2}\int d^p\tau \phi^2\hat{\psi}$. Again, the free bulk case is considered first. The operator $\hat{\mathcal{O}}$ is given by $\hat{\mathcal{O}} = \phi\hat{\psi}$, and the tree-level contribution to its bare two-point function is given by

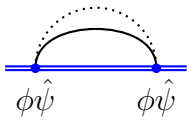

$$= \frac{\mathcal{N}_\phi^2 \mathcal{N}_{\hat{\psi}}^2}{|\tau|^{2(\Delta_\phi + \hat{\Delta}_{\hat{\psi}})}} \,. \tag{6.43}$$

Again, at one loop there is only one divergent diagram , whose divergent can be computed as before

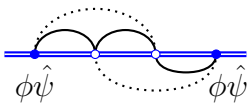

$$= \frac{\left(\mathcal{N}_\phi^2\right)^3 \left(\mathcal{N}_{\hat{\psi}}^2\right)^2 g_0^2}{|\tau|^{2\Delta_\phi + 2\hat{\Delta}_{\hat{\psi}}}} \left(\frac{w^{(p)}_{2\Delta_\phi} w^{(p)}_{2\hat{\Delta}_{\hat{\psi}}}}{w^{(p)}_{2\Delta_\phi + 2\hat{\Delta}_{\hat{\psi}} - p}} \frac{2\pi^{\frac{p}{2}}}{\Gamma\left(\frac{p}{2}\right)} \frac{1}{\varepsilon} + \mathrm{O}(\varepsilon^0) \right) . \tag{6.44}$$

This yields the following renormalisation factor, beta-functions and fixed point

$$\begin{aligned} Z_{\hat{\mathcal{O}}} &= 1 + \frac{\Gamma\left(\frac{p}{2} - \Delta_\phi\right)^2 g^2}{2^{2d-p-1}\pi^{d-\frac{p}{2}}\Gamma\left(\frac{p}{2}\right)\Gamma\left(\frac{d}{2} - \Delta_\phi\right)^2 \varepsilon} + \mathrm{O}\left(g^4\right) , \\ \beta_g &= -\varepsilon g - \frac{\Gamma\left(\frac{p}{2} - \Delta_\phi\right)^2}{2^{2(d-1)-p}\pi^{d-\frac{p}{2}}\Gamma\left(\frac{p}{2}\right)\Gamma\left(\frac{d}{2} - \Delta_\phi\right)^2} g^3 + \mathrm{O}\left(g^4\right) , \\ g_*^2 &= -\frac{2^{2(d-1)-p}\pi^{d-\frac{p}{2}}\Gamma\left(\frac{p}{2}\right)\Gamma\left(\frac{d}{2} - \Delta_\phi\right)^2}{\Gamma\left(\frac{p}{2} - \Delta_\phi\right)^2} \varepsilon + \mathrm{O}(\varepsilon^2) . \end{aligned} \tag{6.45}$$

In this case, the fixed-point value g_*^2 is always negative. Therefore, no real fixed point exists. Moreover, as in the previous case, the situation

[5] Up to an arbitrary positive coefficient in front of ε, as it was discussed at the beginning of Section 6.2.1.

does not change at leading order when the bulk interactions are turned on.

Defect with $(\mathbf{a},\mathbf{b})=(\mathbf{2},\mathbf{2n})$

The last case explicitly analysed is the family given by $a=2$ and $b=2n$ even. The interaction term in (6.16) becomes $\frac{g_0}{2}\int d^p\tau\phi^2\hat{\psi}^{2n}$. The operator $\hat{\mathcal{O}}$ in this case is $\hat{\mathcal{O}}=\phi\hat{\psi}^{2n}$. The tree-level bare two-point function is is given by the following diagram

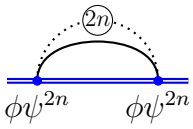

$$= \frac{(2n)!\,\mathcal{N}_\phi^2\left(\mathcal{N}_\psi^2\right)^{2n}}{|x|^{2\Delta_\phi+4n\hat{\Delta}_{\hat{\psi}}}}\,, \tag{6.46}$$

where the dotted line with the label $2n$ represents $2n$ propagators of $\hat{\psi}$. At one loop, there is only one divergent diagram. Since only $Z_{\hat{\mathcal{O}}}$ is needed, it suffices to consider the following diagram

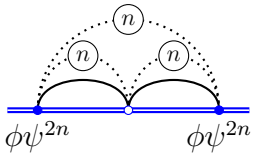

$=$

$$= -\frac{g_0}{2}\,2\binom{2n}{n}^2 n!(2n)!\left(\mathcal{N}_\phi^2\right)^2\left(\mathcal{N}_\psi^2\right)^{3n}\frac{\left(w^{(p)}_{2\Delta_\phi+2n\hat{\Delta}_{\hat{\psi}}}\right)^2}{w^{(p)}_{4\Delta_\phi+4n\hat{\Delta}_{\hat{\psi}}-p}}\frac{1}{|x|^{4\Delta_\phi+6n\hat{\Delta}_{\hat{\psi}}-p}}\,. \tag{6.47}$$

The above quantity diverges as $\varepsilon\to 0$, and the corresponding pole must be cancelled by introducing the wavefunction renormalisation $Z_{\hat{\mathcal{O}}}$. Then, using (6.27), one can extract the beta-function and the fixed point g_*

$$\begin{aligned}
Z_{\hat{\mathcal{O}}} &= 1-\frac{g}{\varepsilon}\frac{2^{1+2\Delta_\phi-p}((2n)!)^2\,\Gamma(\Delta_\phi)}{(4\pi)^{\frac{d-p}{2}}n!\,\Gamma\left(\frac{d}{2}-\Delta_\phi\right)\Gamma\left(\frac{p}{2}\right)}\left(\frac{4^{\frac{p-2\Delta_\phi}{2n}}\Gamma\left(\frac{p-2\Delta_\phi}{2n}\right)}{(4\pi)^{\frac{p}{2}}\Gamma\left(\frac{p}{2}-\frac{p-2\Delta_\phi}{2n}\right)}\right)^n+\mathrm{O}(g^2)\,,\\
\beta_g &= -\varepsilon g+\frac{2^{1+2\Delta_\phi-p}((2n)!)^2\,\Gamma(\Delta_\phi)}{(4\pi)^{\frac{d-p}{2}}n!\,\Gamma\left(\frac{d}{2}-\Delta_\phi\right)\Gamma\left(\frac{p}{2}\right)}\left(\frac{4^{\frac{p-2\Delta_\phi}{2n}}\Gamma\left(\frac{p-2\Delta_\phi}{2n}\right)}{(4\pi)^{\frac{p}{2}}\Gamma\left(\frac{p}{2}-\frac{p-2\Delta_\phi}{2n}\right)}\right)^n g^2+\mathrm{O}(g^3)\,,\\
g_* &= \frac{(4\pi)^{\frac{d-p}{2}}n!\,\Gamma\left(\frac{d}{2}-\Delta_\phi\right)\Gamma\left(\frac{p}{2}\right)}{2^{1+2\Delta_\phi-p}((2n)!)^2\,\Gamma(\Delta_\phi)}\left(\frac{(4\pi)^{\frac{p}{2}}\Gamma\left(\frac{p}{2}-\frac{p-2\Delta_\phi}{2n}\right)}{4^{\frac{p-2\Delta_\phi}{2n}}\Gamma\left(\frac{p-2\Delta_\phi}{2n}\right)}\right)^n\varepsilon+\mathrm{O}(\varepsilon^2)\,.
\end{aligned} \tag{6.48}$$

Using (6.32), one can also extract the one-point function of ϕ^2

$$a_{\phi^2} = \frac{n!\,\Gamma\left(\Delta_\phi - \frac{p}{2}\right)\Gamma\left(\frac{p}{2}\right)^3}{8\Delta_\phi((2n)!)^3(p-1)!}\varepsilon^2 + \mathrm{O}(\varepsilon^3)\,. \tag{6.49}$$

The physically interesting case is $d = 3$, $p = 2$ and $\Delta_\phi = d/4 = 3/4$. This yields the following expression:

$$g_* = \frac{2^{2n}\sqrt{\pi}\,n!}{((2n)!)^2}\Gamma\left(1 - \frac{1}{4n}\right)^n \sin^n\left(\frac{\pi}{n}\right)\varepsilon + \mathrm{O}(\varepsilon^2)\,. \tag{6.50}$$

Notice that the fixed point exists for any n (that is for any even b) above.

As in the discussion of the $(a, b) = (1, 2)$ case, the bulk interaction has not been turned on yet, meaning that these examples provide non-trivial surface defects in three-dimensional GFF theory. If one were to include the bulk interaction, it would still not affect the leading-order computation.

Summary of non-local defects

Here some results for the physically interesting case of $d = 3$ are summarised. In this case, there are two types of defects: lines and surfaces.

- For $p = 1$, the allowed interaction terms are of the form $\phi\hat{\psi}^b$. The case $b = 2$ in GFF theory was studied explicitly, finding the existence of a non-trivial line defect.
- For $p = 2$, one can have interactions $\phi\hat{\psi}^b$ and $\phi^2\hat{\psi}^b$. The first case with $b = 2$ and the second case for $b = 2n$ even were addressed, finding a non-trivial defect only for the second family of interactions. Again, at leading order, the bulk interaction does not affect this result.

For higher values of b, other potentially interesting defect examples could arise. It would also be interesting to investigate whether there are additional constraints on the allowed values of b.

6.2.2 Defects close to $d = 4$

In this section, the generalisation of two simple defects that can be constructed in the short-range $O(N)$ model are explored, starting from the UV theory in $d = 4$ and expanding around $d = 4 - \hat{\varepsilon}$. This section is based on the analysis of [37]. Unlike Section 6.2.1 , where d was kept fixed and the dimension of the scalar field Δ_ϕ was varied, here

one needs to expand around $d = 4$ for the defect action to be weakly relevant.

To explore the LRI fixed points, in Section 6.1, a parameter $0 < \kappa < 1$ was introduced, with $\sigma = 2 - \frac{(1-\kappa)\hat{\varepsilon}}{2}$. This parameterises a straight line in the (d, σ) plane, where κ selects a particular direction in the phase space shown in Figure 6.1. In general, the LRI fixed points in the (d, σ) plane are characterised by the exact relation $\Delta_\phi = \frac{d-\sigma}{2}$. When performing calculations near the local theory in $d = 4$, non-vanishing contributions to the wavefunction renormalisation and the anomalous dimension of the field ϕ arise. Therefore, by enforcing the condition above, one obtains the following expression for σ:

$$\sigma = d - 2\Delta_\phi = 2 + \frac{\kappa - 1}{2}\hat{\varepsilon} + 2\gamma_\phi(\kappa, \hat{\varepsilon})\,, \tag{6.51}$$

where $\gamma_\phi(\kappa, \hat{\varepsilon})$ is the anomalous dimension of the field ϕ, which starts at $\mathrm{O}(\hat{\varepsilon}^2)$. This parametrises a one-parameter family of trajectories, ranging from $\kappa = 0$, where $\gamma_\phi(0, \hat{\varepsilon}) = 0$ and $\sigma = d/2$, to $\kappa = 1$, where $\gamma_\phi(1, \hat{\varepsilon}) = \gamma_{\mathrm{SRI}}$ and the trajectories approach the upper bound of the LRI region, as shown in Figure 6.1.

By making a simple generalisation of the computation for the SRI (or $\kappa = 1$), it is possible to obtain these trajectories at order ε^2. Note that, at this stage, only the homogeneous theory is being considered, without any defect. The first contribution to the renormalisation of the field ϕ appears at two loops, and it gives:

$$Z_\phi = 1 - \frac{(N+2)\,\lambda^2}{18\,(4\pi)^4\,(1+3\kappa)\,\hat{\varepsilon}} + \mathrm{O}(\lambda^3)\,, \tag{6.52}$$

while the coupling renormalisation yields

$$\begin{aligned} Z_\lambda = 1 + \frac{N+8}{3\kappa\,\hat{\varepsilon}}\frac{\lambda}{(4\pi)^2} + \\ + \left(\frac{(N+8)^2}{9\kappa^2\hat{\varepsilon}^2} - \frac{5N + 22 + \kappa(13N+62)}{9(1+3\kappa)\kappa\,\hat{\varepsilon}}\right)\frac{\lambda^2}{(4\pi)^4} + \mathrm{O}(\lambda^3)\,. \end{aligned} \tag{6.53}$$

This leads to the following beta-function

$$\beta_\lambda = -\kappa\,\hat{\varepsilon}\,\lambda + \frac{N+8}{3}\frac{\lambda^2}{(4\pi)^2} - \frac{10N + 44 + \kappa(26N+124)}{9(1+3\kappa)}\frac{\lambda^3}{(4\pi)^4} + \mathrm{O}(\lambda^4)\,, \tag{6.54}$$

which admits a non-trivial fixed point at

$$\frac{\lambda_*}{(4\pi)^2} = \frac{3}{N+8}\kappa\,\hat{\varepsilon} + \frac{6}{(N+8)^3}\frac{5N+22+\kappa\,(13N+62)}{1+3\kappa}\kappa^2\hat{\varepsilon}^2 + \mathrm{O}\left(\hat{\varepsilon}^3\right) . \tag{6.55}$$

From these computations one can immediately derive the anomalous dimension γ_ϕ of ϕ_a at the IR fixed point

$$\gamma_\phi = \beta_\lambda \frac{\partial \ln Z_\phi}{\partial\lambda}\bigg|_{\lambda=\lambda_*} = \frac{\kappa^3(N+2)}{(1+3\kappa)(N+8)^2}\hat{\varepsilon}^2 + \mathrm{O}\left(\hat{\varepsilon}^3\right) . \tag{6.56}$$

This leads to the following family of curves in the (d,σ) plane

$$\sigma = 2 + \frac{\kappa-1}{2}\hat{\varepsilon} - \frac{2\kappa^3(N+2)}{(3\kappa+1)(N+8)^2}\hat{\varepsilon}^2 + \mathrm{O}\left(\hat{\varepsilon}^3\right) . \tag{6.57}$$

Some of these trajectories are shown in Figure 6.2. As a consistency check, one can easily verify that at $\kappa = 1$ one retrieves the expressions for the short-range $O(N)$ model

$$\sigma = 2 - \frac{(N+2)}{2\,(N+8)^2}\hat{\varepsilon}^2 = 2 - \eta_{\mathrm{SRI}}\,. \tag{6.58}$$

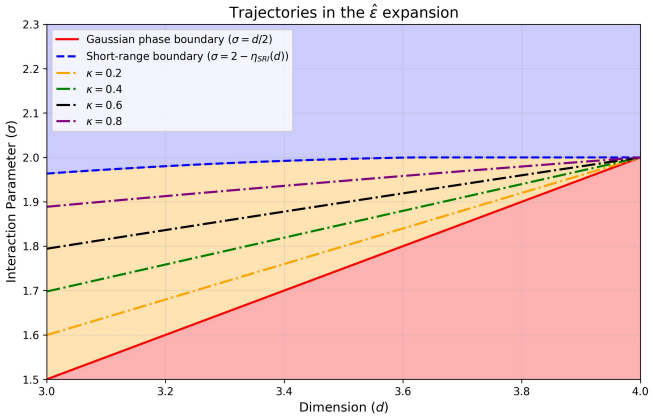

Figure 6.2: The trajectories $\sigma(d)$ such that the condition $\sigma = d - 2\Delta_\phi$ is enforced.

Another useful check, which may be more trivial in flows that do not depend on an extra parameter like κ, is the stability of the bulk IR fixed point. This involves studying the sign of the derivative of β_λ at λ_* and ensuring it is positive

$$\beta'_\lambda(\lambda_*) = \kappa\,\hat{\varepsilon} - \frac{2\,(5N+22+\kappa(13N+62))}{(1+3\kappa)(N+8)^2}\kappa^2\hat{\varepsilon}^2 + \mathrm{O}(\hat{\varepsilon}^3)\,. \tag{6.59}$$

This leads to the following consistency condition

$$\hat{\varepsilon} < \hat{\varepsilon}_{\text{thresh}} = \frac{(1+3\kappa)(N+8)^2}{2\kappa\,(5N+22+\kappa(13N+62))}\,. \tag{6.60}$$

For $0 < \kappa < 1$, this threshold value is always greater than 1, meaning that this stability condition is never a concern for the perturbative treatment considered in this section.

Localized magnetic field

The simplest defect one can consider in the above setup is the analogue of the localised magnetic field introduced in 3.2, given by the action

$$S = S_0 + h_0 \int d\tau \phi_1(\tau)\,, \tag{6.61}$$

where a single field ϕ_1 is integrated along a line. To renormalise the coupling h in the $\hat{\varepsilon}$-expansion, finiteness of the one-point function of ϕ_1 is imposed. The computation is analogous to the local case, up to the appearance of the new parameter κ. The relevant diagrams are shown in Appendix B.4.1. The final result for the coupling renormalisation Z_h is

$$\begin{aligned} Z_h = 1 + \frac{h^2}{3(1+3\kappa)\hat{\varepsilon}}\frac{\lambda}{(4\pi)^2} + \Bigg[\frac{(N+2)h}{18(1+3\kappa)\hat{\varepsilon}} + \\ + \left(\frac{1}{\hat{\varepsilon}^2} - \frac{1+3\kappa^2-(1-\kappa)(\gamma_E-\log 4\pi)}{4\kappa\hat{\varepsilon}}\right)\frac{2(N+8)h^2}{9(1+3\kappa)(1+5\kappa)} \\ + \left(\frac{2}{(1+3\kappa)\hat{\varepsilon}^2} - \frac{1}{\hat{\varepsilon}}\right)\frac{h^4}{12(1+3\kappa)}\Bigg]\frac{\lambda^2}{(4\pi)^4} + \mathrm{O}(\lambda^3)\,. \end{aligned} \tag{6.62}$$

This subsequently yields the following beta-function [6]

$$\begin{aligned} \beta_h = -\frac{\hat{\varepsilon}\,(1+\kappa)}{4}h + \frac{\lambda}{(4\pi)^2}\frac{h^3}{6} + \frac{\lambda^2}{(4\pi)^4}\Bigg(\frac{(N+2)\,\kappa h}{9\,(1+3\kappa)} \\ - \frac{(N+8)\,(1+3\kappa^2-(1-\kappa)\,(\gamma_E-\log(4\pi)))}{36\kappa\,(1+3\kappa)}h^3 - \frac{h^5}{12}\Bigg) + \mathrm{O}(\lambda^3)\,. \end{aligned} \tag{6.63}$$

This beta function reduces to the short range result in the limit $\kappa \to 1$ given in (3.21). The opposite limit, $\kappa \to 0$, is subtle because in (6.62) the single pole in $\hat{\varepsilon}$ is accompanied by a single pole in $\kappa = 0$, leading to a singular limit $\kappa \to 0$ for the beta function (6.63). This pole is cancelled

[6] One should not be worried about the appearence of terms like γ_E or $\log 4\pi$, since two-loop coefficients of the beta function for multiple couplings are scheme dependent.

when one set the bulk coupling to the fixed point λ_* in (6.55). In that case, the limit $\kappa \to 0$ trivially leads to $\beta_h = -\hat{\varepsilon}h/4$, consistently with a Gaussian fixed point. For general κ, instead one has a non-trivial defect fixed point

$$\begin{aligned} h_*^2 = &\frac{(N+8)(1+\kappa)}{2\kappa} + \frac{(5+2(1-\kappa^2)(\log(4\pi)-\gamma_E))\,(N+8)}{8\kappa(1+3\kappa)}\hat{\varepsilon} \\ &+ \frac{(15\kappa^2+27\kappa+17)N^2+8(15\kappa^2+36\kappa+29)N+48(9\kappa^2+22\kappa+19)}{8(1+3\kappa)(N+8)}\hat{\varepsilon} \\ &+ \mathrm{O}(\hat{\varepsilon}^2)\,. \end{aligned} \tag{6.64}$$

In the following, some defect observables at this fixed point are computed.

Scaling dimension. The first observable considered is the scaling dimension of the defect field $\hat{\phi}_1$. This is just a derivative of the beta function: $\Delta_{\hat{\phi}} = 1 + \frac{\partial \beta_h}{\partial h}|_{h=h_*}$, and it is

$$\Delta_{\hat{\phi}} = 1 + \frac{1+\kappa}{2}\hat{\varepsilon} - \frac{1}{8}\left(3+\kappa\left(3(\kappa+2)+\frac{16\kappa^2(N+2)}{(1+3\kappa)(N+8)^2}\right)\right)\hat{\varepsilon}^2 + \mathrm{O}(\hat{\varepsilon}^3)\,. \tag{6.65}$$

It is important to notice that the limit $\kappa \to 0$ should not be considered, since there is no defect fixed point in that direction. The limit $\kappa \to 1$, instead, perfectly reproduces the existing results [32].

One-point function. The next piece of defect CFT data one can easily obtain is the one-point function of the bulk field ϕ_1, which is the observable used to renormalise the defect coupling. Defining

$$\langle \phi_a(x) \rangle = \delta_{a,1} \frac{\mathcal{N}_\phi a_\phi}{|x_\perp|^{\Delta_\phi}}\,, \tag{6.66}$$

and inserting the renormalised coupling in the diagrams in Appendix B.4.1, one gets

$$\begin{aligned} a_\phi^2 = &\frac{(\kappa+1)(N+8)}{8\kappa} + \left(\frac{-15\kappa^2-18\kappa-5}{4(3\kappa+1)} + \frac{3\,(9\kappa^2+10\kappa+3)}{2(3\kappa+1)(N+8)}\right. \\ &\left. + \frac{(3\kappa-1)(\kappa+1)(N+8)}{32\kappa} + \frac{(\kappa+1)^2(N+8)\log(2)}{16\kappa}\right)\hat{\varepsilon} + \mathrm{O}\left(\hat{\varepsilon}^2\right)\,. \end{aligned} \tag{6.67}$$

When $\kappa \to 1$, one recovers the result given in (3.24).

g-function. Another important defect observable is the g-function of this dCFT, which obeys a monotonicity theorem under RG flow as explained in Section 2.3.1. The computation is analogous to the one in [32], with the important difference that one needs to keep a generic value of Δ_ϕ, leading to a dependence on κ. For a free bulk theory, one can compute the defect expectation value of the circular defect exactly either by finding the classical solution to the equation of motion and computing the classical action or by resumming diagrams. The final result is

$$\log g_{\text{free}} = \log \frac{Z_{\text{defect}}}{Z_0} = \frac{2^{1-d}\pi^{\frac{3-d}{2}}\Gamma\left(\frac{1}{2}-\Delta_\phi\right)\Gamma\left(\Delta_\phi\right)R^{2-2\Delta_\phi}}{\Gamma\left(1-\Delta_\phi\right)\Gamma\left(\frac{d}{2}-\Delta_\phi\right)}\,, \tag{6.68}$$

where R is the radius of the circle. Adding the bulk interaction, one has two diagrams up to order $\hat{\varepsilon}$, which were solved in [32] and reviewed in Appendix B.4.2. The final result is

$$\log g = -\frac{(1+\kappa)\hat{\varepsilon}}{16}h^2 + \frac{\kappa h^4 \lambda_*}{192\pi^2(3\kappa+1)} + \mathrm{O}\left(\lambda_*^2\right)\,, \tag{6.69}$$

and using the value of the defect fixed point coupling h_*

$$\log g_{\text{IR}} = -\frac{(\kappa+1)^3(N+8)}{32\kappa(3\kappa+1)}\hat{\varepsilon} + \mathrm{O}\left(\hat{\varepsilon}^2\right) < 0 = \log g_{\text{UV}}\,, \tag{6.70}$$

as one expects from the g-theorem. [7]

Surface defect

Another interesting defect was introduced in the short-range model in Section 3.4: the surface defect. It was realised by integrating ϕ^2 over a two-dimensional plane [8]

$$S = S_0 + h_0 \int d^2\tau\, \phi_a\phi_a(\tau)\,, \tag{6.71}$$

and, contrary to the localised magnetic field, it preserves the full $O(N)$ symmetry.

To renormalise the defect coupling one considers the one-point function of $\phi_a\phi^a$ (a $O(N)$ singlet is needed to get a non-vanishing one-point

[7] More precisely, the quantity that is monotonic under RG flow is the defect entropy, defined by $s = (1 - R\frac{\partial}{\partial R})\log g$. However, as explained in [32], s and $\log g$ agree at leading order.

[8] There is also a symmetry-breaking version of this surface defect obtained by the interaction $h^{ab}\phi_a\phi_b$, with a generic tensor coupling h_{ab}. However, for simplicity only the $O(N)$ symmetric case is considered.

function). When the bulk is free, the beta-function can be computed exactly by going to momentum space and following the procedure described in [125] for resumming the diagrams

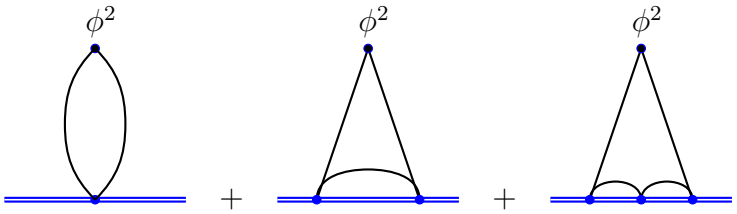

$$+ \quad + \quad + \quad \dots \tag{6.72}$$

This leads to the exact expression for the bare coupling

$$h_0 = \mu^{\frac{1+\kappa}{2}\hat{\varepsilon}} h \left(1 + \frac{2h}{(1+\kappa)\pi\hat{\varepsilon}} + \left(\frac{2h}{(1+\kappa)\pi\hat{\varepsilon}} \right)^2 + \dots \right) = \frac{\mu^{\frac{1+\kappa}{2}\hat{\varepsilon}} h}{1 - \frac{2h}{(1+\kappa)\pi\hat{\varepsilon}}} , \tag{6.73}$$

and consequently to the exact beta-function

$$\beta_h = -\frac{1+\kappa}{2}\hat{\varepsilon} h + \frac{h^2}{\pi} . \tag{6.74}$$

This admits a non-trivial fixed point in $h_* = \frac{\pi(1+\kappa)}{2}\hat{\varepsilon}$.

Reintroducing the bulk coupling, one needs to take into account the wavefunction renormalisation of ϕ^2, which will depend on the parameter κ. More generally, one can compute the renormalisation of the field ϕ^n for any positive integer n. This is given by the following bulk diagrams

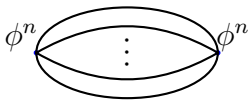

$$= \frac{N n! N_\phi^n}{|x|^{2n\Delta_\phi}} , \tag{6.75}$$

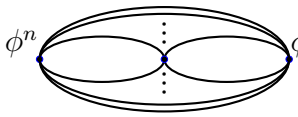

$$= -\frac{N(N+2)n!n(n-1)N_\phi^{n+2}\lambda_0}{12} \frac{\left(w^{(d)}_{4\Delta_\phi}\right)^2}{w^{(d)}_{8\Delta_\phi - d}} \frac{1}{|x|^{(8+2n-4)\Delta_\phi - d}} . \tag{6.76}$$

The second diagram diverges, and one can introduce the wavefunction renormalisation

$$Z_{\phi^n} = 1 - \frac{(N+2)n(n-1)}{6\kappa\,\hat{\varepsilon}} \frac{\lambda}{(4\pi)^2} + \mathrm{O}(\lambda^2) . \tag{6.77}$$

The diagrams for the renormalisation of the defect coupling h are given in Appendix B.4.1. After taking into account the wavefunction renormalisation Z_{ϕ^2}, one finds the following

$$\begin{aligned} h_0 &= \mu^{\frac{1+\kappa}{2}\hat{\varepsilon}} h \left(\frac{1}{1-\frac{2h}{(1+\kappa)\pi\hat{\varepsilon}}} + \frac{(N+2)\lambda}{48\pi^2\kappa\,\hat{\varepsilon}} \right) + \mathrm{O}\left(h^2\lambda, h\lambda^2, \lambda^3\right) , \\ \beta_h &= -\frac{1+\kappa}{2}\hat{\varepsilon}h + \frac{h^2}{\pi} + \frac{N+2}{48\pi^2}h\lambda\,. \end{aligned} \tag{6.78}$$

At $\lambda = \lambda_*$, there is a non-trivial defect fixed point

$$h_* = \frac{N\,(1-\kappa)+8+4\kappa}{2\,(N+8)}\pi\hat{\varepsilon} + \mathrm{O}\left(\hat{\varepsilon}^2\right) . \tag{6.79}$$

As expected, for $\kappa = 1$ one recovers the result of the short-range model [123–125]. In the opposite limit, and in contrast to the case of the localised magnetic field, there is no divergence at $\kappa = 0$. Instead, the fixed point gives $h_* = \frac{\pi}{2}\hat{\varepsilon}$, which is in agreement with the exact result found above for the Gaussian theory (6.74). Another notable difference from the localised magnetic field is that the fixed point is perturbatively small in $\hat{\varepsilon}$, rather than being of order $\hat{\varepsilon}^0$.

Also in this case it is possible to compute some interesting defect observables.

Scaling dimension. As before, a derivative of the beta function for h gives access to the following defect scaling dimension at the fixed point

$$\Delta_{\hat{\phi}^2} = 2 + \frac{8+4\kappa+N(1-\kappa)}{2(N+8)}\hat{\varepsilon} + \mathrm{O}(\hat{\varepsilon}^2)\,, \tag{6.80}$$

Once more, both limits $\kappa = 1$ and $\kappa = 0$ are well defined and they return the expected results for the short range and the Gaussian theory.

One point data. The Feynman diagrams used to renormalise the coupling also give access to the one-point function $\langle\phi^2\rangle$

$$a_{\phi^2} = -\frac{\sqrt{N}(4\kappa+N(1-\kappa)+8)}{4\sqrt{2}(N+8)}\hat{\varepsilon} + \mathrm{O}(\hat{\varepsilon}^2)\,, \tag{6.81}$$

Defect free energy. The last observable discussed is the defect free energy $\mathcal{F}$ introduced in 2.3.1. The computation follows the one in [125], but with generic Δ_ϕ. Summing up the three diagrams shown in Appendix B.4.2 gives the following logarithmic term in the free energy

$$\mathcal{F}_{\text{univ}} = \left(\frac{N(1+\kappa)\hat{\varepsilon}\,h^2}{16\pi^2} - \frac{Nh^3}{12\pi^3} - \frac{N(N+2)\lambda h^2}{384\pi^4} \right) \log\left(\mu R\right) . \tag{6.82}$$

This expression is very similar to the local case [123–125] apart from the κ dependence in the first term. At the defect fixed point one can compute the Weyl anomaly coefficient b finding

$$b_{\rm IR} = -\frac{(8+4\kappa+N(1-\kappa))^3}{64(N+8)^3}\hat{\varepsilon}^3 + \mathrm{O}\left(\hat{\varepsilon}^4\right) < b_{\rm UV} = 0\,, \tag{6.83}$$

which is consistent with the defect b-theorem [16].

6.2.3 Semiclassical construction of defects

In Sections 6.2.1 and 6.2.2, defects for the long-range $O(N)$ model have been realised as fixed points of defect RG flows triggered by interactions that are classically marginal. However, as discussed in Section 3.4.2 strongly relevant interactions might as well originate a defect RG flow that ends in an IR fixed point. For instance, consider the long-range $O(N)$ model with a localised magnetic field on a line. Recall that the action is

$$S = \int d^dx \left(\frac{1}{2}\phi_a \mathcal{L}_\sigma \phi_a + \frac{\lambda_0}{4!}(\phi_a)^2\right) + h_0 \int d\tau\ \phi_1\,. \tag{6.84}$$

With $\sigma = (d+\varepsilon)/2$, the bulk interaction is weakly relevant. However, in this case $\Delta_\phi = (d-\varepsilon)/4$, and the defect interaction is strongly relevant for $2 < d < 4$. Therefore, standard perturbation theory around the trivial vacuum fails. Instead, one needs to carry out an analysis similar to the one of Section 3.4.2, as is discussed in [37].

Semiclassics

The first step to study this model is to look for non-trivial saddle points of the path integral of the form

$$\phi^a_{\rm cl}(x) = \delta_{a1}\frac{\mathcal{N}_\phi\, a_{\rm cl}}{|x_\perp|^{\Delta_{\rm cl}}}\,. \tag{6.85}$$

The non-local equations of motion are

$$-\mathcal{L}_\sigma \phi^a_{\rm cl}(x) = -\frac{2^{\frac{d+\varepsilon}{2}}\Gamma\left(\frac{d-1-\Delta_{\rm cl}}{2}\right)\Gamma\left(\frac{d+\varepsilon+2\Delta_{\rm cl}}{4}\right)\mathcal{N}_\phi\, a_{\rm cl}}{\Gamma\left(\frac{\Delta_{\rm cl}}{2}\right)\Gamma\left(\frac{d-2-\varepsilon-2\Delta_{\rm cl}}{4}\right)|x_\perp|^{\Delta_{\rm cl}+\frac{d+\varepsilon}{2}}}\delta_{a1} = \frac{\lambda_0}{3!}\frac{\mathcal{N}_\phi^3\, {a_{\rm cl}}^3}{|x_\perp|^{3\Delta_{\rm cl}}}\delta_{a1}\,, \tag{6.86}$$

and they are solved by

$$\Delta_{\rm cl} = \frac{d+\varepsilon}{4}\,, \quad \mathcal{N}_\phi^2\, {a_{\rm cl}}^2 = -\frac{6}{\lambda_0}\frac{2^{\frac{d+\varepsilon}{2}}\Gamma\left(\frac{3d-4-\varepsilon}{8}\right)\Gamma\left(\frac{3d+3\varepsilon}{8}\right)}{\Gamma\left(\frac{d-4-3\varepsilon}{8}\right)\Gamma\left(\frac{d+\varepsilon}{8}\right)}\,, \tag{6.87}$$

where as in Section 3.4.2 the solution $a_{\rm cl} > 0$ has been selected. Reasoning as in the previous section,one can conclude that

$$\langle \phi^a(x) \rangle = \delta_{a,1} \frac{\mathcal{N}_\phi \, a_\phi}{|x_\perp|^{\Delta_\phi}} \,. \tag{6.88}$$

with

$$\Delta_\phi = \frac{d-\varepsilon}{4} \,, \quad {a_\phi}^2 = {a_{\rm cl}}^2 (1 + \mathrm{O}(\varepsilon)) = -\frac{(N+8)\Gamma\left(\frac{3d-4}{4}\right)}{2^{\frac{d}{2}-1}\Gamma\left(\frac{d-4}{4}\right)\Gamma\left(\frac{d}{2}\right)\varepsilon} + \mathrm{O}\left(\varepsilon^0\right) \,. \tag{6.89}$$

Note that for $d = 4 + \mathrm{O}(\varepsilon)$ the classical contribution vanishes, since one gets perturbatively close to the trivial vacuum. As in Section 3.4.2, by considering the expectation value of the equation of motion, one can compute the $\mathrm{O}(\hat{\varepsilon})$ contribution to the coefficient a_ϕ near $d = 4$, where the defect becomes weakly-coupled. This result can then be matched to the results of Section 6.2.2.

The matching procedure works as follows. In this section, the defect conformal manifold (shown in Figure 6.1) was parametrised using the coordinates (d, ε), near the crossover with GFF. In contrast, in Section 6.2.2, the coordinates $(\hat{\varepsilon}, k)$ were used near the point $d = 4$. To switch between these coordinate systems, one needs to ensure that the same point (d, σ) is being described. The corresponding condition is $d = 4 - \hat{\varepsilon}$ and $\varepsilon = \hat{\varepsilon}/k + \mathrm{O}(\hat{\varepsilon}^2)$.

By considering the expectation value of the equation of motion and switching to the $(\hat{\varepsilon}, k)$ coordinates, one obtains

$$a_\phi^2 = \frac{(N+8)(\kappa+1)}{8\,\kappa} + \mathrm{O}(\hat{\varepsilon}), \tag{6.90}$$

which precisely matches the results in (6.66) and (6.67).

Quantum corrections

In order to compute quantum fluctuations around the new saddle point, the action has to be expanded around it

$$S'[\delta\phi^a] = S_{\rm bulk}[\phi^a_{\rm cl} + \delta\phi^a] - S_{\rm bulk}[\phi^a_{\rm cl}] = \int d^d x \, \frac{1}{2} \Bigg(\Big(\delta^{ab} \mathcal{L}_\sigma + \frac{\lambda_0 \bar{\phi}^2}{6|x_\perp|^{2\Delta_{\rm cl}}} \left(\delta^{ab} + 2\delta^{a1}\delta^{b1} \right) \Big) \delta\phi_a \delta\phi_b + \frac{\lambda_0 \bar{\phi}}{6|x_\perp|^{\Delta_{\rm cl}}} \, \delta\phi_a \delta\phi_a \delta\phi_1 + \tfrac{\lambda_0}{4!} (\delta\phi_a)^2 \Bigg) \,. \tag{6.91}$$

For convenience, the definition $\bar{\phi} = \mathcal{N}_\phi \, a_{\rm cl}$ has been used. A similar analysis can also be done for a $O(N)$ breaking surface defect [125].

In (6.91), there are new quadratic and cubic terms that break both Poincaré symmetry and $O(N)$ symmetry to $O(N-1)$, as expected. The quadratic term comes with coefficient $\lambda_0\bar{\phi}^2$, which, by (6.87), is a pure number. One can either try to invert the quadratic part of the action or treat this new term as a perturbation. In the latter case, since the coefficient is not small, one must always consider an arbitrary number of insertions of this term. This is what will be done in the following, since the inversion of the quadratic operator turns out to be a very difficult task. On the other hand, since $\lambda_0\bar{\phi} \sim \sqrt{\lambda_0}$, the cubic term is perturbatively small.

As an instructive example, one can consider the computation of the leading-order quantum corrections to the order parameter $\langle\delta\phi_a(x)\rangle$. For concreteness, the focus will be on the case $d = 3$, which is the physically relevant one. The following analysis is similar to the one carried out for the extraordinary surface transition in [132]. However, this case is more complicated due to the fact that here there is a line defect instead of a boundary. The diagrams contributing to this one-point function at order $\sqrt{\lambda_0}$ all belong to a single family, which can be represented as follows

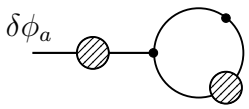

(6.92)

where the dots represent the quadratic and cubic interactions, and the "bubble" is the dressed propagator defined by

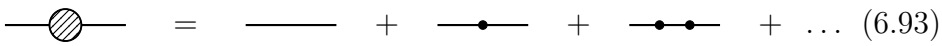

(6.93)

In (6.92) there is always at least one quadratic interaction inserted in the loop to avoid tadpole contributions. This diagram is already difficult to compute analytically, mainly because the terms in (6.93) involve challenging integrals, whose results must then be resummed.

To begin, one can extract the divergent part of (6.92). It turns out that the divergence arises only from the following diagram

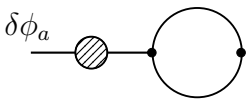

(6.94)

This can be verified by checking all the other diagrams and observing that they do not exhibit logarithmic divergences. To evaluate (6.94), one can use the following recursion relation

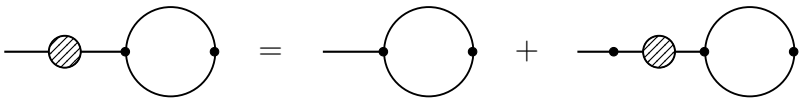

(6.95)

The first diagram on the right-hand side can be easily computed

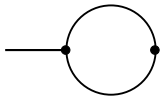

$$= \delta_{a1} \frac{A_0}{|x_\perp|^{\frac{3-3\varepsilon}{4}}} ,$$

$$A_0 = \frac{\sqrt{\lambda_0}(N+8)\Gamma\left(\frac{1}{4}\right)}{2^{\frac{15}{4}}\sqrt{3}\,\pi^{\frac{5}{2}}}\left(\frac{1}{\varepsilon}+\right. \tag{6.96}$$

$$\left.+\frac{\left(48-2\pi+3\gamma_E+10\sqrt{2}\log\left(2-\sqrt{2}\right)+\left(13-5\sqrt{2}\right)\log(2)\right)}{4}+\mathrm{O}(\varepsilon)\right).$$

Using dimensional analysis, one can make the following ansatz for the left-hand side

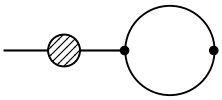

$$= \delta_{a1} \frac{A}{|x_\perp|^{\frac{3-3\varepsilon}{4}}} . \tag{6.97}$$

Substituting this ansatz into the recursion relation in (6.95), and evaluating the integral in the last term on the right-hand side, yields a linear equation that can be solved for A

$$A = \frac{\sqrt{\lambda_0}(N+8)\Gamma\left(\frac{1}{4}\right)}{2^{\frac{19}{4}}\sqrt{3}\,\pi^{\frac{5}{2}}}\left(\frac{1}{\varepsilon}+\right. \tag{6.98}$$

$$\left.+\frac{32-2\pi+3\gamma_E+13\log(2)-3\sqrt{2}\log\left(2\sqrt{2}+3\right)}{4}+\mathrm{O}(\varepsilon)\right).$$

As it was argued, (6.98) captures the full divergence of the more complicated diagram in (6.92). A non-trivial consistency check is that this divergence exactly cancels the one arising from the coupling renormalisation in the classical term. More specifically, one has

$$\langle\phi_a(x)\rangle = \phi^a_{\mathrm{cl}} + \langle\delta\phi_a(x)\rangle\,, \tag{6.99}$$

where $\phi^a_{\mathrm{cl}} \sim 1/\sqrt{\lambda_0}$ as given by (6.87). Since the bulk renormalises independently, one also has that $\lambda_0 = \mu^\varepsilon\lambda(1+\lambda(N+8)/(12\pi^2\varepsilon)+\mathrm{O}(\lambda^2))$, according to (6.11). Therefore, the first term in (6.92) has a divergence at order $\sqrt{\lambda}$, which is exactly cancelled by the divergence in the second term that was just computed. This ensures that $\langle\phi_a(x)\rangle$ remains finite. The finite term corresponds to the order ε^0 correction to (6.89). Part of this finite term is given in (6.98), while the rest comes from diagrams that contain more than one quadratic interaction in the loop. Their contributions can be collected into one single diagram

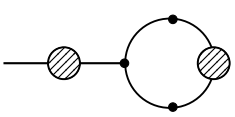

(6.100)

Furthermore, using a recursion similar to the one in (6.95), it suffices to compute the following

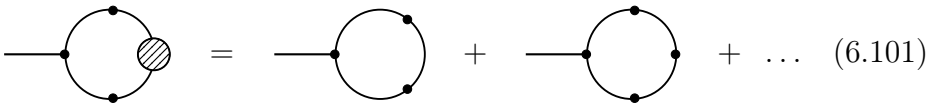

(6.101)

Unfortunately, performing this computation analytically is difficult. However, all the diagrams in the sum in (6.101) are finite for $\varepsilon = 0$ and can be evaluated numerically. The result of the sum can then be extrapolated using standard numerical techniques, such as Padé approximation.

Chapter 7

Outlook

This thesis explored various aspects of conformal defects in conformal field theories, with an emphasis on developing and applying analytic bootstrap techniques, on the one hand, and investigating the realisations of conformal defects through defect renormalisation group flows, on the other. As remarked in the introduction, for the sake of concreteness, this thesis focused on conformal defects in the $O(N)$ model and similar models. These are of interest both for their physical applications in condensed matter theory and from a more abstract, theoretical perspective. However, given that these methods have proven to be highly effective in this context, and that they are, in principle, easily generalisable, a natural future direction is the direct application of similar methods to other examples of defect CFTs.

For instance, the analytic bootstrap analysis of the localised magnetic field in the ε-expansion, discussed in Section 4.2, already has several possible extensions to similar contexts. For example, one could perform a similar analysis on the same defect by applying the same analytic bootstrap techniques to the large-N expansion instead of the ε-expansion, or to other correlators beyond the one considered. This would provide interesting complementary defect data to those obtained in Section 4.2. Other interesting possibilities arise from considering slightly different dCFTs where analytic bootstrap techniques can still be applied. Examples include the defects introduced in the long-range $O(N)$ model in Section 6.2, or other order defects that can be constructed in bulk CFTs with different symmetries and potentials, or that involve fermions, such as those described in [178, 179]. Another intriguing follow-up could be to investigate similar defects in the higher-derivative theories introduced in [180]. These theories are known to be scale-invariant [51], and it would be interesting to explore the properties of the fixed point of a defect RG flow in a scale-invariant but not conformally invariant bulk CFT.

The analysis of the magnetic impurity in the free bulk theory in Section 4.3.1, which can be performed to all orders in ε, and the existence of the "non-local" defects in generalised free field theories, as shown in Section 6.2.1, also provide an intriguing prompt for future research: *what are the possible conformal defects for Gaussian bulk theories*? In fact, several recent works have already addressed aspects of this problem [121, 181–183, 122], but a complete classification has yet to be established.

The transdimensional defects introduced in Chapter 5 also admit a multitude of possible natural generalisations. On the one hand, additional observables or higher-order results could be computed in the models introduced, using the same ideas. These could then be used to extrapolate numerical information about potentially physically relevant non-local CFTs and new dCFTs. For example, the non-local interacting family of three-dimensional CFTs, with a light spectrum given by (5.29), could be studied using analytic and numerical bootstrap methods and large-N techniques, with the aim of obtaining interesting non-perturbative results. Another natural extension would be to define transdimensional defects for other bulk fixed points beyond the $O(N)$ model. The only requirement is that the model admits a perturbative defect that can be consistently defined in non-integer dimensions. Examples include scalar models with different bulk symmetries [178] and theories with fermionic degrees of freedom [184, 178, 179]. A further natural question that arises in light of these transdimensional defects is the existence of defect conformal manifolds composed of dCFTs, where the dimension of the defect is not constant. This could potentially connect together known examples of dCFTs, and interesting structures may emerge.

In the context of defects in the long-range $O(N)$ model introduced in Section 3.4, there are several ways to continue the analysis. The first, of course, is to apply analytic and numerical bootstrap techniques to systematically extract information about these defects. In this case, Monte Carlo simulations could also be employed. In a different direction, one could explore defects in other regions of the phase diagram shown in Figure 6.1, beyond those discussed in Chapter 6. Specifically, Chapter 6 focused on the region around the corner at $d = 4$ and near the crossover at $\sigma = d/2$. However, one could also consider the "upper" crossover, which marks the boundary between the LRI and SRI phases. A novel approach to studying this crossover was proposed in [170], and it would be interesting to introduce defects into that picture.

Finally, in Section 3.4.2, the question of understanding the existence of fixed points for strongly-relevant defect RG flows was discussed, and an initial approach to partially address this problem was outlined in Section 6.2.3. However, providing a complete solution to this problem appears to be a challenging task. On the one hand, it would be interesting to expand on the analysis presented in Section 6.2.3, based on semiclassical analysis and perturbation theory around new saddle points. In fact, this approach has been successfully applied to boundary CFTs [132], although the case with higher co-dimension seems to be significantly more difficult. On the other hand, the transdimensional defects introduced in Chapter 5 could also play a role in addressing this question. Indeed, one could study a defect fixed point near a value of the defect dimension that makes the defect RG flow weakly relevant, and then extrapolate using the techniques from Section 5.1 to other values of interest. This is perhaps one of the most intriguing problems involving defects that could be tackled in the near future. It is not entirely unlikely that a better understanding of strongly relevant defect RG flows could also shed light on how a theory evolves into a strongly coupled regime along an ordinary RG flow.

Appendices

Appendix A

Bulk and defect blocks

The bulk blocks appearing in (2.63) are not known in closed form but can be expressed as a sum of Harish-Chandra functions [79]. In radial coordinates, they take the form

$$f_{\Delta,\ell}(r,w) = 2^{-\ell} f^{HS}_{\Delta,\ell}(r,w) + \frac{\Gamma(\ell+d-2)\Gamma(-\ell-\frac{d-2}{2})}{2^\ell \Gamma(\ell+\frac{d-2}{2})\Gamma(-\ell)} \frac{\Gamma(\frac{\ell+d-p-1}{2})\Gamma(\frac{1-\ell}{2})}{\Gamma(\frac{\ell+d-1}{2})\Gamma(\frac{1-\ell-p}{2})} f^{HS}_{\Delta,2-d-\ell}(r,w)\,, \tag{A.1}$$

where $f^{HS}_{\Delta,\ell}(r,w)$ is given by the following double infinite sum

$$\begin{aligned} f^{HS}_{\Delta,\ell}(r,w) = \sum_{m=0}^{\infty}\sum_{n=0}^{\infty} &\left[(1-rw)(1-\tfrac{r}{w})\right]^{\frac{\Delta-\ell}{2}+m+n} h_n(\Delta,\ell) \\ & h_m(1-\ell,1-\Delta)\frac{4^{m-n}}{n!m!}\frac{(\frac{\Delta+\ell}{2})_{n-m}}{(\frac{\Delta+\ell}{2}-\frac{1}{2})_{n-m}}\,{}_4F_3\Big(-n,-m,\tfrac{1}{2}, \\ & \tfrac{\Delta-\ell-d}{2}+1;-\tfrac{\Delta+\ell}{2}+1-n,\tfrac{\Delta+\ell}{2}-m,\tfrac{\Delta-\ell-d+3}{2};1\Big)(1-r^2)^{\ell-2m} \\ & {}_2F_1\big(\tfrac{\Delta+\ell}{2}-m+n,\tfrac{\Delta+\ell}{2}-m+n,\Delta+\ell-2(m-n),1-r^2\big)\,, \end{aligned} \tag{A.2}$$

with

$$h_n(\Delta,\ell) = \frac{\left(\frac{\Delta}{2}-\frac{1}{2}\right)_n\left(\frac{\Delta}{2}-\frac{p}{2}\right)_n\left(\frac{\Delta+\ell}{2}\right)_n}{\left(\Delta-\frac{d}{2}+1\right)_n\left(\frac{\Delta+\ell}{2}+\frac{1}{2}\right)_n}\,. \tag{A.3}$$

An important feature of the bulk blocks is their analytic structure in the variable w. Since they are proportional to $\left(\frac{(1-rw)(w-r)}{rw}\right)^{\frac{\Delta-\ell}{2}} = \xi^{\frac{\Delta-\ell}{2}}$, for generic Δ they have a branch cut between $w=0$ and $w=r$. This feature, together with the convergence of the bulk OPE around $w=r$, allows to evaluate the discontinuity of the two-point function as

$$\text{Disc}F(r,w) = \sum_{\mathcal{O}} \lambda_{\phi\phi\mathcal{O}}\, a_{\mathcal{O}}\, \text{Disc}\left[\xi^{-\Delta_\phi} f_{\Delta,\ell}(r,w)\right]\,. \tag{A.4}$$

An important property of the bulk blocks is their analytic structure in the variable w. Since they are proportional to $\xi^{\frac{\Delta-\ell}{2}} = \left(\frac{(1-rw)(w-r)}{rw}\right)^{\frac{\Delta-\ell}{2}}$, they have a branch cut between $w=0$ and $w=r$ for generic Δ. This feature, combined with the convergence of the bulk OPE around $w=r$, allows the discontinuity of the two-point function to be evaluated as

$$\text{Disc}F(r,w) = \sum_{\mathcal{O}} \lambda_{\phi\phi\mathcal{O}}\, a_{\mathcal{O}}\, \text{Disc}\left[\xi^{-\Delta_\phi} f_{\Delta,\ell}(r,w)\right] . \tag{A.5}$$

The defect blocks in (2.64) in radial coordinates are defined as

$$\begin{aligned}\hat{f}_{\hat{\Delta},s}(r,w) = r^{\hat{\Delta}}\, {}_2F_1\left(\hat{\Delta}, \frac{p}{2}, \hat{\Delta}+1-\frac{p}{2}, r^2\right)(2w)^{-s} \\ {}_2F_1\left(-s, \frac{d-p}{2}-1, 2-\frac{d-p}{2}-s, w^2\right) .\end{aligned} \tag{A.6}$$

The functions $F_1(z,\bar{z})$ and $F_2(z,\bar{x})$ introduced in (3.28) in the analysis of the localised magnetic field can be expressed as linear combinations of $F_S(z,\bar{z})$, $F_T(z,\bar{z})$ and of $\hat{F}_S(z,\bar{z})$, $\hat{F}_T(z,\bar{z})$ defined in (3.33) and (3.37)

$$\begin{aligned}F_1(z,\bar{z}) &= F_S(z,\bar{z}) - \tfrac{1}{N} F_T(z,\bar{z}) = \hat{F}_V(z,\bar{z}) , \\ F_2(z,\bar{z}) &= F_T(z,\bar{z}) = \hat{F}_S(z,\bar{z}) - \hat{F}_V(z,\bar{z}) .\end{aligned} \tag{A.7}$$

Appendix B

Explicit computations

B.1 Computation of the one-loop bulk two-point function for the localised magnetic field

B.1.1 The correlator from the dispersion relation

As it was discussed in the main text, the discontinuity of the correlator contains a non trivial term that gives rise to a very complicated integral in the dispersion formula. Here it will be shows the computation of that integral, and in particular it will be given a derivation of $I(r,w)$ (4.35), namely the non trivial contribution to the full correlators (4.36) (4.38) . To begin, it is possible to write the non trivial part of the discontinuity (4.34) as a sum of hypergeometric functions, using the definition of the bulk block (A.2), and then replacing the hypergeometric function with its definition as a sum, and finally exchanging the order of the sums. The result is

$$\begin{aligned}
&\frac{4\pi\sqrt{rw}\left(F\left(\sin^{-1}\left(\sqrt{r}\sqrt{\frac{r-w}{1-rw}}\right)|\frac{(rw-1)^2}{(r-w)^2}\right)-F\left(\sin^{-1}\left(\frac{\sqrt{\frac{r-w}{1-rw}}}{\sqrt{r}}\right)|\frac{(rw-1)^2}{(r-w)^2}\right)\right)}{r-w} = \\
&= \sum_{n=0}^{\infty}\frac{i\pi 2^{1-2n}r}{1+2n}\left(\frac{(r-w)(rw-1)}{w}\right)^n {}_2F_1\left(n+1,n+1;2n+2;1-r^2\right) = \\
&= \sum_{n=0}^{\infty}\sum_{m=0}^{\infty}\frac{i\pi 2^{1-2n}r}{1+2n}\left(\frac{(r-w)(rw-1)}{w}\right)^n \frac{(1-r^2)^m((n+1)_m(n+1)_m)}{m!(2n+2)_m} = \\
&= \sum_{m=0}^{\infty}\frac{2i\pi r\left(1-r^2\right)^m}{m+1}{}_3F_2\left(\frac{1}{2},m+1,m+1;\frac{m}{2}+1,\frac{m}{2}+\frac{3}{2};\frac{(r-w)(rw-1)}{4w}\right).
\end{aligned} \tag{B.1}$$

It turns out that this expansion of the discontinuity can be easily integrated term by term in the dispersion relation and one can find the function $I(r,w)$. Indeed, plugging the previous expression into the dispersion relation (4.8) and changing variable from w' to $x = \left(\frac{(1-rw')(w'-r)}{4w'}\right)$,

one finds

$$\begin{aligned} I(r,w) &= \int_{-\infty}^{0} dx \sum_{m=0}^{\infty} \tfrac{4rw(1-r^2)^m\, {}_3F_2\left(\frac{1}{2},m+1,m+1;\frac{m}{2}+1,\frac{m}{2}+\frac{3}{2};x\right)}{(m+1)(r^2(-w)+rw^2+r+4wx-w)} = \\ &= \sum_{m=0}^{\infty} \frac{2^{1-m}rw(1-r^2)^m G^{4,2}_{4,4}\left(\frac{4w}{wr^2-(w^2+1)r+w}\middle|\begin{matrix}0,0,\frac{m}{2},\frac{m+1}{2}\\ -\frac{1}{2},0,m,m\end{matrix}\right)}{(m!)(r^2(-w)+rw^2+r-w)}, \end{aligned} \tag{B.2}$$

where G is the Meijer G-function, and it was assumed

$$\Re\left(\frac{r\left(-rw+w^2+1\right)}{w}\right) \leqslant 1 \vee \frac{r\left(-rw+w^2+1\right)}{w} \notin \mathbb{R}\,. \tag{B.3}$$

To rewrite the previous expression in a closed form one can use the integral representation of the Meijer G-function

$$\begin{aligned} &G^{m,n}_{p,q}\left(z\middle|\begin{matrix}a_1,\ldots,a_n,a_{n+1},\ldots,a_p\\ b_1,\ldots,b_m,b_{m+1},\ldots,b_q\end{matrix}\right) = \\ &\quad = \frac{1}{2\pi i}\int_{\mathcal{L}} ds\, \frac{\prod_{k=1}^{n}\Gamma\left(-s-a_k+1\right)\prod_{k=1}^{m}\Gamma\left(s+b_k\right)z^{-s}}{\prod_{k=n+1}^{p}\Gamma\left(s+a_k\right)\prod_{k=m+1}^{q}\Gamma\left(-s-b_k+1\right)}\,. \end{aligned} \tag{B.4}$$

Plugging the integral representation representation in (B.2), and exchanging sum and integral, one gets

$$\begin{aligned} &I(r,w) = \sum_{m=0}^{\infty}\int ds\, \tfrac{2^{1-m}rw\left(1-r^2\right)^m}{\Gamma(m+1)(w-r)(rw-1)}\tfrac{2^{m+1}\Gamma(1-s)^2\Gamma(2s-1)\Gamma(m+s)^2}{\Gamma(m+2s)}\left(\tfrac{4w}{(r-w)(rw-1)}\right)^{-s} = \\ &= -\int_{\mathcal{L}} ds\, \frac{\pi^2 r 4^{1-s}\csc^2(\pi s)}{2s-1}\,{}_2F_1\left(s,s;2s;1-r^2\right)\left(\frac{w}{(r-w)(rw-1)}\right)^{1-s} = \\ &= \sum_{n=0}^{\infty}\frac{\partial}{\partial t}\left(\left(\tfrac{(r-w)(rw-1)}{w}\right)^{n+t}\tfrac{4^{-n-t}r}{2n+2t+1}\,{}_2F_1\left(n+t+1,n+t+1;2(n+t+1);1-r^2\right)\right) = \\ &= \sum_{n=0}^{\infty}\frac{\partial}{\partial t}\left(\left(\tfrac{(r-w)(rw-1)}{(1+r)^2w}\right)^{n+t}\tfrac{4r}{(1+r)^2(2n+2t+1)}\,{}_2F_1\left(\tfrac{1}{2},n+t+1;n+t+\tfrac{3}{2};\tfrac{(1-r)^2}{(r+1)^2}\right)\right) = \\ &= \frac{\partial}{\partial t}\left(\left(\tfrac{(r-w)(rw-1)}{(1+r)^2w}\right)^{t}\tfrac{4r}{(1+r)^2(2t+1)}F^{112}_{101}\left(\begin{matrix}1+t:\frac{1}{2};\frac{1}{2}+t,1;\\ \frac{3}{2}+t:-;1+t;\end{matrix}\quad\left(\tfrac{1-r}{1+r}\right)^2,\tfrac{(r-w)(rw-1)}{(1+r)^2w}\right)\right)\Bigg|_{t=0}. \end{aligned} \tag{B.5}$$

The final result is expressed in terms of a derivative of a Kampé de Fériet function [138], which is defined by

$$F^{ABB'}_{CDD'}\left(\begin{matrix}(a):(b);(b');\\ (c):(d);(d');\end{matrix}\quad x,y\right) = \sum_{m=0}^{\infty}\sum_{n=0}^{\infty}\frac{\prod_{j=1}^{A}(a_j)_{m+n}\prod_{j=1}^{B}(b_j)_m\prod_{j=1}^{B'}(b'_j)_n}{\prod_{j=1}^{C}(c_j)_{m+n}\prod_{j=1}^{D}(d_j)_m\prod_{j=1}^{D'}(d'_j)_n}\frac{x^m}{m!}\frac{y^n}{n!}. \tag{B.6}$$

This sum converges absolutely if $A+B = C+D+1$, $A+B' = C+D'+1$, $|x| < 1$ and $|y| < 1$, which in this case, together with (B.3), imply

$$0 < r < 1 \wedge \Bigg((0 < w < 1 \wedge 0 < r \leqslant w) \vee (w = 1 \wedge 0 < r < 1) \vee \\ \vee \left(w > 1 \wedge 0 < r \leqslant \frac{1}{w} \right) \Bigg) . \tag{B.7}$$

One can extend the result to all other values by exploiting the symmetry of the correlator with respect to $r \leftrightarrow \frac{1}{r}$ and $w \leftrightarrow \frac{1}{w}$ [18].

B.1.2 Generating function of the bulk inversion

The first few orders in the $z = 1$ expansion of the one-loop generating function $C_T^t(z,\beta)$ (4.51) read

$$\begin{aligned} C_T^t(z,\beta) = a_\phi^{2\,(0)} \Bigg(& (1-z)^{\Delta_\phi} \Bigg(\frac{\sqrt{\pi}\,\Gamma\left(\frac{\beta+1}{2}\right)\Gamma\left(1-\frac{\Delta_\phi}{2}\right)^2\Gamma\left(\frac{\beta}{2}+\Delta_\phi-1\right)}{\Gamma\left(\frac{\beta+2}{4}\right)^2\Gamma\left(\frac{1}{4}(\beta-2\Delta_\phi+4)\right)\Gamma\left(\frac{1}{4}(\beta+2\Delta_\phi)\right)} + \\ & + \Bigg(\frac{(z-1)^2\left(-\beta^3-4\beta^2\Delta_\phi-6\beta^2-4\beta\Delta_\phi^2-20\beta\Delta_\phi-8\beta-4\Delta_\phi^2-16\Delta_\phi\right)}{192(\beta+1)} + \\ & + \frac{(z-1)\left(\beta^3+4\beta^2\Delta_\phi+4\beta^2+4\beta\Delta_\phi^2+12\beta\Delta_\phi+4\beta+4\Delta_\phi^2+8\Delta_\phi\right)}{16(\beta+1)(\beta+2\Delta_\phi+2)} + \\ & + \frac{2}{(z-1)(\beta+2\Delta_\phi-2)} - \frac{1}{2} \Bigg)(1-z)^{\frac{\beta}{2}+\Delta_\phi} \Bigg) \times \\ & \times \Bigg(\frac{\Gamma\left(\frac{\beta}{2}\right)^4 \sin^2\left(\frac{\pi\Delta_\phi}{2}\right)}{\pi^2\Gamma(\beta-1)\Gamma(\beta)} + \frac{\left(\Delta_\phi^2+2\Delta_\phi\right)(z-1)^2\Gamma\left(\frac{\beta}{2}\right)^4 \sin^2\left(\frac{\pi\Delta_\phi}{2}\right)}{8\pi^2\Gamma(\beta-1)\Gamma(\beta)} + \\ & - \frac{\left(\Delta_\phi^3+6\Delta_\phi^2+8\Delta_\phi\right)(z-1)^3\Gamma\left(\frac{\beta}{2}\right)^4 \sin^2\left(\frac{\pi\Delta_\phi}{2}\right)}{48\pi^2\Gamma(\beta-1)\Gamma(\beta)} - \frac{\Delta_\phi(z-1)\Gamma\left(\frac{\beta}{2}\right)^4 \sin^2\left(\frac{\pi\Delta_\phi}{2}\right)}{2\pi^2\Gamma(\beta-1)\Gamma(\beta)} \Bigg) \Bigg) \Bigg) + \\ & - a_\phi^{2\,(1)} \frac{\Gamma\left(\frac{\beta}{4}\right)^2(1-z)^{\Delta_\phi}\Gamma\left(\frac{\beta}{4}+\frac{\Delta_\phi}{2}-\frac{1}{2}\right)}{\Gamma\left(\frac{\beta}{2}-\frac{1}{2}\right)\left(2^{\frac{\beta}{2}-\Delta_\phi+1}\Gamma\left(\frac{\Delta_\phi}{2}\right)^2\right)\Gamma\left(\frac{\beta}{4}-\frac{\Delta_\phi}{2}+1\right)} + \mathrm{O}((z-1)^4), \end{aligned} \tag{B.8}$$

where Δ_ϕ needs to be expanded at one loop. The singlet contribution is simply $C_S^t(z,\beta) = \frac{1}{N} C_T^t(z,\beta)$.

B.1.3 Feynman diagrams

The bulk two-point function of two fundamental fields in the presence of the defect $\langle \phi_a(x)\phi_b(y)\rangle_{\mathcal{D}}$ can be calculated perturbatively by evaluating

Feynman diagrams at the fixed point. In particular, to the first order in ε (hence at one loop) there are two disconnected contributions, which are given by the one-loop correction to the bulk propagator and the one-loop correction to the product of one-point functions

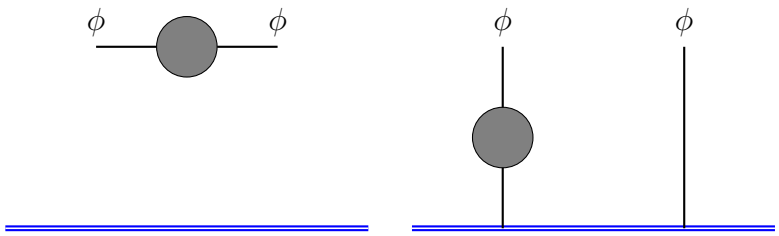

(B.9)

where the blue double line at the bottom represents the defect $\mathcal{D}$, whereas black lines are scalar propagators with a generic one-loop correction represented as a grey circle. These two contributions naturally provide the corrections to the defect and bulk identity in (4.36) and (4.38). The only connected diagram is the cross diagram

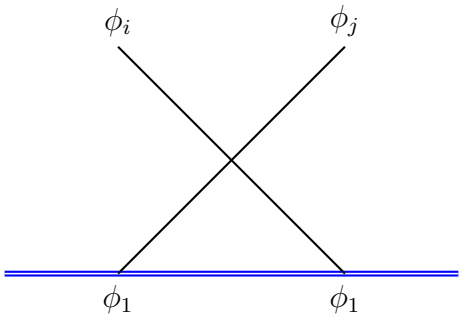

(B.10)

The contribution of the diagram (B.10) is given by

$$-\mathcal{N}_\phi^2\,(\delta_{ij}+2\delta_{i1}\delta_{j1})\,\frac{\lambda h^2}{2!}\int d\tau_1\int d\tau_2\int d^{4-\varepsilon}q\;G(x-q)G(y-q)\\ G(q-x(\tau_1))G(q-x(\tau_2))\,, \tag{B.11}$$

where $|\dot{x}(\tau_{1,2})|=1$, $\mathcal{N}_\phi$ is chosen to normalise the bulk two-point function in the absence of the defect, and $G(x)$ is the free propagator

$$G(x)=\frac{1}{(d-2)\Omega_{d-1}|x|^{d-2}}=\frac{1}{4\pi^2|x|^2}+\mathrm{O}(\varepsilon)\,,\quad \mathcal{N}_\phi=2\pi+\mathrm{O}(\varepsilon)\,. \tag{B.12}$$

Since at the fixed point $\lambda_*\propto\varepsilon$, one can set $\varepsilon=0$ in all the other terms. Evaluating at the fixed point, Inserting (B.12) into (B.11) and

performing the τ_2 and τ_2 integrals one gets

$$\begin{aligned} -(\delta_{ij}+2\delta_{i1}\delta_{j1})\frac{3}{8\pi^2}\int d^4q\,\frac{1}{|q_\perp|^2\,|x-q|^2\,|y-q|^2} = \\ = (\delta_{ij}+2\delta_{i1}\delta_{j1})\,\frac{I(x,y)}{8|x_\perp||y_\perp|}\,, \end{aligned} \tag{B.13}$$

where $I(x,y)$ is exactly the conformally invariant function defined in (4.35), but expressed in the coordinates (x,y). Thanks to conformal invariance, it is enough to evaluate $I(x,y)$ for $x_\parallel = y_\parallel = 0$. However, the integral in (B.13) is very hard to solve analytically and a general closed form has not been found. Nevertheless, it is still possible to reduce it to a more useful one-dimensional integral representation which can be used to obtain series expansions and other analytic considerations.

First of all, one can derive the integral representation. The starting point is

$$I(x,y) = -\tfrac{3}{\pi^2}\int d^3q_\perp \int dq_\parallel\, \tfrac{|x_\perp||y_\perp|}{|q_\perp|^2\,(q_\parallel^2+|x_\perp-q_\perp|^2)\,(q_\parallel^2+|y_\perp-q_\perp|^2)}\,. \tag{B.14}$$

One can introduce a Feynman parameter α for the last two factor in the denominator

$$I(x,y) = -\tfrac{3}{\pi^2}\int_0^1 d\alpha \int d^3q_\perp \int dq_\parallel\, \tfrac{|x_\perp||y_\perp|}{|q_\perp|^2\left(q_\parallel^2+\alpha|x_\perp-q_\perp|^2+(1-\alpha)|y_\perp-q_\perp|^2\right)^2}\,. \tag{B.15}$$

Now it is possible to perform the $q_\parallel$ integral and rearrange to obtain

$$I(x,y) = -\frac{3}{2\pi}\int_0^1 d\alpha \int d^3q_\perp\, \frac{|x_\perp||y_\perp|}{|q_\perp|^2\;(|q_\perp-\tilde{q}_\perp|^2+L^2)^{\frac{3}{2}}}\,, \tag{B.16}$$

where

$$\tilde{q}_\perp = \alpha x_\perp + (1-\alpha)y_\perp\,, \quad L^2 = \alpha(1-\alpha)|x_\perp-y_\perp|^2\,. \tag{B.17}$$

Introducing another Feynman parameter ξ, one gets

$$I(x,y) = -\tfrac{9}{4\pi}\int_0^1 d\alpha \int_0^1 d\xi \int d^3q_\perp\, \tfrac{\xi^{\frac{1}{2}}\cdot|x_\perp||y_\perp|}{(|q_\perp-\xi\tilde{q}_\perp|^2+\xi(1-\xi)|\tilde{q}_\perp|^2+\xi L^2)^{\frac{5}{2}}}\,. \tag{B.18}$$

After the shift $q_\perp \to q_\perp + \xi\tilde{q}_\perp$, the integral over $q_\perp$ becomes easy and it gives

$$I(x,y) = -3|x_\perp||y_\perp| \int_0^1 d\alpha \int_0^1 d\xi\, \frac{1}{\xi^{\frac{1}{2}}\,(L^2+(1-\xi)|\tilde{q}_\perp|^2)}\,. \tag{B.19}$$

It is now convenient to pass to lightcone coordinates. Changing variable $\xi = \eta^2$ and rearranging one gets

$$I(z,\bar{z}) = -6\sqrt{z\bar{z}}\int_0^1 d\alpha \int_0^1 d\eta \, \frac{1}{(1+\alpha(z\bar{z}-1)-\eta^2(1+(z-1)\alpha)(1+(\bar{z}-1)\alpha))} \,. \quad \text{(B.20)}$$

At this point one can obtain two different representations by integrating either in α or in η. Integrating over α one gets

$$I(z,\bar{z}) = -6\sqrt{z\bar{z}}\int_0^1 d\eta \, \frac{\log\left[P(z,\bar{z},\eta)+\sqrt{Q(z,\bar{z},\eta)}\right]-\log\left[P(z,\bar{z},\eta)-\sqrt{Q(z,\bar{z},\eta)}\right]}{\sqrt{Q(z,\bar{z},\eta)}} \,, \quad \text{(B.21)}$$

where $P(z,\bar{z},\eta)$ and $Q(z,\bar{z},\eta)$ are the following polynomials

$$\begin{aligned} P(z,\bar{z},\eta) &= 1 + z\bar{z} - \eta^2(z+\bar{z}), \\ Q(z,\bar{z},\eta) &= (z\bar{z}-1)^2 - 2\eta^2(z+\bar{z}+z\bar{z}(z+\bar{z}-4)) + \eta^4(z-\bar{z})^2 \,. \end{aligned} \quad \text{(B.22)}$$

Alternatively, it is possible to perform the integral over η in (B.20) to get

$$I(z,\bar{z}) = -6\sqrt{z\bar{z}}\int_0^1 d\alpha \, \frac{\tanh^{-1}\left[\frac{(1+(z-1)\alpha)(1+(\bar{z}-1)\alpha}{1+\alpha(z\bar{z}-1)}\right]}{\sqrt{(1+(z-1)\alpha)(1+(\bar{z}-1)\alpha)(1+\alpha(z\bar{z}-1))}} \,. \quad \text{(B.23)}$$

Both expressions (B.21) and (B.23) can be used to obtain series expansions of $I(z,\bar{z})$. Moreover, from (B.23) it is also possible to extract in a closed form the term in $I(z,\bar{z})$ proportional to $\log(1-\bar{z})$. Indeed in the limit $\bar{z} \to 1$ the argument of the hyperbolic arcotangent goes to 1 giving a logarithmic divergence, whereas the denominator remains finite. The logarithmic term is therefore given by

$$I(z,\bar{z})_{\log(\bar{z}-1)} = 3\sqrt{z\bar{z}}\,\log(\bar{z}-1)\int_0^1 d\alpha \, \frac{1}{\sqrt{(1+(z-1)\alpha)(1+(\bar{z}-1)\alpha)(1+\alpha(z\bar{z}-1))}} \,. \quad \text{(B.24)}$$

The result of this integral can be expressed in terms of incomplete elliptic integrals of the first kind $F(\varphi,k)$

$$\begin{aligned} &I(z,\bar{z})_{\log(\bar{z}-1)} = \\ &= 6\sqrt{z\bar{z}}\log(\bar{z}-1)\left(\frac{F\left(\sin^{-1}\left(\sqrt{\frac{\bar{z}-z}{\bar{z}-1}}\right),\frac{z(\bar{z}-1)^2}{(\bar{z}-z)(z\bar{z}-1)}\right)-F\left(\sin^{-1}\left(\sqrt{\frac{\bar{z}-z}{z\bar{z}-z}}\right),\frac{z(\bar{z}-1)^2}{(\bar{z}-z)(z\bar{z}-1)}\right)}{\sqrt{(\bar{z}-z)(z\bar{z}-1)}}\right) \,. \end{aligned} \quad \text{(B.25)}$$

B.2 Computation of the β-function for the magnetic impurity

In this appendix, the three-loop beta function for the interacting Wilson line is calculated for both the free and interacting bulk cases [35].

The method employed was introduced in [185], with a recent review available in [186].

Moreover, in Section B.2.7 the two-point function of two defect spin operators (3.82) is explicitly computed at two loops.

B.2.1 Summary of the strategy

The goal ultimate goal is to express the bare coupling ζ_0 in terms of the renormalized coupling ζ, given in the MS scheme by

$$\zeta_0 = \mu^{\varepsilon/2}\zeta\Bigg(1 + \frac{a_{11}\zeta^2 + a_{12}\zeta^4 + a_{13}\zeta^6}{\varepsilon} + \frac{a_{22}\zeta^4 + a_{23}\zeta^6}{\varepsilon^2} + \frac{a_{33}\zeta^6}{\varepsilon^3} + \mathrm{O}(\zeta^8)\Bigg)\,. \tag{B.26}$$

From this one can extract the beta function from the condition that $d\zeta_0/d\mu = 0$, namely

$$\beta(\zeta) = -\frac{\varepsilon}{2}\,\zeta + a_{11}\zeta^3 + 2a_{12}\zeta^5 + 3a_{13}\zeta^7 + \mathrm{O}(\zeta^9)\,. \tag{B.27}$$

As usual, one also finds the relation between lower and higher order poles

$$a_{22} = \frac{3}{2}\,a_{11}^2\,, \qquad a_{33} = \frac{5}{2}\,a_{11}^3\,, \qquad a_{23} = \frac{11}{3}\,a_{11}a_{12}\,. \tag{B.28}$$

The goal of the rest of this appendix is to compute the vertex $\mathcal{V}(x)$ at three loops.

In order to determine the coefficients a_{ij} in equation (B.26), one has to demand that physical observables are finite when expressed in terms of ζ. As argued in the main text, a good such observable is the vertex function

$$\mathcal{V}(x) = \frac{\mathrm{Tr}\,\langle\phi(x)\mathcal{D}_j(0,\tau)\rangle}{\mathrm{Tr}\,\langle\mathcal{D}_j(0,\tau)\rangle}\,, \tag{B.29}$$

In order to determine the coefficients a_{ij} in equation (B.26), it is necessary to require that physical observables remain finite when expressed in terms of ζ. As discussed in the main text, a suitable observable for this purpose is the vertex function.

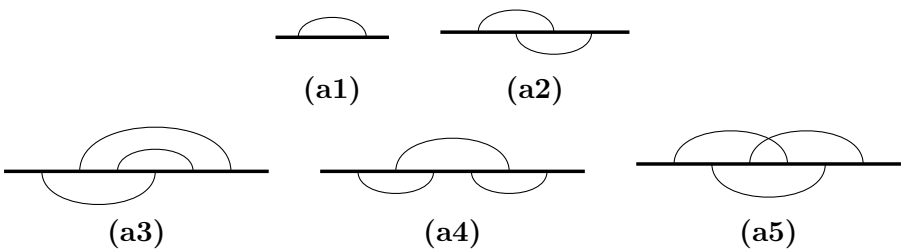

Figure B.1: One-, two-, and three-loop propagator diagrams.

B.2.2 Expectation value of defect at three loops

The calculation begins with the expectation value of the defect. Since $\langle \operatorname{Tr} \mathcal{D}(\tau) \rangle$ exponentiates, it is convenient to consider its logarithm. The final result is presented first, with the derivation provided below

$$\begin{aligned} \frac{\log \left\langle \operatorname{Tr} \mathcal{D}(\tau) \right\rangle}{j(j+1)(2j+1)} &= \zeta_0^2 \, \mathbf{(a1)} - \zeta_0^4 \, \mathbf{(a2)} \\ &\quad + \zeta_0^6 \left(2\mathbf{(a3)} + 2\mathbf{(a4)} + \mathbf{(a5)} \right) + \dots \end{aligned} \tag{B.30}$$

In this expression, **(a1)**–**(a5)** are integrals represented diagrammatically in figure B.1. The thick horizontal line represents the defect, and the thin black lines are ϕ propagators. The integrals are computed in the range $[0, \tau]$, time-ordering is implicit, and propagators are unit normalised. For example

$$\mathbf{(a1)} \;=\; \text{  } \;=\; \int\limits_{0<\tau_1<\tau_2<\tau} \frac{d\tau_1 \, d\tau_2}{\tau_{21}^{2-\varepsilon}} \,, \tag{B.31}$$

$$\mathbf{(a2)} \;=\; \text{  } \;=\; \int\limits_{0<\tau_1<\tau_2<\tau_3<\tau_4<\tau} \frac{d\tau_1 \, d\tau_2 \, d\tau_3 \, d\tau_4}{(\tau_{31}\tau_{42})^{2-\varepsilon}} \,. \tag{B.32}$$

Although these integrals are not difficult to compute, they are not required, as their contribution will cancel between the numerator and denominator in equation (B.29).

The derivation of equation (B.30) can now be explained. Although the procedure is tedious, it can be automated with the assistance of `mathematica`. The first step involves computing $\langle \mathcal{D}(\tau) \rangle$ up to order ζ_0^6 by performing all possible Wick contractions. Each diagram consists of a product of an integral and a trace. The traces are of the form $\operatorname{Tr} T_{a_1} T_{a_2} \dots T_{a_l}$, with all indices $a_1, \dots, a_l$ contracted. These traces can be computed by repeatedly applying the commutation relations in equation (3.42), a process that was automated using a computer.

With regard to the integrals, a large number are found, many more than those shown in figure B.1. However, many of these integrals factorise into products of lower-point integrals. To illustrate this, an example is provided. Consider the following sum of diagrams.

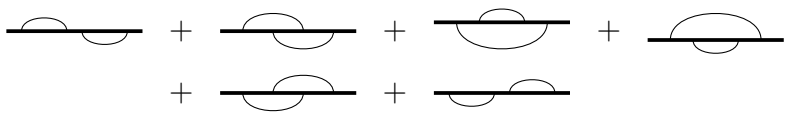

(B.33)

Since all possible orderings of points are accounted for, this sum is equivalent to the diagram **(a1)** squared. Each diagram appears twice, resulting in

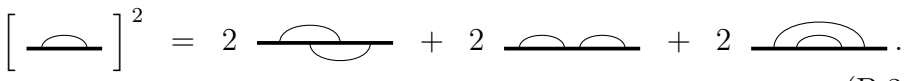

(B.34)

Similar expression can be found for other products of diagrams, even when the diagrams being multiplied are different, or there are several copies of each. The central idea is that a product of diagrams is equal to the sum of all time-ordered diagrams such that the relative order of the legs in each subdiagram is preserved. Formulated in this way, this is a combinatorial problem that can be automated. By factorizing sums of diagrams as in this example, one can observe that the result exponentiates, and obtain equation (B.30).

B.2.3 Expectation value of vertex at three loops

The full vertex $\mathcal{V}(x)$ is now considered. Again, the final result is presented first, with the derivation provided below

$$\begin{aligned}\frac{\mathcal{V}(x)}{\zeta_0\sqrt{\kappa}j(j+1)} &= \mathbf{(b1)} - \mathbf{(b2)}\zeta_0^2 + \big(\mathbf{(b3)} + 2\mathbf{(b4)} + 2\mathbf{(b5)}\big)\zeta_0^4 \\ &\quad + \Big(- 2\mathbf{(b6)} - 4\mathbf{(b7)} - \mathbf{(b8)} - \mathbf{(b9)} - 2\mathbf{(b10)} \\ &\qquad - 2\mathbf{(b11)} - 2\mathbf{(b12)} - 2\mathbf{(b13)} - 2\mathbf{(b14)} - 4\mathbf{(b15)} \\ &\qquad + 2(2j(j+1) - 5)\mathbf{(b16)} + 4(j(j+1) - 2)\mathbf{(b17)} \\ &\qquad - 2\mathbf{(b18)} - 4\mathbf{(b19)} + 2(2j(j+1) - 5)\mathbf{(b20)} \\ &\qquad + (2j(j+1) - 7)\mathbf{(b21)}\Big)\zeta_0^6 + \dots \ .\end{aligned} \tag{B.35}$$

The diagrams **(b1)**–**(b21)** are presented in figure B.2. In this figure, the cross $\times$ represents the point where the bulk field $\phi(x)$ is connected to the defect. For example, if the bulk field sits at $x = (w, x_\perp)$, where

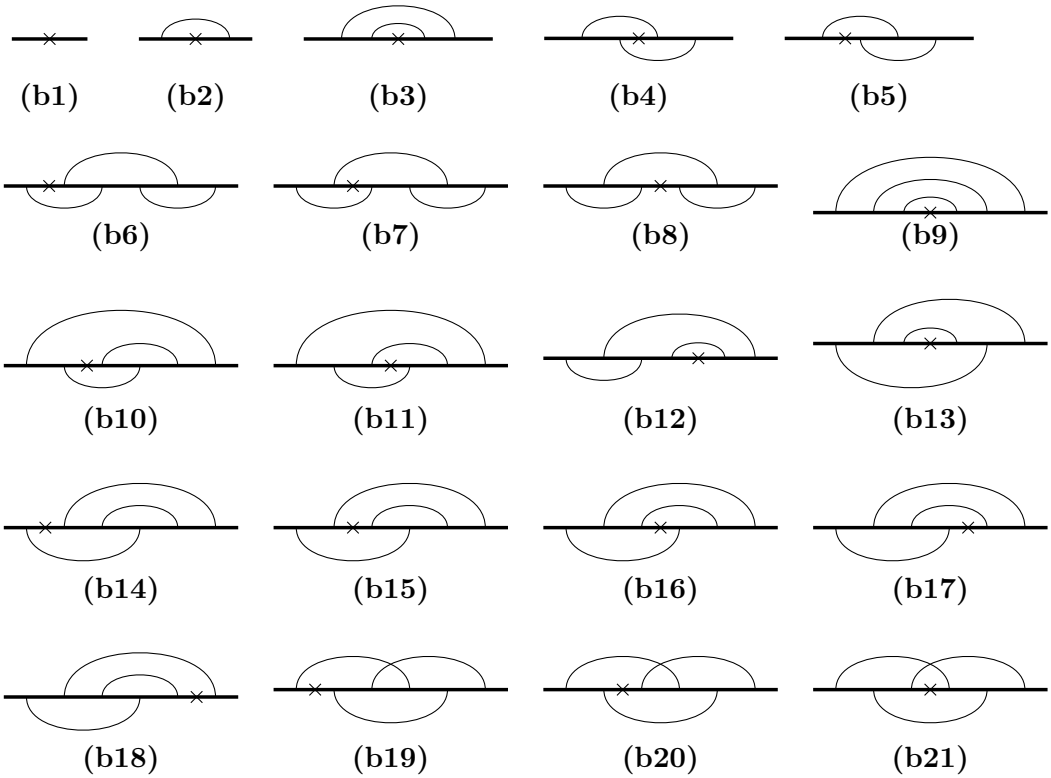

Figure B.2: Vertex diagrams up to three loops.

$x_\perp$ are directions orthogonal to the defect, then

$$\textbf{(b5)} \;=\; \quad =\quad \int_{0<\tau_1<\tau_2<\tau_3<\tau_4<\tau_5<\tau} \frac{d\tau_1\, d\tau_2\, d\tau_3\, d\tau_4\, d\tau_5}{\tau_{41}^{2-\varepsilon}\tau_{53}^{2-\varepsilon}(|x_\perp|^2+(w-\tau_2)^2)^{1-\frac{\varepsilon}{2}}}\,. \tag{B.36}$$

The value of these integrals is crucial for obtaining the beta function, and the method for calculating them is explained in Section B.2.4.

Regarding the derivation of equation (B.35), it follows the same procedure as before. First, all Wick contractions contributing to $\mathrm{Tr}\langle\phi(x)\mathcal{D}(\tau)\rangle$ are generated. For each term, the traces are computed using the commutation relations (3.42), and the integrals are factorised using relations analogous to (B.34). It can be observed that the result is proportional to the right-hand side of (B.35), multiplied by $\mathrm{Tr}\langle\mathcal{D}(\tau)\rangle$ as in (B.30). Although these steps are tedious, they have been automated using a computer.

B.2.4 Integrals

To obtain the beta function, the remaining task is to extract the divergent part of the integrals in equation (B.35). For illustration, diagram **(b5)** in (B.37) is computed in detail. The method is then generalised and automated for all other diagrams.

The first observation is that, since only the divergent part of $\mathcal{V}(x)$ is of interest, it is convenient to place the insertion of $\phi(x)$ far from the defect. More precisely, if $x=(w,x_\perp)$, then $|x_\perp|\gg\tau$ is assumed, where τ is the length of the defect operator $\mathcal{D}(\tau)$. In this limit, the dependence on $\vec{x}$, w, and τ_2 drops out

$$\overline{\textbf{(b5)}} \;\equiv\; \lim_{|x_\perp|\to\infty} |x_\perp|^{2-\varepsilon}\,\textbf{(b5)} = \int_{0<\tau_1<\tau_2<\tau_3<\tau_4<\tau_5<\tau} \frac{d\tau_1\, d\tau_2\, d\tau_3\, d\tau_4\, d\tau_5}{\tau_{41}^{2-\varepsilon}\tau_{53}^{2-\varepsilon}}\,. \tag{B.37}$$

An important observation is that the variables can be integrated in any order. Since τ_2 does not appear in the integrand, it is convenient to perform its integration first.

$$\overline{\textbf{(b5)}} = \int_{0<\tau_1<\tau_3<\tau_4<\tau_5<\tau} d\tau_1\, d\tau_3\, d\tau_4\, d\tau_5 \int_{\tau_1}^{\tau_3} \frac{d\tau_2}{\tau_{41}^{2-\varepsilon}\tau_{53}^{2-\varepsilon}} = \int_{1345} \frac{\tau_{31}}{\tau_{41}^{2-\varepsilon}\tau_{53}^{2-\varepsilon}}\,. \tag{B.38}$$

In the second equality, shorthand notation $\int_{ij\ldots k} = \int_{0<\tau_i<\tau_j<\ldots<\tau_k<\tau}$ is introduced, and $d\tau_i$ is omitted for conciseness. The strategy is to continue selecting the simplest variable for integration at each step. For example, since τ_4 appears only once, its integral is straightforward.

$$\overline{\textbf{(b5)}} = \int_{135} \int_{\tau_3}^{\tau_5} d\tau_4 \, \frac{\tau_{31}}{\tau_{41}^{2-\varepsilon}\tau_{53}^{2-\varepsilon}} = \tag{B.39}$$
$$= \frac{1}{\varepsilon - 1} \int_{135} \left[\tau_{51}^{\varepsilon}\tau_{53}^{\varepsilon-2} - \tau_{51}^{\varepsilon-1}\tau_{53}^{\varepsilon-1} - \tau_{31}^{\varepsilon}\tau_{53}^{\varepsilon-2} \right].$$

On the right-hand side, the relation $\tau_{31} = \tau_{51} - \tau_{53}$ was used to simplify the result. An important observation is that, as integration proceeds, many terms are generated, each of which requires a specific order of integration to minimise complexity. For the first two terms in (B.39), it is best to integrate τ_1 and τ_3 first, followed by τ_5. This approach ensures that all integrals are elementary

$$\int_{135} \left[\tau_{51}^{\varepsilon}\tau_{53}^{\varepsilon-2} - \tau_{51}^{\varepsilon-1}\tau_{53}^{\varepsilon-1} \right] = \int_0^{\tau} d\tau_5 \int_0^{\tau_5} d\tau_3 \int_0^{\tau_3} d\tau_1 \left[\tau_{51}^{\varepsilon}\tau_{53}^{\varepsilon-2} - \tau_{51}^{\varepsilon-1}\tau_{53}^{\varepsilon-1} \right]$$
$$= \frac{\tau^{2\varepsilon+1}}{2(\varepsilon-1)\varepsilon^2(2\varepsilon+1)}. \tag{B.40}$$

Instead, for the last term in (B.39) it is better to integrate first τ_1 and τ_5, and only then τ_3:

$$\int_{135} \tau_{31}^{\varepsilon}\tau_{53}^{\varepsilon-2} = \int_0^{\tau} d\tau_3 \int_{\tau_3}^{\tau} d\tau_5 \int_0^{\tau_3} d\tau_1 \, \tau_{31}^{\varepsilon}\tau_{53}^{\varepsilon-2} =$$
$$= \int_0^{\tau} d\tau_3 \, \frac{\tau_3^{\varepsilon+1}(\tau-\tau_3)^{\varepsilon-1}}{(\varepsilon-1)(\varepsilon+1)} = \frac{2\Gamma(\varepsilon-1)\Gamma(\varepsilon+2)}{\Gamma(2\varepsilon+3)} \, \tau^{2\varepsilon+1}. \tag{B.41}$$

The final τ_3 integral is known as the Euler integral. By selecting an appropriate order of integration, this more challenging integral was encountered only at the last step. Had a less optimal order of integration been chosen, intermediate results would have involved hypergeometric functions, with simplification occurring only at the final stage.

For completeness, the value of the diagram of interest is

$$\overline{\textbf{(b5)}} = \left(\frac{1}{2\varepsilon^2(2\varepsilon+1)} - \frac{2\Gamma(\varepsilon)\Gamma(\varepsilon+2)}{\Gamma(2\varepsilon+3)} \right) \frac{\tau^{2\varepsilon+1}}{(\varepsilon-1)^2}. \tag{B.42}$$

The approach used in computing diagram **(b5)** can now be applied to all other integrals. To summarise, the first step is to take the limit

$|x_\perp| \gg \tau$, which significantly simplifies the form of the integral. Next, the variables τ_i that appear at most once in the integrand are integrated. This process generates many terms, and for each term, different orderings may be required to minimise complexity. At times, relations of the form $\tau_{ij} = \tau_{ik} + \tau_{kj}$ are useful for simplifying intermediate expressions. Ultimately, only two integrals remain that are not elementary

$$H_1 = \int_0^\tau du\, u^a(\tau - u)^b\,, \quad H_2 = \int_0^\tau du \int_0^u dv\, u^a(u-v)^b(\tau - v)^c\,. \tag{B.43}$$

These integrals might appear in the last integration step, or as a subdiagram of a larger diagram. Fortunately, these integrals can be evaluated straightforwardly

$$H_1 = \frac{\Gamma(a+1)\Gamma(b+1)}{\Gamma(a+b+2)}\,\tau^{a+b+1}\,, \tag{B.44}$$

$$H_2 = \frac{\Gamma(a+b+2)\Gamma(b+c+2)}{(b+1)\Gamma(a+2b+c+4)} \times {}_3F_2\left(\begin{matrix} b+1, a+b+2, b+c+2 \\ b+2, a+2b+c+4 \end{matrix}; 1\right)\tau^{a+b+c+2}\,. \tag{B.45}$$

By implementing this algorithm in `mathematica`, all integrals in figure B.2 can be computed in closed form.

B.2.5 Computation of the β-function

All that is left is to combine all the ingredients. All integrals in figure B.2 are computed using the method of section B.2.4. Then these values are inserted in equation (B.29) for the vertex $\mathcal{V}(x)$. Demanding the result to be finite, gives the bare coupling in terms of the renormalized one, the result being presented in (3.44). As an important sanity check, the higher-order poles satisfy the consistency conditions (B.28). The bare coupling leads to the beta function (3.45). In the limit of large quantum number $j \to \infty$, the beta function agrees with that of [33], providing another sanity check.

B.2.6 β-function in the interacting bulk case

This section extends the previous results to calculate $\beta(\zeta)$ for the case of an interacting bulk. The calculation is carried out to order $\lambda\zeta^3$, where a single Feynman diagram contributes to the vertex renormalisation. The result of this computation was presented without derivation

in [116], while the explicit derivation is provided in [35].

At the order under consideration, most contributions to the beta function arise from diagrams without bulk interaction or from corrections to the bulk propagator. The only exception is the diagram

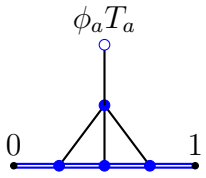

(B.46)

where the length of the defect operator is taken to be one, since the integral is homogeneous.

First, the symmetry factor of this diagram is computed. It is important to note that T_a also participates in the trace, as shown in the definition of the vertex (3.43). One of the three legs attached to the defect carries a generator T_a with the same index as the external field ϕ_a, while the other two legs carry generators T_b with contracted indices. Of the three possible channels, in two of them the contracted generators T_b are inserted next to each other, simplifying to $j(j+1)T_a$. The remaining channel is $T_b T_a T_b = (j(j+1)-1)T_a$. This leads to an overall contribution of $\left(j(j+1)-\frac{1}{3}\right)T_a$. It should also be noted that the integral is path-ordered, but due to permutation symmetry, it can be divided by 3! and instead, the unordered integral can be computed. Therefore, the contribution of this diagram to the vertex is

$$\frac{\mathcal{V}_\lambda(x)}{\zeta_0\sqrt{\kappa}j(j+1)} = -\frac{\lambda_0\,\zeta_0^2\,\kappa^2}{6}\left(j(j+1)-\frac{1}{3}\right)I(x)\,, \tag{B.47}$$

where the integral is

$$\begin{aligned} I(x) = &\int \frac{d^{4-\varepsilon}y}{\left((x_\parallel - y_\parallel)^2 + |x_\perp - y_\perp|^2\right)^{\frac{2-\varepsilon}{2}}} \\ &\times \left(\int_0^1 \frac{dt}{\left(|y_\perp|^2 + (t-y_\parallel)^2\right)^{\frac{2-\varepsilon}{2}}}\right)^3 . \end{aligned} \tag{B.48}$$

For the present purposes, it suffices to extract the leading contribution in the limit $|x_\perp| \to \infty$, which is also divergent in the limit $\varepsilon \to 0$. It is important to note that divergences of the form $\frac{1}{\varepsilon}$ arise only for small values of $|y_\perp|$ and when $y_\parallel$ is near the interval $[0,1]$. The only other region where the integrand becomes unbounded is when y approaches

the external point x; however, for any dimension d, the integral remains finite

$$\int_{|x-y|<l} \frac{d^d y}{|x-y|^{d-2}} = \frac{\Omega_{d-1} l^2}{2}\,, \tag{B.49}$$

where Ω_{d-1} is the volume of the $d-1$-dimensional sphere.

Without loss of generality, one can set $x_\perp = \left(\frac{1}{2}, L, 0, \dots\right)$, and then pass to cylindrical coordinates $\left(y_\parallel, y_\perp\right) \to \left(y_\parallel, \rho, \theta, \dots\right)$

$$I(L) = \int_0^\infty d\rho \int_{-\infty}^{+\infty} dy_\parallel \int_0^\pi d\theta \int d\Omega_{1-\varepsilon} \\ \frac{\rho^{2-\varepsilon}\,(\sin\theta)^{1-\varepsilon}}{\left(\left(\frac{1}{2}-y_\parallel\right)^2+\rho^2+L^2-2\rho L\cos\theta\right)^{\frac{2-\varepsilon}{2}}} \left(\int_0^1 \frac{dt}{\left(\rho^2+(t-y_\parallel)^2\right)^{\frac{2-\varepsilon}{2}}}\right)^3 . \tag{B.50}$$

The leading term as $L \to \infty$ is of interest. As mentioned earlier, in order to extract the divergent part, ρ and $y_\parallel$ can be considered to be bounded. Therefore, one has

$$I(L) \sim \frac{1}{L^{2-\varepsilon}} \int_0^\delta d\rho \int_{-\delta}^{1+\delta} dy_\parallel \int_0^\pi d\theta \int d\Omega_{1-\varepsilon}\; \rho^{2-\varepsilon}\,(\sin\theta)^{1-\varepsilon} \times \\ \times \left(\int_0^1 \frac{dt}{\left(\rho^2+(t-y_\parallel)^2\right)^{\frac{2-\varepsilon}{2}}}\right)^3 + \mathrm{O}(\varepsilon^0)\,, \tag{B.51}$$

where $\delta > 0$ is some arbitrarily small parameter. The integrals over dt, $d\Omega_{1-\varepsilon}$ and $d\theta$ are easily performed and one finds

$$I(L) \sim \frac{1}{L^{2-\varepsilon}} \frac{2\pi^{\frac{3-\varepsilon}{2}}}{\Gamma\left(\frac{3-\varepsilon}{2}\right)} \int_0^\delta d\rho \int_{-\delta}^{1+\delta} dy_\parallel\, \rho^{-4+2\varepsilon} \Big((1-y_\parallel) \\ {}_2F_1\left(\tfrac{1}{2}, 1-\tfrac{\varepsilon}{2}; \tfrac{3}{2}; -\tfrac{(1-y_\parallel)^2}{\rho^2}\right) + y_\parallel\, {}_2F_1\left(\tfrac{1}{2}, 1-\tfrac{\varepsilon}{2}; \tfrac{3}{2}; -\tfrac{y_\parallel^2}{\rho^2}\right)\Big)^3 . \tag{B.52}$$

Computing this integral in full generality is hard, but since $\rho < \delta$ is small, one can simply expand the integrand. The key point is that only powers $\rho^{-1+c\varepsilon}$ give divergent contributions, since

$$\int_0^\delta d\rho\, \rho^{-1+c\varepsilon} = \frac{1}{c\varepsilon} + \mathrm{O}(\varepsilon^0)\,. \tag{B.53}$$

All in all, only one term contributes to the divergence, and the remaining $d\rho$ and $dy_\parallel$ integrations are elementary

$$\begin{aligned} I(L) \sim & \frac{1}{L^{2-\varepsilon}} \frac{2\pi^{\frac{3-\varepsilon}{2}}}{\Gamma\left(\frac{3-\varepsilon}{2}\right)} \frac{\pi^{\frac{3}{2}}\Gamma\left(\frac{1-\varepsilon}{2}\right)^3}{8\,\Gamma\left(1-\frac{\varepsilon}{2}\right)^3} \\ & \times \int_0^\delta d\rho \int_{-\delta}^{1+\delta} dy_\parallel\, \rho^{-1+2\varepsilon} \left(\mathrm{sgn}(1-y_\parallel) + \mathrm{sgn}(y_\parallel)\right)^3 = \\ & = \frac{1}{L^{2-\varepsilon}} \frac{2\pi^4}{\varepsilon} + \mathrm{O}(\varepsilon^0)\,. \end{aligned} \tag{B.54}$$

Inserting this into (B.47) one finally gets

$$\frac{\mathcal{V}_\lambda(L)}{\zeta_0\sqrt{\kappa} j(j+1)} \sim -\frac{1}{L^2} \frac{\lambda_0 \zeta_0^2}{48\,\varepsilon} \left(j(j+1) - \frac{1}{3} \right), \tag{B.55}$$

which when combined with the free-theory contributions and with the two-loop correction to the bulk propagator, leads to (3.47).

B.2.7 Two-point function of defect spin operators

The two-loop contribution to the two-point function (3.82) is computed here. Similarly to what has been done at one loop in 3.3.3, one needs to compute connected diagrams. To get them, at two loops one will not only need to subtract the order zero connected contribution times pieces of two-loops bubble, but also the order one connected contributions times pieces of one-loop bubbles. This is illustrated with an example

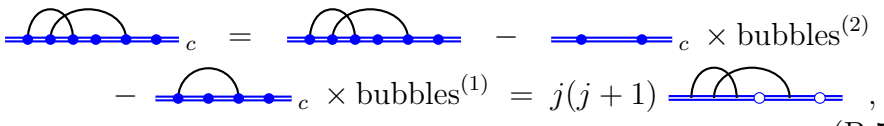

(B.56)

where the last diagram denotes just a kinematical integral stripped of the color factor. At the end of this procedure, one is left with the following

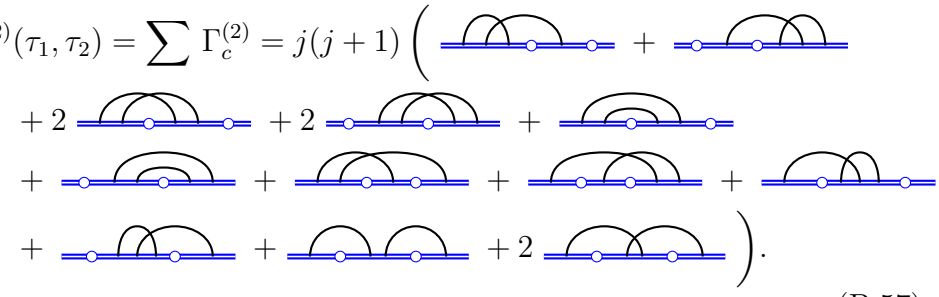

(B.57)

This sum of kinematical terms can be reorganised and further simplified since an exponentiation of the previous orders occurs. Indeed one has

$I_c^{(2)}(\tau_1,\tau_2) =$ 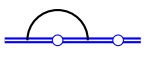 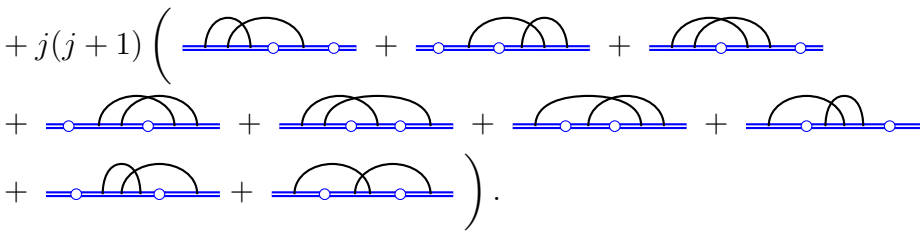

(B.58)

Moreover, one can note that specular diagrams yield the same contribution. Hence one is left with the evaluation of only five diagrams. The integrals are not difficult and the result is

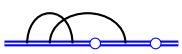 $= \zeta_0^4\,|\tau_1-\tau_2|^{2\varepsilon}\,\dfrac{\delta_{ab}}{3}\,\dfrac{2^{-1-2\varepsilon}\,\Gamma\left(\frac{1}{2}-\varepsilon\right)\Gamma(\varepsilon-1)}{\sqrt{\pi}(\varepsilon-1)\varepsilon},$

 $= \zeta_0^4|\tau_1-\tau_2|^{2\varepsilon}\dfrac{\delta_{ab}}{3}\left(\dfrac{1}{2(\varepsilon-1)\varepsilon^2(2\varepsilon-1)}-\dfrac{\Gamma(\varepsilon-1)\Gamma(-2\varepsilon)}{\Gamma(2-\varepsilon)}\right),$

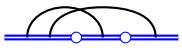 $= \zeta_0^4\,|\tau_1-\tau_2|^{2\varepsilon}\,\dfrac{\delta_{ab}}{3}\left(-\dfrac{1}{2(\varepsilon-1)^2\varepsilon^2}+\dfrac{\Gamma(\varepsilon-1)\Gamma(-2\varepsilon)}{\Gamma(2-\varepsilon)}\right),$

 $= \zeta_0^4\,|\tau_1-\tau_2|^{2\varepsilon}\,\dfrac{\delta_{ab}}{3}\left(\dfrac{-1+\frac{2^{1-2\varepsilon}\sqrt{\pi}\,\varepsilon\Gamma(\varepsilon)}{\Gamma\left(\frac{1}{2}+\varepsilon\right)}}{2(\varepsilon-1)^2\,\varepsilon^2}\right),$

 $= \zeta_0^4\,|\tau_1-\tau_2|^{2\varepsilon}\,\dfrac{\delta_{ab}}{3}\left(\dfrac{-\Gamma(1+\varepsilon)^2+\Gamma(1+2\varepsilon)}{(\varepsilon-1)^2\,\varepsilon^2\,\Gamma(1+2\varepsilon)}\right).$

(B.59)

Substituting these into (B.58) gives the two loops contribution to the bare two-point function, which can then be used to compute the renormalised one.

B.3 Diagrams and recursion for transdimensional defects

In this appendix the integrals appearing in Sections 5.1.1 and 5.1.2 are evaluated.

The first diagrams are those contributing to the bulk one-point function

of $\phi_a\phi_b$

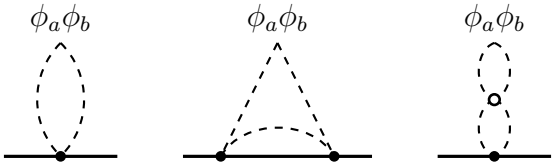

(B.60)

It is convenient to define $(h_0)_{ab} = \mu^{\varepsilon+\delta}(h_{ab} + \mathcal{Z}_{h,ab})$, where $\mathcal{Z}_{h,ab}$ is an additive counterterm, and proceed to renormalise the coupling such that the bulk one-point function $\langle\phi_a\phi_b(x_\perp, 0)\rangle$ is finite, as in [123–125] but with non-zero δ. Note that now the renormalised bulk one-point function also includes the wavefunction renormalisation factors Z_S^{-1} and Z_T^{-1} of the bulk operators S and T_{ab}.

The diagrams in (B.60) are regulated with both ε and δ and can be renormalised with

$$\mathcal{Z}_{h,ab} = \frac{2\lambda h_{ab}}{\varepsilon} + \frac{\lambda\delta_{ab}h_{cc}}{\varepsilon} + \frac{h_{ac}h_{cb}}{\varepsilon+\delta} + \mathrm{O}(h^3, h^2\lambda, h\lambda^2)\,. \tag{B.61}$$

To specify the renormalisation scheme at higher orders, note that the Feynman integrals admit the unique decomposition

$$I_L(\varepsilon,\delta) = \sum_{k=0}^{L}\prod_{i=1}^{k}\frac{D_L}{\varepsilon+\alpha_{k,i}\delta} + g(\varepsilon,\delta)\,, \tag{B.62}$$

with D_L and $\alpha_{k,i}$ real constants and $g(\varepsilon,\delta)$ regular near $\varepsilon = \delta = 0$. The reason for this form is that the integrals depend on δ only through the defect dimension p, and one also knows that by taking $\delta \to 0$ while keeping ε finite, one should retrieve the divergent integrals of the surface defect. From (B.61) one obtains the beta function

$$\beta_{ab} = -(\varepsilon+\delta)h_{ab} + (\delta_{ab}h_{cc} + 2h_{ab})\,\lambda + h_{ac}h_{cb} + \mathrm{O}(h^2\lambda, h\lambda^2)\,, \tag{B.63}$$

where, besides the rescaling $\lambda \to 16\pi^2\lambda$, $h \to 2\pi h$ has also been rescaled.

Next, Feynman diagrams of higher order in h are considered, which allow to write expressions that are exact in δ, at leading order in ε. The corrections to the middle diagram in (B.60) with one bulk vertex and a minimal number of defect vertices are

(B.64)

To simplify the expressions, it is convenient to treat explicitly only for the $O(N)$ symmetric defect, so $h_{ab} = h\delta_{ab}$, but the same calculations can be used for the symmetry breaking defect.

For the first graph in (B.64), one can take the bulk external point to be $x = (x_\perp, x_\parallel) = (\mathbf{1}, 0)$, where $\mathbf{1}$ is any unit vector normal to the defect, and find (up to symmetry factors, couplings and indices)

$I(x_\perp) =$ 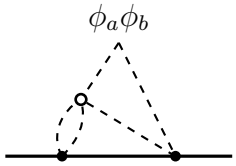

$= \int d^{4-\varepsilon}y \int d^{2+\delta}\tau_1 \int d^{2+\delta}\tau_2\, G(y-\tau_1)^2\, G(y-\tau_2)\, G(y-\tau_2)\, G(x-y)\,.$ (B.65)

The integral over τ_1 is trivial. After that, one is left with

$$I(x_\perp) = \mathcal{N}_\phi^{10} \frac{\pi^{1+\frac{\delta}{2}}\Gamma\left(1-\varepsilon-\frac{\delta}{2}\right)}{\Gamma(2-\varepsilon)} \int d^{2-\varepsilon-\delta}y_\perp \int d^{2+\delta}y_\parallel \int d^{2+\delta}\tau_2 \frac{1}{|y_\perp|^{2-2\varepsilon-\delta}\left(|y_\perp|^2+|\tau_2-y_\parallel|^2\right)^{1-\frac{\varepsilon}{2}}\left(1+\tau_2^2\right)^{1-\frac{\varepsilon}{2}}\left(|y_\perp-\mathbf{1}|^2+|y_\parallel|^2\right)^{1-\frac{\varepsilon}{2}}}\,, \tag{B.66}$$

where $\mathcal{N}_\phi^2$ is defined in (5.5). To evaluate this integral, it is convenient to go to defect momentum space. In fact, the two defect integrals are a convolution of the last three propagators, thus they can be exchanged for a single integral over the parallel momentum of the product of the defect Fourier transform of such propagators. The defect Fourier transforms of the last three propagators can be represented using Schwinger parameters

$$\int \frac{d^{2+\delta}y_\parallel}{(2\pi)^{2+\delta}} \frac{e^{ip_\parallel\cdot y_\parallel}}{\left(|y_\perp|^2+|y_\parallel|^2\right)^{1-\frac{\varepsilon}{2}}} = \\ = \frac{\pi^{1+\frac{\delta}{2}}}{\Gamma\left(1-\frac{\varepsilon}{2}\right)} \int_0^\infty du\, u^{-1-\frac{\varepsilon+\delta}{2}} \exp\left(-u|y_\perp|^2 - \frac{|p_\parallel|^2}{4u}\right). \tag{B.67}$$

After having introduced three parameters u_1, u_2 and u_3, one can easily perform first the $y_\perp$ integration and then the $p_\parallel$ integration. One is left with

$$I(x_\perp) = \frac{\Gamma\left(\frac{1}{2}-\frac{\varepsilon+\delta}{2}\right)\Gamma\left(1-\varepsilon-\frac{\delta}{2}\right)}{2^{10-\varepsilon-\delta}\pi^{3-\frac{5}{2}(\varepsilon+\delta)}\sin\left(\frac{\pi\varepsilon}{2}\right)\Gamma\left(\frac{3}{2}-\frac{\varepsilon}{2}\right)} \int_0^\infty du_1 \int_0^\infty du_2 \int_0^\infty du_3 \\ e^{-u_2-u_3} \frac{(u_1u_2u_3(u_1+u_2))^{-\varepsilon/2}}{(u_1(u_2+u_3)+u_2u_3)^{1+\delta/2}}\, {}_1\tilde{F}_1\left(\frac{\varepsilon}{2}; 1-\frac{\varepsilon+\delta}{2}; \frac{u_2^2}{u_1+u_2}\right), \tag{B.68}$$

where ${}_1\tilde{F}_1$ is the regularised confluent hypergeometric function

$$ {}_1\tilde{F}_1(a;b;z) = \frac{1}{\Gamma(a)} \sum_{k=0}^{\infty} \frac{\Gamma(a+k)}{k!\,\Gamma(b+k)} z^k \,. \tag{B.69} $$

The prefactor outside the integral has a simple pole, whereas the integral over the parameter u_1 is still divergent in the limit $\varepsilon \to 0$ and $\delta \to 0$ (the other integrals are finite). To extract the divergent terms one first expands the hypergometric and then perform the u_1 integral. Crucially, only the first term of the expansion (B.69) contributes to the divergence of I, since all other terms are of order $\mathrm{O}(\varepsilon, \delta)$. Therefore, one finds

$$ I = K(\varepsilon,\delta) \int_0^\infty du_2 \int_0^\infty du_3\, f(u_2,u_3,\varepsilon,\delta) + \text{finite}\,, \tag{B.70} $$

where now the integrals are convergent and the poles are explicit in $K(\varepsilon,\delta)$ and $f(u_2,u_3,\varepsilon,\delta)$. The integral is still hard to compute, since $f(u_2,u_3,\varepsilon,\delta)$ contains Gauss's hypergeometric functions ${}_2F_1$. To extract the divergent behaviour in the form of (B.62), one can make the substitution $\delta \to \alpha\varepsilon$ and then expand in series of ε, neglecting regular terms. The integrals become easy and can be performed. At the end, exploiting the parameter α, one can reconstruct the dependence on ε and δ, finding

$$ I = \frac{1}{256\pi^6\,\varepsilon(2\varepsilon+\delta)} + \frac{1+\gamma_E+\log\pi}{256\pi^6\varepsilon} + \frac{1}{128\pi^6(2\varepsilon+\delta)} + \text{finite}\,. \tag{B.71} $$

Alternatively, the integral may be computed as follows. The relevant divergence comes from the region where the bulk interaction point gets close to the defect (the divergence associated with the interaction point getting close to the external point is accounted for with Z_{ϕ^2}). To compute the divergence, one replaces integrate only over $|y_\perp| < \eta$ with η small. The integral becomes considerably simpler because one can replace, *e.g.* $|y_\perp - \mathbf{1}| \to 1$. One needs to first do all other integrations, expanding in $y_\perp$ and keeping terms divergent neat $y_\perp \sim 0$. Then one does the the final integral over $y_\perp$ to recover (B.71).

The second diagram in (B.64) is easier, but one first evaluates a subdiagram which (up to symmetry factors, couplings and indices) is

$$ I'(\tau) = \quad \hat{\phi}_a(0) \qquad \hat{\phi}_a(\tau) \quad = \int d^{4-\varepsilon}x \int d^{2+\delta}\tau_1\, G(x-\tau_1)^2\, G(x)\, G(x-\tau) $$

$$ = \frac{\mathcal{N}_\phi^8}{\tau^{2-3\varepsilon-\delta}} \int d^{4-\varepsilon}x \int \frac{d^{2+\delta}\tau_1}{\left(|x_\perp|^2+|x_\parallel|^2\right)^{1-\frac{\varepsilon}{2}} \left(|x_\perp|^2+|x_\parallel-\tau_1|^2\right)^{2-\varepsilon} \left(|x_\perp|^2+|x_\parallel-\mathbf{1}|^2\right)^{1-\frac{\varepsilon}{2}}} \,. \tag{B.72} $$

This integral can be computed exactly by integrating over τ_1 and then introducing a Feynman parameter for the first and the third propagators and yields

$$I'(\tau) = \frac{1}{\tau^{2-3\varepsilon-\delta}} \frac{\Gamma\left(1-\frac{3\varepsilon+\delta}{2}\right)}{2^{8+\varepsilon+\delta}\pi^{2-\frac{3\varepsilon+\delta}{2}} \sin\left(\pi\frac{\varepsilon}{2}\right)\sin\left(\pi\frac{2\varepsilon+\delta}{2}\right)\Gamma\left(\frac{3-\varepsilon}{2}\right)\Gamma\left(1-\frac{\varepsilon+\delta}{2}\right)\Gamma\left(\frac{1}{2}+\frac{2\varepsilon+\delta}{2}\right)} . \tag{B.73}$$

From this one can find the pole structure in the form (B.62)

$$I'(\tau) = \frac{1}{\tau^{2-3\varepsilon-\delta}}\left(\frac{1}{64\pi^5\,\varepsilon\left(\varepsilon+\frac{1}{2}\delta\right)} + \frac{\gamma_E+\log\pi}{64\pi^5\varepsilon} + \right. \\ \left. + \frac{2+\gamma_E+\log\pi}{128\pi^5\left(\varepsilon+\frac{1}{2}\delta\right)} + \mathrm{O}(\varepsilon^0,\delta^0)\right) . \tag{B.74}$$

Then the second diagram of (B.64) follows easily from (B.73) by integrating over τ.

No the problem of evaluating high orders in δ is considered. The effective defect-to-defect propagator (5.19) is

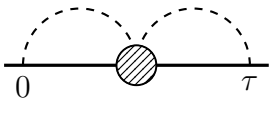

$$= \sum_{k=0}^{\infty} h_0^k \frac{a_k}{|\tau|^{2-(k+1)\varepsilon-k\delta}} ,$$

$$a_k = \frac{(-1)^k\Gamma\left(\frac{\varepsilon+\delta}{2}\right)^{k+1}\Gamma\left(1-\frac{k+1}{2}\varepsilon-\frac{k}{2}\delta\right)}{2^{k+2}\pi^{2-\frac{k+1}{2}\varepsilon-\frac{k}{2}\delta}\Gamma\left(\frac{k+1}{2}(\varepsilon+\delta)\right)} . \tag{B.75}$$

As before, diagrams are stripped of indices, which however can be easily restored.

This can then be inserted into (5.20), but it is still difficult to solve in general the remaining integrals. However, for the purposes of Section 5.1.2 it is sufficient to compute them in two specific instances. The first one is the case where the two external points coincide, which is diagram (5.18a). This gives an effective one-point function that reads

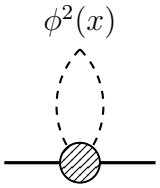

$$= \sum_{k=0}^{\infty} h_0^{k+1} \frac{b_k}{|x_\perp|^{2-(k+2)\varepsilon-(k+1)\delta}} , \tag{B.76}$$

with

$$b_k = \frac{(-1)^k\Gamma\left(\frac{\varepsilon+\delta}{2}\right)^k\Gamma\left(1-\frac{k}{2}\varepsilon-\frac{k-1}{2}\delta\right)\Gamma\left(1-\frac{k+1}{2}\varepsilon-\frac{k}{2}\delta\right)\Gamma\left(1-\frac{k+2}{2}\varepsilon-\frac{k+1}{2}\delta\right)}{2^{k+4-(k+1)\varepsilon-k\delta}\pi^{\frac{3}{2}-\frac{k+2}{2}\varepsilon-\frac{k+1}{2}\delta}\Gamma\left(1+\frac{\delta}{2}\right)\Gamma\left(\frac{3}{2}-\frac{k+1}{2}\varepsilon-\frac{k}{2}\delta\right)} . \tag{B.77}$$

The renormalised one-point function in (5.10) is obtained by substituting the renormalised coupling in (B.76) and evaluating at the non-trivial fixed point of (5.7). By expanding in ε and δ one can check that the series agrees with the result given in (5.10).

The last building block needed for renormalisation is the limit of (5.20) with one point close to the defect and one far away. Including an extra propagator between these points, this is

$$\int d^{2+\delta}x_{\parallel}\left(\quad\right) = \sum_{k=0}^{\infty} \frac{h_0^{k+1}}{|y_\perp|^{2-(k+4)\varepsilon-(k+3)\delta}}\left(c_k + d_k\left(\frac{|x_\perp|}{|y_\perp|}\right)^{\varepsilon+\delta} + \mathrm{O}\left(\frac{|x_\perp|}{|y_\perp|}\right)\right), \tag{B.78}$$

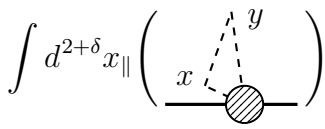

where $x = (x_\parallel, x_\perp)$, $y = (y_\parallel, y_\perp)$, and

$$c_k = \frac{(-1)^k\Gamma\left(\frac{\varepsilon+\delta}{2}\right)^{k+2}\Gamma\left(1-\frac{k+2}{2}\varepsilon-\frac{k+1}{2}\delta\right)\Gamma\left(1-\frac{k+3}{2}\varepsilon-\frac{k+2}{2}\delta\right)\Gamma\left(1-\frac{k+4}{2}\varepsilon-\frac{k+3}{2}\delta\right)}{2^{k+8-(k+3)\varepsilon-(k+2)\delta}\pi^{\frac{7}{2}-\frac{k+4}{2}\varepsilon-\frac{k+3}{2}\delta}\Gamma\left(1+\frac{\delta}{2}\right)\Gamma\left(\frac{3}{2}-\frac{k+3}{2}\varepsilon-\frac{k+2}{2}\delta\right)}, \tag{B.79}$$

and

$$d_k = \frac{(-1)^k\Gamma\left(-\frac{\varepsilon+\delta}{2}\right)\Gamma\left(\frac{\varepsilon+\delta}{2}\right)^{k+1}\Gamma\left(1-\frac{k+1}{2}\varepsilon-\frac{k}{2}\delta\right)\Gamma\left(1-\frac{k+2}{2}\varepsilon-\frac{k+1}{2}\delta\right)\Gamma\left(1-\frac{k+3}{2}\varepsilon-\frac{k+2}{2}\delta\right)}{2^{k+8-(k+2)\varepsilon-(k+1)\delta}\pi^{\frac{7}{2}-\frac{k+4}{2}\varepsilon-\frac{k+3}{2}\delta}\Gamma\left(1+\frac{\delta}{2}\right)\Gamma\left(\frac{3}{2}-\frac{k+2}{2}\varepsilon-\frac{k+1}{2}\delta\right)}. \tag{B.80}$$

These results can be used to compute the remaining integrals in (5.18) using the very same techniques as for the integrals in (B.64) evaluated above. For each bubble, the diagrams in (5.18) have one infinite sum that is difficult to perform in closed form. Still, the integrals involved in (5.18) are computed term by term. This reduces the renormalisation process to a completely algorithmic procedure that can be implemented in *Mathematica*.

The contributions to diagrams (b), (c), and (d) in (5.18) can be split into two parts: one where the bulk interaction point is integrated close to the defect, and one where it is integrated over a distance greater than some finite value. The latter is already made finite by (5.6) and by the wavefunction renormalisation of ϕ^2 in the bulk theory. For this reason, this contribution can be neglected, since at this order one only needs to keep $\mathrm{O}(\lambda^0 h^k)$ finite terms and $\mathrm{O}(\lambda h^k)$ divergent terms. In particular, this justifies the use of the expansion (B.78) in diagram (c). Finally, it is easy to reintroduce factors associated with sums over indices: they are just 1 for diagram (a) and $(N+2)/3$ for diagrams (b),

(c), and (d).

Keeping explicit all the sums of each bubble, the integrals in (5.18) (with $|x_\perp| = 1$), accounting also for symmetry factors are as follows. Diagram (5.18a) is already given in (B.76) and (B.77). For diagram (5.18b)

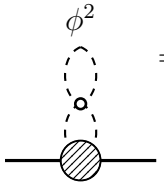

$$= 3\lambda_0 \sum_{k=0}^{\infty} \frac{(-h_0)^{k+1}\Gamma\left(1-\frac{\varepsilon}{2}\right)\Gamma\left(1-\varepsilon-\frac{\delta}{2}\right)\Gamma\left(\frac{\varepsilon+\delta}{2}\right)^k\Gamma\left(-\frac{k+1}{2}\varepsilon-\frac{k}{2}\delta\right)}{2^{k+6-(k+2)\varepsilon-k\delta}\pi^{1-\frac{k+3}{2}\varepsilon-\frac{k+1}{2}\delta}\Gamma\left(1+\frac{\delta}{2}\right)\Gamma\left(\frac{3}{2}-\frac{\varepsilon}{2}\right)} \times \frac{\Gamma\left(1-\frac{k}{2}\varepsilon-\frac{k-1}{2}\delta\right)\Gamma\left(1-\frac{k+2}{2}\varepsilon-\frac{k+1}{2}\delta\right)}{\Gamma\left(1-\frac{\varepsilon+\delta}{2}\right)\Gamma\left(\frac{3}{2}-\frac{k+1}{2}\varepsilon-\frac{k}{2}\delta\right)} \,. \tag{B.81}$$

For diagram (5.18c)

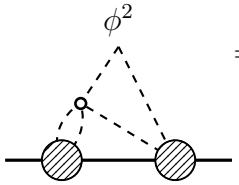

$$\begin{aligned} &= 3\lambda_0 \sum_{k_1=0}^{\infty}\sum_{k_2=0}^{\infty} \frac{(-h_0)^{k_1+k_2+2}\Gamma\left(\frac{\varepsilon+\delta}{2}\right)^{k_1+k_2}\Gamma\left(1-\frac{k_1}{2}\varepsilon-\frac{k_1-1}{2}\delta\right)}{2^{6+k_1+k_2-(k_1+k_2+2)\varepsilon-(k_1+k_2)\delta}\pi^{1-\frac{k_1+k_2+4}{2}\varepsilon-\frac{k_1+k_2+2}{2}\delta}} \\ &\quad \times \frac{\Gamma\left(1-\frac{k_2+2}{2}\varepsilon-\frac{k_2+1}{2}\delta\right)\Gamma\left(1-\frac{k_2+1}{2}\varepsilon-\frac{k_2}{2}\delta\right)}{\Gamma\left(1+\frac{\delta}{2}\right)^2\Gamma\left(1-\frac{\varepsilon+\delta}{2}\right)\Gamma\left(\frac{3}{2}-\frac{k_1+1}{2}\varepsilon-\frac{k_1}{2}\delta\right)} \\ &\times \left(\frac{2^{\varepsilon+\delta}\Gamma\left(\frac{\varepsilon+\delta}{2}\right)\Gamma\left(1-\frac{k_1+2}{2}\varepsilon-\frac{k_1+1}{2}\delta\right)\Gamma\left(-\frac{k_1+1}{2}\varepsilon-\frac{k_1}{2}\delta\right)\Gamma\left(1-\frac{k_2+3}{2}\varepsilon-\frac{k_2+2}{2}\delta\right)}{\Gamma\left(\frac{3}{2}-\frac{k_2+2}{2}\varepsilon-\frac{k_2+1}{2}\delta\right)} \right. \\ &\quad \left. + \frac{\Gamma\left(-\frac{\varepsilon+\delta}{2}\right)\Gamma\left(-\frac{k_1+2}{2}\varepsilon-\frac{k_1+1}{2}\delta\right)\Gamma\left(1-\frac{k_1+1}{2}\varepsilon-\frac{k_1}{2}\delta\right)\Gamma\left(1-\frac{k_2}{2}\varepsilon-\frac{k_2-1}{2}\delta\right)}{\Gamma\left(\frac{3}{2}-\frac{k_2+1}{2}\varepsilon-\frac{k_2}{2}\delta\right)} \right) . \end{aligned} \tag{B.82}$$

For diagram (5.18d), after a suitable shift in the summation indices one finds

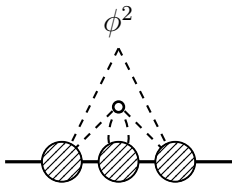

$$\begin{aligned} &= -3\lambda_0 \sum_{k_1=0}^{\infty}\sum_{k_2=0}^{\infty}\sum_{k_3=k_1+k_2}^{\infty} \frac{(-h_0)^{k_3+3}\Gamma\left(\frac{\varepsilon+\delta}{2}\right)^{k_3}}{2^{7+k_3-(k_3+3)\varepsilon-(k_3+1)\delta}\pi^{-\frac{3}{2}-\frac{k_3+5}{2}\varepsilon-\frac{k_3+3}{2}\delta}} \\ &\quad \times \frac{\Gamma\left(1-\frac{k_2}{2}\varepsilon-\frac{k_2-1}{2}\delta\right)\Gamma\left(\frac{k_2+3}{2}\varepsilon+\frac{k_2+2}{2}\delta\right)}{\Gamma\left(1-\frac{\varepsilon+\delta}{2}\right)\sin\left(\pi\left(\frac{k_2+2}{2}\varepsilon+\frac{k_2+1}{2}\delta\right)\right)\sin\left(\pi\left(\frac{k_2+1}{2}\varepsilon+\frac{k_2}{2}\delta\right)\right)} \\ &\quad \times \frac{\Gamma\left(1-\frac{k_3+3}{2}\varepsilon-\frac{k_3+1}{2}\delta\right)\Gamma\left(1-\frac{k_3+5}{2}\varepsilon-\frac{k_3+3}{2}\delta\right)\Gamma\left(1-\frac{k_3+4}{2}\varepsilon-\frac{k_3+2}{2}\delta\right)}{\Gamma\left(1+\frac{\delta}{2}\right)^2\Gamma\left(\frac{1}{2}+\frac{k_2+2}{2}\varepsilon+\frac{k_2+1}{2}\delta\right)\Gamma\left(\frac{3}{2}-\frac{k_2+1}{2}\varepsilon-\frac{k_2}{2}\delta\right)\Gamma\left(\frac{3}{2}-\frac{k_3+4}{2}\varepsilon-\frac{k_3+2}{2}\delta\right)} \,. \end{aligned} \tag{B.83}$$

Note that k_1 does not appear explicitly in the terms of the sum, so its sum can be replaced with a combinatorial factor to speed up calculations: $\sum_{k_1=0}^{\infty}\sum_{k_2=0}^{\infty}\sum_{k_3=k_1+k_2}^{\infty} \to \sum_{k_2=0}^{\infty}\sum_{k_3=k_2}^{\infty}(k_3-k_2+1)$.

From these expressions, one can set $h_0 = \mu^{\varepsilon+\delta} Z_{h,\lambda}\, h$ and extract the counterterms $Z_{h,\lambda}$, and then compute the beta function by imposing

$\mu\frac{d}{d\mu}h_0 = 0$. It is

$$\beta_h = -(\varepsilon+\delta)h + h^2 + \lambda\,(N+2)\sum_{k=0}^{\infty}\beta_{1,k}h^k + \mathrm{O}(\lambda^2,\lambda\varepsilon)\,. \tag{B.84}$$

Since at the bulk fixed point $\lambda_* \propto \varepsilon$, at this order one can just keep the order ε^0 term in the coefficients $\beta_{1,k}$.[1] The coefficients up to order $k = 11$ are

$$\begin{aligned}
&\beta_{1,1} = 1\,, \qquad \beta_{1,2} = -2\,, \qquad \beta_{1,3} = 2\,, \qquad \beta_{1,4} = -3 + \tfrac{1}{2}\zeta(3)\,,\\
&\beta_{1,5} = \tfrac{14}{3} - \tfrac{2}{3}\zeta(3) - \tfrac{3}{4}\zeta(4)\,, \qquad \beta_{1,6} = -\tfrac{15}{2} + \zeta(3) + \tfrac{9}{8}\zeta(4) + \tfrac{9}{8}\zeta(5)\,,\\
&\beta_{1,7} = \tfrac{62}{5} - \tfrac{8}{5}\zeta(3) - \tfrac{9}{5}\zeta(4) - \tfrac{9}{5}\zeta(5) + \tfrac{1}{10}\zeta(3)^2 - \tfrac{27}{16}\zeta(6)\,,\\
&\beta_{1,8} = -21 + \tfrac{8}{3}\zeta(3) + 3\zeta(4) + 3\zeta(5) - \tfrac{1}{6}\zeta(3)^2 + \tfrac{45}{16}\zeta(6) - \tfrac{3}{8}\zeta(3)\zeta(4)\\
&\qquad\qquad + \tfrac{83}{32}\zeta(7)\,,\\
&\beta_{1,9} = \tfrac{254}{7} - \tfrac{32}{7}\zeta(3) - \tfrac{36}{7}\zeta(4) - \tfrac{36}{7}\zeta(5) + \tfrac{2}{7}\zeta(3)^2 - \tfrac{135}{28}\zeta(6)\\
&\qquad\qquad + \tfrac{9}{14}\zeta(3)\zeta(4)\zeta(7) - \tfrac{249}{56} + \tfrac{9}{14}\zeta(3)\zeta(5) - \tfrac{117}{32}\zeta(8)\,,\\
&\beta_{1,10} = -\tfrac{255}{4} + 8\zeta(3) + 9\zeta(4) + 9\zeta(5) - \tfrac{1}{2}\zeta(3)^2 + \tfrac{135}{16}\zeta(6) - \tfrac{9}{8}\zeta(3)\zeta(4)\\
&\qquad + \tfrac{249}{32}\zeta(7) - \tfrac{9}{8}\zeta(3)\zeta(5) + \tfrac{819}{128}\zeta(8) + \tfrac{1}{48}\zeta(3)^3 - \tfrac{81}{64}\zeta(4)\zeta(5) + \tfrac{2515}{384}\zeta(9)\,,\\
&\beta_{1,11} = \tfrac{1022}{9} - \tfrac{128}{9}\zeta(3) - 16\zeta(4) - 16\zeta(5) + \tfrac{8}{9}\zeta(3)^2 - 15\zeta(6) + 2\zeta(3)\zeta(4)\\
&\qquad - \tfrac{83}{6}\zeta(7) + 2\zeta(3)\zeta(5) - \tfrac{91}{8}\zeta(8) - \tfrac{1}{27}\zeta(3)^3 + \tfrac{9}{4}\zeta(4)\zeta(5) + \tfrac{15}{8}\zeta(3)\zeta(6)\\
&\qquad\qquad - \tfrac{2515}{216}\zeta(9) - \tfrac{1}{8}\zeta(3)^2\zeta(4) + \tfrac{9}{8}\zeta(5)^2 + \tfrac{83}{48}\zeta(3)\zeta(7) - \tfrac{2149}{256}\zeta(10)\,.
\end{aligned} \tag{B.85}$$

The beta-function can be used to compute the fixed point coupling

$$h_* = \delta + \varepsilon - \frac{N+2}{N+8}\varepsilon\sum_{k=0}^{\infty}\beta_{1,k+1}\delta^k\,. \tag{B.86}$$

Now the diagrams contributing to $\langle\hat\phi(0)\hat\phi(\tau)\rangle$ will be considered. At first order in λ and to all orders in h, they are

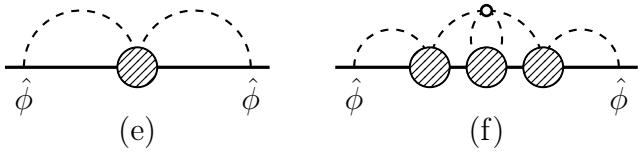

(B.87)

Diagram (e) is already computed in (B.75). For (f), one can rely on the

[1] In the dimensional regularisation with two regulators that is being used, the beta-function coefficients are ratios of homogeneous polynomials of the same degree in the two regulators (see e.g. (B.89)). At order ε^0, this reduces to the numbers below.

immediate generalisation of I' as defined in (B.72) and find (at $\tau = 1$)

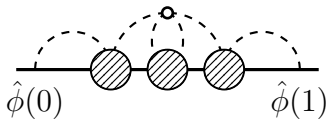

$$= -3\lambda_0 \sum_{k_1=0}^{\infty}\sum_{k_2=0}^{\infty}\sum_{k_3=k_1+k_2}^{\infty} \frac{(-h_0)^{k_3+1}\Gamma\left(\frac{\varepsilon+\delta}{2}\right)^{k_3}}{2^{4+k_3+\varepsilon+\delta}\pi^{-1-\frac{k_3+3}{2}\varepsilon-\frac{k_3+1}{2}\delta}} \times \frac{\Gamma\left(\frac{k_2+3}{2}\varepsilon+\frac{k_2+2}{2}\delta\right)\Gamma\left(1-\frac{k_2}{2}\varepsilon-\frac{k_2-1}{2}\delta\right)}{\Gamma\left(1+\frac{\delta}{2}\right)\Gamma\left(1-\frac{\varepsilon+\delta}{2}\right)\sin\left(\pi\left(\frac{k_2+2}{2}\varepsilon+\frac{k_2+1}{2}\delta\right)\right)\sin\left(\pi\left(\frac{k_2+1}{2}\varepsilon+\frac{k_2}{2}\delta\right)\right)} \times \frac{\Gamma\left(1-\frac{k_3+3}{2}\varepsilon-\frac{k_3+1}{2}\delta\right)}{\Gamma\left(\frac{1}{2}+\frac{k_2+2}{2}\varepsilon+\frac{k_2+1}{2}\delta\right)\Gamma\left(\frac{3}{2}-\frac{k_2+1}{2}\varepsilon-\frac{k_2}{2}\delta\right)\Gamma\left(\frac{k_3+3}{2}\varepsilon+\frac{k_3+2}{2}\delta\right)} \,. \tag{B.88}$$

As in (B.83), k_1 does not appear in the sum, so one can reduce the expression to a double sum.

From these diagrams one can extract the counterterms contributing to the wavefunction renormalisation of $\hat{\phi}_0^a = Z_{\hat{\phi}}\,\hat{\phi}^a$; they are

$$\begin{aligned} Z_{\hat{\phi}} = 1 &- \frac{h}{\varepsilon+\delta} + \lambda\,\frac{N+2}{2\varepsilon+\delta}\Bigg(h - \frac{3\varepsilon+\delta}{3\varepsilon+2\delta}h^2 \\ &+ \frac{8(\varepsilon+\delta)(5\varepsilon+2\delta) - \varepsilon\delta\zeta(2) - 4(\varepsilon+\delta)(2\varepsilon+\delta)\zeta(3)}{4(3\varepsilon+2\delta)(4\varepsilon+3\delta)}h^3 \\ &- \frac{1}{4(3\varepsilon+2\delta)(4\varepsilon+3\delta)(5\varepsilon+4\delta)}\Big(8(\varepsilon+\delta)^2(25\varepsilon+11\delta) + \varepsilon\delta(\varepsilon-\delta)\zeta(2) \\ &- \left(32\varepsilon^3 + 81\varepsilon^2\delta + 66\varepsilon\delta^2 + 16\delta^3\right)\zeta(3) - 18(\varepsilon+\delta)^2(2\varepsilon+\delta)\zeta(4)\Big)h^4 \\ &+ \mathrm{O}(h^5)\Bigg) + \mathrm{O}(\lambda^2) \;+\; \text{higher order poles}\,. \end{aligned} \tag{B.89}$$

Higher order poles are omitted since they can be easily reconstructed using the 't Hooft relations. It is not necessary to compute more terms, since it is already easy to guess the series for the anomalous dimension of $\hat{\phi}$ at the fixed point,

$$\gamma_{\hat{\phi}} = \left[\frac{d\log Z_{\hat{\phi}}}{dh}\beta_h + \frac{d\log Z_{\hat{\phi}}}{d\lambda}\beta_\lambda\right]_{\lambda_*,h_*} = \delta + \varepsilon - \frac{N+2}{N+8}\varepsilon\sum_{k=0}^{\infty}(-\delta)^k + \mathrm{O}(\varepsilon^2)\,. \tag{B.90}$$

Using this anomalous dimension one finds (5.26).

Finally, the dimension $\hat{\Delta}_{\partial_\perp\hat{\phi}}$ of the defect operator $\partial_\perp\hat{\phi}$ can be computed from the defect two-point function $\langle\partial_\perp\hat{\phi}(0)\partial_\perp\hat{\phi}(\tau)\rangle$. Up to order one in λ and at all orders in h is given by the diagrams [2] (with $SO(d-p)$

[2] Note that a single normal derivative of the free defect-to-defect propagator $\partial_\perp G(x-y)\big|_{x_\perp=y_\perp=0}$ vanishes, so extra bubbles as in (B.87) do not contribute.

indices of $\partial_\perp\hat\phi$ indices contracted)

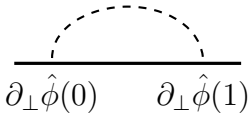

$$= \frac{(2-\varepsilon-\delta)\Gamma\left(2-\frac{\varepsilon}{2}\right)}{2\pi^{2-\frac{\varepsilon}{2}}}\,, \tag{B.91}$$

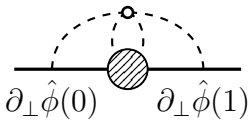

$$= -3\lambda_0 \sum_{k=0}^{\infty} \frac{(-h_0)^{k+1}((k+1)\varepsilon+k\delta)\Gamma\left(\frac{\varepsilon+\delta}{2}\right)^k}{2^{3+k+\varepsilon+\delta}\pi^{-1-\frac{k+3}{2}\varepsilon-\frac{k+1}{2}\delta}\Gamma\left(1+\frac{\delta}{2}\right)\Gamma\left(1-\frac{\varepsilon+\delta}{2}\right)} \tag{B.92}$$

$$\times \frac{\Gamma\left(1-\frac{k}{2}\varepsilon-\frac{k-1}{2}\delta\right)\Gamma\left(2-\frac{k+3}{2}\varepsilon-\frac{k+1}{2}\delta\right)}{\sin\left(\pi\left(\frac{k+2}{2}\varepsilon+\frac{k+1}{2}\delta\right)\right)\sin\left(\pi\left(\frac{k+1}{2}\varepsilon+\frac{k}{2}\delta\right)\right)\Gamma\left(\frac{1}{2}+\frac{k+2}{2}\varepsilon+\frac{k+1}{2}\delta\right)\Gamma\left(\frac{3}{2}-\frac{k+1}{2}\varepsilon-\frac{k}{2}\delta\right)}\,.$$

The simple poles of the wavefunction renormalisation of $\partial_\perp\hat\phi_0^a = Z_{\partial_\perp\hat\phi}\,\partial_\perp\hat\phi^a$ are

$$\begin{aligned} Z_{\partial_\perp\hat\phi} = 1 + \lambda\frac{N+2}{2\varepsilon+\delta}\Big(&\frac{h}{2} - \frac{\varepsilon+\delta}{4(3\varepsilon+2\delta)}h^2 + \frac{6(\varepsilon+\delta)^2+\varepsilon\delta\zeta(2)}{8(3\varepsilon+2\delta)(4\varepsilon+3\delta)}h^3 \\ &- \frac{30(\varepsilon+\delta)^3+3\varepsilon\delta(\varepsilon+\delta)\zeta(2)+2\varepsilon\delta(2\varepsilon+\delta)\zeta(3)}{16(3\varepsilon+2\delta)(4\varepsilon+3\delta)(5\varepsilon+4\delta)}h^4 \\ &+ \frac{528(\varepsilon+\delta)^4+72\varepsilon\delta(\varepsilon+\delta)^2\zeta(2)+16\varepsilon\delta(\varepsilon+\delta)(\varepsilon+2\delta)\zeta(3)}{64(3\varepsilon+2\delta)(4\varepsilon+3\delta)(5\varepsilon+4\delta)(6\varepsilon+5\delta)}h^5 \\ &+ \frac{3\varepsilon\delta\left(4\varepsilon^2+17\delta\varepsilon+12\delta^2\right)\zeta(4)}{64(3\varepsilon+2\delta)(4\varepsilon+3\delta)(5\varepsilon+4\delta)(6\varepsilon+5\delta)}h^5 + \mathrm{O}(h^6)\Big) + \mathrm{O}(\lambda^2) \\ &+ \text{ higher order poles}\,. \end{aligned} \tag{B.93}$$

From these terms it is already possible to guess the series for the anomalous dimension of $\partial_\perp\hat\phi$ at the fixed point

$$\begin{aligned} \gamma_{\partial_\perp\hat\phi} = \left[\frac{d\log Z_{\partial_\perp\hat\phi}}{dh}\beta_h + \frac{d\log Z_{\partial_\perp\hat\phi}}{d\lambda}\beta_\lambda\right]_{\lambda_*,h_*} &= \\ = -\frac{N+2}{N+8}\varepsilon\sum_{k=1}^{\infty}\frac{\delta^k-(-2\delta)^k}{3\cdot 2^k} &+ \mathrm{O}(\varepsilon^2)\,. \end{aligned} \tag{B.94}$$

Using this anomalous dimension one finds (5.27).

B.4 Diagrams for defects in the long-range O(N) model

In this appendix, several diagrams in useful integrals needed for the computations of Chapter 6 are listed.

B.4.1 Diagrams for the defect coupling renormalisation

In this section, the diagrams that are relevant to the renormalisation of defect couplings h in Section 6.2.2 are reported. The first set of diagrams relates to the case of the localised magnetic field. Recall the notation $w_A^{(d)} = (4\pi)^{d/2} 2^{-A} \Gamma\left(\frac{d-A}{2}\right) / \Gamma\left(\frac{A}{2}\right)$

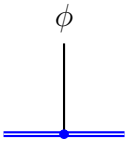

$$= -\mathcal{N}_\phi^2 h_0 \frac{\sqrt{\pi}\Gamma\left(\Delta_\phi - \frac{1}{2}\right)}{\Gamma(\Delta_\phi)} \frac{1}{|x_\perp|^{2\Delta_\phi - 1}} , \tag{B.95}$$

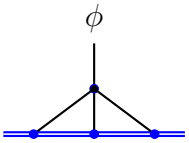

$$= \frac{\left(\mathcal{N}_\phi^2\right)^4 \lambda_0 h_0^3}{6} \left[\frac{\sqrt{\pi}\Gamma\left(\Delta_\phi - \frac{1}{2}\right)}{\Gamma(\Delta_\phi)}\right]^4 \frac{w_{2\Delta_\phi - 1}^{(d-1)} w_{6\Delta_\phi - 3}^{(d-1)}}{w_{8\Delta_\phi - 3 - d}^{(d-1)}} \frac{1}{|x_\perp|^{8\Delta_\phi - d - 3}} , \tag{B.96}$$

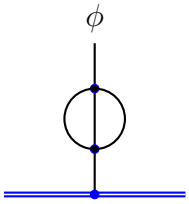

$$= -\frac{(N+2)\left(\mathcal{N}_\phi^2\right)^5 \lambda_0^2 h_0}{18} \frac{\pi^{\frac{3}{2}} \Gamma\left(\Delta_\phi - \frac{1}{2}\right)^2 \Gamma\left(3\Delta_\phi - \frac{1}{2}\right)}{\Gamma(\Delta_\phi)^2 \Gamma(3\Delta_\phi)} \frac{w_{6\Delta_\phi - 1}^{(d-1)} \left[w_{2\Delta_\phi - 1}^{(d-1)}\right]^2}{w_{10\Delta_\phi - 2d - 1}^{(d-1)}} \frac{1}{|x_\perp|^{10\Delta_\phi - 2d - 1}} , \tag{B.97}$$

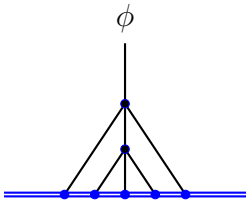

$$= -\frac{\left(\mathcal{N}_\phi^2\right)^7 \lambda_0^2 h_0^5}{12} \left[\frac{\sqrt{\pi}\Gamma\left(\Delta_\phi - \frac{1}{2}\right)}{\Gamma(\Delta_\phi)}\right]^7 \frac{\left[w_{2\Delta_\phi - 1}^{(d-1)}\right]^2 w_{6\Delta_\phi - 3}^{(d-1)} w_{12\Delta_\phi - d - 5}^{(d-1)}}{w_{8\Delta_\phi - d - 3}^{(d-1)} w_{14\Delta_\phi - 2d - 5}^{(d-1)}} \frac{1}{|x_\perp|^{14\Delta_\phi - 2d - 5}} , \tag{B.98}$$

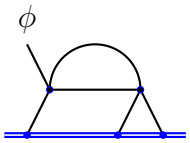

$$= -\frac{(N+8)\left(\mathcal{N}_\phi^2\right)^6 \lambda_0^2 h_0^3}{36} \frac{\Gamma\left(\Delta_\phi - \frac{1}{2}\right)^4 \pi^{\frac{5}{2}} \Gamma\left(2\Delta_\phi - \frac{1}{2}\right)}{\Gamma(\Delta_\phi)^4 \Gamma(2\Delta_\phi)} \times$$
$$\times \frac{w_{4\Delta_\phi - 1}^{(d-1)} w_{4\Delta_\phi - 2}^{(d-1)} w_{2\Delta_\phi - 1}^{(d-1)} w_{10\Delta_\phi - d - 3}^{(d-1)}}{w_{8\Delta_\phi - d - 2}^{(d-1)} w_{12\Delta_\phi - 2d - 3}^{(d-1)}} \frac{1}{|x_\perp|^{12\Delta_\phi - 2d - 3}} . \tag{B.99}$$

The second set of diagrams appears in the renormalisation of the surface defect coupling

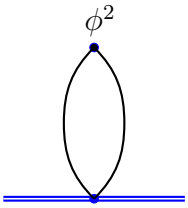

$$= -2h_0 \left(\mathcal{N}_\phi^2\right)^2 N \frac{\pi}{2\Delta_\phi - 1} \frac{1}{|x_\perp|^{4\Delta_\phi - 2}} , \tag{B.100}$$

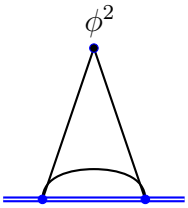

$$= 4 \left(\mathcal{N}_\phi^2\right)^3 N h_0^2 \frac{\pi^3 \Gamma\left(2\Delta_\phi - 1\right)^2 \Gamma\left(3\Delta_\phi - 2\right)}{\Gamma(\Delta_\phi)^3 \Gamma\left(4\Delta_\phi - 2\right) \sin(\pi\Delta_\phi)} \frac{1}{|x_\perp|^{6\Delta_\phi - 4}} , \tag{B.101}$$

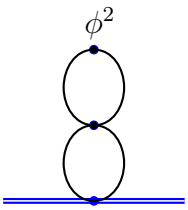

$$= \frac{h_0 \lambda_0 \left(\mathcal{N}_\phi^2\right)^4 N(N+2)}{3} \frac{\left[w^{(d)}_{4\Delta_\phi}\right]^2}{w^{(d)}_{8\Delta_\phi - d}} \frac{\pi}{4\Delta_\phi - 1 - \frac{d}{2}} \frac{1}{|x_\perp|^{8\Delta_\phi - d - 2}} . \tag{B.102}$$

B.4.2 Diagrams for the g-function close to four dimensions

First, the diagrams useful to the computation of the g-function close to four dimensions for the localised magnetic field are listed. The second diagram is challenging to compute exactly, and the result up to $\mathrm{O}(\hat{\varepsilon})$ given below makes use of the integral (B.115).

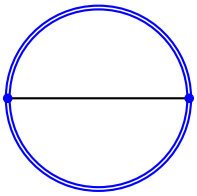

$$= \mathcal{N}_\phi^2 2^{1-2\Delta_\phi} h_0^2 R^{2-2\Delta_\phi} \pi \frac{\Gamma\left(\frac{1}{2} - \Delta_\phi\right) \sqrt{\pi}}{\Gamma\left(1 - \Delta_\phi\right)} , \tag{B.103}$$

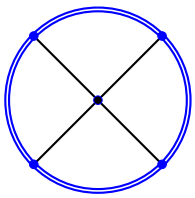

$$= -\frac{\lambda_0 h_0^4}{384\pi^2} + \mathrm{O}(\hat{\varepsilon}) . \tag{B.104}$$

Second, the free energy for the surface defect is computed using the diagrams below

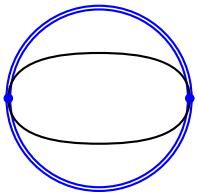

$$= h_0^2 \left(\mathcal{N}_\phi^2\right)^2 N \oint \frac{d^2x d^2y}{|x-y|^{4\Delta_\phi}} = -h_0^2 \left(\mathcal{N}_\phi^2\right)^2 N \frac{(2R)^{4(1-\Delta_\phi)}\pi^2}{2\Delta_\phi - 1}\,, \tag{B.105}$$

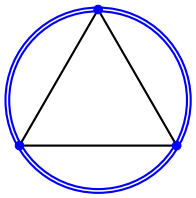

$$= -h_0^3 \left(\mathcal{N}_\phi^2\right)^3 \frac{4N}{3} R^{6(1-\Delta_\phi)} \frac{8\pi^{\frac{9}{2}}\Gamma\left(2-3\Delta_\phi\right)}{\Gamma\left(\frac{3}{2}-\Delta_\phi\right)^3}\,, \tag{B.106}$$

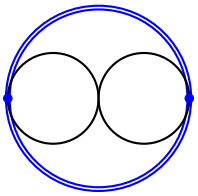

$$= -\lambda_0 h_0^2 \left(\mathcal{N}_\phi^2\right)^4 \frac{N(N+2)}{6} \frac{\left[w^{(d)}_{4\Delta_\phi}\right]^2}{w^{(d)}_{8\Delta_\phi - d}} \frac{(2R)^{d+4-8\Delta_\phi}\pi^2}{\frac{d}{2}+1-4\Delta_\phi}\,. \tag{B.107}$$

B.4.3 Useful integrals

The diagrams above make use of the following integrals.

Integral over a bulk vertex

$$I(x) := \int \frac{d^d y}{|x-y|^A |y|^B} = \frac{w^{(d)}_A w^{(d)}_B}{w^{(d)}_{A+B-d}} \frac{1}{|x|^{A+B-d}}\,. \tag{B.108}$$

Integral over a defect vertex

$$\int \frac{d^p \tau}{|x-x(\tau)|^\alpha} = \frac{\pi^{\frac{p}{2}}\Gamma\left(\frac{\alpha-p}{2}\right)}{\Gamma\left(\frac{\alpha}{2}\right)} \frac{1}{|x_\perp|^{\alpha-p}}\,. \tag{B.109}$$

Integral over a bulk vertex with defect propagator

$$\int \frac{d^d y}{|x-y|^\alpha \left|y_\parallel\right|^\beta} = \frac{\pi^{\frac{d-p}{2}}\Gamma\left(\frac{\alpha-d+p}{2}\right)}{\Gamma\left(\frac{\alpha}{2}\right)} \frac{w^{(p)}_{\alpha-d+p} w^{(p)}_\beta}{w^{(p)}_{\alpha+\beta-d}} \frac{1}{\left|x_\parallel\right|^{\alpha+\beta-d}}\,. \tag{B.110}$$

Three propagators

The following integral is used in the renormalisation of the surface defect coupling, and is particularly challenging to compute by hand (borrowing notation from [125], see [187] for a derivation). One way to proceed is to use Schwinger parametrisation and the inversion formula for the gamma function

$$\begin{aligned} F &= \int \frac{d^d k d^d l}{\left(k^2+m^2\right)^{\lambda_1}\left[(k+l)^2\right]^{\lambda_2}\left(l^2+m^2\right)^{\lambda_3}} \\ &= \frac{\pi^d \Gamma\left(\lambda_1+\lambda_2-\frac{d}{2}\right)\Gamma\left(\lambda_2+\lambda_3-\frac{d}{2}\right)\Gamma\left(\frac{d}{2}-\lambda_2\right)\Gamma(\lambda_1+\lambda_2+\lambda_3-d)}{\Gamma(\lambda_1)\Gamma(\lambda_3)\Gamma(\lambda_1+2\lambda_2+\lambda_3-d)\Gamma\left(\frac{d}{2}\right)} \frac{1}{\left(m^2\right)^{\lambda_1+\lambda_2+\lambda_3-d}} . \end{aligned} \tag{B.111}$$

Circular integral over one angle

$$\begin{aligned} \oint \frac{d\tau}{|x-x(\tau)|^{2\Delta}} &= \int_{-\pi}^{\pi} \frac{R d\theta}{\left(\left|x_{\parallel}\right|^2+\left|x_{\perp}\right|^2+R^2-2R\left|x_{\parallel}\right|\cos\theta\right)^{\Delta}} \\ &= \frac{2\pi R}{\left[\left(\left|x_{\parallel}\right|+R\right)^2+\left|x_{\perp}\right|^2\right]^{\Delta}} {}_2F_1\left(\frac{1}{2},\Delta;1,\frac{4R\left|x_{\parallel}\right|}{\left(\left|x_{\parallel}\right|+R\right)^2+\left|x_{\perp}\right|^2}\right) , \end{aligned} \tag{B.112}$$

where the integral representation of the hypergeometric function ${}_2F_1$ has been used.

Circular integral over two angles

$$\oint \frac{d\tau_1 d\tau_2}{|x(\tau_1)-x(\tau_2)|^{2\Delta}} = 4^{1-\Delta} R^{2-2\Delta} \pi \frac{\Gamma\left(\frac{1}{2}-\Delta\right)\sqrt{\pi}}{\Gamma(1-\Delta)} . \tag{B.113}$$

Second diagram in the g-function for the localised magnetic field

The computation of diagram (B.104) is intricate. Calculating it amounts to evaluating the following quantity

$$-\frac{\lambda_0 h_0^4}{4!}\left(\mathcal{N}_\phi^2\right)^4 \int d^d x \left(\oint \frac{d\tau}{|x-x(\tau)|^{2\Delta_\phi}}\right)^4 = -\frac{\lambda_0 h_0^4}{4!} I . \tag{B.114}$$

The integral over the circular defect can be computed using equation (B.112). It simplifies to

$$\begin{aligned} I = 2\pi (2\pi R)^4 \left(\mathcal{N}_\phi^2\right)^4 S_{2-\varepsilon} \int_0^\infty dr \int_0^\infty dz \frac{r z^{3-\varepsilon}}{\left((r+R)^2+z^2\right)^{4-(1+\kappa)\varepsilon}} \times \\ \times \left[{}_2F_1\left(\tfrac{1}{2},1-\tfrac{(1+\kappa)\varepsilon}{4};1,\tfrac{4rR}{(r+R)^2+z^2}\right)\right]^4 . \end{aligned} \tag{B.115}$$

It is enough to give I to order $\mathrm{O}\left(\hat{\varepsilon}^0\right)$, since $\lambda_* \sim \hat{\varepsilon}$ and h_* is finite. The remaining integral can be conducted using appendix B in [32] and it evaluates to $I = 1/(16\pi^2)$ in the limite $\hat{\varepsilon} \to 0$.

Spherical integration over two angles

$$\oint \frac{d^2\tau_1 d^2\tau_2}{|x(\tau_1) - x(\tau_2)|^{2\Delta}} = \frac{(2R)^{4-2\Delta}\pi^2}{1-\Delta}\,. \tag{B.116}$$

Bibliography

[1] A. A. Belavin, A. M. Polyakov and A. B. Zamolodchikov, *"Infinite Conformal Symmetry in Two-Dimensional Quantum Field Theory"*, Nucl. Phys. B 241, 333 (1984).

[2] F. Dolan and H. Osborn, *"Conformal four point functions and the operator product expansion"*, Nucl. Phys. B 599, 459 (2001), hep-th/0011040.

[3] R. Rattazzi, V. S. Rychkov, E. Tonni and A. Vichi, *"Bounding scalar operator dimensions in 4D CFT"*, JHEP 0812, 031 (2008), arxiv:0807.0004.

[4] Z. Komargodski and A. Zhiboedov, *"Convexity and Liberation at Large Spin"*, JHEP 1311, 140 (2013), arxiv:1212.4103.

[5] A. Fitzpatrick, J. Kaplan, D. Poland and D. Simmons-Duffin, *"The Analytic Bootstrap and AdS Superhorizon Locality"*, JHEP 1312, 004 (2013), arxiv:1212.3616.

[6] S. Caron-Huot, *"Analyticity in Spin in Conformal Theories"*, JHEP 1709, 078 (2017), arxiv:1703.00278.

[7] S. El-Showk, M. F. Paulos, D. Poland, S. Rychkov, D. Simmons-Duffin and A. Vichi, *"Solving the 3D Ising Model with the Conformal Bootstrap"*, Phys. Rev. D 86, 025022 (2012), arxiv:1203.6064.

[8] S. El-Showk, M. F. Paulos, D. Poland, S. Rychkov, D. Simmons-Duffin and A. Vichi, *"Solving the 3d Ising Model with the Conformal Bootstrap II. c-Minimization and Precise Critical Exponents"*, J. Stat. Phys. 157, 869 (2014), arxiv:1403.4545.

[9] F. Kos, D. Poland, D. Simmons-Duffin and A. Vichi, *"Precision Islands in the Ising and $O(N)$ Models"*, JHEP 1608, 036 (2016), arxiv:1603.04436.

[10] K. G. Wilson, *"Confinement of Quarks"*, Phys. Rev. D 10, 2445 (1974).

[11] I. Affleck, *"Conformal field theory approach to the Kondo effect"*, Acta Phys. Polon. B 26, 1869 (1995), cond-mat/9512099.

[12] K. Jensen and A. O'Bannon, *"Holography, Entanglement Entropy, and Conformal Field Theories with Boundaries or Defects"*, Phys. Rev. D 88, 106006 (2013), arxiv:1309.4523.

[13] D. Gaiotto, A. Kapustin, N. Seiberg and B. Willett, *"Generalized Global Symmetries"*, JHEP 1502, 172 (2015), arxiv:1412.5148.

[14] P. Liendo, L. Rastelli and B. C. van Rees, *"The Bootstrap Program for Boundary CFT_d"*, JHEP 1307, 113 (2013), arxiv:1210.4258.

[15] F. Gliozzi, P. Liendo, M. Meineri and A. Rago, *"Boundary and Interface CFTs from the Conformal Bootstrap"*, JHEP 1505, 036 (2015), arxiv:1502.07217, [Erratum: JHEP 12, 093 (2021)].

[16] K. Jensen and A. O'Bannon, *"Constraint on Defect and Boundary Renormalization Group Flows"*, Phys. Rev. Lett. 116, 091601 (2016), arxiv:1509.02160.

[17] M. Billo, V. Goncalves, E. Lauria and M. Meineri, *"Defects in conformal field theory"*, JHEP 1604, 091 (2016), arxiv:1601.02883.

[18] M. Lemos, P. Liendo, M. Meineri and S. Sarkar, *"Universality at large transverse spin in defect CFT"*, JHEP 1809, 091 (2018), arxiv:1712.08185.

[19] A. Bissi, T. Hansen and A. Söderberg, *"Analytic Bootstrap for Boundary CFT"*, JHEP 1901, 010 (2019), arxiv:1808.08155.

[20] D. Mazáč, L. Rastelli and X. Zhou, *"An analytic approach to $BCFT_d$"*, JHEP 1912, 004 (2019), arxiv:1812.09314.

[21] E. Lauria, M. Meineri and E. Trevisani, *"Spinning operators and defects in conformal field theory"*, JHEP 1908, 066 (2019), arxiv:1807.02522.

[22] P. Liendo, Y. Linke and V. Schomerus, *"A Lorentzian inversion formula for defect CFT"*, JHEP 2008, 163 (2020), arxiv:1903.05222.

[23] C. P. Herzog and A. Shrestha, *"Two point functions in defect CFTs"*, JHEP 2104, 226 (2021), arxiv:2010.04995.

[24] G. Cuomo, Z. Komargodski and A. Raviv-Moshe, *"Renormalization Group Flows on Line Defects"*, Phys. Rev. Lett. 128, 021603 (2022), arxiv:2108.01117.

[25] C. P. Herzog and V. Schaub, *"A sum rule for boundary contributions to the trace anomaly"*, JHEP 2201, 121 (2022), arxiv:2107.11604.

[26] L. Bianchi and D. Bonomi, *"Conformal dispersion relations for defects and boundaries"*, arxiv:2205.09775.

[27] J. Barrat, A. Gimenez-Grau and P. Liendo, *"A dispersion relation for defect CFT"*, arxiv:2205.09765.

[28] A. Allais, *"Magnetic defect line in a critical Ising bath"*, https://arxiv.org/abs/1412.3449.

[29] M. Vojta, C. Buragohain and S. Sachdev, *"Quantum impurity dynamics in two-dimensional antiferromagnets and superconductors"*, Physical Review B 61, 15152 (2000).

[30] S. Sachdev, C. Buragohain and M. Vojta, *"Quantum Impurity in a Nearly Critical Two-Dimensional Antiferromagnet"*, Science 286, 2479 (1999), Publisher: American Association for the Advancement of Science, https://www.science.org/doi/10.1126/science.286.5449.2479.

[31] F. Parisen Toldin, F. F. Assaad and S. Wessel, *"Critical behavior in the presence of an order-parameter pinning field"*, Physical Review B 95, 014401 (2017).

[32] G. Cuomo, Z. Komargodski and M. Mezei, *"Localized magnetic field in the O(N) model"*, JHEP 2202, 134 (2022), arxiv:2112.10634.

[33] G. Cuomo, Z. Komargodski, M. Mezei and A. Raviv-Moshe, *"Spin impurities, Wilson lines and semiclassics"*, JHEP 2206, 112 (2022), arxiv:2202.00040.

[34] L. Bianchi, D. Bonomi and E. de Sabbata, *"Analytic bootstrap for the localized magnetic field"*, JHEP 2304, 069 (2023), arxiv:2212.02524.

[35] L. Bianchi, D. Bonomi, E. de Sabbata and A. Gimenez-Grau, *"Analytic bootstrap for magnetic impurities"*, JHEP 2405, 080 (2024), arxiv:2312.05221.

[36] E. de Sabbata, N. Drukker and A. Stergiou, *"Transdimensional Defects"*, arxiv:2411.17809.

[37] L. Bianchi, L. S. Cardinale and E. de Sabbata, *"Defects in the long-range O(N) model"*, arxiv:2412.08697.

[38] J. D. Qualls, *"Lectures on Conformal Field Theory"*, arxiv:1511.04074.

[39] S. Rychkov, *"EPFL Lectures on Conformal Field Theory in D>= 3 Dimensions"*.

[40] J. Penedones, *"TASI lectures on AdS/CFT."*, arxiv:1608.04948, in: *"Theoretical Advanced Study Institute in Elementary Particle Physics: New Frontiers in Fields and Strings"*, 75–136p.

[41] D. Simmons-Duffin, *"The Conformal Bootstrap"*, arxiv:1602.07982, in: *"Theoretical Advanced Study Institute in Elementary Particle Physics: New Frontiers in Fields and Strings"*, 1–74p.

[42] H. Osborn, *"Lectures on conformal field theories"*.

[43] J. M. Meineri and J. Penedones, *"Conformal Field Theory and Gravity, EPFL doctoral course"*.

[44] S. M. Chester, *"Weizmann lectures on the numerical conformal bootstrap"*, Phys. Rept. 1045, 1 (2023), arxiv:1907.05147.

[45] R. Blumenhagen and E. Plauschinn, *"Introduction to conformal field theory: with applications to String theory"*.

[46] S. Ribault, *"Conformal field theory on the plane"*, arxiv:1406.4290.

[47] M. Schottenloher, *"A mathematical introduction to conformal field theory"*.

[48] J. Polchinski, *"Scale and Conformal Invariance in Quantum Field Theory"*, Nucl. Phys. B 303, 226 (1988).

[49] D. Dorigoni and V. S. Rychkov, *"Scale Invariance + Unitarity => Conformal Invariance?"*, arxiv:0910.1087.

[50] A. Dymarsky, Z. Komargodski, A. Schwimmer and S. Theisen, *"On Scale and Conformal Invariance in Four Dimensions"*, JHEP 1510, 171 (2015), arxiv:1309.2921.

[51] A. Gimenez-Grau, Y. Nakayama and S. Rychkov, *"Scale without conformal invariance in dipolar ferromagnets"*, Phys. Rev. B 110, 024421 (2024), arxiv:2309.02514.

[52] M. S. Costa, J. Penedones, D. Poland and S. Rychkov, *"Spinning Conformal Correlators"*, JHEP 1111, 071 (2011), arxiv:1107.3554.

[53] M. S. Costa, J. Penedones, D. Poland and S. Rychkov, *"Spinning Conformal Blocks"*, JHEP 1111, 154 (2011), arxiv:1109.6321.

[54] M. S. Costa and T. Hansen, *"Conformal correlators of mixed-symmetry tensors"*, JHEP 1502, 151 (2015), arxiv:1411.7351.

[55] P. Di Francesco, P. Mathieu and D. Senechal, *"Conformal Field Theory"*, Springer-Verlag (1997), New York.

[56] S. Weinberg, *"The Quantum theory of fields. Vol. 1: Foundations"*, Cambridge University Press (2005).

[57] M. F. Paulos, S. Rychkov, B. C. van Rees and B. Zan, *"Conformal Invariance in the Long-Range Ising Model"*, Nucl. Phys. B 902, 246 (2016), arxiv:1509.00008.

[58] R. Haag, *"Local Quantum Physics"*, Springer (1996), Berlin.

[59] F. A. Dolan and H. Osborn, *"On short and semi-short representations for four-dimensional superconformal symmetry"*, Annals Phys. 307, 41 (2003), hep-th/0209056.

[60] F. Gieres, *"Dirac's formalism and mathematical surprises in quantum mechanics"*, Rept. Prog. Phys. 63, 1893 (2000), quant-ph/9907069.

[61] D. Poland, S. Rychkov and A. Vichi, *"The Conformal Bootstrap: Theory, Numerical Techniques, and Applications"*, Rev. Mod. Phys. 91, 015002 (2019), arxiv:1805.04405.

[62] D. Pappadopulo, S. Rychkov, J. Espin and R. Rattazzi, *"OPE Convergence in Conformal Field Theory"*, Phys. Rev. D 86, 105043 (2012), arxiv:1208.6449.

[63] S. Rychkov and P. Yvernay, *"Remarks on the Convergence Properties of the Conformal Block Expansion"*, Phys. Lett. B 753, 682 (2016), arxiv:1510.08486.

[64] F. Dolan and H. Osborn, *"Conformal partial waves and the operator product expansion"*, Nucl.P̃hys.B̃ 678, 491 (2004), hep-th/0309180.

[65] F. Dolan and H. Osborn, *"Conformal Partial Waves: Further Mathematical Results"*, arxiv:1108.6194.

[66] D. Simmons-Duffin, *"The Lightcone Bootstrap and the Spectrum of the 3d Ising CFT"*, JHEP 1703, 086 (2017), arxiv:1612.08471.

[67] D. Simmons-Duffin, D. Stanford and E. Witten, *"A spacetime derivation of the Lorentzian OPE inversion formula"*, JHEP 1807, 085 (2018), arxiv:1711.03816.

[68] D. Carmi and S. Caron-Huot, *"A Conformal Dispersion Relation: Correlations from Absorption"*, JHEP 2009, 009 (2020), arxiv:1910.12123.

[69] A. Bissi, A. Sinha and X. Zhou, *"Selected topics in analytic conformal bootstrap: A guided journey"*, Phys. Rept. 991, 1 (2022), arxiv:2202.08475.

[70] T. Takayanagi, *"Holographic Dual of BCFT"*, Phys. Rev. Lett. 107, 101602 (2011), arxiv:1105.5165.

[71] L. Bianchi, M. Meineri, R. C. Myers and M. Smolkin, *"Rényi entropy and conformal defects"*, JHEP 1607, 076 (2016), arxiv:1511.06713.

[72] A. Gadde, *"Conformal constraints on defects"*, JHEP 2001, 038 (2020), arxiv:1602.06354.

[73] C. Herzog, *"Conformal field theory with boundaries and defects"*.

[74] P. Kravchuk, A. Radcliffe and R. Sinha, *"Effective theory for fusion of conformal defects"*, arxiv:2406.04561.

[75] N. B. Agmon and Y. Wang, *"Classifying Superconformal Defects in Diverse Dimensions Part I: Superconformal Lines"*, arxiv:2009.06650.

[76] M. Billò, M. Caselle, D. Gaiotto, F. Gliozzi, M. Meineri and R. Pellegrini, *"Line defects in the 3d Ising model"*, JHEP 1307, 055 (2013), arxiv:1304.4110.

[77] J. Padayasi, A. Krishnan, M. A. Metlitski, I. A. Gruzberg and M. Meineri, *"The extraordinary boundary transition in the 3d O(N) model via conformal bootstrap"*, arxiv:2111.03071.

[78] N. Drukker, Z. Kong and G. Sakkas, *"Broken Global Symmetries and Defect Conformal Manifolds"*, Phys. Rev. Lett. 129, 201603 (2022), arxiv:2203.17157.

[79] M. Isachenkov, P. Liendo, Y. Linke and V. Schomerus, *"Calogero-Sutherland Approach to Defect Blocks"*, JHEP 1810, 204 (2018), arxiv:1806.09703.

[80] F. Gliozzi, *"More constraining conformal bootstrap"*, Phys. Rev. Lett. 111, 161602 (2013), arxiv:1307.3111.

[81] F. Gliozzi and A. Rago, *"Critical exponents of the 3d Ising and related models from Conformal Bootstrap"*, JHEP 1410, 042 (2014), arxiv:1403.6003.

[82] F. Gliozzi, *"Truncatable bootstrap equations in algebraic form and critical surface exponents"*, JHEP 1610, 037 (2016), arxiv:1605.04175.

[83] M. F. Sohnius and P. C. West, *"Conformal Invariance in N=4 Supersymmetric Yang-Mills Theory"*, Phys. Lett. B 100, 245 (1981).

[84] D. Anselmi, *"Renormalization"*, Independently published (2019).

[85] J. C. Collins, *"Renormalization : An Introduction to Renormalization, the Renormalization Group and the Operator-Product Expansion"*, Cambridge University Press (1984), Cambridge.

[86] A. B. Zamolodchikov, *"Irreversibility of the Flux of the Renormalization Group in a 2D Field Theory"*, JETP Lett. 43, 730 (1986).

[87] Z. Komargodski and A. Schwimmer, *"On Renormalization Group Flows in Four Dimensions"*, JHEP 1112, 099 (2011), arxiv:1107.3987.

[88] H. Casini and M. Huerta, *"On the RG running of the entanglement entropy of a circle"*, Phys. Rev. D 85, 125016 (2012), arxiv:1202.5650.

[89] N. Drukker and D. J. Gross, *"An Exact prediction of N=4 SUSYM theory for string theory"*, J. Math. Phys. 42, 2896 (2001), hep-th/0010274.

[90] T. Shachar, R. Sinha and M. Smolkin, *"RG flows on two-dimensional spherical defects"*, SciPost Phys. 15, 240 (2023), arxiv:2212.08081.

[91] L. Onsager, *"Crystal statistics. 1. A Two-dimensional model with an order disorder transition"*, Phys. Rev. 65, 117 (1944).

[92] M. Aizenman, *"Proof of the Triviality of phi**4 in D-Dimensions Field Theory and Some Mean Field Features of Ising Models for D>4"*, Phys. Rev. Lett. 47, 1 (1981).

[93] J. Frohlich, *"On the Triviality of Lambda (phi**4) in D-Dimensions Theories and the Approach to the Critical Point in D >= Four-Dimensions"*, Nucl. Phys. B 200, 281 (1982).

[94] M. Aizenman and H. Duminil-Copin, *"Marginal triviality of the scaling limits of critical 4D Ising and ϕ^4_4 models"*, Annals Math. 194, 163 (2021), arxiv:1912.07973.

[95] J. Henriksson, *"The critical O(N) CFT: Methods and conformal data"*, arxiv:2201.09520.

[96] I. R. Klebanov and A. M. Polyakov, *"AdS dual of the critical O(N) vector model"*, Phys. Lett. B 550, 213 (2002), hep-th/0210114.

[97] A. Altland and B. Simons, *"Condensed Matter Field Theory"*, Cambridge University Press (2023).

[98] G. Parisi, *"Field theoretic approach to second order phase transitions in two-dimensional and three-dimensional systems"*, J. Stat. Phys. 23, 49 (1980).

[99] K. G. Wilson and M. E. Fisher, *"Critical exponents in 3.99 dimensions"*, Phys. Rev. Lett. 28, 240 (1972).

[100] H. Kleinert and V. Schulte-Frohlinde, *"Critical properties of phi**4-theories"*.

[101] M. Moshe and J. Zinn-Justin, *"Quantum field theory in the large N limit: A Review"*, Phys. Rept. 385, 69 (2003), hep-th/0306133.

[102] J. Rong, *"Local/Short-range conformal field theories from long-range perturbation theory"*, arxiv:2406.17958.

[103] S. Giombi and V. Kirilin, *"Anomalous dimensions in CFT with weakly broken higher spin symmetry"*, JHEP 1611, 068 (2016), arxiv:1601.01310.

[104] F. P. Toldin, F. F. Assaad and S. Wessel, *"Critical behavior in the presence of an order-parameter pinning field"*, Physical Review B 95, (2017).

[105] S. Ebadi et al., *"Quantum phases of matter on a 256-atom programmable quantum simulator"*, Nature 595, 227 (2021), arxiv:2012.12281.

[106] B. M. Law, *"Wetting, adsorption and surface critical phenomena"*, Progress in Surface Science 66, 159 (2001).

[107] M. Fisher and P. de Gennes, *" Phenomenes aux parois dans un melange binaire critique"*, World Scientific Simple Views on Condensed Matter, 237–241 (2003).

[108] A. Hanke, *"Critical Adsorption on Defects in Ising Magnets and Binary Alloys"*, Phys. Rev. Lett. 84, 2180 (2000), https://link.aps.org/doi/10.1103/PhysRevLett.84.2180.

[109] A. Allais and S. Sachdev, *"Spectral function of a localized fermion coupled to the Wilson-Fisher conformal field theory"*, Phys. Rev. B 90, 035131 (2014), arxiv:1406.3022.

[110] A. Gimenez-Grau, E. Lauria, P. Liendo and P. van Vliet, *"Bootstrapping line defects with O(2) global symmetry"*, JHEP 2211, 018 (2022), arxiv:2208.11715.

[111] A. Kapustin, *"Wilson-'t Hooft operators in four-dimensional gauge theories and S-duality"*, Phys. Rev. D 74, 025005 (2006), hep-th/0501015.

[112] S. Liu, H. Shapourian, A. Vishwanath and M. A. Metlitski, *"Magnetic impurities at quantum critical points: Large N expansion and connections to symmetry protected topological states"*, Physical Review B 104, (2021).

[113] M. Beccaria, S. Giombi and A. A. Tseytlin, *"Wilson loop in general representation and RG flow in 1D defect QFT"*, J. Phys. A 55, 255401 (2022), arxiv:2202.00028.

[114] A. M. Sengupta, *"Spin in a fluctuating field: The Bose(+Fermi) Kondo models"*, Phys. Rev. B 61, 4041 (2000), https://link.aps.org/doi/10.1103/PhysRevB.61.4041.

[115] S. Sachdev, *"Static hole in a critical antiferromagnet: Field theoretic renormalization group"*, Physica C 357, 78 (2001), cond-mat/0011233.

[116] S. Sachdev, *"Static hole in a critical antiferromagnet: field-theoretic renormalization group"*, Physica C: Superconductivity 357-360, 78 (2001).

[117] L. Bianchi, L. Griguolo, M. Preti and D. Seminara, *"Wilson lines as superconformal defects in ABJM theory: a formula for the emitted radiation"*, JHEP 1710, 050 (2017), arxiv:1706.06590.

[118] D. Gaiotto, D. Mazac and M. F. Paulos, *"Bootstrapping the 3d Ising twist defect"*, JHEP 1403, 100 (2014), arxiv:1310.5078.

[119] N. Gorini, L. Griguolo, L. Guerrini, S. Penati, D. Seminara and P. Soresina, *"Constant primary operators and where to find them: the strange case of BPS defects in ABJ(M) theory"*, JHEP 2302, 013 (2023), arxiv:2209.11269.

[120] N. Drukker and Z. Kong, *"1/3 BPS loops and defect CFTs in ABJM theory"*, JHEP 2306, 137 (2023), arxiv:2212.03886.

[121] E. Lauria, P. Liendo, B. C. Van Rees and X. Zhao, *"Line and surface defects for the free scalar field"*, JHEP 2101, 060 (2021), arxiv:2005.02413.

[122] V. Bashmakov and J. Sisti, *"Exploring Defects with Degrees of Freedom in Free Scalar CFTs"*, arxiv:2410.01716.

[123] M. Trépanier, *"Surface defects in the O(N) model"*, JHEP 2309, 074 (2023), arxiv:2305.10486.

[124] A. Raviv-Moshe and S. Zhong, *"Phases of surface defects in Scalar Field Theories"*, JHEP 2308, 143 (2023), arxiv:2305.11370.

[125] S. Giombi and B. Liu, *"Notes on a surface defect in the O(N) model"*, JHEP 2312, 004 (2023), arxiv:2305.11402.

[126] S. Harribey, W. H. Pannell and A. Stergiou, *"Multiscalar critical models with localised cubic interactions"*, arxiv:2407.20326.

[127] O. Diatlyk, Z. Sun and Y. Wang, *"Surprises in the ordinary: $O(N)$ invariant surface defect in the ϵ-expansion"*, arxiv:2411.16522.

[128] H. W. Diehl and M. Shpot, *"Massive field theory approach to surface critical behavior in three-dimensional systems"*, Nucl. Phys. B 528, 595 (1998), cond-mat/9804083.

[129] A. Krishnan and M. A. Metlitski, *"A plane defect in the 3d O(N) model"*, SciPost Phys. 15, 090 (2023), arxiv:2301.05728.

[130] H. Osborn and A. Stergiou, *"Seeking fixed points in multiple coupling scalar theories in the ϵ expansion"*, JHEP 1805, 051 (2018), arxiv:1707.06165.

[131] S. Harribey, I. R. Klebanov and Z. Sun, *"Boundaries and interfaces with localized cubic interactions in the $O(N)$ model"*, JHEP 2310, 017 (2023), arxiv:2307.00072.

[132] M. A. Shpot, *"Boundary conformal field theory at the extraordinary transition: The layer susceptibility to $O(\varepsilon)$"*, JHEP 2101, 055 (2021), arxiv:1912.03021.

[133] L. F. Alday and S. Caron-Huot, *"Gravitational S-matrix from CFT dispersion relations"*, JHEP 1812, 017 (2018), arxiv:1711.02031.

[134] L. F. Alday, J. Henriksson and M. van Loon, *"An alternative to diagrams for the critical O(N) model: dimensions and structure constants to order $1/N^2$"*, JHEP 2001, 063 (2020), arxiv:1907.02445.

[135] A. Gimenez-Grau, *"Probing magnetic line defects with two-point functions"*, arxiv:2212.02520.

[136] L. F. Alday, J. Henriksson and M. van Loon, *"Taming the ϵ-expansion with large spin perturbation theory"*, JHEP 1807, 131 (2018), arxiv:1712.02314.

[137] J. Henriksson and M. Van Loon, *"Critical O(N) model to order ϵ^4 from analytic bootstrap"*, J. Phys. A 52, 025401 (2019), arxiv:1801.03512.

[138] H. M. Srivastava and M. C. Daoust, *"A Note on the Convergence of KAMPÉ DE FÉRIET's Double Hypergeometric Series"*, Mathematische Nachrichten 53, 151 (1972).

[139] L. F. Alday, *"Solving CFTs with Weakly Broken Higher Spin Symmetry"*, JHEP 1710, 161 (2017), arxiv:1612.00696.

[140] J. Henriksson, S. R. Kousvos and A. Stergiou, *"Analytic and Numerical Bootstrap of CFTs with $O(m) \times O(n)$ Global Symmetry in 3D"*, SciPost Phys. 9, 035 (2020), arxiv:2004.14388.

[141] J. Henriksson and A. Stergiou, *"Perturbative and Nonperturbative Studies of CFTs with MN Global Symmetry"*, SciPost Phys. 11, 015 (2021), arxiv:2101.08788.

[142] A. Gimenez-Grau and P. Liendo, *"Bootstrapping Monodromy Defects in the Wess-Zumino Model"*, arxiv:2108.05107.

[143] S. Kehrein, F. Wegner and Y. Pismak, *"Conformal symmetry and the spectrum of anomalous dimensions in the N vector model in four epsilon dimensions"*, Nucl. Phys. B 402, 669 (1993).

[144] P. Dey, A. Kaviraj and A. Sinha, *"Mellin space bootstrap for global symmetry"*, JHEP 1707, 019 (2017), arxiv:1612.05032.

[145] T. Huber and D. Maitre, *"HypExp: A Mathematica package for expanding hypergeometric functions around integer-valued parameters"*, Comput. Phys. Commun. 175, 122 (2006), hep-ph/0507094.

[146] T. Huber and D. Maitre, *"HypExp 2, Expanding Hypergeometric Functions about Half-Integer Parameters"*, Comput. Phys. Commun. 178, 755 (2008), arxiv:0708.2443.

[147] S. Teber, *"Electromagnetic current correlations in reduced quantum electrodynamics"*, Phys. Rev. D 86, 025005 (2012), arxiv:1204.5664.

[148] D. M. McAvity and H. Osborn, *"Conformal field theories near a boundary in general dimensions"*, Nucl. Phys. B 455, 522 (1995), cond-mat/9505127.

[149] M. Beccaria, G. V. Dunne and A. A. Tseytlin, *"BPS Wilson loop in $\mathcal{N} = 2$ superconformal $SU(N)$ orientifold gauge theory and weak-strong coupling interpolation"*, JHEP 2107, 085 (2021), arxiv:2104.12625.

[150] H. W. Diehl and S. Dietrich, *"Field-theoretical approach to static critical phenomena in semi-infinite systems"*, Z. Phys. B 42, 65 (1981).

[151] H. W. Diehl and M. Shpot, *"Surface critical behavior in fixed dimensions $d < 4$: Nonanalyticity of critical surface enhancement and massive field theory approach"*, Phys. Rev. Lett. 73, 3431 (1994), cond-mat/9409064.

[152] D. J. Binder and S. Rychkov, *"Deligne categories in lattice models and quantum field theory, or making sense of $O(N)$ symmetry with non-integer N"*, JHEP 2004, 117 (2020), arxiv:1911.07895.

[153] M. Hogervorst, S. Rychkov and B. C. van Rees, *"Unitarity violation at the Wilson-Fisher fixed point in $4-\epsilon$ dimensions"*, Phys. Rev. D 93, 125025 (2016), arxiv:1512.00013.

[154] I. Bertan, I. Sachs and E. D. Skvortsov, *"Quantum ϕ^4 theory in AdS_4 and its CFT dual"*, JHEP 1902, 099 (2019), arxiv:1810.00907.

[155] M. E. Fisher, S.-k. Ma and B. G. Nickel, *"Critical Exponents for Long-Range Interactions"*, Phys. Rev. Lett. 29, 917 (1972).

[156] N. Chai, M. Goykhman and R. Sinha, *"Long-range vector models at large N"*, JHEP 2109, 194 (2021), arxiv:2107.08052.

[157] L. Fei, S. Giombi and I. R. Klebanov, *"Critical $O(N)$ models in $6-\epsilon$ dimensions"*, Phys. Rev. D 90, 025018 (2014), arxiv:1404.1094.

[158] L. Fei, S. Giombi, I. R. Klebanov and G. Tarnopolsky, *"Three loop analysis of the critical O(N) models in $6-\varepsilon$ dimensions"*, Phys. Rev. D 91, 045011 (2015), arxiv:1411.1099.

[159] J. A. Gracey, *"Four loop renormalization of ϕ^3 theory in six dimensions"*, Phys. Rev. D 92, 025012 (2015), arxiv:1506.03357.

[160] O. Antipin, J. Bersini, F. Sannino, Z.-W. Wang and C. Zhang, *"More on the cubic versus quartic interaction equivalence in the $O(N)$ model"*, Phys. Rev. D 104, 085002 (2021), arxiv:2107.02528.

[161] S. M. Chester, S. S. Pufu and R. Yacoby, *"Bootstrapping $O(N)$ vector models in $4 < d < 6$"*, Phys. Rev. D 91, 086014 (2015), arxiv:1412.7746.

[162] A. Stergiou, *"Symplectic critical models in $6+\epsilon$ dimensions"*, Phys. Lett. B 751, 184 (2015), arxiv:1508.03639.

[163] J. A. Gracey, *"Six dimensional QCD at two loops"*, Phys. Rev. D 93, 025025 (2016), arxiv:1512.04443.

[164] H. Osborn and A. Stergiou, *"C_T for non-unitary CFTs in higher dimensions"*, JHEP 1606, 079 (2016), arxiv:1603.07307.

[165] J. Sak, *"Low-temperature renormalization group for ferromagnets with long-range interactions"*, Phys. Rev. B 15, 4344 (1977), https://link.aps.org/doi/10.1103/PhysRevB.15.4344.

[166] J. Sak, *"Recursion Relations and Fixed Points for Ferromagnets with Long-Range Interactions"*, Phys. Rev. B 8, 281 (1973), https://link.aps.org/doi/10.1103/PhysRevB.8.281.

[167] M. Aizenman and R. Fernández, *"Critical exponents for long-range interactions"*, Letters in Mathematical Physics 16, 39 (1988), https://doi.org/10.1007/BF00398169.

[168] S. Hernández-Cuenca, *"Wormholes and Factorization in Exact Effective Theory"*, arxiv:2404.10035.

[169] C. C. Behan, *"Bootstrapping some continuous families of conformal field theories"*.

[170] C. Behan, L. Rastelli, S. Rychkov and B. Zan, *"A scaling theory for the long-range to short-range crossover and an infrared duality"*, J. Phys. A 50, 354002 (2017), arxiv:1703.05325.

[171] L. Caffarelli and L. Silvestre, *"An extension problem related to the fractional Laplacian"*, Communications in partial differential equations 32, 1245 (2007).

[172] J. Honkonen and M. Y. Nalimov, *"Crossover between field theories with short-range and long-range exchange or correlations"*, Journal of Physics A: Mathematical and General 22, 751 (1989).

[173] S. Giombi and H. Khanchandani, *"$O(N)$ models with boundary interactions and their long range generalizations"*, JHEP 2008, 010 (2020), arxiv:1912.08169.

[174] K. Ohno and Y. Okabe, *"The 1/n expansion for the extraordinary transition of semi-infinite system"*, Progress of theoretical physics 72, 736 (1984).

[175] M. A. Metlitski, *"Boundary criticality of the O(N) model in $d = 3$ critically revisited"*, SciPost Phys. 12, 131 (2022), arxiv:2009.05119.

[176] I. Buhl-Mortensen, M. de Leeuw, A. C. Ipsen, C. Kristjansen and M. Wilhelm, *"A Quantum Check of AdS/dCFT"*, JHEP 1701, 098 (2017), arxiv:1611.04603.

[177] C. Kristjansen and K. Zarembo, *"'t Hooft loops in N=4 super-Yang-Mills"*, arxiv:2412.01972.

[178] W. H. Pannell and A. Stergiou, *"Line defect RG flows in the ε expansion"*, JHEP 2306, 186 (2023), arxiv:2302.14069.

[179] J. Barrat, P. Liendo and P. van Vliet, *"Line defect correlators in fermionic CFTs"*, arxiv:2304.13588.

[180] M. Safari, A. Stergiou, G. P. Vacca and O. Zanusso, *"Scale and conformal invariance in higher derivative shift symmetric theories"*, JHEP 2202, 034 (2022), arxiv:2112.01084.

[181] L. Bianchi, A. Chalabi, V. Procházka, B. Robinson and J. Sisti, *"Monodromy defects in free field theories"*, JHEP 2108, 013 (2021), arxiv:2104.01220.

[182] A. Chalabi, C. P. Herzog, K. Ray, B. Robinson, J. Sisti and A. Stergiou, *"Boundaries in Free Higher Derivative Conformal Field Theories"*, arxiv:2211.14335.

[183] L. Di Pietro, E. Lauria and P. Niro, *"Conformal boundary conditions for a 4d scalar field"*, SciPost Phys. 16, 090 (2024), arxiv:2312.11633.

[184] S. Giombi, E. Helfenberger and H. Khanchandani, *"Line Defects in Fermionic CFTs"*, arxiv:2211.11073.

[185] V. S. Dotsenko and S. N. Vergeles, *"Renormalizability of Phase Factors in the Nonabelian Gauge Theory"*, Nucl. Phys. B 169, 527 (1980).

[186] M. Beccaria, S. Giombi and A. A. Tseytlin, *"Higher order RG flow on the Wilson line in $\mathcal{N} = 4$ SYM"*, arxiv:2110.04212.

[187] V. A. Smirnov, *"Feynman integral calculus"*, Springer (2006), Berlin, Heidelberg.